

2-27-7  
NATIONAL ADVISORY COMMITTEE FOR AERONAUTICS

# WARTIME REPORT

ORIGINALY ISSUED  
September 1943 as  
Advance [REDACTED] Report 3I15

AERODYNAMIC AND HYDRODYNAMIC TESTS OF A FAMILY OF MODELS  
OF FLYING-BOAT HULLS DERIVED FROM A STREAMLINE BODY

NACA MODEL 84 SERIES

By John B. Parkinson, Roland E. Olson,  
Eugene C. Draley, and Arvo A. Luoma

Langley Memorial Aeronautical Laboratory  
Langley Field, Va,



WASHINGTON

NACA WARTIME REPORTS are reprints of papers originally issued to provide rapid distribution of advance research results to an authorized group requiring them for the war effort. They were previously held under a security status but are now unclassified. Some of these reports were not technically edited. All have been reproduced without change in order to expedite general distribution.

NATIONAL ADVISORY COMMITTEE FOR AERONAUTICS

AD VAN  REPORT

AERODYNAMIC AND HYDRODYNAMIC TESTS OF A FAMILY OF MODELS  
OF FLYING-BOAT HULLS DERIVED FROM A STREAMLINE BODY -  
NACA MODEL 84 SERIES

By John B. Parkinson, Roland E. Olson,  
Eugene C. Draley, and Arvo A. Luoma

SUMMARY

A series of related forms of flying-boat hulls representing various degrees of compromise between aerodynamic and hydrodynamic requirements was tested in NACA tank 1 and in the NACA 8-foot high-speed tunnel. The purpose of the investigation was to provide information regarding the penalties in water performance resulting from further aerodynamic refinement and as a corollary, to provide information regarding the penalties in range or pay load resulting from the retention of certain desirable hydrodynamic characteristics. The information should form a basis for over-all improvements in hull form.

The related models of the series were based on an arbitrary streamline body of revolution. The variations in form were developed in such a way as to show clearly the effect of conventional departures from the ideal streamline body made in the design of flying-boat hulls.

The models were 114.85 inches long and the diameter of the basic streamline form was 15.92 inches. In the hydrodynamic tests, resistance and trim or trimming moments were measured at all speeds and loads of interest and the spray patterns were photographed. In the aerodynamic tests, lift, drag, and pitching moment were measured with transition fixed at 5 percent of the length, at speeds up to 420 miles per hour, and at Reynolds numbers up to 30,000,000.

The results of the investigation are summarized as follows:



### (1) Effect of varying height of bow

Increasing the height of the bow by warping the form decreases the trim and increases the resistance at low speeds. A low bow runs cleaner in smooth water than a high bow of the same length because of the increased fore-and-aft curvature of the high bow. Increasing the height of a well-faired bow by warping the form has only a small adverse effect on the aerodynamic drag.

### (2) Effect of varying height of stern

Increasing the height of the stern by warping the basic form but holding the afterbody position fixed, increases resistance and trim at speeds below the hump, decreases the hump speed, and does not affect the value of the maximum resistance at the hump. A low stern runs awash and requires a higher position of the tail surfaces relative to the dock. Increasing the height of the stern by warping the basic form but holding the afterbody position fixed has a large adverse effect on the aerodynamic drag; varying the height of the stern of the streamline body alone has no adverse effect on the drag but increases the angle of minimum drag as would be expected.

### (3) Effect of increasing angle of dead rise at bow

Increasing the angle of dead rise at the bow by dropping the keel line reduces only slightly the resistance at low speeds but results in a large improvement in cleanness of running. The modification is out of the water at the hump speed, and for a well-faired form has little or no effect on the aerodynamic drag.

### (4) Effect of decreasing angle of dead rise on afterbody

Decreasing the angle of dead rise on the afterbody decreases the trim at speeds up to and including the hump speed. The decrease in trim reduces the resistance at these speeds and tends to increase the clearance of the tail extension.

### (5) Effect of increasing depth of step

Increasing the depth of the step by raising the afterbody parallel to itself has only a small effect on resistance and spray at low speeds and decreases resistance at planing speeds. Too shallow a step results in a violent instability at high speeds that is most pronounced when the afterbody keel approaches the horizontal. Increasing the depth of step from 2.5 to 4.4 percent of the beam increases the aerodynamic drag only 2 percent.

### (6) Effect of increasing angle of afterbody keel

Increasing the angle of afterbody keel results in large increases in trim and resistance at the hump speed, most of the increase in resistance being attributed to the increase in trim; it lowers the resistance at planing speeds. A low angle of afterbody keel results in the cleanest running at low speeds. Increasing the angle of afterbody keel increases the trim at which the violent instability resulting from too shallow a step will be encountered.

### (7) Effect of addition of chine flare

Chine flare added exterior to the straight bottom sections of the forebody has only a small effect on the resistance and trim up to and including the hump speed but results in a marked improvement in cleanness of running. Chine flare added to the afterbody reduces the resistance at the hump speed and slightly increases the resistance at planing speeds.

### (8) Effect of addition of third planing surface

The addition of a third planing surface on the model with the lowest stern has a negligible effect on the trim and resistance - a remarkable result because the stern sections without the planing surface are circular and heavily wetted. The addition of the planing surface somewhat reduces the wetting of the stern.

### (9) Effect of rounded chines at bow

Bounding the chines at the bow results in very poor spray characteristics in smooth water and probably would be impracticable in rough water.

## (10) Design charts

The results of general free-to-trim and fixed-trim tests of a model incorporating the most promising of the forms tested are presented in the form of design charts for estimating static water lines and take-off performance. The aerodynamic data, because of their unique character, are presented completely for use in estimating the effect of the variables investigated on aerodynamic performance.

It is concluded that the aerodynamic drag of a planing type of hull need not be more than 25 percent greater than that of the streamline body from which it is derived. This difference might be reduced by the development of a form of afterbody that has less influence on the flow than does the conventional pointed type.

## INTRODUCTION

The aerodynamic drag of hulls is an important factor in the design of Long-range flying boats, not only because of its effect on speed but also because of its influence on pay load, which is more important. Because of the long distance involved in transoceanic routes, the fuel load must be a large part of the useful load carried. The pay load on such flights is small and its size is largely dependent on the magnitude of the fuel load, even in cases of the largest craft now built or contemplated. Under these conditions of operation, the weight of the fuel required for power to overcome the drag of the hull is large in terms of pay load. The further development of the planing type of hull for long-range flying boats, therefore, should be toward forms that combine the lowest possible aerodynamic drag with satisfactory hydrodynamic qualities.

The first step by the NACA in furthering this development was the investigation of two forms of hull in which the fore and after planing surfaces were shaped to follow as closely as possible an arbitrary streamline body derived from a solid of revolution (reference 1). The forms were generally satisfactory in the tank although they showed some evidence of "sticking" and high-water resistance at high speeds and some "dirtiness" at low speeds. Their aerodynamic drag was low enough, however, to warrant the acceptance of a certain degree of poor water performance.

I-277

It was evident from the tank tests of these models that the limitations on reductions in aerodynamic drag imposed by the hydrodynamic requirements were not definite enough to provide simple guides for the most favorable compromise, it was therefore decided to obtain hydrodynamic and aerodynamic information on a series of related forms of hull representing various degrees of compromise between the requirements in the air and on the water, These data would make it possible to obtain an idea of the cost in water performance to be paid for further aerodynamic refinement and of the cost in range or pay load to be paid for certain desirable hydrodynamic characteristics and would be further guides for over-all improvements in form. The NACA model 84 series of hulls was designed for this purpose,

The models of the series were made generally similar to model 74-A (reference 1) except that a V-section was adopted for the planing surfaces instead of the section with rounded keel incorporated in that model. The use of the V-section resulted in slightly greater departure from the form of the basic streamline body than was the case with the earlier models but seemed to be preferable for operation in waves. In the design of the series, the plan forms of the streamline body and the planing surfaces were held constant. The variations of form included in the scope of the investigation are as follows:

- Height of bow
- Height of stern
- Angle of dead rise at bow
- Angle of dead rise on afterbody
- Depth of step
- Angle of afterbody keel
- Addition of chine flare
- Addition of third planing surface on tail
- Rounding of chines at bow
- Depth of streamline body

The models of the series were tested in NACA tank 1 to obtain the effects of the variations in form on the water resistance, flow, and general behavior. The aerodynamic tests were made in the NACA 8-foot high-speed tunnel and provided an unusual opportunity to obtain the effects on the aerodynamic forces at high values of the Reynolds number. The tests in both the tank and the wind tunnel were made with models of the hull alone and hence do not include the effects of interferences between the hull and

the aerodynamic surfaces or the possible effects of the changes in form on the dynamic stability.

## DESCRIPTION OF MODELS

The lines of the NACA model 84 series, illustrating the mutual relationships of the variations in form, are shown in figure 1. Enlarged body plans showing the shape of the transverse sections in detail are given in figure 2. The numerical values of the offsets used in the construction of the models are included in Tables I to III for use in reproducing the detailed form of the sections.

The basic forms in all cases were derived from the arbitrary body of revolution, having a fineness ratio of 7.22 and maximum ordinate at 30 percent of the length, described in reference 1. Because of the anticipated use of supercharged hulls for long-range seaplanes, the basic forms were considered to represent the circular shell under internal pressure and the modifications for water performance were, in general, made exterior to them.

The basic cross section of the planing surfaces is a straight V having an angle of dead rise of  $20^{\circ}$ . The sides of the V were drawn tangent to or as close to the circular section of the basic form as the proper longitudinal form of the planing surfaces would allow. Typical relationships between the sections of the planing surfaces and those of the basic forms are indicated on the body plans.

In all the models, the axis of the body of revolution was taken as the base line. The variations in height of bow and in height of stern were obtained by bending the axis (center of radii) vertically upward from station 10, which is at the maximum ordinate, toward the ends. In the variations of the bow, the sections of bows 1, 2, and 3 and the sections of bows 2B and 3B are the same, the differences being in their vertical position. The axis of bow 1 is horizontal and coincides with the base line. The chines at the bow are located in a plane passing through the axis of revolution of the basic form. The curvature of the axes of bows 3 and 3B is such as to give a horizontal deck line forward. The heights of the axes of bows 2 and 2B are one-half those of bows 3 and 3B; thus the variations in height of bow sections in the series are linear. In

the variations of the stern, the height of the basic form **was** changed but that of the planing surfaces **was** held constant. The axis of stern 1 is horizontal and coincides with the base line. This stern **was** not included in the hull models because the tail obviously is too low for a suitable support for tail surfaces and for proper location of the after planing surface exterior to the basic form. The curvature of the axis of the basic form of stern 3 is such as to give a horizontal deck line aft. The heights of the axes of sterns 2 and 2C are one-half those of stern 3 and the height of the axis of stern 4 is 1.5 times those of stern 3; thus the variations in the height of the basic form aft and in the vertical distance between the basic form and the after planing surface are linear.

In bows 1, 2, and 3, the V-bottom sections are tangent to the basic streamline form and have a constant angle of dead rise of  $20^{\circ}$ . These sections result in a developable bottom surface and a minimum departure from the basic form for V-sections exterior to it. In bows 2B and 3B, the original keel line was dropped to give a progressive increase in angle of dead rise from  $20^{\circ}$  at station 10 to  $60^{\circ}$  at the bow. This modification results in greater departure from the basic form but provides a sharper entrance for the immersed portion of the hull.

The chine flare is exterior to and tangent to the straight V-sections and therefore slightly reduces the effective dead rise. Forward of station 10, its width is one-fifth the half-breadth and it is curved to be horizontal at the chine. Aft of station 10, the width of the chine flare is arbitrarily reduced to 18 percent of the half-breadth at the step and the angle of the chine is slightly above the horizontal. In this region, the width inboard of the flare is constant. On the afterbody, the form of the flare at each station is the same as at the step. The models were originally made with the flare, which was removed during the tank tests by planing it off.

The models of the series were made with a common depth of step of 2.58 percent of the beam at the step and an angle of afterbody keel of  $5.50^{\circ}$ . These values resulted in the highest position of the afterbody planing surface for stern 2 without cutting into the basic form aft and represented the lower limits of depth and angle used in practice. Higher values were obtained with removable blocks fitted in stern 4, which had sufficient clearance between the highest afterbody position and the

basic form to avoid cutting into it. Five blocks were provided as follows:

Block	Depth of step, percent	Angle of afterbody
4D	3.55	5.50
4E	4.52	5.50
4F	2.58	7.25
4G	2.58	9.00

Block 4 was made with chine flare, which was subsequently removed. For simplicity, the remaining blocks were made with straight V-sections and the models were tested with chine flare on the forebody only,

An additional block, block 4H, having straight V-sections with the angle of dead rise decreased from  $20^\circ$  at the step to  $0^\circ$  at the stern post was provided for stern 4. In this block, the depth of step was 2.58 percent of the beam at the step and the angle of afterbody keel was  $7.25^\circ$ .

Stern 2C is the same as stern 2 except that the shape of the basic form was altered to provide a third planing surface under the tail for cleaner running during immersion at low speeds. The surface has straight V-sections with  $20^\circ$  angle of dead rise and fades out above the afterbody planing surface in the usual manner. In this case, the surface cuts into that of the basic form; it is unlikely that this part of the hull would be supercharged. Stern 2 was chosen for this modification because of the additional dirtiness expected with the low tail, which would not be so marked in the case of the higher tails.

Bow 1A is the same as bow 1 except that the chines are rounded forward of station 7 using an expanding radius as shown on the body plan (fig. 2(a)). This modification was applied only to the low bow because the hydrodynamic effect of the rounded chines would be less marked in the case of the higher bows.

Figure 3 shows profiles of the models tested in the

L-277  
wind tunnel in the present; investigation. Nose 1 and tail 1 reproduce the body of revolution from which the models of the series were derived and the combination represents the streamline body of lowest drag with which the drags of the hull models may be compared. In the second form, the depth of the original body is arbitrarily increased 50 percent by inserting a uniform spacer at the axis of revolution. This modification does not affect the hydrodynamic characteristics and therefore was not included in the tank series. The rest of the forms investigated are the same as those tested in the tank.

The models of the series are identified in the data from the tests according to table IV. The models were made of laminated white pine in sections, divided vertically at station 10 (maximum beam) and horizontally along the axes of the basic forms. The bow and the stern sections were bolted together internally and the top and bottom halves were held together by through bolts; the recesses for the nuts of these bolts were filled with beeswax and plasticine. This arrangement provided the variety of forms described with the minimum of component parts and a means of increasing the depth of any model by spacers, as in model 84-1,

For the tank tests, the models were filled by several coats of thinned varnish and finished with three coats of grey pigmented varnish rubbed between coats. Special care was taken to prevent swelling of the pieces because of moisture, and the slight ledges at the joints found on assembly were satisfactorily faired with beeswax.

For the aerodynamic tests, from 14 to 20 coats of lacquer were sprayed on the models and the lacquer was sanded between coats. The final coat of lacquer was finished by sanding in the direction of air flow with No. 400 carborundum paper until the models were aerodynamically smooth. Unfortunately, the photographs indicate a degree of irregularity and roughness that did not exist. This appearance of roughness was caused by the variation in shades of the filler and the paint that were used.

## HYDRODYNAMIC TESTS

### Apparatus and Procedure

NACA tank 3, in which the models were towed, is de-



scribed in reference 2. The most comprehensive description of the present equipment and of methods of testing may be found in reference 3.

Most of the variations in the series are of such a nature that the parts changed are clear of the water except at low speeds when the models are deeply immersed. At these speeds, the water forces predominate and the trim is not greatly influenced by the position of the center of gravity or by external moments applied by the propellers and aerodynamic surfaces. It was therefore considered adequate to investigate the effect of the variations by general free-to-trim tests up to the speed at which the afterbody planing surface was first clear of the water. This procedure provided representative information on resistance and flow about the models at trims corresponding to those encountered in practice. At the same time it greatly reduced the testing required to obtain similar information by general tests at fixed trim,

In the case of variations in the form that are normally wetted at planing speeds, the usual general tests at fixed trim were made over a wide range of speed, load, and trim to determine the effect of the variations in form on the resistance and behavior at high speeds and in addition to provide data for design purposes. All the models were tested by the general free-to-trim method at low speeds and models 84-AF, 84-SI?-1, 84-EF-3, and 84-EF-4 were tested by the general fixed-trim method.

In the free-to-trim tests, the model was free to pivot about an assumed center of gravity and was balanced about this point. For convenience, the pivot was located above the deck line on the assumption that small changes in vertical position would have small effect on the trim. Model 84-EF, having the low bow and high stern, was tested first with three longitudinal positions of the center of gravity. From the results of these tests, the position 7.20 inches forward of the step was chosen as a suitable common position for all the models and as the center of moments for the tests at fixed trim,

The appearance of excessive dirtiness and spray at the bow at low speeds was assumed to indicate the maximum practical load and was found to be that corresponding to a load coefficient of 0.8 at the hump speed. It was not considered advisable to go to higher load coefficients with the length-beam ratio used in the series even in the case of the higher bows.

In judging the effects of the variations on water performance, the flow and spray were considered the most important hydrodynamic data because of the small effect of most of the variations in form on the resistance at the hump speed. A large number of photographs of the spray patterns were obtained to record the effect on the spray pattern of the changes in form and to aid in determining suitable compromises with the aerodynamic properties as determined in the wind-tunnel tests. Tests involving variations in the form of bow generally were photographed from ahead of the model in order to obtain indications of the relative heights of the bow spray; and tests involving variations in the form aft were photographed from behind to record the spray pattern in the region of the tail extension.

### Results and Discussion

The results of the model 84 series tests were reduced to the usual coefficients based on Froude's law to make them independent of size. In this case, the maximum beam was chosen as the characteristic dimension. The nondimensional coefficients are defined as follows:

- $C_{\Delta}$  load coefficient ( $\Delta/wb^3$ )
- $C_R$  resistance coefficient ( $R/wb^3$ )
- $C_V$  speed coefficient ( $V/\sqrt{gb}$ )
- $C_M$  trim-sine-cosine coefficient ( $M/wb^4$ )
- $C_d$  draft coefficient ( $d/b$ )

where

- $\Delta$  load on water, pounds
- $w$  specific weight of water, pounds per cubic foot  
(63.3 for these tests; usually taken as 64 for sea water)
- $b$  maximum beam, feet
- $R$  resistance, pounds
- $V$  speed, feet per second

- g acceleration of gravity, 32.2 feet per second per second
- M trimming moment, pound-feet
- d draft at main step, feet

Any consistent system of units may be used. The moment data are referred to the center of moments shown in figure 1. Tail-heavy moments are considered positive. Trim is the angle between the base line of the model and the horizontal.

Selection of the longitudinal position of the center of gravity.- The results of the general free-to-trim tests of model 84-EF at three fore-and-aft positions of the center of gravity are shown in figure 4. Moving the center of gravity from 5.7 inches to 7.2 inches forward of the step caused a small decrease in trim and a small reduction in resistance. Changing the position from 7.2 inches to 8.7 inches forward of the step produced a negligible variation in resistance. At the most forward position, the low trim made the bow appear dirty and the model displayed a greater tendency toward longitudinal instability. The intermediate position, 7.2 inches forward of the step, was used for the rest of the investigation.

Effect of varying the height of the bow.- Raising the bow, if the forebody length is kept constant, reduces the buoyant and hydrodynamic lift of the forebody at low speeds. This reduction results in the decrease in trim at low speeds shown in the general free-to-trim curves of figure 5. The decrease in trim is accompanied by a definite increase in resistance for the higher bows, models 84-BF and 84-CF. In the case of the higher bows, the increased convexity of the buttock lines produces a more blunt entrance into the water, causes a turbulent bow wave (figs. 8 to 11) to be thrown forward, and increases the resistance. The approximate heights and densities of the spray for the three bows may be compared in the photographs of figures 6 to 11. The low bow, model 84-AF, representing the smallest departure from a streamline form, not only has the lowest resistance but also is the cleanest running bow.

Removing the chine flare did not change the order of merit of the bows but accentuated the increased turbulence of the high bow. The use of any of the bows without the chine flare is inadvisable, however, because of the height and the amount of the spray at low speeds (figs. 7, 9, 11).

It must be remembered that the curves and photographs given were obtained from tests made under relatively smooth water conditions. If the hulls were tested in rough water, the low bow would be very dirty because it does not have sufficient clearance. It is thought, therefore, that a moderate departure from the basic form, produced by raising the bow, would be preferable for cleanness at low speeds. If the forebody was lengthened at the same time the bow was raised, the entrance in the water would be less abrupt and the spray characteristics would be improved. A higher bow of this type might be more favorable even in smooth water,

Effect of varying the height of the stern.— A comparison of the resistance and trim curves for three heights of the stern is made in figure 12. This investigation was made by the general free-to-trim method because the portion of the hull that was varied is completely clear of the water just over the hump speed. The discontinuity near the hump speed, which is associated with the clearing of the tail from the water, occurs at a lower speed as the tail is raised. The maximum resistance is about the same for the three models but the speed at which it occurs is lower for the high sterns.

Below hump speed the model with the low stern, model 84-DF, has the lowest resistance and trim. The decreased trim indicates that the round tail, which is wetted at those speeds (fig. 13), instead of producing hydrodynamic suction actually develops hydrodynamic lift. The low trim is the greatest factor in producing a reduction in the resistance because the model is then running at an attitude nearer the trim for minimum water resistance.

The effect on the spray produced by varying the height of the stern can be seen by studying the stern photographs of figures 6, 7, and 13 to 16. At low speeds, the sides of the stern of model 84-DF are wetted out to the tail; whereas the sides of the high sterns are relatively dry. The photographs show that the tail extension for the high sterns is clear of the water at lower speeds, as was indicated on the resistance curves. After the tail extension is clear of the water, the models are all at about the same trim and the spray patterns are similar.

Although the low stern, model 84-DF, has the lowest hydrodynamic resistance and is the nearest approach in the series to a streamline form, the photographs show that it is impractical because the deck of the tail, on which the control surfaces are attached, is actually subnorged at

some speeds and loads. Provision would have to be made to give the tail assembly greater clearance if this form of hull were to be used.

Removing the flare from the chines of the models did not change the relative performance of the tail extensions,

Effect of increasing the angle of dead rise at bow.-

The effect of increasing the angle of dead rise of the intermediate bow, model 84-33', and of the high bow, model 84-CF, is shown in the general free-to-trim curves (fig. 17). With the angle of dead rise increased forward, a slight reduction in the resistance is obtained before the hump speed, whereas the change in trim produced by this variation is negligible. With the chine flare removed, the reduction in resistance was slightly greater. At the hump speed, the portion of the hull affected by this change in form is completely clear of the water.

The main effect, of the variation in dead rise at the bow is the change produced in the flow and the spray originating at the bow. A comparison of figures 8 with 18, 9 with 19, 10 with 20, and 11 with 21 shows that the finer entrance (finer water lines) of the hull, obtained by increasing the dead rise, definitely improved the cleanness of running at low speeds. Instead of a heavy turbulent wave being shoved forward, models 84-BF, 84-CF, 84-B, and 84-C, the bow wave is lighter and most of the water is thrown laterally, models 84-FF, 84-CF, 84-F, 84-G. The removal of the chine flare probably accentuates this improvement in spray characteristics. The bow of model 84-FF appeared to be the best in the series,

Effect of a decreasing angle of dead rise on the afterbody.- The results of the general free-to-trim tests of model 84-EF-4 and model 84-EF-6 are compared in figure 22. The decreasing dead rise aft increases the lift of the afterbody and therefore reduces the trim. A reduction in trim of  $2^{\circ}$  is obtained at the hump. The corresponding reduction in resistance is about 15 percent. Most of the reduction in resistance is due to the lower trim.

The effect of angle of dead rise on the afterbody is shown in figures 23 and 24. Model 84-EF-6 runs a little cleaner than model 84-EF-4 because of the decreased trim that tends to bring the afterbody and tail extension clear of the water.

Model 84-EF-6 showed the least tendency toward a lateral instability at low speeds that seemed to be inherent in the series. In the photographs of model 84-EF-4 (fig. 23) at a speed coefficient of  $C_V = 2.33$  and a load coefficient of  $C_\Delta = 0.4$ , a laterally projected jet of water, originating under the afterbody is seen striking the side of the wake. With the heavy loads,  $C_\Delta = 0.6$  and  $C_\Delta = 0.8$ , this jet has a high-enough velocity to bounce back, hitting the side of the model forward of the stern post. This flow is generally unsymmetrical and causes the model to swing laterally on the suspension. The instability is accompanied by a discontinuity in the resistance. With a decreasing dead rise on the afterbody, model 84-EF-6, the unsymmetrical flow apparently was reduced and the lateral instability was negligible.

It is doubtful if this instability is serious, inasmuch as it is present in most models with pointed afterbodies that are tested in the tank. The method of towing probably magnifies this characteristic.

Effect of increasing the depth of the step.— At low speeds, the variation of depth of step has only a small effect on either the resistance or the spray (figs. 25 and 26 to 28). At the hump speed with the heaviest load on the models, increasing the depth of step from 0.40 inch, model 84-EF-1, to 0.70 inch, model 84-EF-3, resulted in a maximum increase in trim of about  $1^\circ$  and a corresponding increase in resistance of approximately 5 percent. The greater part of this change in resistance is due to the change in trim. This fact is evident if the resistance for model 84-EF-3 is determined from the general test data (see fig. 40) using the same trims obtained for model 84-EF-1 in figure 25.

The only visible effect on the spray at low speeds is the clearing of the afterbody from the water at a lower speed for the greater depth of step. (See figs. 26 to 28.)

In figure 29, the resistance coefficients at high speeds for 0.40-inch and 0.70-inch depths of step are compared at attitudes of the hull (trim  $\tau$  for minimum water resistance, for  $5^\circ$ , and for  $6^\circ$ ) which are practical for the operation of the hull and presumably can be obtained with the control moment available at these speeds. The effects of increasing the depth of step were similar to those reported in, reference 4. Increasing the depth of the step by raising the afterbody provides greater clearance and reduces the resistance.

In figure 29, model 84-EF-1, no data are shown for the light loads at  $5^\circ$  and  $6^\circ$  trim because of a sticking and accompanying vertical instability not present at the trim for minimum water resistance. A similar sticking and instability is reported in reference 1. When the trim of the hull is such that the afterbody keel is nearly horizontal, the flow from the main step suddenly covers the entire afterbody planing surface and the resistance and draft are suddenly increased. The flow then changes, permitting the model to rise again. Often the model jumped completely clear of the water. The instability did not appear at the trim for minimum water resistance because the attitude of the hull was below the range in which the afterbody surfaces are parallel to the water. At a trim of  $8^\circ$  at high speeds, the forebody of the model is clear of the water for light loads and the resistance and spray are the same as obtained when a hull is running on the afterbody only. Increasing the depth of step to 0.70 inch (4.4 percent of the beam) by raising the entire afterbody apparently removed the tendency toward instability,

It was difficult to interpret the sticking and instability in terms of full-scale performance because no attempt was made to obtain dynamic similarity. The mass moving vertically included the heavy model, the towing gate, and counterweights used for adjusting the load on the model. The model was also being towed at fixed trims and any changes in moment had no effect on the attitude of the hull.

Later experience with dynamic models indicates that the depths of step used in the series were too small for present-day take-off speeds. Depths of step from 6 to 10 percent of the beam are now considered necessary to avoid dangerous instability at high-water speeds induced by the sticking observed in the present tests.

Effect of angle of afterbody keel.— A comparison of the low-speed performance for three angles of afterbody keel is presented in figure 30. As the angle of afterbody keel is increased, the buoyancy and the hydrodynamic lift of the afterbody are reduced for any definite trim. To compensate for this decrease in lift the model tends to assume a higher trim. At very low speeds, this increase in trim is small and the change in resistance is negligible. The maximum effect is found at the hump speed at which an increase in angle of afterbody keel of  $3\frac{1}{2}^\circ$  caused a maximum increase in trim of about  $4^\circ$  and an accompanying

increase in free-to-trim resistance of about 25 percent. Most of the increase in resistance is due to the change in trim, the higher trim causing a greater departure from the trim for minimum water resistance.

The spray photographs for the variations of angle of afterbody keel are given in figures 23, 26, and 31. With the high angles of afterbody keel, the roach from the afterplaning surfaces continues to strike the tail extensions at slightly higher speeds. The greater clearance provided by the high angle of afterbody keel causes the afterbody to come out of the water at a lower speed. From observations and photographs it is concluded that at low speeds the model with the low angle of afterbody keel, model 84-SF-1, was the cleanest running.

In the investigation of the effect of this variation on high-speed performance, angles of afterbody keel of  $5.50^\circ$  and  $7.25^\circ$  were used. Using a higher angle is not advisable because it obviously causes too great an increase in the hump resistance. The results of the tests are compared (fig. 32) at the trim for minimum water resistance and at  $5^\circ$  and  $6^\circ$  fixed trim. The same conclusions may be drawn from these tests as were reported in reference 5. By increasing the angle of afterbody keel a greater clearance is obtained for the afterbody and the area of the afterplaning surface struck by water from the main step is reduced.

Comparison of the curves shows that a greater difference in resistance is obtained at  $6^\circ$  trim than at  $5^\circ$  trim. A greater difference is also obtained at  $5^\circ$  then at the trim for minimum water resistance, which is generally lower than  $5^\circ$ . The higher trims cause the afterbody to approach the horizontal and consequently to be in a position to be wetted by the flow from the main step. The model with a higher angle of afterbody keel in combination with a shallow step displayed the same vertical instability noted in the investigation of the effect of depth of step. The angle at which the instability occurs is changed to correspond to the angle at which the afterbody keel is parallel to the water surface. For model 84-EF-4 with a  $7.25^\circ$  angle of afterbody keel, this instability first appeared for a load of  $C_\Delta = 0.05$  at a trim of  $7^\circ$ . At a trim of  $8^\circ$ ,  $C_\Delta = 0.10$  was also unstable. The vertical motion was very slight at a trim of  $3^\circ$ .

These tests indicate that an angle of afterbody keel



from  $5^{\circ}$  to  $7^{\circ}$  is the most suitable compromise for satisfactory resistance at the hump speed and at planing speeds. A form of hull with a decreasing dead rise on the afterbody in combination with a higher angle of afterbody keel, as in model 84-EF-6 might be used. This combination would improve the resistance at the hump and automatically maintain increased clearance of the afterbody for good high-speed performance.

Effect of the addition of chine flare.— In order to investigate the effect of the chine flare, the original models were tested with the flare removed. The results of the general free-to-trim tests are summarized in figure 33, and the effect of the addition of chine flare on the spray characteristics is shown in figures 15, 16, and 26.

In figure 33 a comparison is made of the effect of adding chine flare to the forebody alone, model 84-EF-1, and to both the forebody and afterbody, model 84-EF. The following comparisons are made with model 84-E, on which the flare was removed. The addition of the chine flare on the forebody alone resulted in a small increase in trim before the hump, the resistance remaining about the same. At the hump, the effect on either the trim or the resistance is negligible. The influence on the spray characteristics was very masked. It is difficult to determine the effect of the flare on the spray from the stern photographs (figs. 16 and 26). At speeds near the hump, the model without the flare has a higher and more dense bow blister. The observations indicated, however, that a chine flare on the forebody is desirable throughout the low-speed range. This conclusion is similar to that drawn from the results of tests reported in reference 6, for corresponding widths and angles of flare. The addition of chine flare to both the forebody and afterbody, model 84-EF, not only improved the spray characteristics but also caused a decrease in trim at the hump of  $1^{\circ}$  and a decrease in resistance of 8 percent. Most of the change in resistance is due to the reduction in trim. The presence of the flare on the afterbody increases the lift of the afterbody and causes the hull to assume a more favorable attitude. The photographs (fig. 15) show the spray and the wave form. The chine flare on the afterbody apparently has little effect on the spray produced by the afterbody. The curves (figs. 5, 12, and 17) show the same reduction in trim and resistance. The bow photographs (figs. 6 and 7, 8 and 9, 10 and 11) may be compared to see the effectiveness of flare on both forebody and afterbody in controlling the spray.

The relative effect of the flare on the afterbody at high speeds may be seen by comparing the fixed-trim tests of model 84-AF and model 84-EF-1 (fig: 34). These models are similar except for the tail extension which **does** not affect the performance at high speeds. The effect of the flare on the afterbody at planing speeds is to increase the resistance,

Effect of the addition of a third planing surface.-

In order to investigate further the effect of the flow around the stern, a planing surface with sharp chines was added to the original round tail. The results of the general free-to-trim tests are given in figure 35. The effect of adding the chines and the planing surface to the tail, model 84-9, is small, indicating that the rounded tail, model 84-I, produces no tendency toward sticking. There is a negligible decrease in trim just before the hump if the third planing surface is added. The discontinuity at the hump, associated with the clearing of the tail from the water, occurs at a higher speed for model 84-H with the added planing area.

The photographs (figs. 14 and 36) show very little difference in spray for the two models. The amount of loose water thrown vertically, when the roach strikes the tip of the tail, is greater for the round tail. With a low afterbody this effect may be very important. The water striking the tip of the tail seems to have no effect on the trim.

Effect of chines on the bow.- The general free-to-trim results with the chines on the bow, model 84-8, and with the chines rounded, model 84-J, are presented in figure 37. Although the chines on the bow have little effect on either the trim or the resistance, the photographs (figs. 7 and 38) show very large differences in the spray. Instead of having the spray deflected downward, the model with rounded chines has a large amount of loose water thrown up and forward. These photographs indicate that a fading cut of the chines at the bow is definitely undesirable even in smooth water.

Design charts.- Complete data for model 84-EF-3 are presented for design purposes. The detailed general free-to-trim curves are included in figure 39. The results of the fixed-trim tests are presented in the form of charts (fig. 40). The use of these charts is explained in reference 1. The trims and drafts at rest, covering a practical

range of loads, are given in figure 41. Typical spray patterns at high speeds near the trim for minimum water resistance are shown in figure 42. The low-speed photographs are presented in figure 28. Because of the large amount of other data presented in this report, corresponding design data for models; 84-~~EF~~-4 and 84-AF have been omitted.

## AERODYNAMIC TESTS

### Apparatus and Methods

Apparatus.— Seven combinations of the BACA model 84-series flying-boat hulls were tested in the NACA 8-foot high-speed tunnel and measurements of aerodynamic drag, lift, and pitching moment were made. The present tests were primarily concerned with the drag. For purposes of comparison, similar data were obtained by testing three streamline bodies from which the hull shapes were derived. Figure 3 illustrates the various combinations aerodynamically tested.

Two vertical streamline struts supported the models and those struts, which were attached to the balance ring of the tunnel, were braced laterally by additional struts. Fairing enclosed the forward vertical strut for most of its length and completely shielded the lateral brace. Pitch-angle changes were obtained by pivoting the model at the front strut and then raising or lowering the rear strut as desired. Figure 43 shows a streamline model and its supporting struts in the wind tunnel. Figure 44 illustrates the method of supporting the model by wires for tare runs in such a way that the model was supported in place without touching the struts.

Methods.— Aerodynamic measurements of drag, lift, and pitching moment were made at 260 miles per hour for a range of pitch angle  $\alpha$  from  $-4^\circ$  to  $12^\circ$  in increments of  $4^\circ$ . The base line used for pitch-angle measurements was that defined in Description of Models. From these data, the angle of minimum drag was determined.

With the model set at the angle of minimum drag, force measurements were made at velocities from 100 to about 420 miles per hour and at a Reynolds number of 30,000,000 based on fuselage length, data being obtained at eight different velocities. This investigation is the only one of its type

in which data were obtained at such high speeds, through and above the actual speed range encountered in flight, and at such large Reynolds numbers.

Tare runs were made with the plain and warped streamline bodies. At the pitch angle of  $0^\circ$ , force measurements were made for velocities from 100 to 420 miles per hour; at a constant speed of 260 miles per hour, similar measurements were made for various pitch angles from  $-4^\circ$  to  $12^\circ$ . The tare force values thus obtained with streamline bodies were used, with the hull-model data, these force values being interpolated and extrapolated when necessary to determine the tare forces on struts for the different minimum pitch angles at which the hull models were tested.

### Precision

The errors that affect the absolute accuracy of the drag results can be divided into accidental errors and systematic errors. The accidental errors are the only ones that affect comparative results and are indicated by the scatter of the tare results plus the scatter of results. The sum of these variations is of the order of 2 percent of the drag.

The systematic errors consist of horizontal buoyancy and tunnel-wall effects. Horizontal-buoyancy corrections ranged from 5.5 to 6.5 percent of the minimum drag. These corrections were made. No tunnel-wall corrections were made but the constriction correction, which is probably the greater part of the total correction, would be about 2.4 percent, consequently, the error due to wall effects was probably less than 3 percent.

The errors in lift coefficient  $C_L$  and pitching-moment coefficient  $C_M$  for comparative purposes would best be indicated by the point scatter and are  $\pm 0.003C_L$  and  $\pm 0.001C_M$ .

### Results and Discussion

The aerodynamic force measurements, except as may be noted otherwise in the figures, were made with fixed transition that was produced by placing a ring of carborundum grains 5 percent aft of the bow. In this way, air-flow conditions were produced that approximated the actual conditions at full-scale Reynolds numbers (figs. 43 and 45). (See reference 7.)

**Drag** coefficients based on both maximum cross-sectional area and  $(\text{volume})^{2/3}$  of models are presented. The coefficients and symbols used are as follows:

$$C_{DA} = \frac{D}{qA} \qquad C_{DV} = \frac{D}{q(\text{volume})^{2/3}}$$

where

$C_{DA}$  drag coefficient based on maximum cross-sectional area of model

$C_{DV}$  drag coefficient based on  $(\text{volume})^{2/3}$  of the model

$D$  drag of model, pounds

$q$  dynamic pressure, pounds per square foot  $\left(\frac{1}{2}\rho v^2\right)$

$A$  maximum cross-sectional area of model, square feet

and the volume of the model is measured in cubic feet,

**Lift** and pitching-moment coefficients are based on  $(\text{volume})^{2/3}$  of models.

$$C_L = \frac{\text{Lift}}{q(\text{volume})^{2/3}}$$

and

$$C_M = \frac{M_C}{q(\text{volume})^{2/3} l}$$

where

$C_L$  lift coefficient

$C_M$  pitching-moment coefficient

$M_C$  moment about point of intersection of base line and line perpendicular to base line passing through axis of rotation, inch-pounds (See fig. 3.)

$l$  model length, inches

The data are presented as curves of drag coefficient, at

the angle of minimum drag against the Reynolds number  $R$  based on hull length. Drag-coefficient data as well as important dimensions of the models are given in table V. Lift and pitching-moment coefficients are plotted against pitch angle for a velocity of 260 miles per hour.

Varying the height of tail of the streamline models had no effect on the value of the minimum drag coefficient, but an increase in height of the tail increased the angle of minimum drag as would be expected (fig. 46).

Increasing the depth of the plain streamline body by the addition of an 8-inch spacer block decreased the minimum drag coefficient, based on area, by about 5 percent; but, based on  $(\text{volume})^{2/3}$ , the minimum drag coefficient increased about 6.5 percent (fig. 47). The reason for this variation may be readily seen when the figures for the area and  $(\text{volume})^{2/3}$  for spacer with nose 1 and tail 1 are compared with corresponding values for nose 1 and tail 1 without the spacer. (See table y.) The increase in  $(\text{volume})^{2/3}$  with the spacer is not so great as the increase in cross-sectional area; the drag coefficient based on area is therefore smaller than the drag coefficient based on  $(\text{volume})^{2/3}$ .

Increasing the height of bow of the hull models increased the minimum drag coefficient; the value for the high bow was 4 percent greater than the value for the low bow, whereas bow 2 showed only slight increases in the order of 1 or 2 percent. These results indicate that hydrodynamic characteristics will probably be the deciding factor in the choice of bows. An increase in the height of bows shows a corresponding decrease in the angle of minimum drag (fig. 48).

In figure 49 it is shown that increasing the angle of dead rise at the bow had little or no effect on the minimum drag or angle of minimum drag. This result indicates that bows with greater angles of dead rise may be used with no detrimental effects to air drag.

Increasing the height of the stern of the hull models increased the drag coefficient; the minimum drag coefficient, based on area, for bow 1 and stern 4 was about 19 percent greater than the corresponding value for bow 1 and stern 2 and, based on  $(\text{volume})^{2/3}$ , about 17 percent greater

(fig. 50). Bow 1 and stern 3 showed an increase in minimum drag coefficient over that for bow 1 and stern 2, based on area, of 7 percent and, based on (volume)<sup>a/3</sup>, of about 6.5 percent. In view of the fact that the variations in tail height of the warped streamline bodies caused no changes in the magnitude of the drag of these bodies, as previously noted, the increases in drag of the hull models, due to changes in tail height, are apparently ~~due~~ to the larger pointed afterbody sections which accompany the higher tail locations and are not directly due to the changes in tail height. Hartman's tests (reference 8) substantiate this point by showing large drag differences between two hull models, models 36 and 40, which differed mainly in that one hull had a large afterbody, whereas the other one did not.

Increasing the depth of step 75 percent increased the minimum drag coefficient by only 2 percent and had no effect on the angle of minimum drag (fig. 51).

The lift and the pitching-moment data are presented in figures 52 to 54. In the application of these data to the design of flying boats, it must be remembered that these data apply for the hull alone and do not include interference effects of the wing and other parts.

In résumé, increasing the height of the bow, the angle of dead rise at the bow, or the depth of step of the hull models did not produce any great changes in drag. Increasing the height of stern, however, produced relatively large changes in the drag with indications that those changes were mainly due to the effects of the pointed afterbody.

#### CONCLUDING REMARKS

The small effects on the drag coefficient of the variations in the form of bow tested indicate that the method used in deriving the lines results in a satisfactory aerodynamic form of bow over a wide range of height of bow. There is little evidence of significant increases in drag resulting from cross flow over the chines at the bow even in the case of the greatest departure from the basic form. It is inferred from the results that sufficient chine flare to control the bow wave at low speeds would have a negligible adverse effect on the drag; likewise, fading out the chines at the bow would have only a small favorable effect. With the correct form and location of chine, an increase in

dead rise forward by dropping the keel line also has a negligible effect on drag.

The photographs of the bow waves at low speeds indicate that chine flare and increased dead rise at the bow are definitely desirable for cleanness of running even in smooth water. Rounding the chines at any point likely to be wetted in service appears very inadvisable. When all the factors are considered, bow 2B with chine flare is the most suitable for the hull loadings investigated. Various alternatives in form of bow appear to be possible without large increases in drag, provided that close adherence to the streamline body is maintained and the chines are correctly located.

The raising of the streamline body aft has no effect; on the drag but, when the hydrodynamic surfaces are added, there is a large adverse effect. The most suitable compromise among aerodynamic, hydrodynamic, and structural requirements is more difficult to obtain. The tail surfaces must in any case have sufficient clearance to avoid excessive damage from spray. Because, when used with a pointed afterbody, the low tail is aerodynamically and hydrodynamically better except for the decreased clearance, the best compromise might be to use the low tail with a pylon to carry the aerodynamic surfaces.

The increase in the drag of the hulls over that of the streamline body is attributed mainly to a strong disturbance of the streamline flow caused by the afterbody volume external to the basic form. For this reason, it is inferred that small changes in form, such as the addition of chine flare or decrease in the angle of dead rise near the stern post, would have little effect on the air flow over the after portion or on the drag of the hull. On the other hand, these small changes result in a pronounced decrease in water resistance at the hump speed and in only a small adverse effect on the water resistance at high planing speeds; they therefore appear to be over-all improvements in form if structurally feasible.

Because of the small increase in aerodynamic drag caused by increase in depth of step and the masked hydrodynamic instability resulting from too shallow a step, it appears inadvisable to attempt to obtain appreciable reductions in drag by this means, particularly when the take-off speed is high. The effect of small changes in depth of step on water resistance can be neglected. Far-



ther investigations using a free dynamically correct model are required to determine the minimum allowable depth of step for a given hull, and these investigations would have to be correlated with full-size behavior to be of practical value. Before this is done, a minimum depth of step of at least 8 percent of the beam should be used for the hulls of the series.

The angle of afterbody keel has a large effect on the trim and water resistance at the hump speed and it must be fairly low to control properly the trim at this stage of the take-off. Unfortunately, it was not possible to obtain its effect on the aerodynamic drag of the series because of the limited availability of the high-speed tunnel. In the case of model 11-A (NACA T.B. No. 525), an increase in angle of afterbody keel resulted in an increase in drag, presumably because of increased turbulence behind the step. In the case of the NACA 84 series, however, there is the possibility that a higher angle of afterbody keel would decrease the interference with the flow over the streamline body, which would have a favorable effect. A further investigation of this effect is desirable.

The present method of obtaining low-enough hull drag for long-range seaplanes is by reducing the beam and frontal area. This procedure results in high beam loadings and excessive spray, which lead to higher positions of the wings and engines and a high position of the center of gravity. The spray and hydrodynamic stability then become important limitations of the take-off weight and the payload. Consideration should therefore be given to methods of obtaining low drag by aerodynamic refinement while retaining the more moderate beam loadings. The present investigation indicates that the aerodynamic drag coefficient of a planing type of hull need not be more than 25 percent greater than that of the body of revolution from which it is derived. This differential might be reduced by the development of a form of afterbody that has less influence on the streamline flow over the after portion of the basic form than does the conventional pointed type.

Langley Memorial Aeronautical Laboratory,  
National Advisory Committee for Aeronautics,  
Langley Field, Va.

## REFERENCES

1. Truscott, Starr, Parkinson, J. B., Ebert, John W., Jr., and Valentine, E. Floyd: Hydrodynamic and Aerodynamic Tests of Models of Flying-Boat Hulls Designed for Low Aerodynamic Drag. N.A.C.A. Models 74, 74-A, and 75. T.N. No. 668, NACA, 1938.
2. Truscott, Starr: The N.A.C.A. Tank - A High-Speed Towing Basin for Testing Models of Seaplane Floats. Rep. No. 470, NACA, 1933.
3. Truscott, Starr: The Enlarged N.A.C.A. Tank and Some of Its Work. T.M. No. 918, NACA, 1939.
4. Bell, Joe W.: The Effect of Depth of Step on the Water Performance of a Flying-Boat Hull Model - N.A.C.A. Model 11-C. T.N. No. 535, NACA, 1935.
5. Allison, John M.: The Effect of the Angle of Afterbody Keel on the Water Performance of a Flying-Boat Hull Model. T.N. No. 541, NACA, 1935.
6. Boll, Joe W., and Olson, Roland E.: Tank Tests to Determine the Effects of the Chine Flare of a Flying-Boat Hull. T.N. No. 725, NACA, 1939.
7. Draley, Eugene C.: High-Speed Drag Tests of Several Fuselage Shapes in Combination with a Wing, NACA A.C.R., Bug. 1940.
8. Hartman, Edwin P.: The Aerodynamic Drag of Flying-Boat Hull Models as Measured in the N.A.C.A. 20-Foot Wind Tunnel - I. T.N. No. 525, NACA, 1935.

## BIBLIOGRAPHY

- Coombes, L. P., and Clark, X. W.: The Air Drag of Hulls. Aircraft Engineering, vol. IX, no. 106, Dec. 1937, pp. 315-321, 328.
- Cowley, W. L., and Warden, R.: Tests of Models of High Speed Seaplanes for the Schneider Trophy Contest of 1927. Section I, R. & M. No. 1296, British A.R.C., 1927.
- Cowley, W. L., and Warden, R.: Tests of Models of High Speed Seaplanes for the Schneider Trophy Contest of 1927. Section II. Tests on the Gloster IV Models. R. & M. No. 1297, British A.R.C., 1928.
- Cowley, W. L., and Warden, R.: Tests on Models of High Speed Seaplanes for the Schneider Trophy Contest of 1927. Section III. Tests on the Crusader Models. R. & M. No. 1298, British A.R.C., 1928.
- Cowley, W. L., and Warden, R.: Tests on Quarter Scale Models of High Speed Seaplanes for the Schneider Trophy Contest of 1927. Section IV. Comparison with Full Scale and Conclusions. R. & M. No. 1299, British A.R.C., 1929.
- Dawson, John R., and Hartman, Edwin P.: Hydrodynamic and Aerodynamic Tests of Four Models of Outboard Floats (N.A.C.A. Models 51-A, 51-B, 51-C, and 51-D). T.N. No. 678, NACA, 1938.
- Diehl, Walter S.: Engineering Aerodynamics. The Ronald Press Co., rev. ed., 1936, pp. 290-297.
- Diehl, Walter S.: Tests on Airplane Fuselages, Floats and Hulls. Rep, Bo. 236, NACA, 1926.
- Göthert, B., and Ribnitz, W.: Des Luftwiderstand von Schwimmern und Flugbooten. Luftwissen, Bd. 6, Nr. 3, March 1939, pp. 101-107.
- Jones, R., and Pell, G. N.: The Resistance of Flying Boat Hulls. R. & M. Bo. 461, British R.B.C., 1918.

L-277  
Parkinson, J. B. , and House, R. O.: Hydrodynamic and Aerodynamic Tests of Models of Floats for Single-Float Seaplanes. N.A.C.A. Models 41-D, 41-E, 61-A, 73, and 73-A. T.N. No 656, NACA, 1938.

Parkinson, John B., Olson, Roland E., and House, Rufus O.: Hydrodynamic and Aerodynamic Tests of a Family of Models of Seaplane Floats with Varying Angles of Dead Rise. N.A.C.A. Models 57-A, 57-B, and 57-C, T.N. No. 716, NACA, 1939.



TABLE I - NACA MODEL 84 SERIES. OFFSETS FOR BOWS 1, 1A, 2, 2B, 3, AND 3B

NACA

[All values in in.]

Station	Distance from F.P.	D			R		a		b	c		d		e		r		r <sub>1</sub>
		Bow 1, 1A	Bow 2, 2B	Bow 3, 3B			Bow 1, 1A, 2, 3	Bow 2B, 3B		Bows 1, 2, 3	Bows 2B, 3B	Bows 1, 1A, 2, 3	Bows 2B, 3B			Bows 1, 2, 3	Bows 2B, 3B	
F.P.	0	0	3.37	6.74	0	1.24	0	0	0	0	0	0	0	0	0	0.73	0.29	1.24
1	.60	0	3.16	6.32	0	1.04	1.33	2.68	.97	.92	.82	.88	.54	.99	.99	1.78	.77	1.63
2	2.85	0	2.46	4.92	3.04	3.16	3.25	5.56	2.36	2.26	2.05	2.14	1.56	2.43	2.43	2.44	1.14	1.53
3	5.10	0	1.90	3.80	4.16	4.16	4.45	6.77	3.38	3.08	2.87	2.98	2.35	3.33	3.33	3.32	1.85	1.03
4	9.60	0	1.14	2.29	5.67	5.67	6.04	7.88	4.38	4.18	4.00	4.65	3.51	4.54	4.54	4.22	2.62	.51
5	14.10	0	.67	1.33	6.63	6.63	7.07	8.25	5.13	4.90	4.77	5.07	4.35	5.30	5.30	4.45	3.34	.19
6	18.60	0	.37	.74	7.22	7.22	7.70	8.36	5.59	5.34	5.26	5.33	4.90	5.78	5.78	4.57	3.96	.04
7	23.10	0	.17	.35	7.61	7.61	8.10	8.42	5.89	5.62	5.60	5.47	5.26	6.09	6.09	4.57	4.34	.00
8	27.60	0	.07	.15	7.81	7.81	8.32	8.45	6.05	5.77	5.77	5.56	5.45	6.25	6.25	4.64	4.57	.00
9	32.10	0	.01	.03	7.93	7.93	8.47	8.49	6.14	5.86	5.86	5.66	5.56	6.34	6.34	4.66	4.66	.00
10	36.60	0	.00	.00	7.96	7.96	8.58	8.58	6.25	5.97	5.97	5.66	5.66	6.37	6.37	4.66	4.66	.00

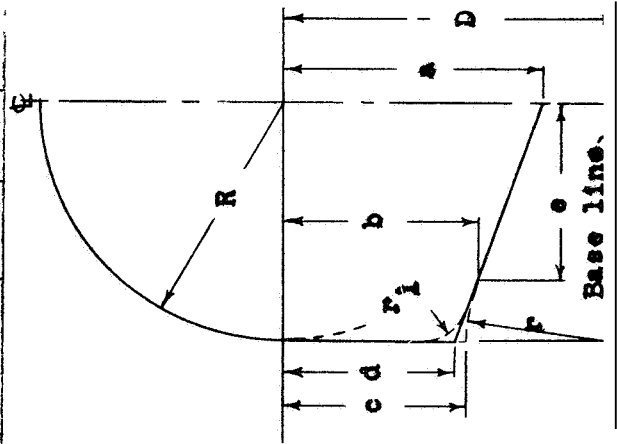
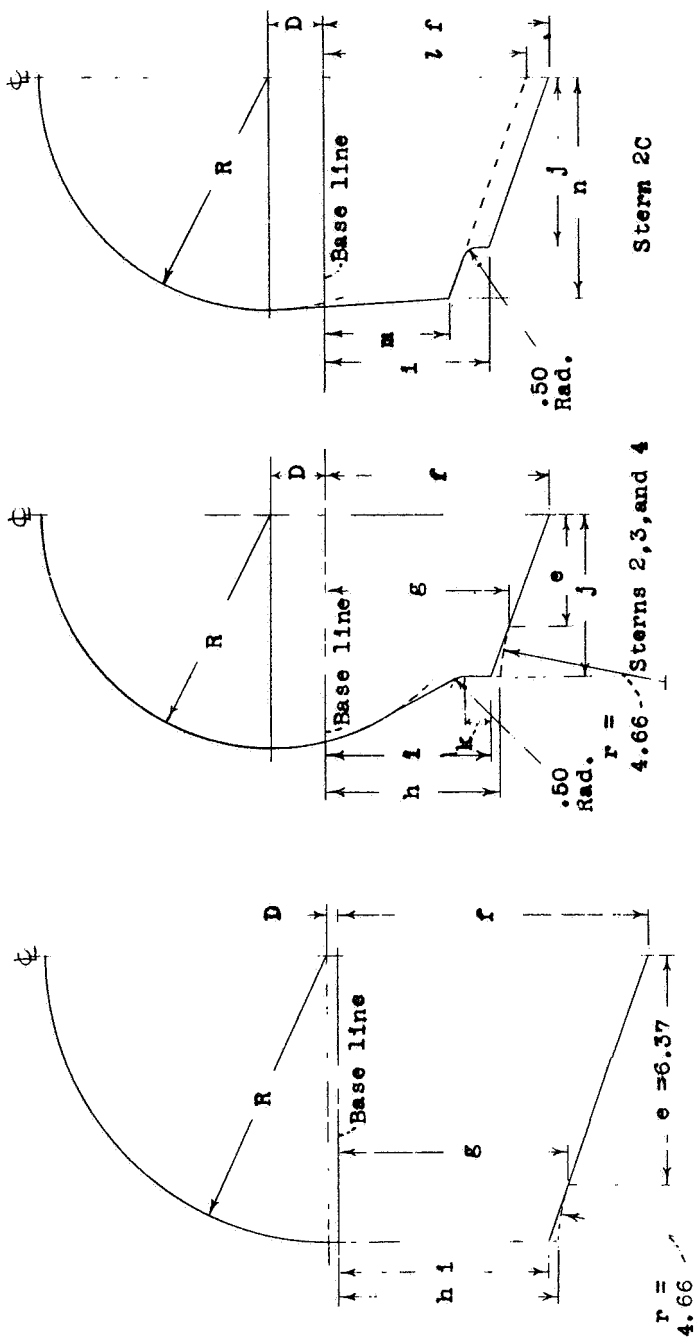


TABLE II. - NACA MODEL 84 S IES. OFFSETS FOR STERNS 2, 2C, 3, AND 4

[All values in in.]

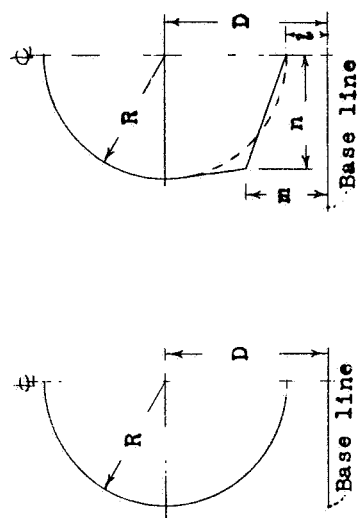
Station	Distance from P.P.	D			R	e	f	g	h	i	j	k				Stern 2C only	
		Stern 2, 2C	Stern 3	Stern 4								Stern 2	Stern 3	Stern 4	1		n
10	36.60	0.00	0.00	0.00	7.96	6.37	8.58	6.25	5.97	5.66							
11	41.10	.01	.02	.03	7.94	6.37	8.68	6.35	6.07	5.76							
12	45.60	.04	.09	.13	7.87	6.37	8.78	6.45	6.17	5.89							
13F	50.10	.10	.21	.31	7.75	6.37	8.88	6.55	6.27	6.04							
13A	50.10	.10	.21	.31	7.75	6.37	8.88	6.55	6.27	6.04							
14	54.60	.19	.38	.57	7.58	6.14	8.05	5.80	5.52	5.29							
15	59.10	.29	.59	.88	7.37	5.76	7.62	5.51	5.23	5.00							
16	63.60	.42	.85	1.27	7.11	5.15	7.18	5.30	5.02	4.79							
17	68.10	.58	1.16	1.74	6.80	4.27	6.75	5.19	4.91	4.68							
18	72.60	.75	1.51	2.26	6.45	3.11	6.32	5.19	4.91	4.68							
19	77.10	.95	1.91	2.86	6.05	1.58	5.88	5.15	5.03	4.80							
20	81.60	1.17	2.35	3.37	5.61	.00	5.45	5.15	5.17	5.08							
21	83.33	1.42	2.84	3.79	5.12		5.28		5.28								
22	86.10	1.68	3.37	4.26	4.59												
23	90.60	1.97	3.95	5.02	4.01												
24	95.10	2.26	4.57	5.83	3.39												
25	99.60	2.61	5.23	6.84	2.73												
26	104.10	2.96	5.93	7.89	2.03												
27	108.60	3.32	6.64	8.96	1.23												
28	112.80	3.73	7.37	9.90	.87												
29	114.00	3.43	6.87	10.47	.51												
30	114.60	3.52	6.98	10.56	.00												
A.P.	114.85		7.04	10.56													

L-277



Stations 10 to 13

Stations 14 to 21



Sterns 2, 3, and 4

Stern 2C

Stations 22 to 30



TABLE III. - ADDITIONAL OFFSETS<sup>1</sup> FOR VARIATIONS IN AFTERBODY BOTTOM OF STERN 4

[Keel and buttock lines are straight]

Station	Distance from P.P.	J.D			J.E			J.F			J.G			J.H		
		f	i	k	f	i	k	f	i	k	f	i	k	f	i	k
Depth of step		0.95			0.70			0.40			0.40			w		
Angle of keel		5.50°			5.50°			7.25°			9.00°			7.25°		
13A	50.10	8.33	5.49		8.18	5.34		8.48	5.64		8.48	5.64		8.48	5.66	
14	54.60	7.90	5.14	0.23	7.75	4.99	0.08	7.91	5.15	0.29	7.77	5.01	0.10	7.91	5.57	0.71
15	59.10	7.47	4.85	.44	7.32	4.70	.29	7.34	4.72	.31	7.06	4.44	.03	7.34	5.48	1.07
16	63.60	7.03	4.64	.70	6.88	4.49	.55	6.76	4.37	.43	6.34	3.95	.01	6.76	5.38	1.44
17	68.10	6.60	4.53	1.01	6.45	4.38	.86	6.19	4.12	.60	5.63	3.56	.04	6.19	5.27	1.75
18	72.60	6.17	4.53	1.36	6.02	4.38	1.21	5.62	3.98	.81	4.92	3.28	.11	5.62	5.11	1.94
19	77.10	5.73	4.65	1.76	5.58	4.50	1.61	5.04	3.96	1.07	4.20	3.12	.23	5.04	4.85	1.96
20	81.60	5.30	4.93	2.45	5.15	4.78	2.30	4.47	4.10	1.62	3.49	3.12	.64	4.47	4.45	1.97
21	83.33	5.13	5.13	3.00	4.98	4.98	2.85	4.25	4.25	2.12	3.22	3.22	1.09	4.25	4.25	2.12

<sup>1</sup>For remaining offsets and typical section, see table II.

TABLE IV. - NACA MODEL 84 SERIES

Model	Bow	Stern	Description
84-0	Nose 1	Tail 1	Basic body of revolution
84-1	Nose 1	Tail 1	Same with depth increased
84-A	1	3	Low bow, intermediate stern
84-AF	1	3	Same with chine flare
84-B	2	3	Intermediate bow, intermediate stern
84-BF	2	3	Same with chine flare
84-C	3	3	High bow, intermediate stern
84-CF	3	3	Same with chine flare
84-D	1	2	Low bow, low stern
84-DF	1	2	Same with chine flare
84-E	1	4	Low bow, high stern
84-EF	1	4	Same with chine flare
84-EF-1	1	4	{ Same with chine flare on forebody only, block 4
84-EF-2	1	4	{ Same as 84-EF-1 except depth of step increased, blocks 4D and 4E, respectively
84-EF-4	1	4	{ Same as 84-EF-1 except angle of afterbody keel increased, blocks 4F and 4G, respectively
84-EF-5	1	4	{ Same as 84-EF-4, block 4F except angle of dead rise decreased on afterbody, block 4H
84-F	2B	3	{ Same as 84-B except angle of dead rise increased at bow
84-FF	2B	3	{ Same with chine flare
84-G	3B	3	{ Same as 84-C except angle of dead rise increased at bow
84-GF	3B	3	{ Same with chine flare
84-6	1	2c	{ Same as 84-D except third planing surface added on tail
84-J	1 A	3	{ Same as 84-A except chines rounded at bow

L-277

TABLE V. - BASIC DIMENSIONS AND MINIMUM AERODYNAMIC DRAG  
CHARACTERISTICS OF STREAMLINE AND HULL MODELS

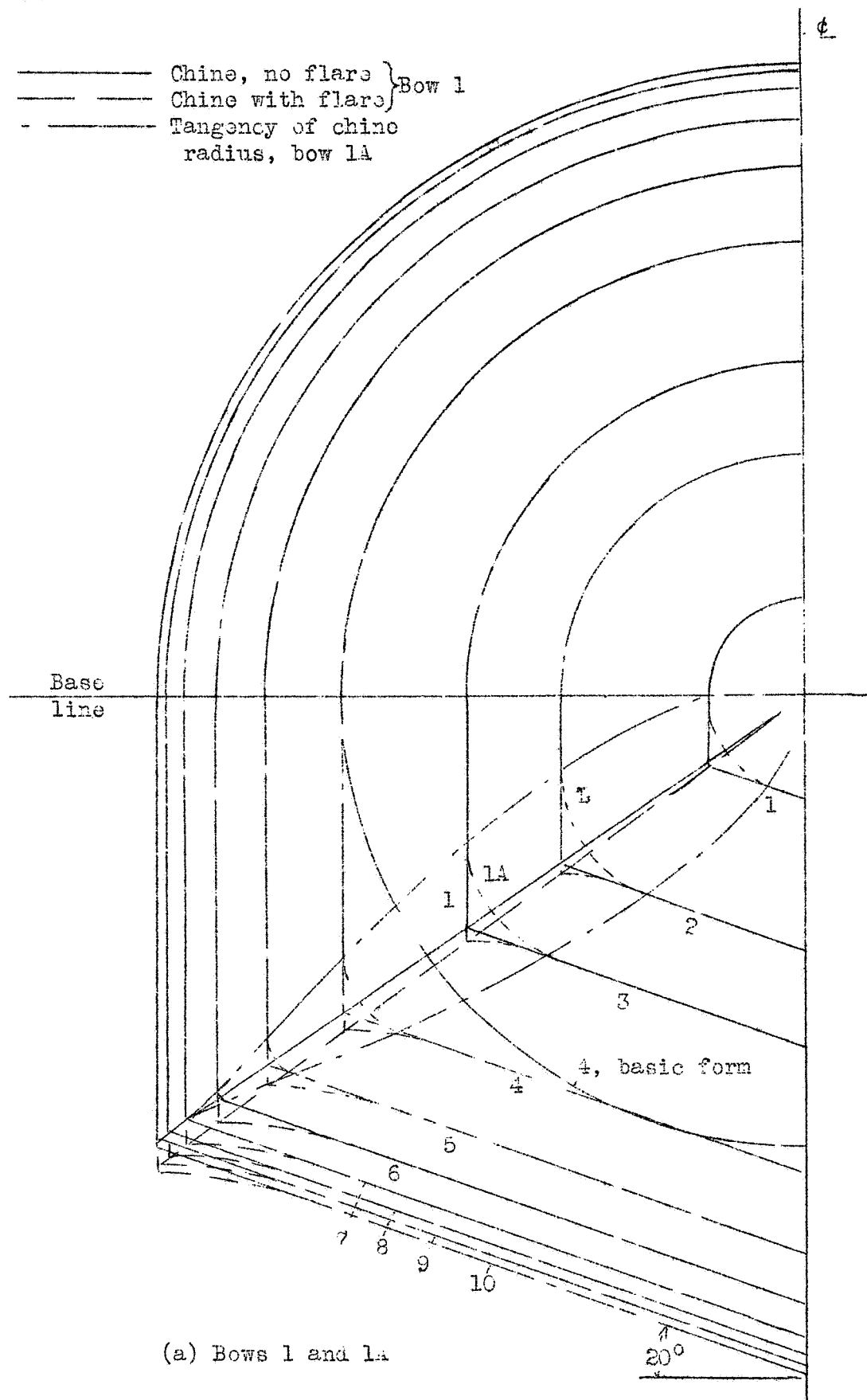
Model		Dimensions			Coefficients		Pitch angle (deg)
Bow	Stern	Area A (sq ft)	Volume (cu ft)	(Volume) <sup>2/3</sup> (ft <sup>2</sup> )	Min. C <sub>DA</sub> (1)	Min. C <sub>Dv</sub> (2)	
Streamline bodies							
1	1	1.382	8.042	4.0139	0.0808	0.0278	0
1	3	1.382	8.042	4.0139	.0808	.0278	4
1	1 Plus 8" spacer	2.262	14.245	5.8764	.0767	.0296	0
Hull bodies							
1	2	1.468	8.564	4.1859	0.0909	0.0319	0.6
1	3	1.468	8.663	4.2180	.0973	.0340	2
2B	3	1.468	8.747	4.2453	.0980	.0340	0
2	3	1.468	8.663	4.2180	.0980	.0341	0
3	3	1.468	8.663	4.2180	.1010	.0353	0
1	4	1.468	8.765	4.2511	.1084	.0373	3.1
1	4E	1.468	8.704	4.2317	.1106	.0382	3.1

$${}^1C_{DA} = \frac{D}{qA}$$

$${}^2C_{DV} = \frac{D}{q(\text{volume})^{2/3}}$$

Fig. 1. Lines of NACA Model 84 Series, showing variations in form investigated.

————— Chine, no flare } Bow 1  
 ————— Chine with flare }  
 - - - - - Tangency of chine  
 radius, bow 1A



(a) Bows 1 and 1A

L-277

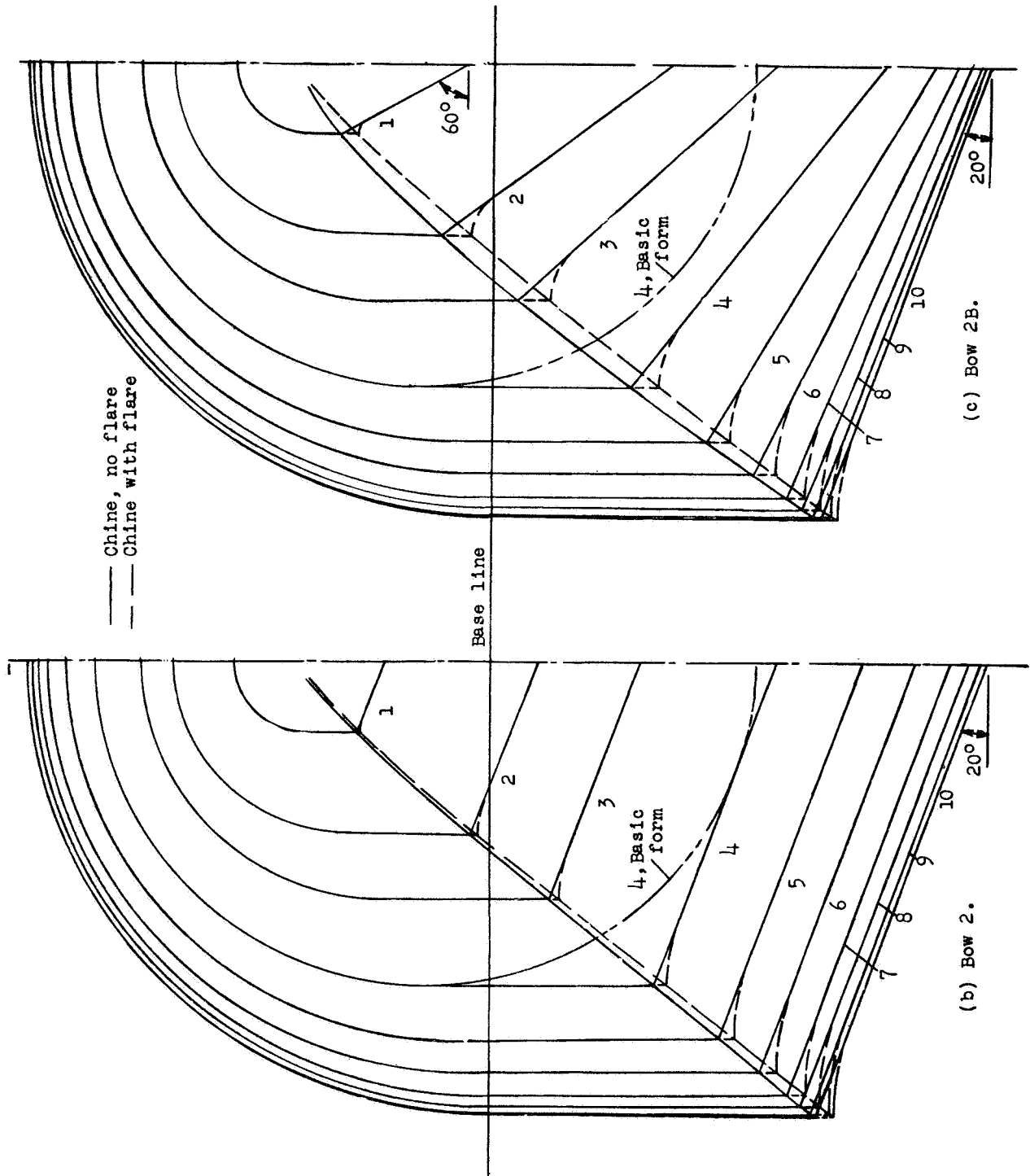


Figure 2.- Continued.

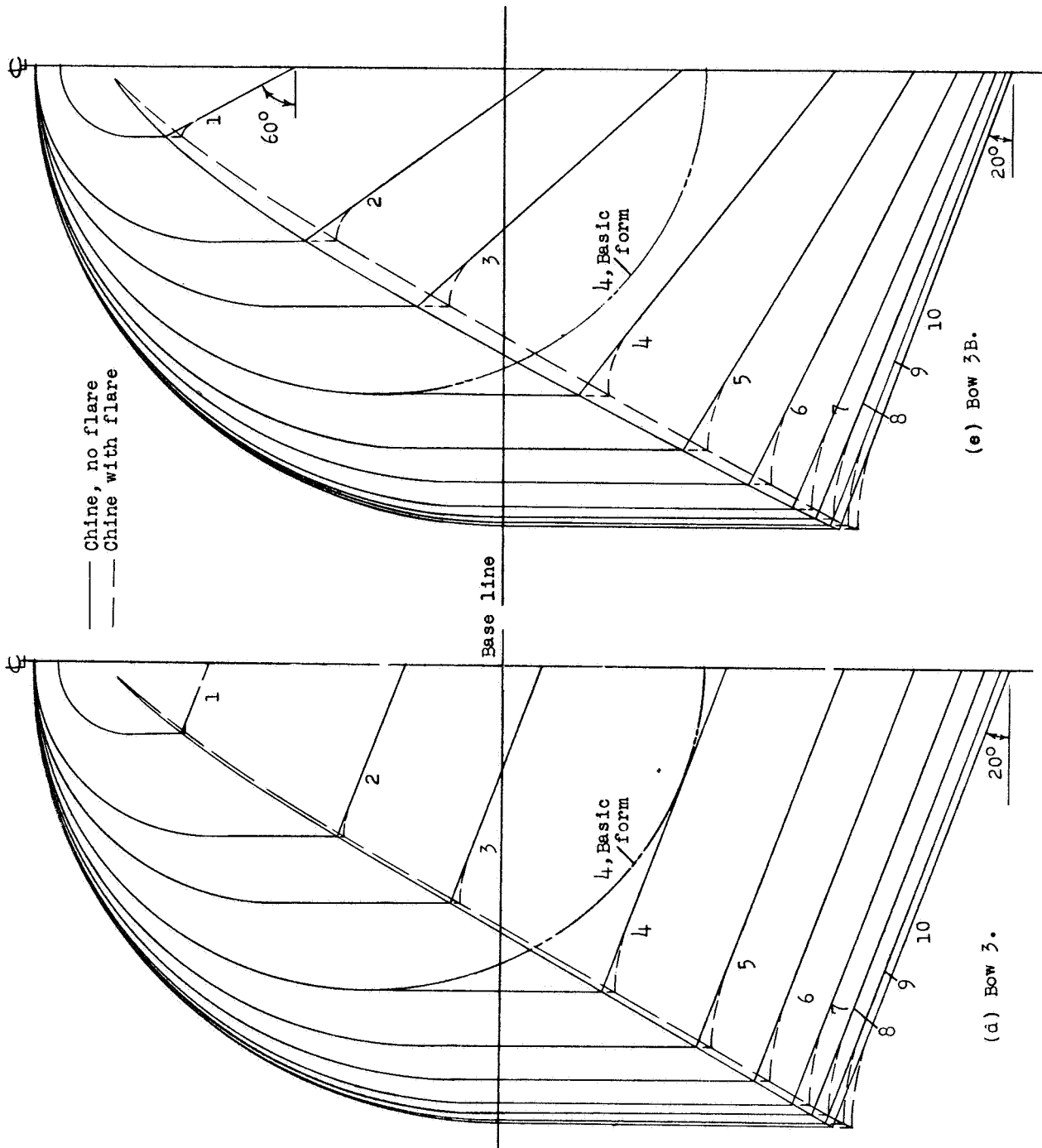
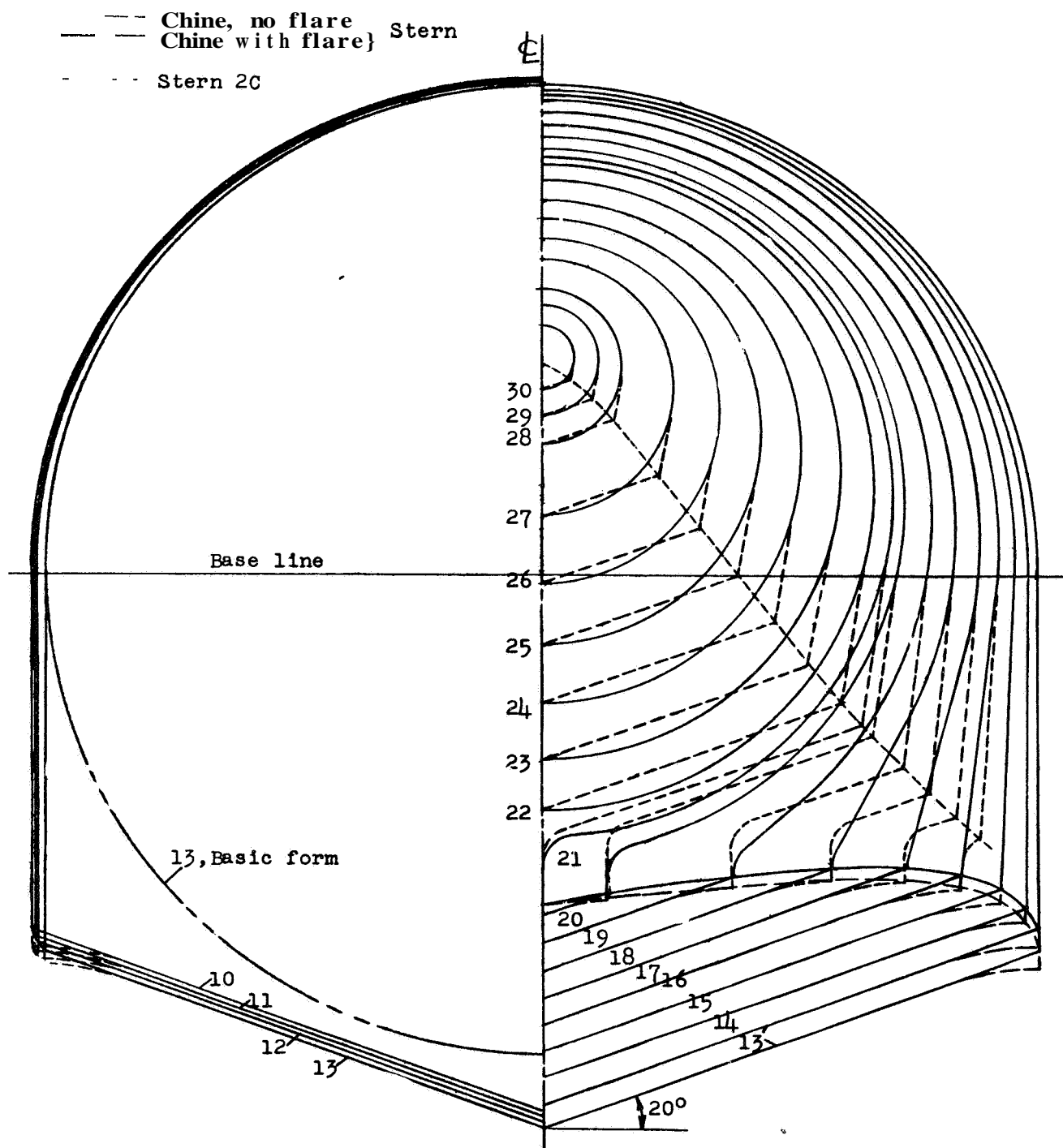


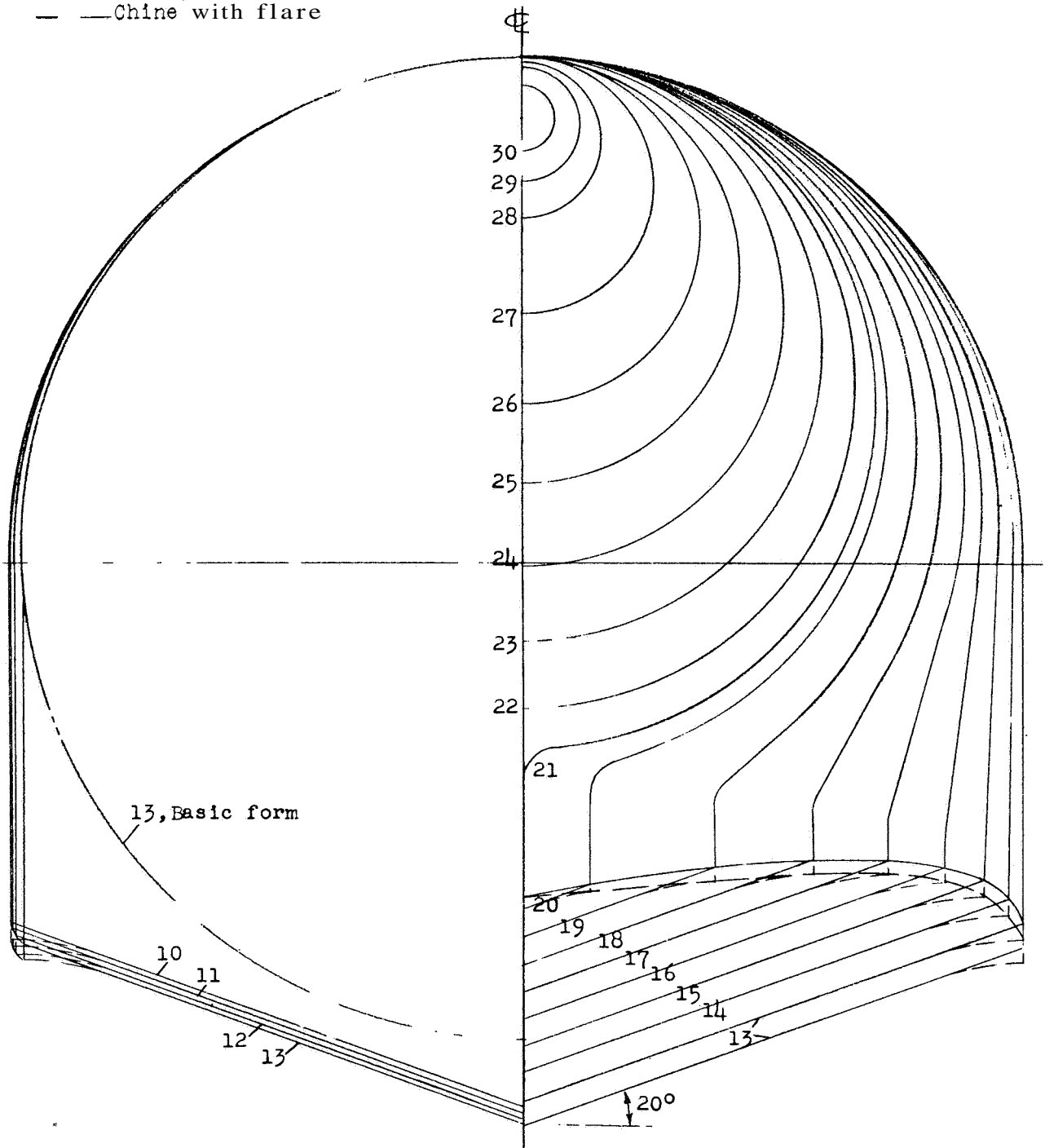
Figure 2 - Continued.



(f) Sterns 2 and 2C.  
Figure 2.- Continued.



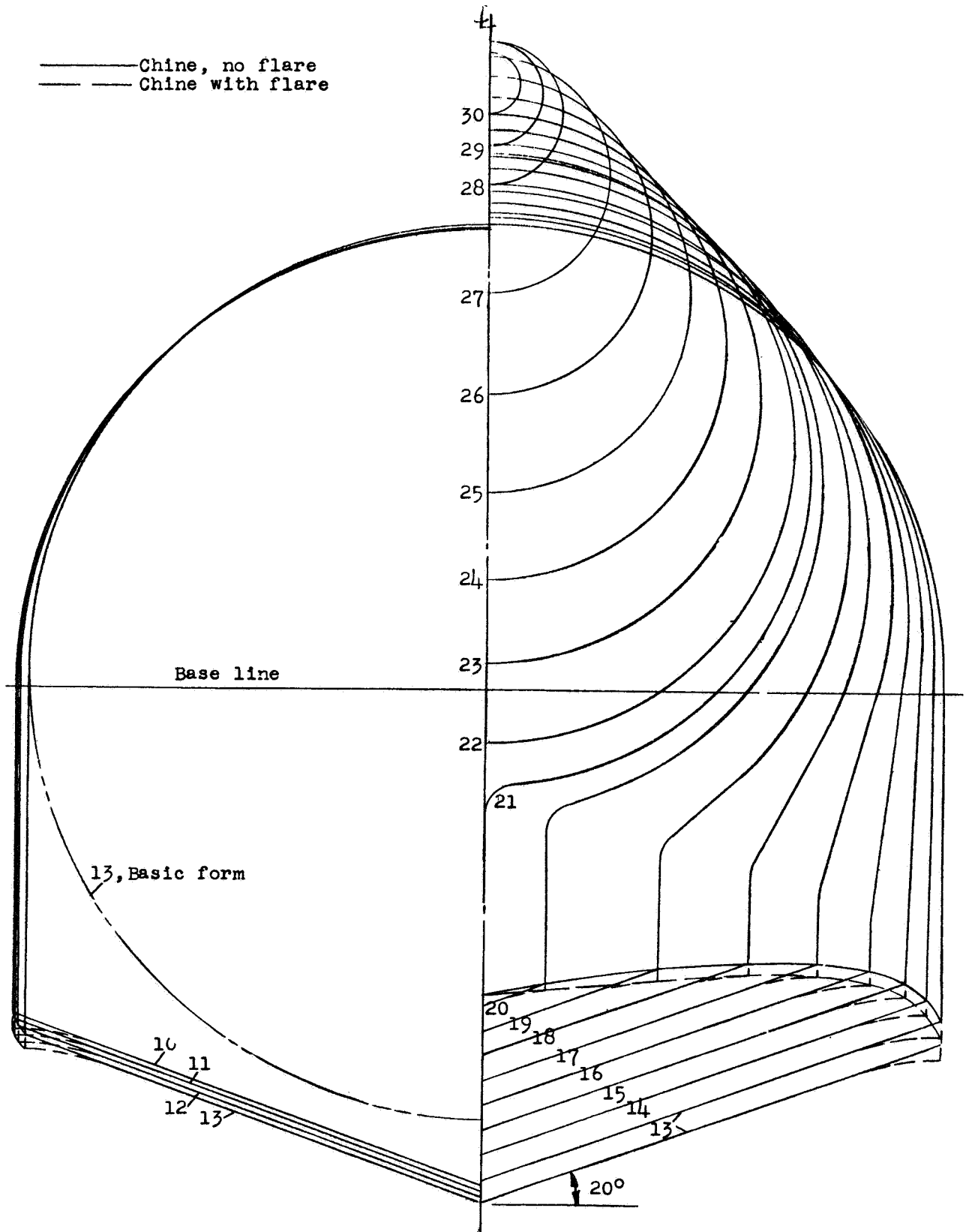
— Chine, no flare  
 - - - Chine with flare



(g) Stern 3.

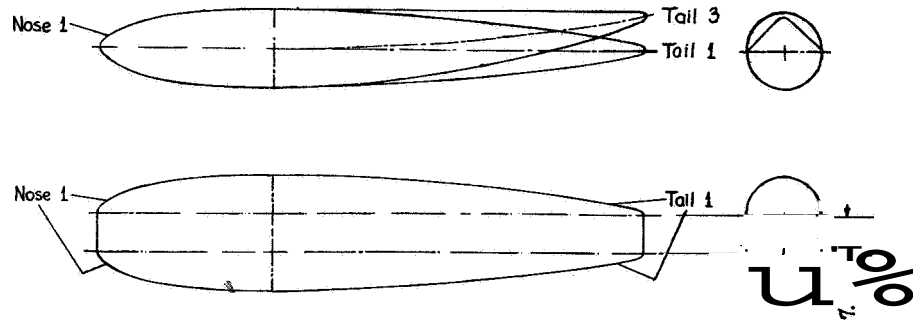
Figure 2.- Continued.

L-277



(h) Stern 4.

Figure 2.- Concluded.



Basic Streamline Shapes

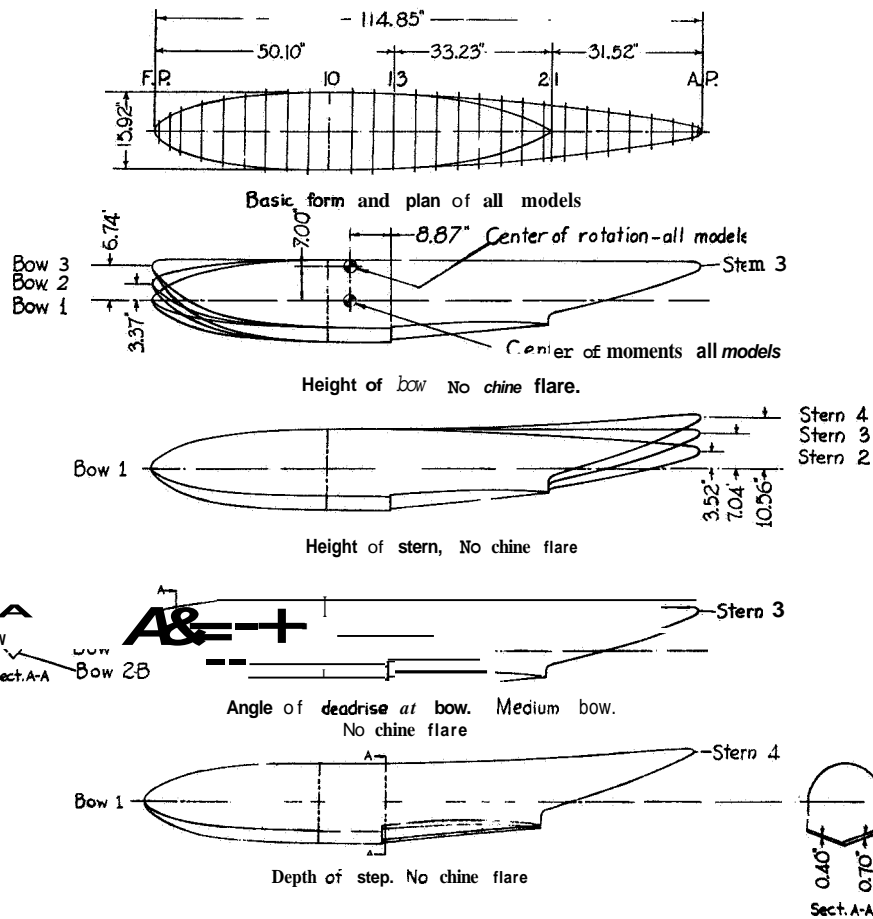


Fig 3.- Lines of NACA Model 84 Series, showing form tested in wind tunnel.

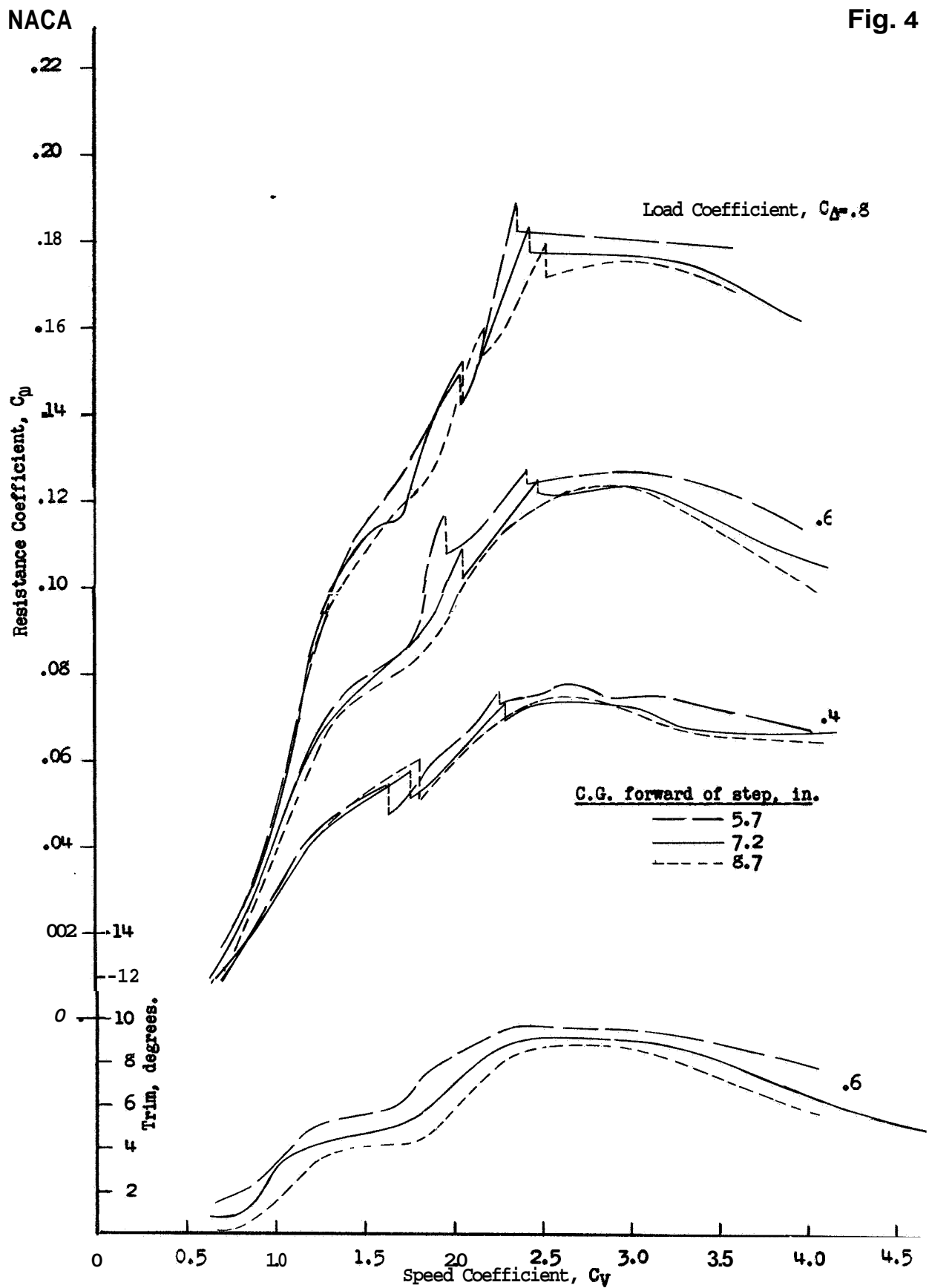


Figure 4 .-Effect of longitudinal position of the center-of-gravity. Model 84EF.

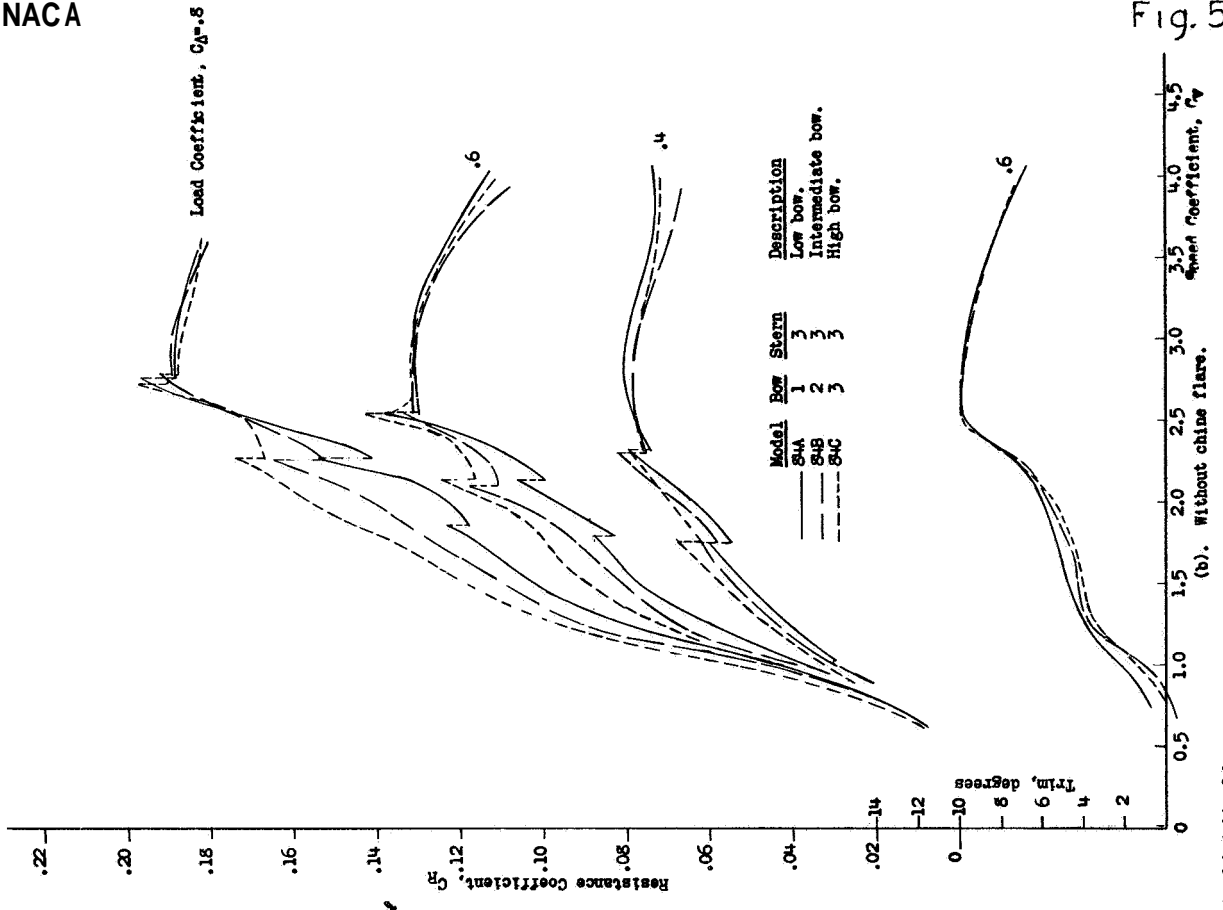
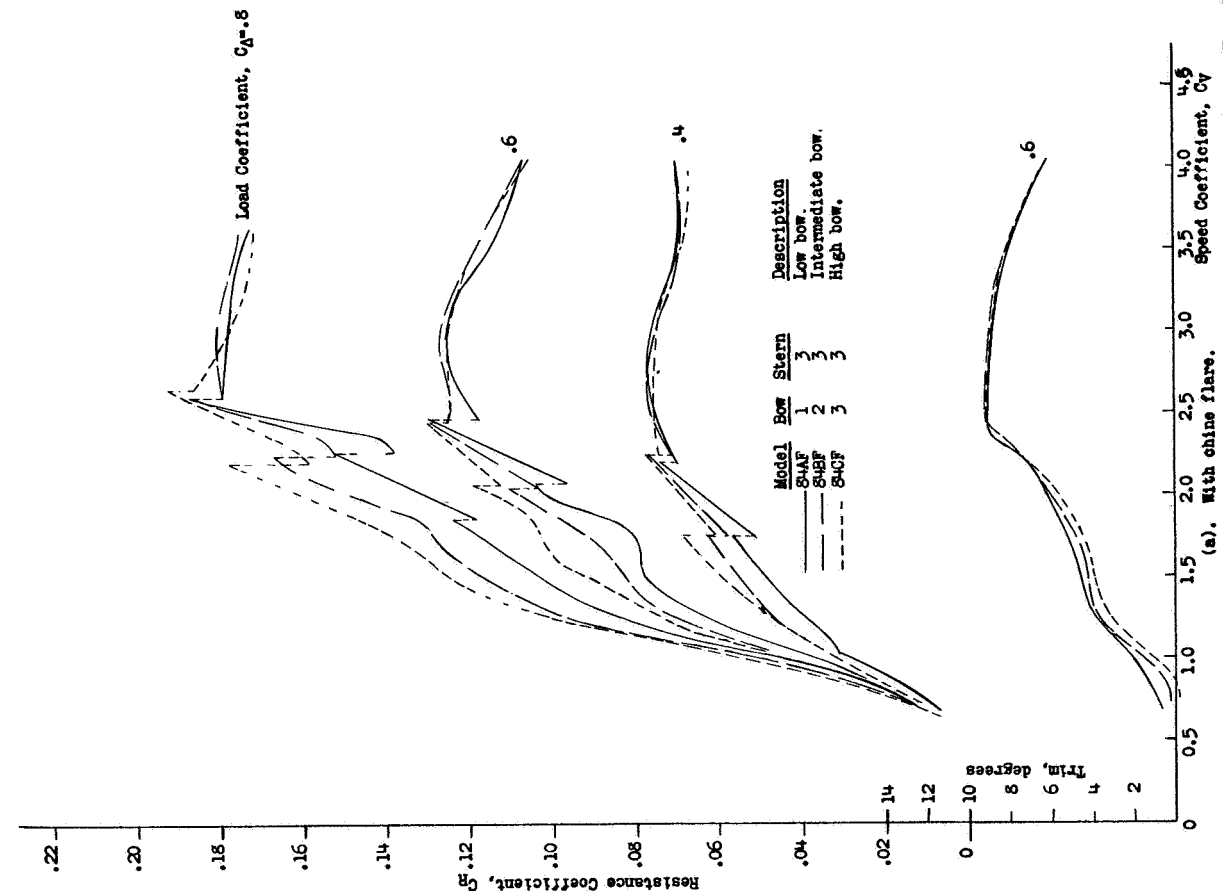


Figure 5. Effect of height of bow.

L-277

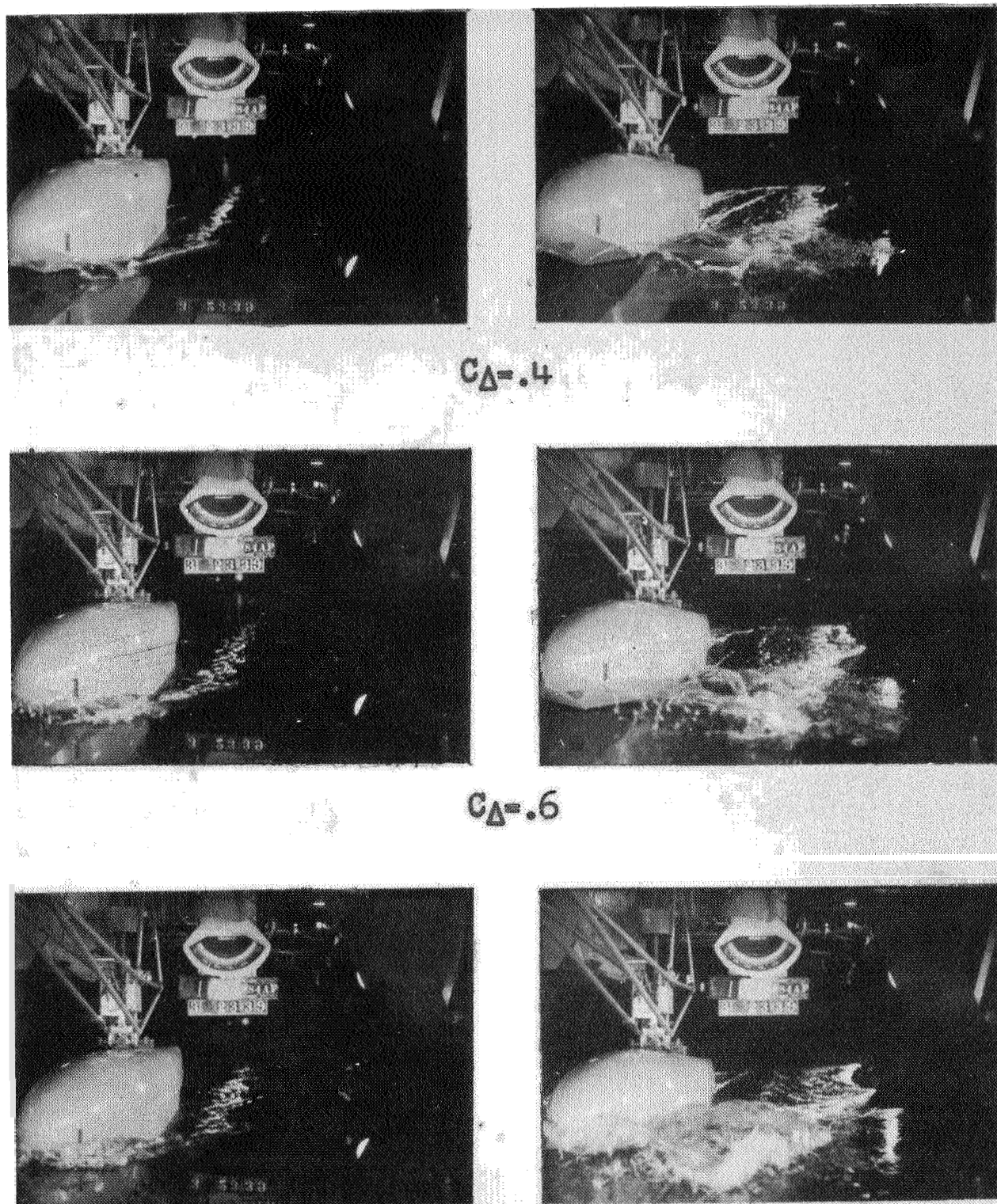
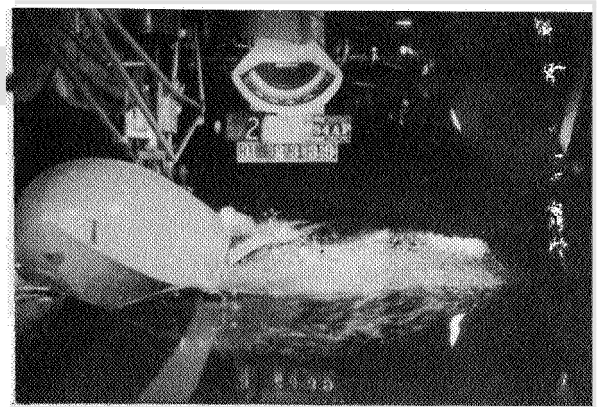
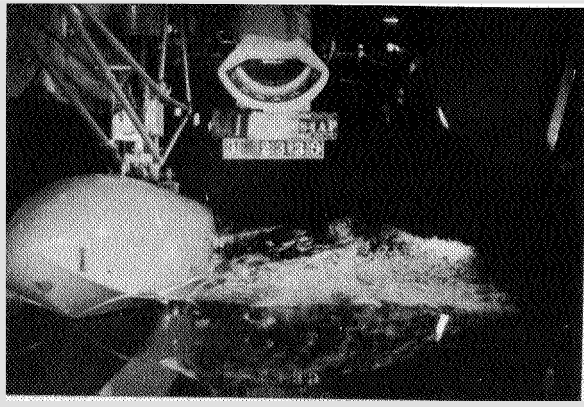
 $C_D = .75$  $C_D = .8$  $C_D = 1.18$ 

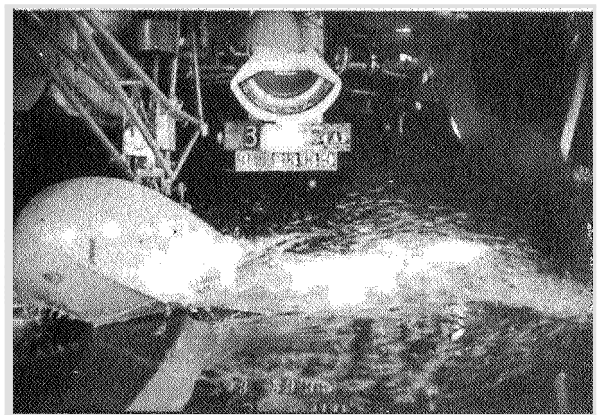
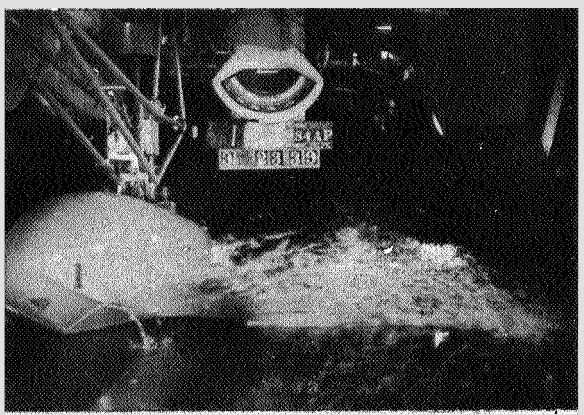
Figure 6 (a). - Model 84AF. Bow 1, Stern 3.  
With chine flare.

NACA  
10475

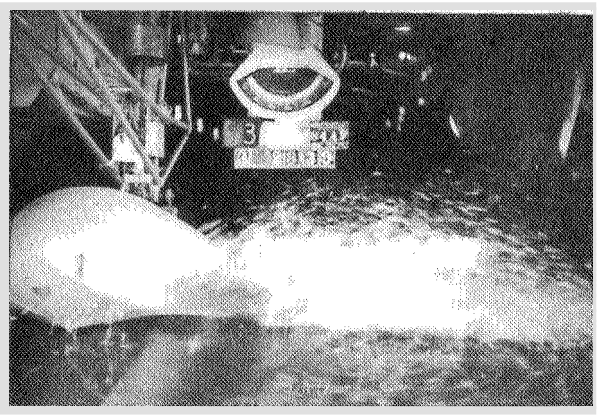
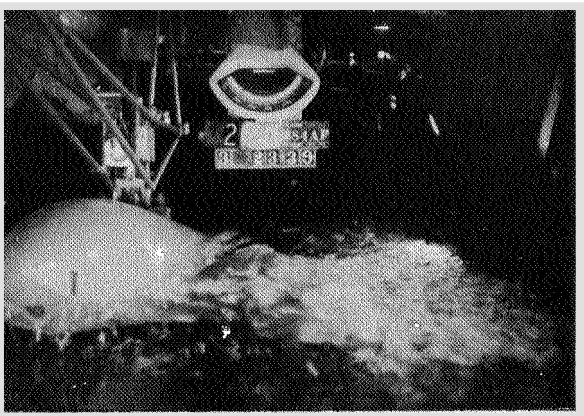
L-277



$C_D = .4$



$C_D = .6$



$C_V = 1.75$

$C_D = .8$

$C_V = 2.14$

Figure 6 (b). Model 84AF

277  
109



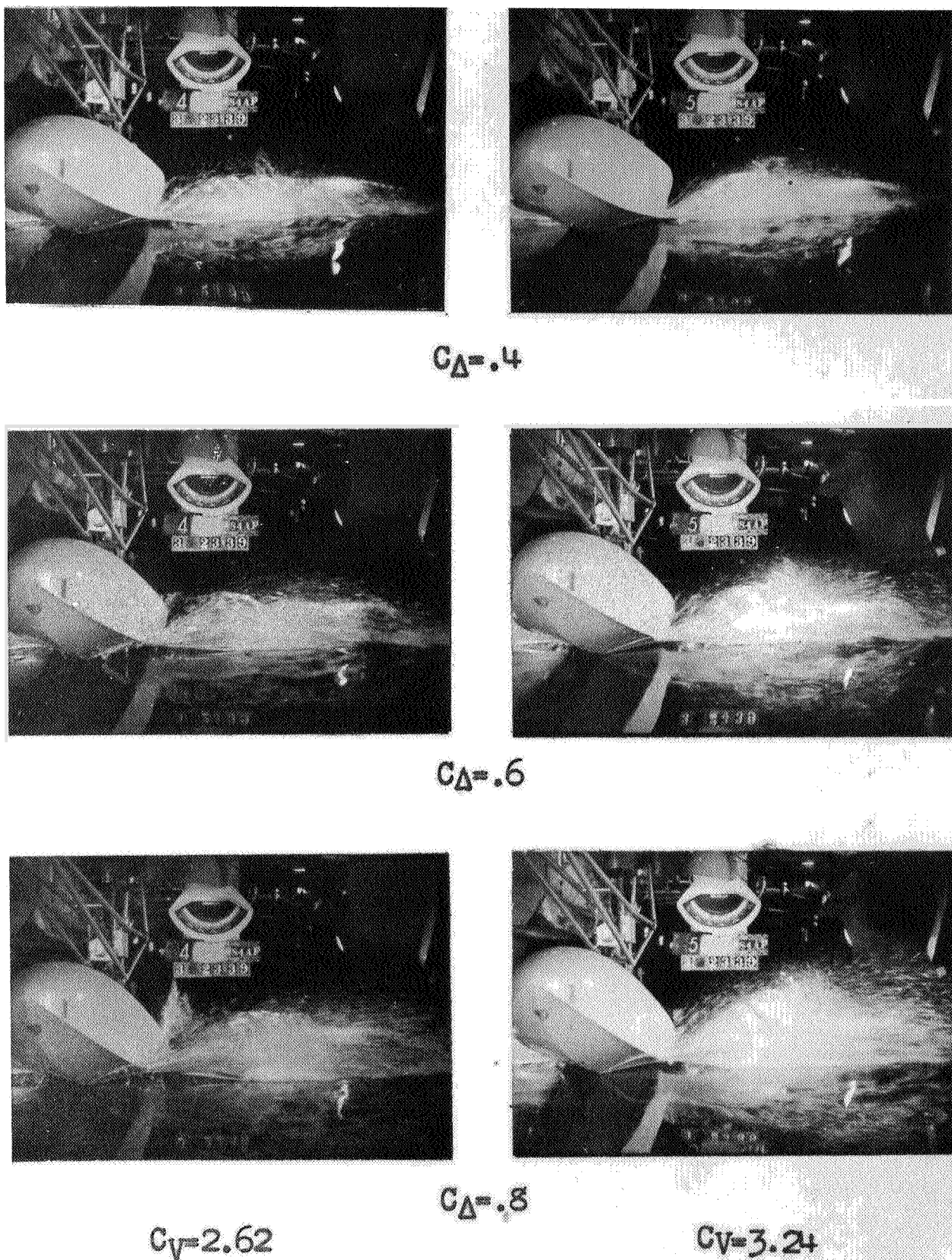
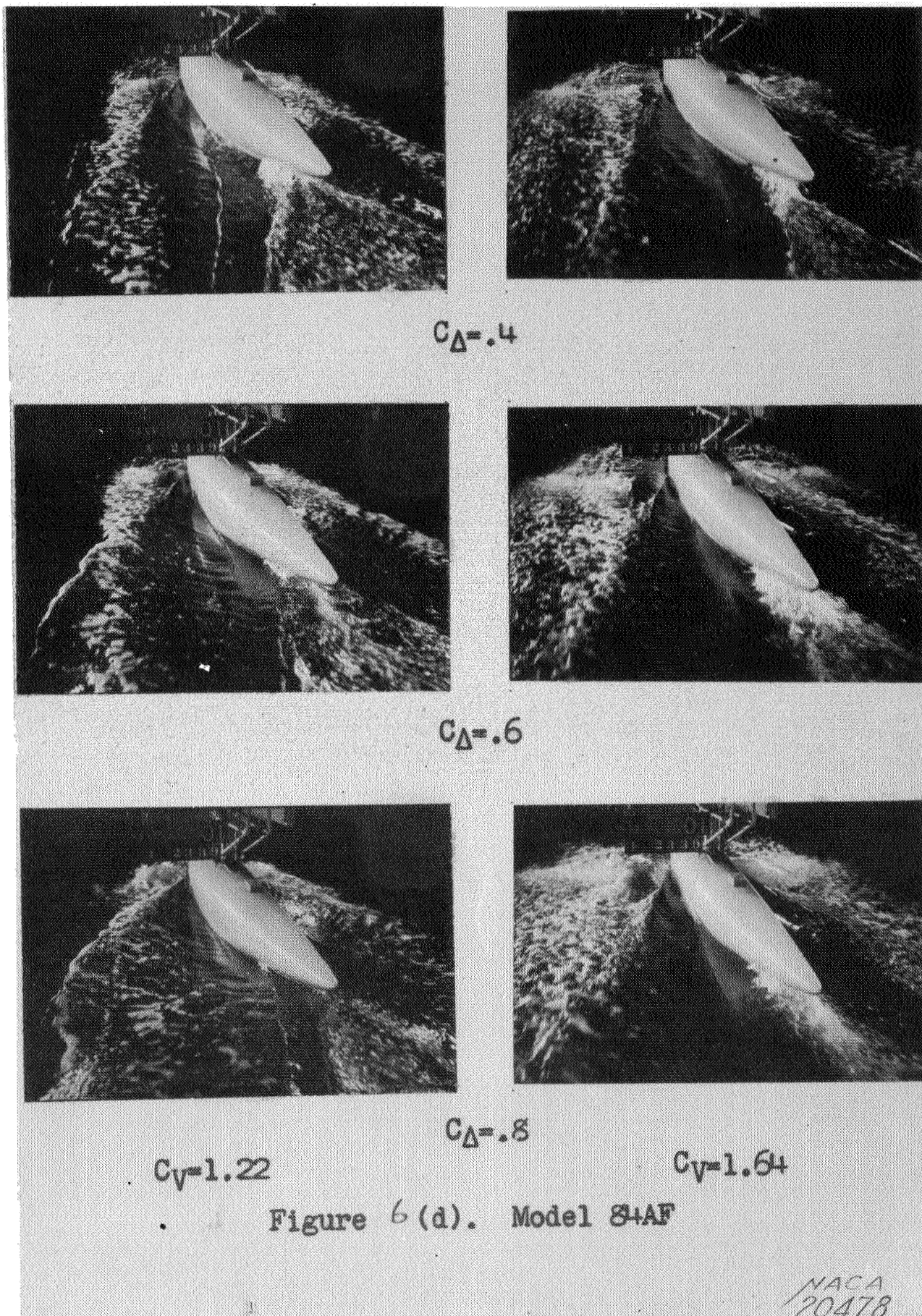
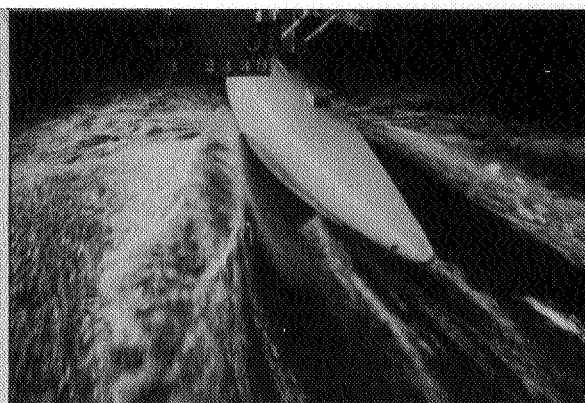
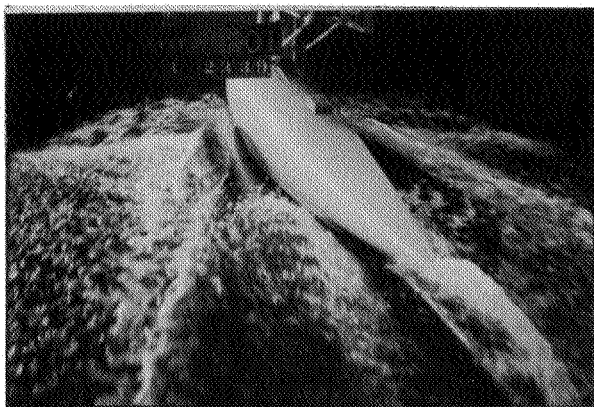


Figure 6 (c). Model 84AF

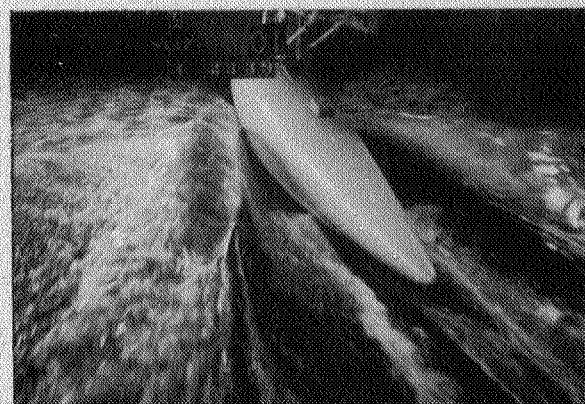
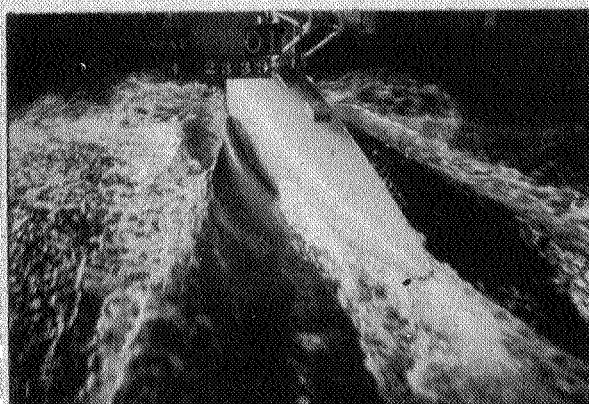




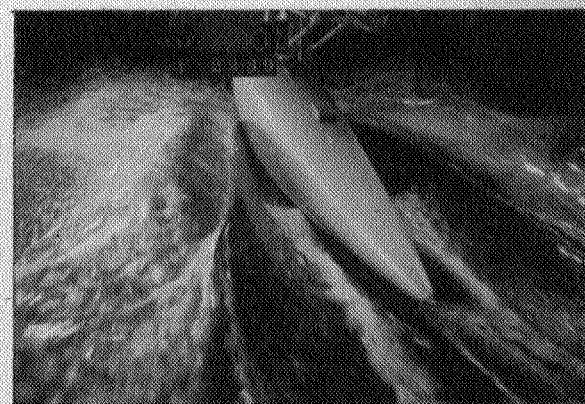
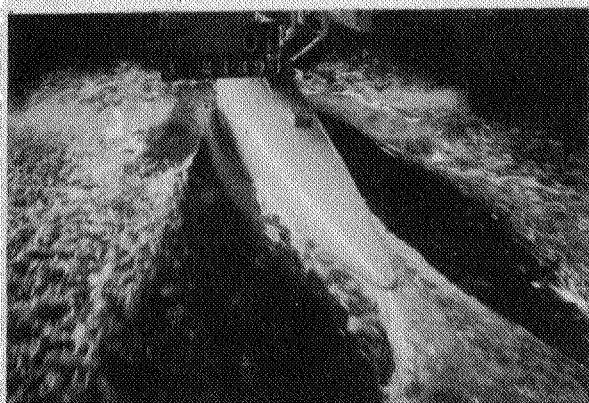
L-277



$C_D = .4$



$C_D = .6$



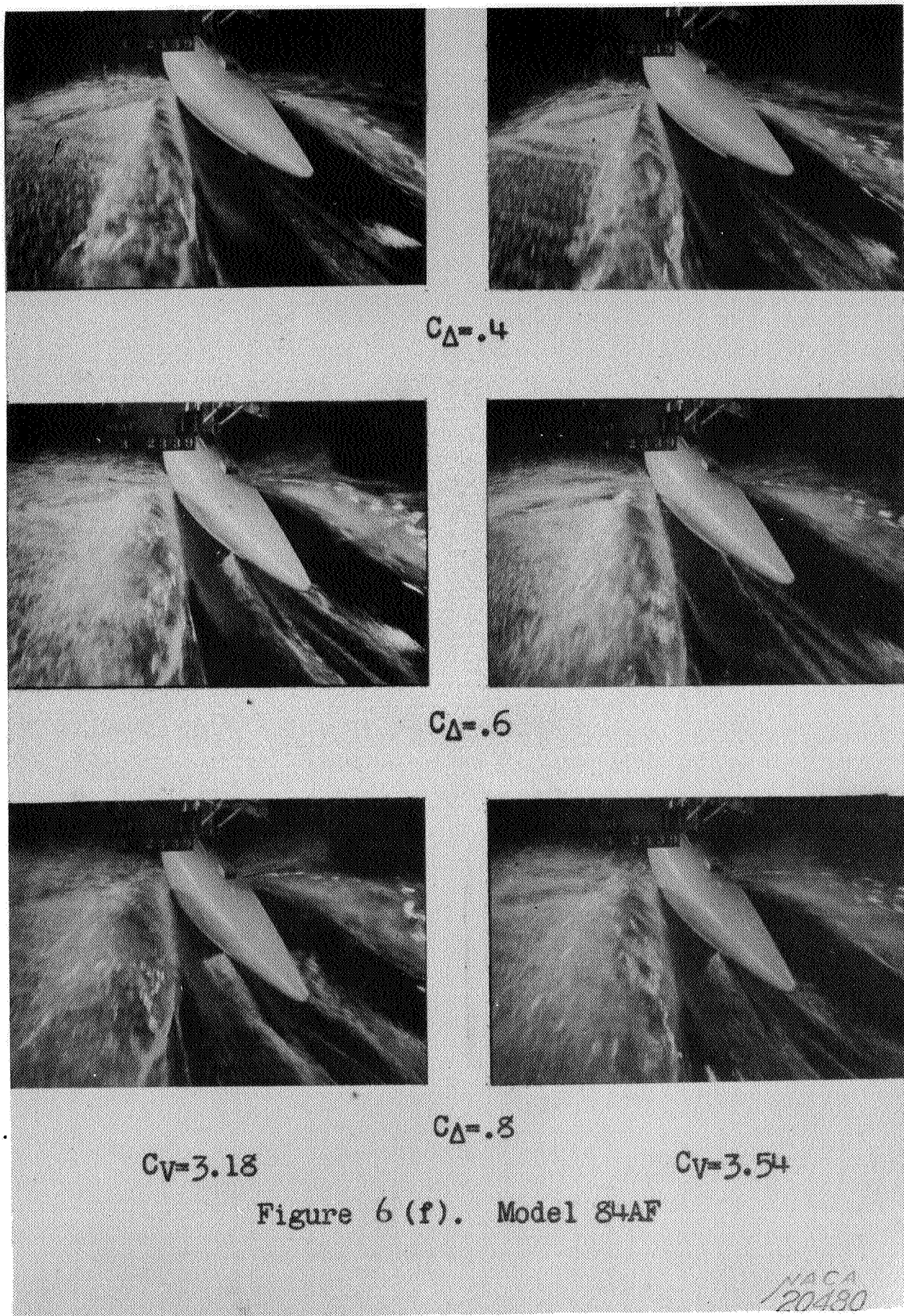
$C_V = 2.14$

$C_D = .8$

$C_V = 2.64$

Figure 6 (e). Model 84AF





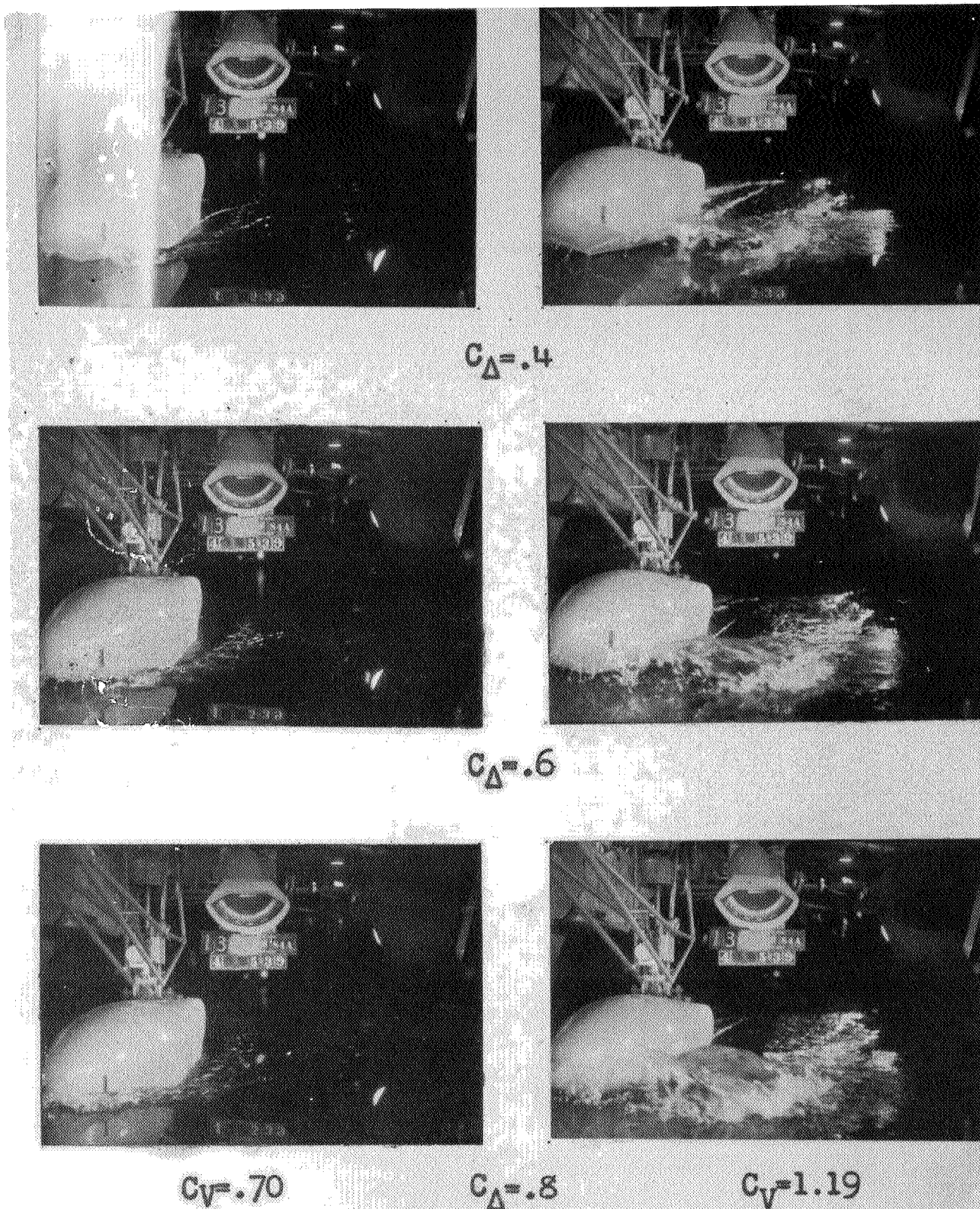


Figure 7 (a). Model 84A, Bow 1, Stern 3.  
Without chine flare.



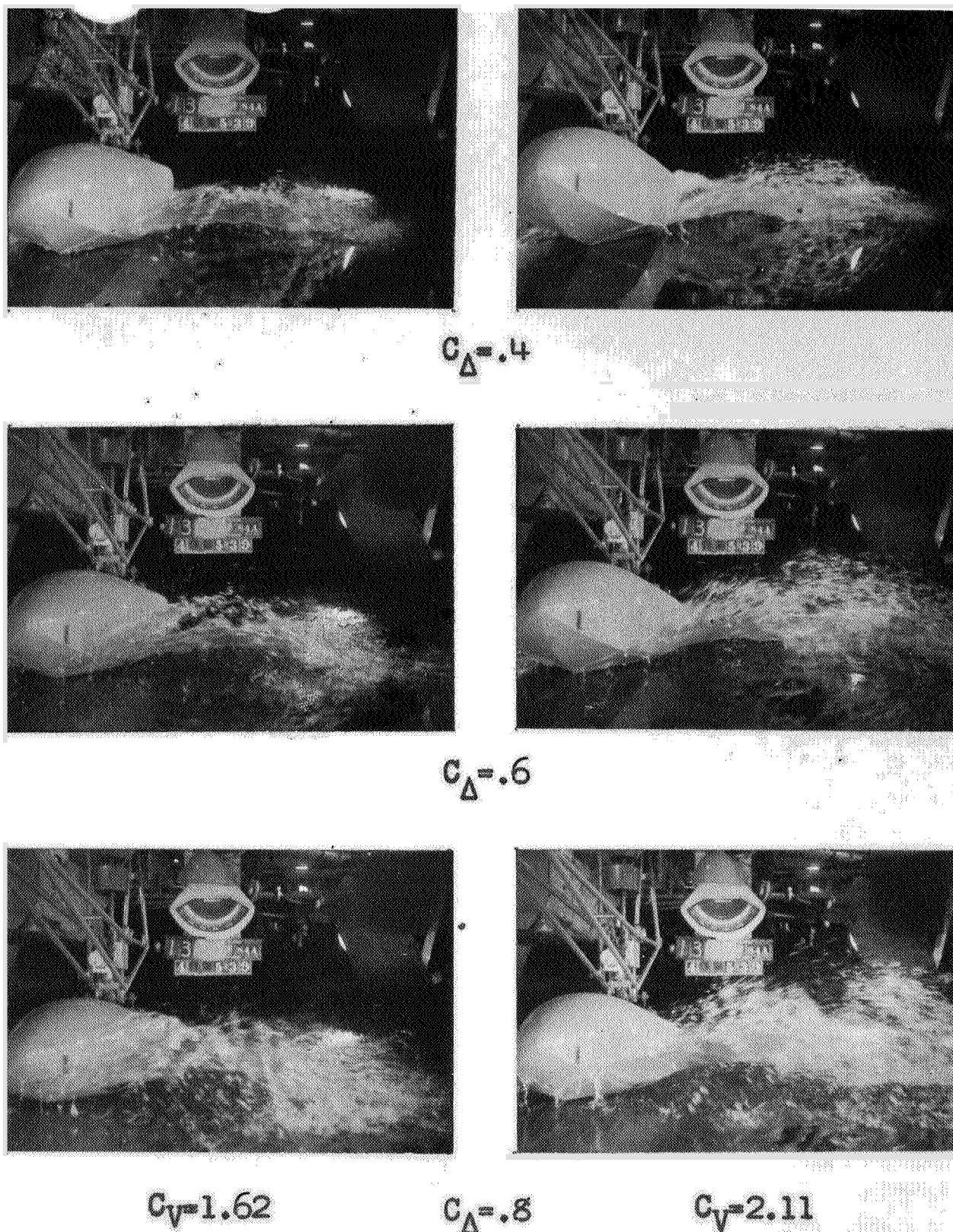


Figure 7 (b). Model 84A

L-277

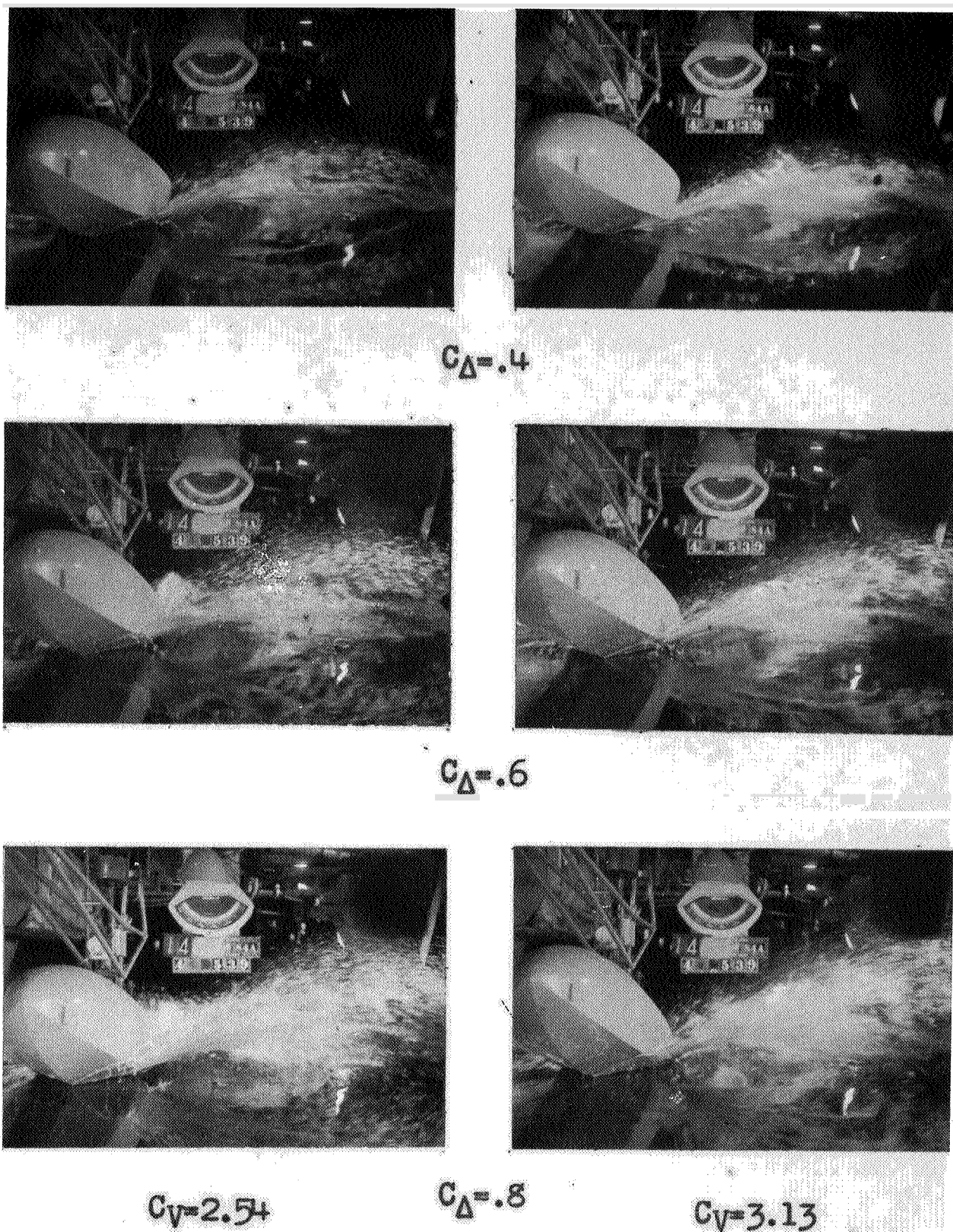


Figure 7 (c). Model 84A

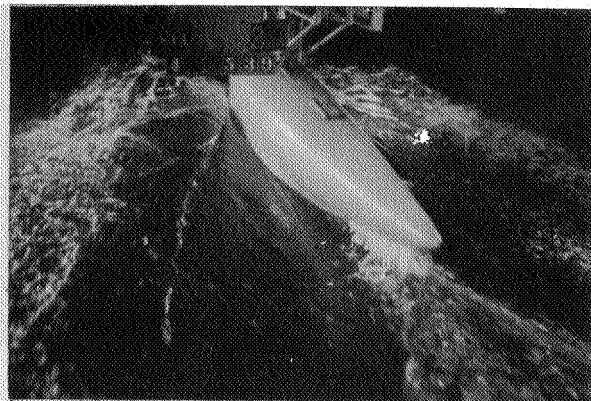
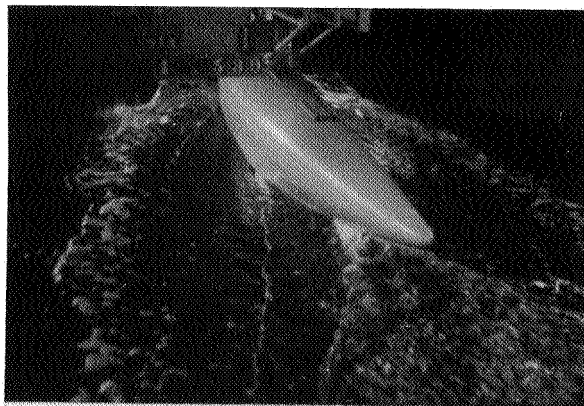
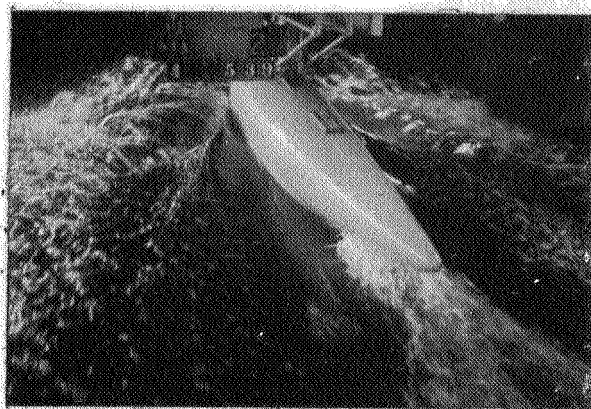
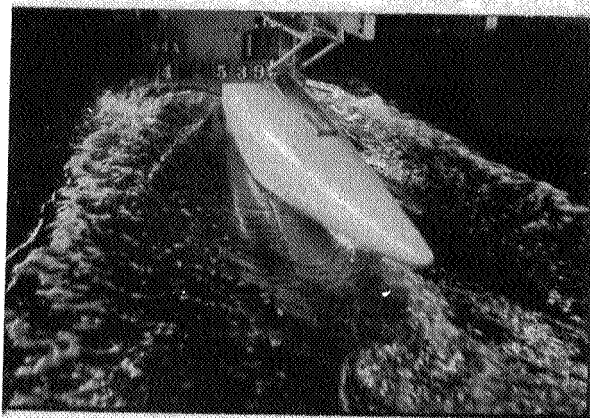
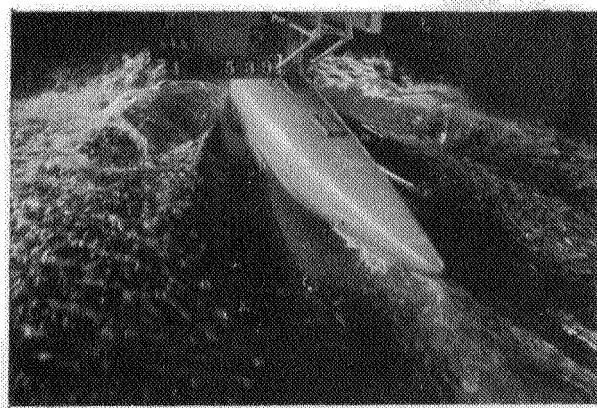
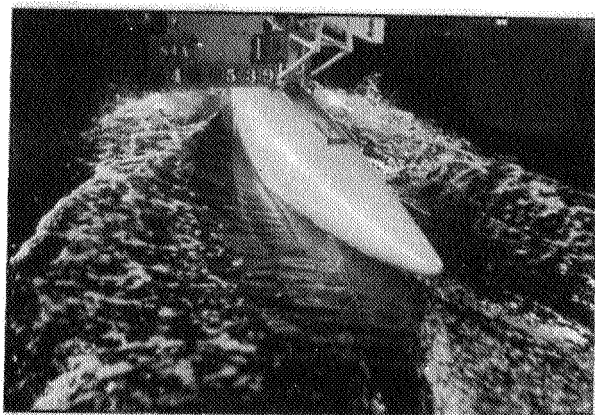

 $C_D = .4$ 

 $C_D = .6$ 

 $C_V = 1.22$ 
 $C_D = .8$ 
 $C_V = 1.71$ 

Figure 7 (d). Model 84A



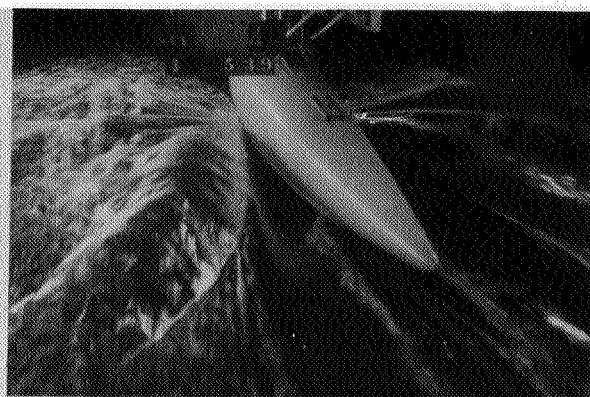
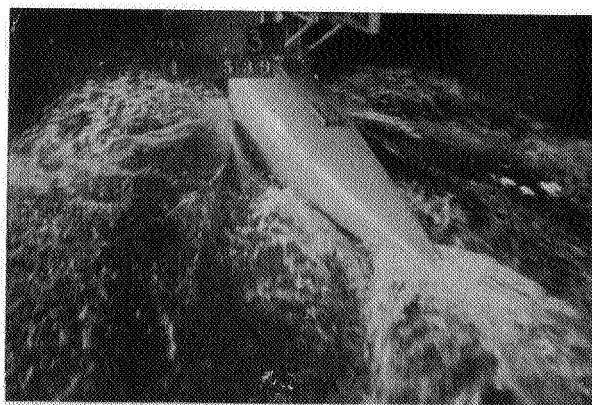
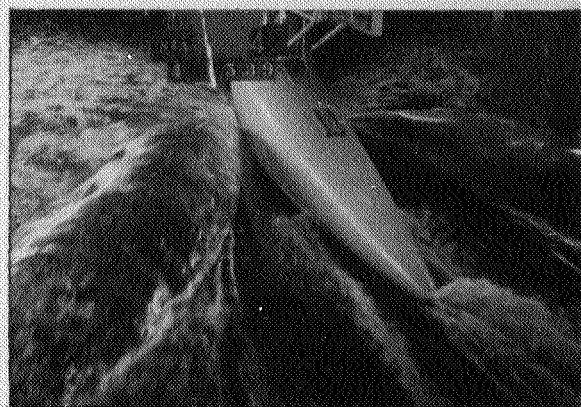
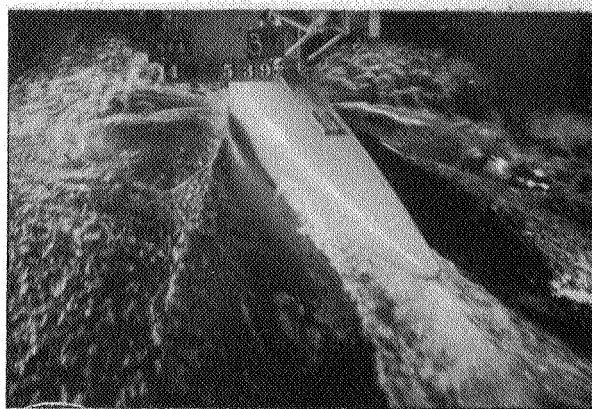
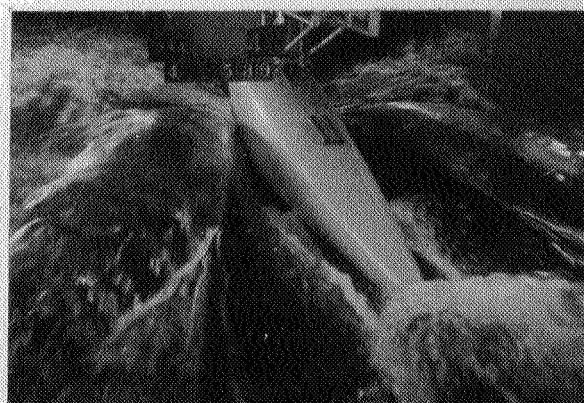
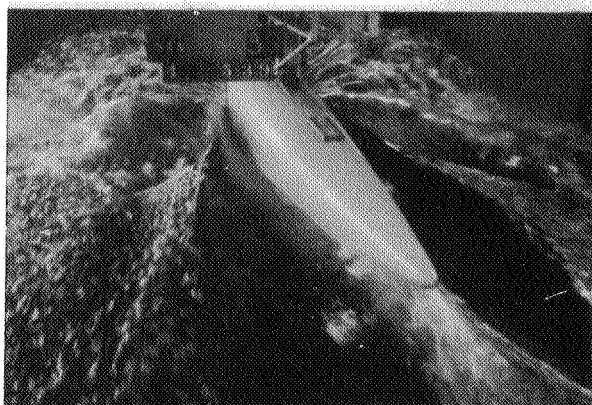
 $C_D = .4$  $C_D = .6$  $C_V = 2.09$  $C_D = .8$  $C_V = 2.63$ 

Figure 7 (e). Model 84A



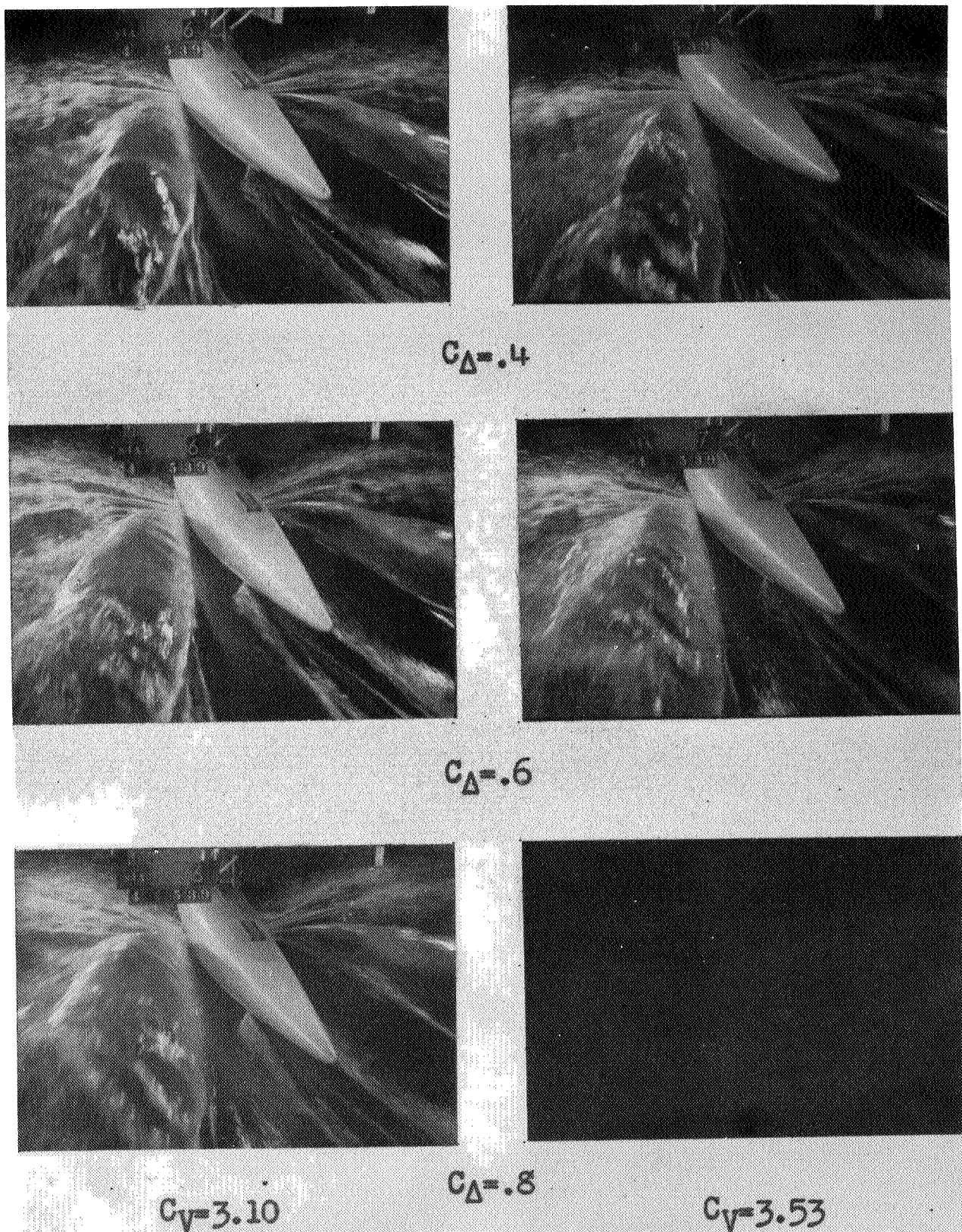


Figure 7 (f). Model 84A.

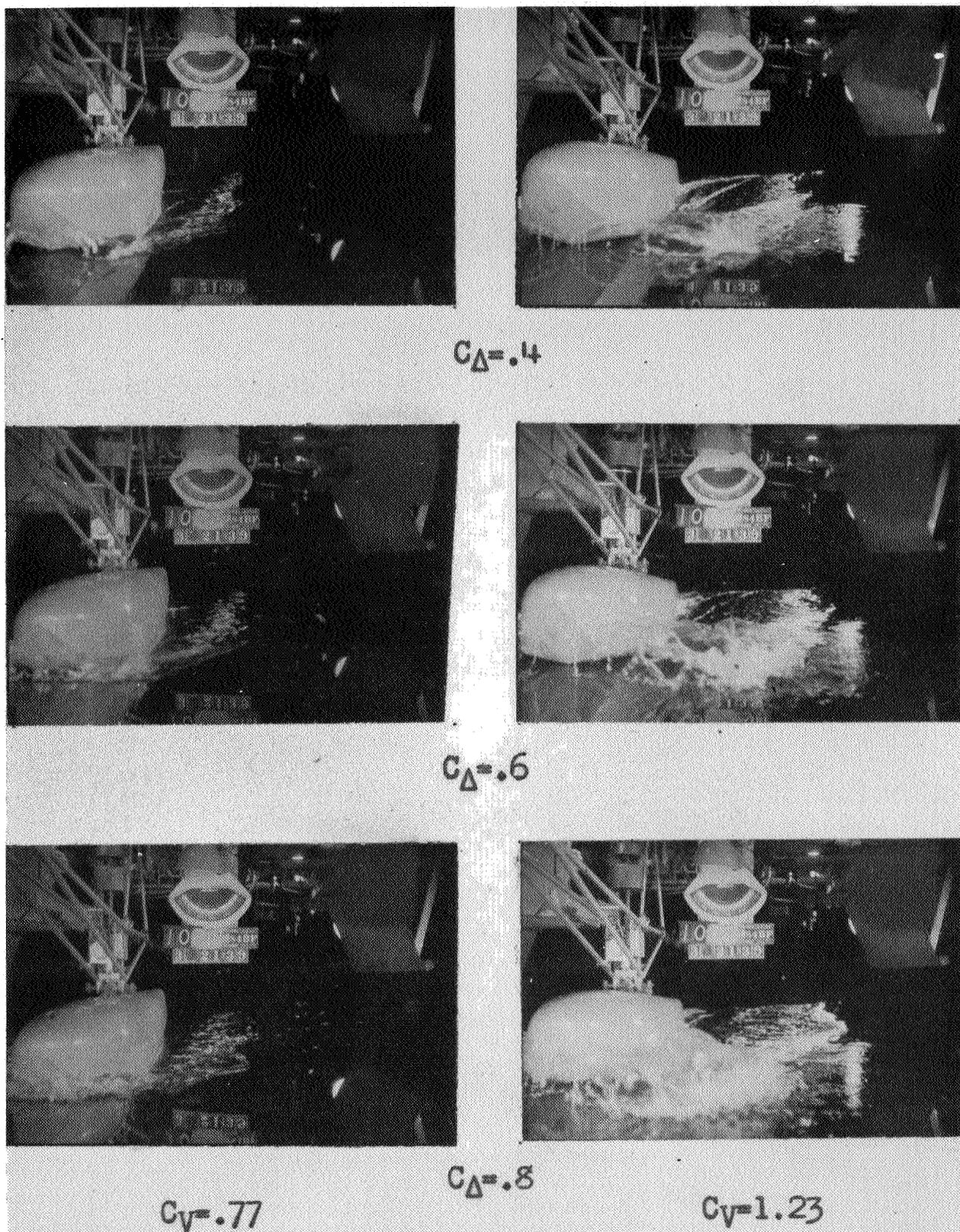
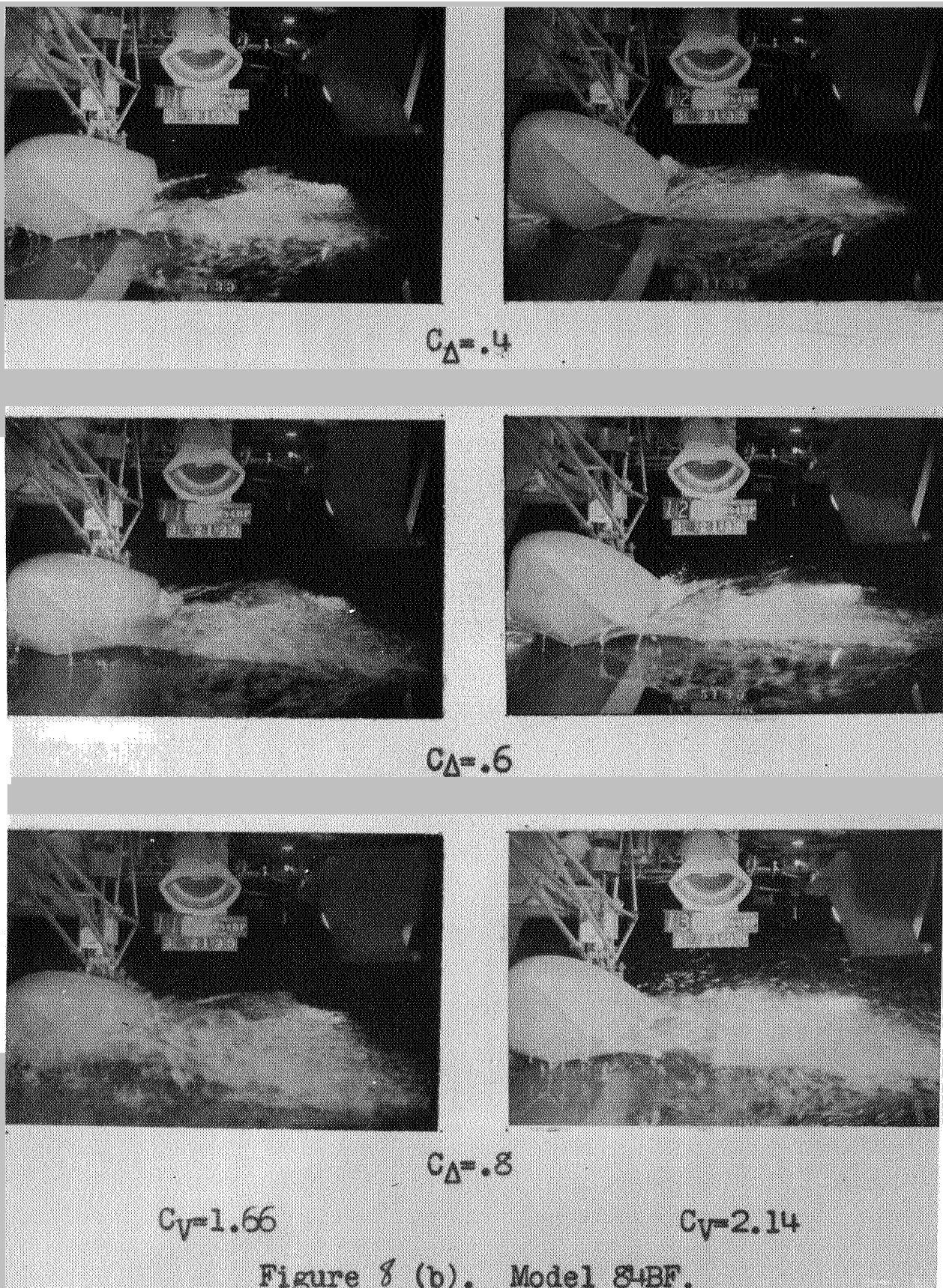


Figure 8 (a). Model 84BF, Bow 2, Stern 3  
With chine flare



L-277



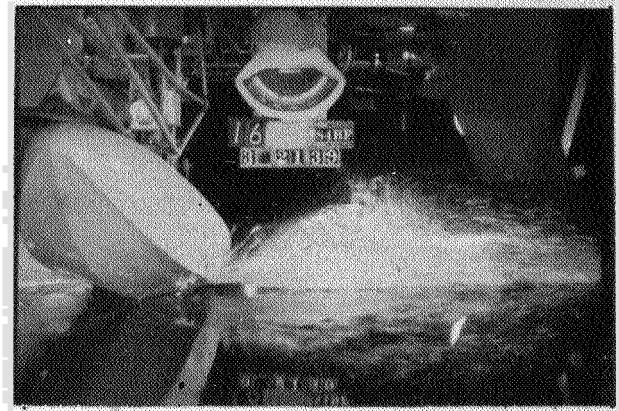
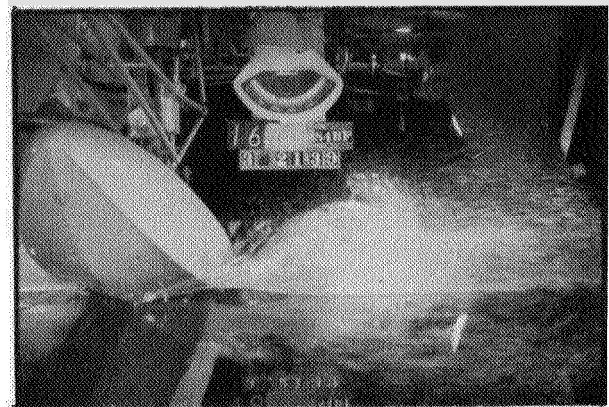
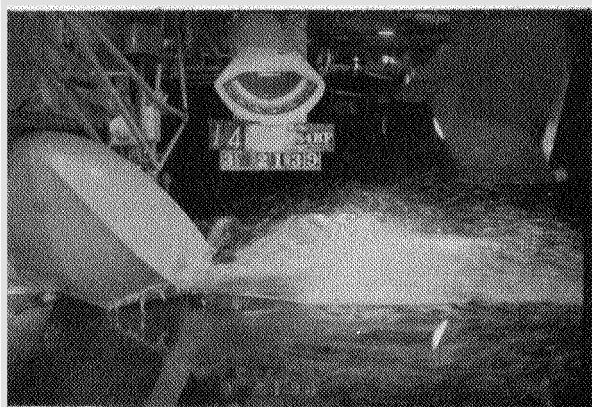

 $C_{\Delta} = .4$ 

 $C_{\Delta} = .6$ 

 $C_{\Delta} = .8$ 
 $C_V = 2.75$ 
 $C_V = 3.26$ 

Figure 8 (c). Model 84BF.



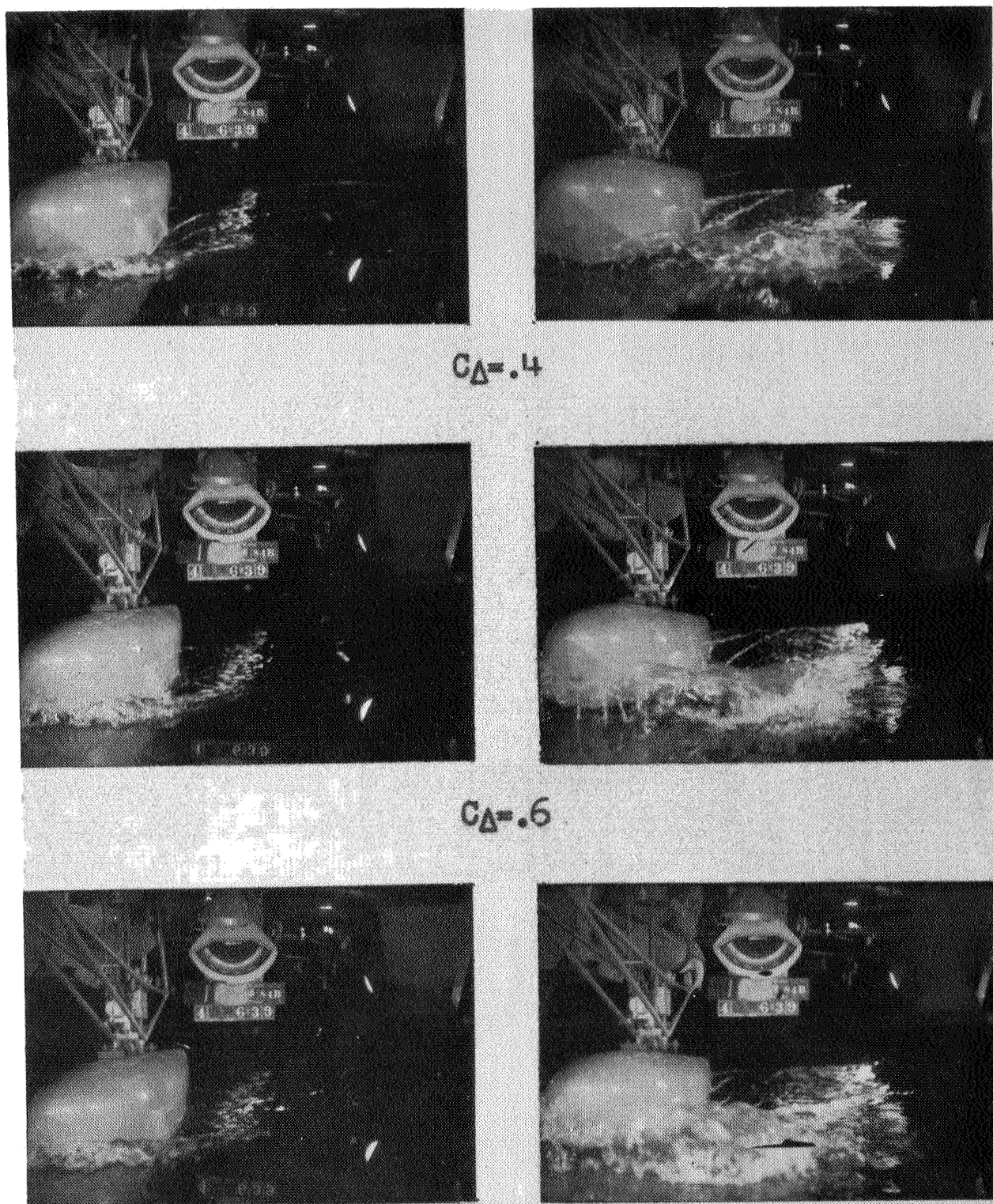
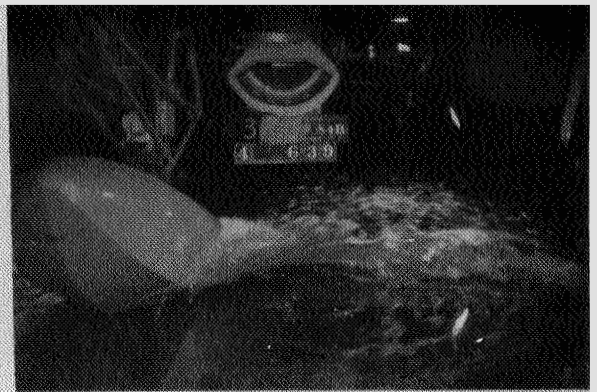
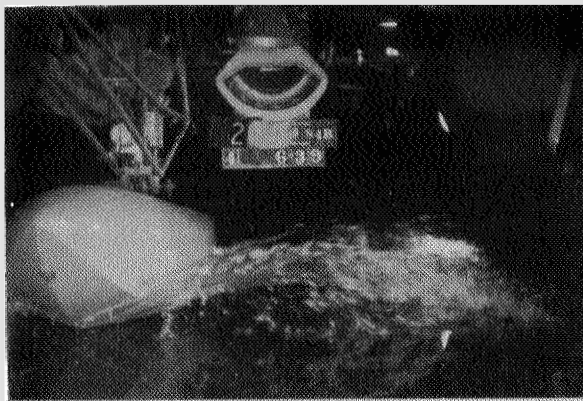


Figure 9 (a) Model 84B, Bow2, Stern 3.

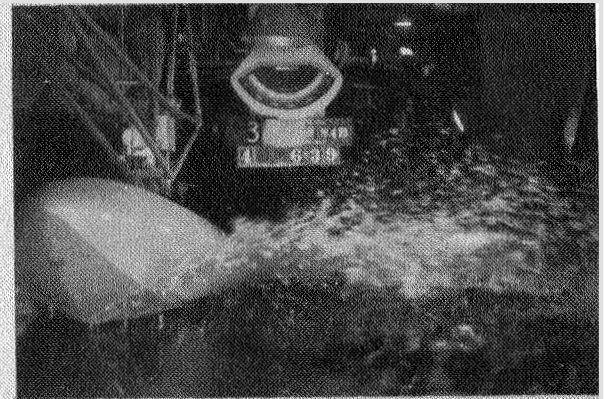
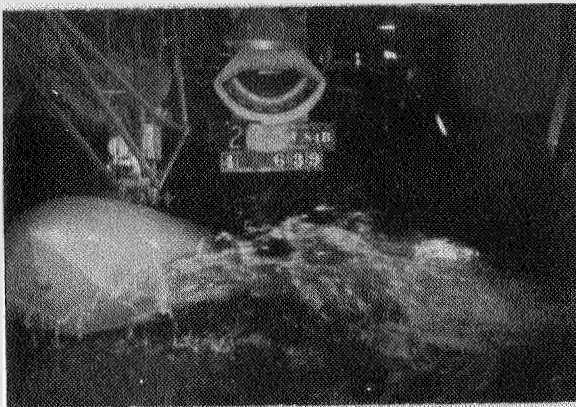
Without chine flare

NACA  
20490

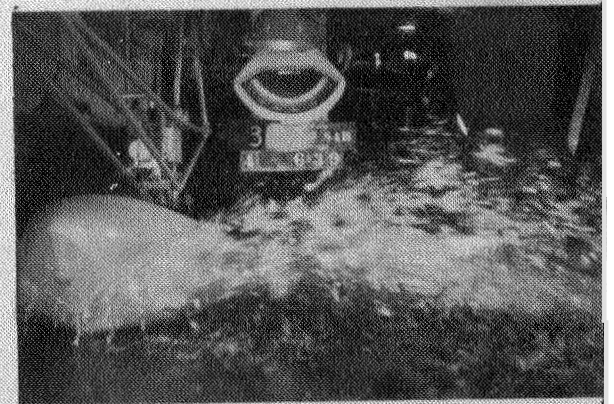
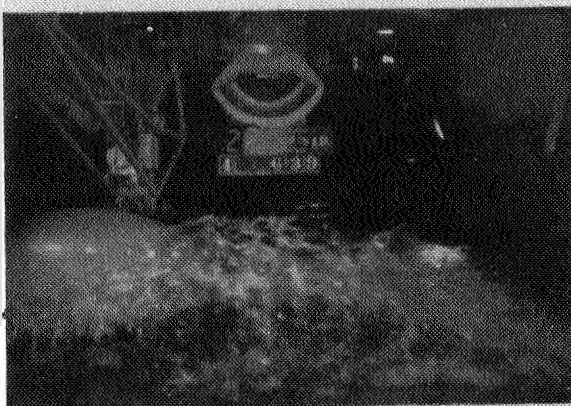
L-277



$C_D = .4$



$C_D = .6$



$C_D = .8$

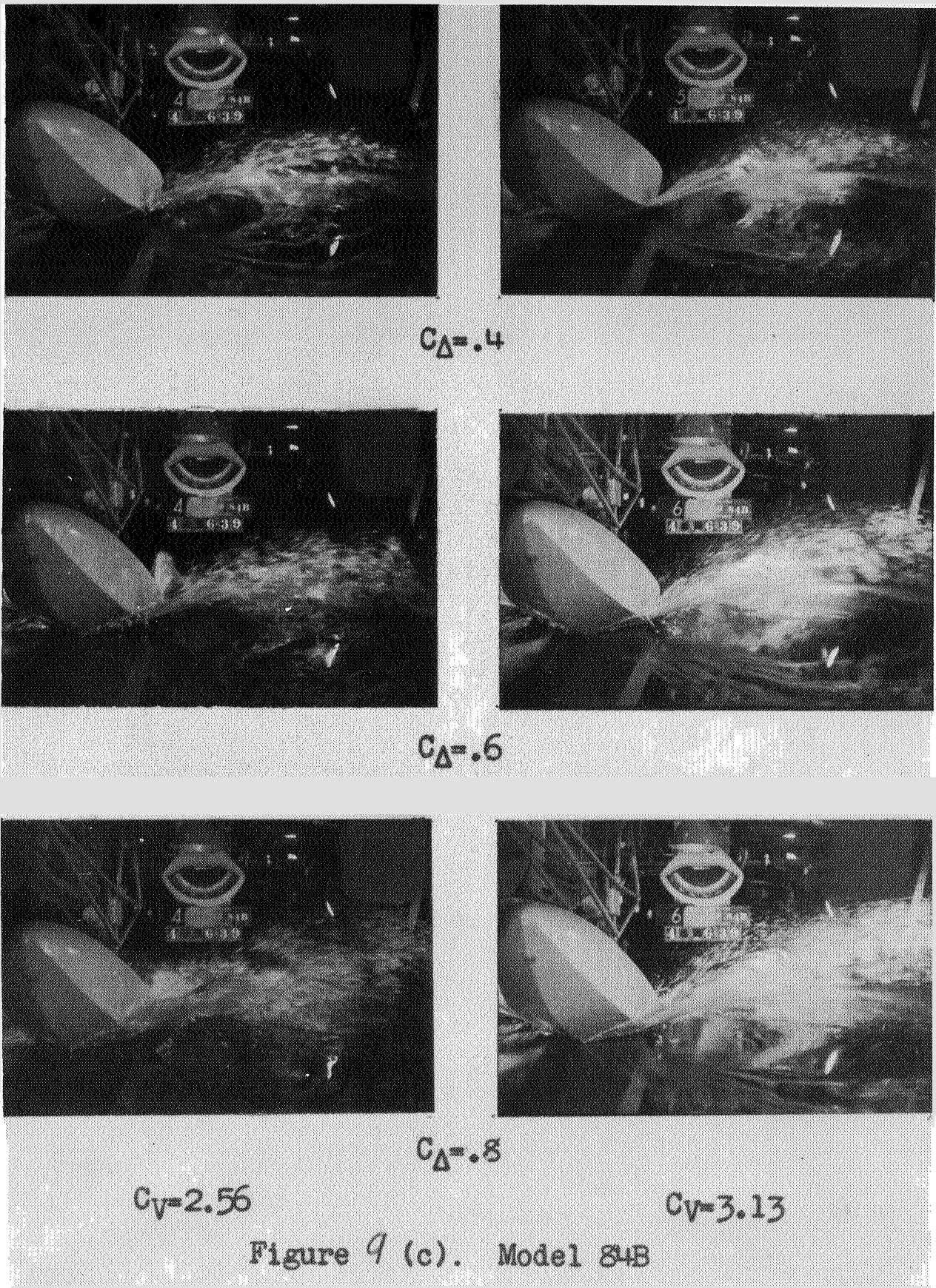
$C_V = 1.65$

$C_V = 2.06$

Figure 9 (b). Model 84B

NACA  
20491





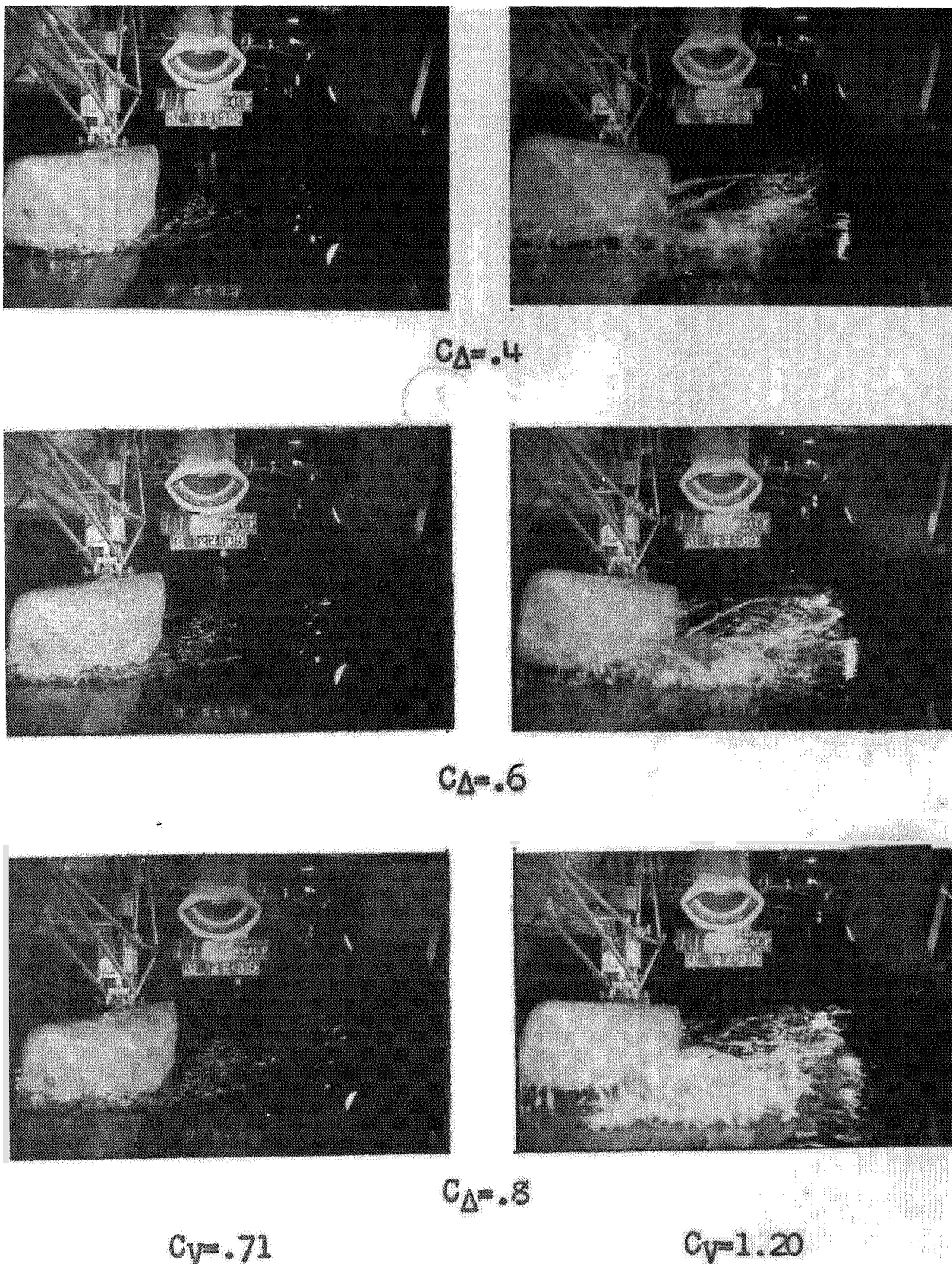


Figure 10 (a). Model 84CF, Bow 3, Stern 3.  
With chine flare.



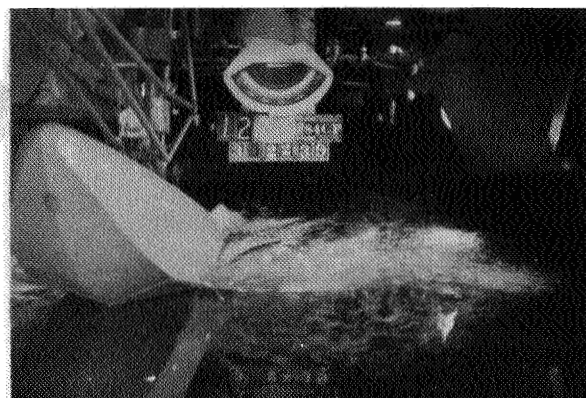
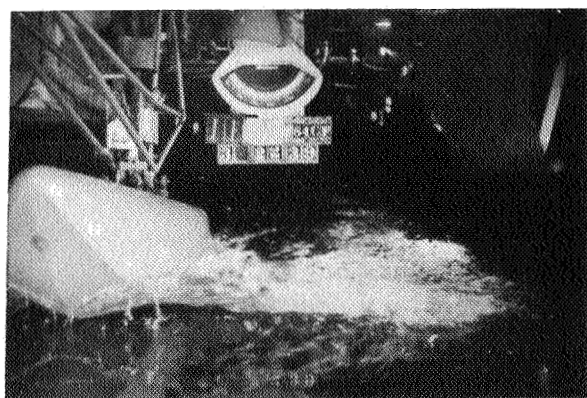
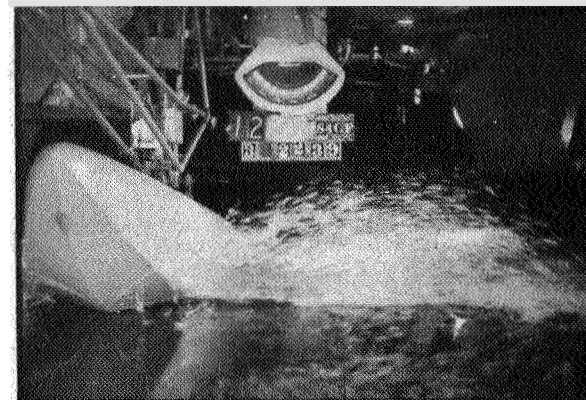
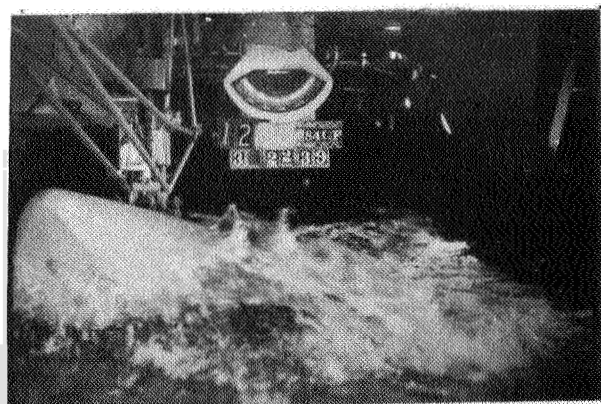
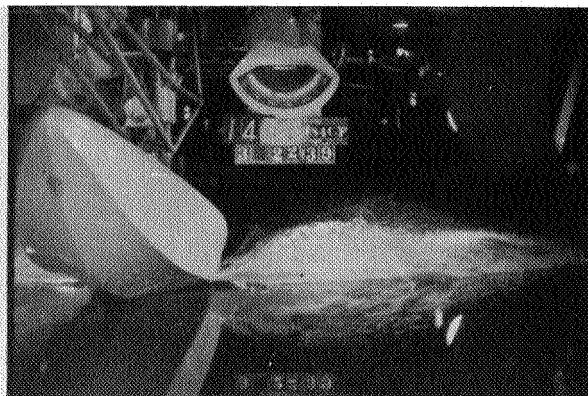
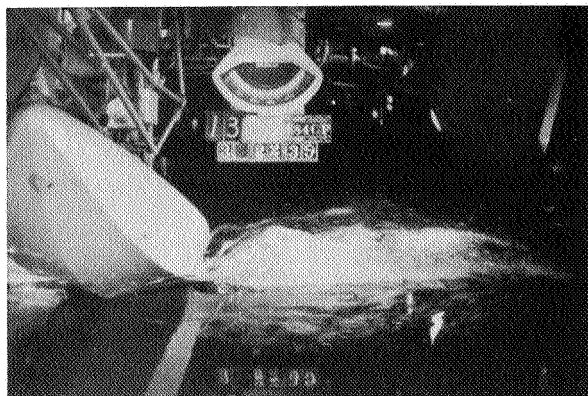
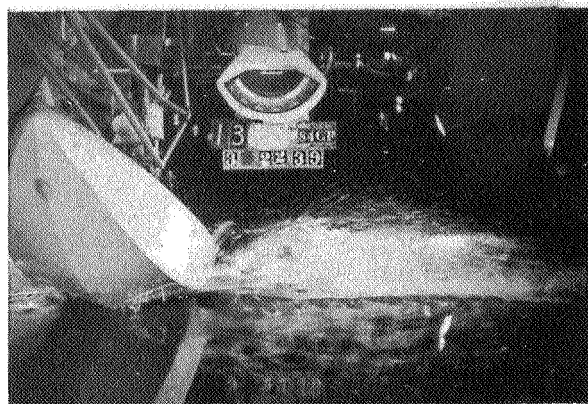

 $C_{\Delta} = .4$ 

 $C_{\Delta} = .6$ 

 $C_{\Delta} = .8$ 
 $C_V = 1.64$ 
 $C_V = 2.10$ 

Figure 10 (b). Model 84CF.


 $C_{\Delta} = .4$ 

 $C_{\Delta} = .6$ 

 $C_{\Delta} = .8$ 
 $C_v = 2.58$ 
 $C_v = 3.15$ 

Figure 10 (c). Model 84CF.



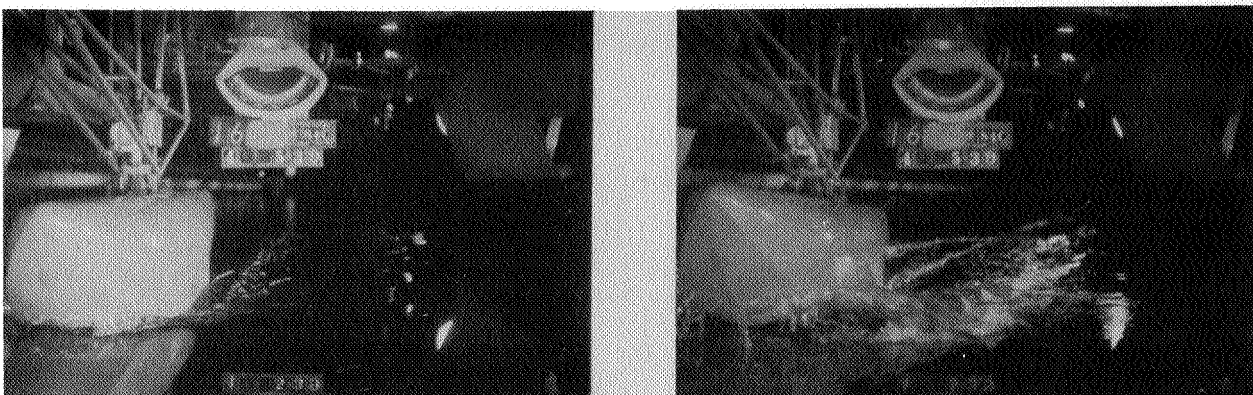
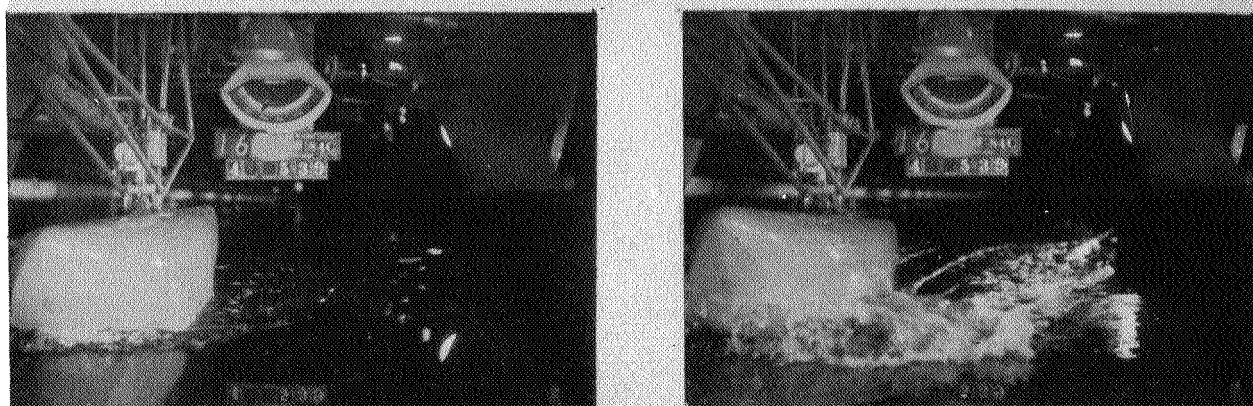
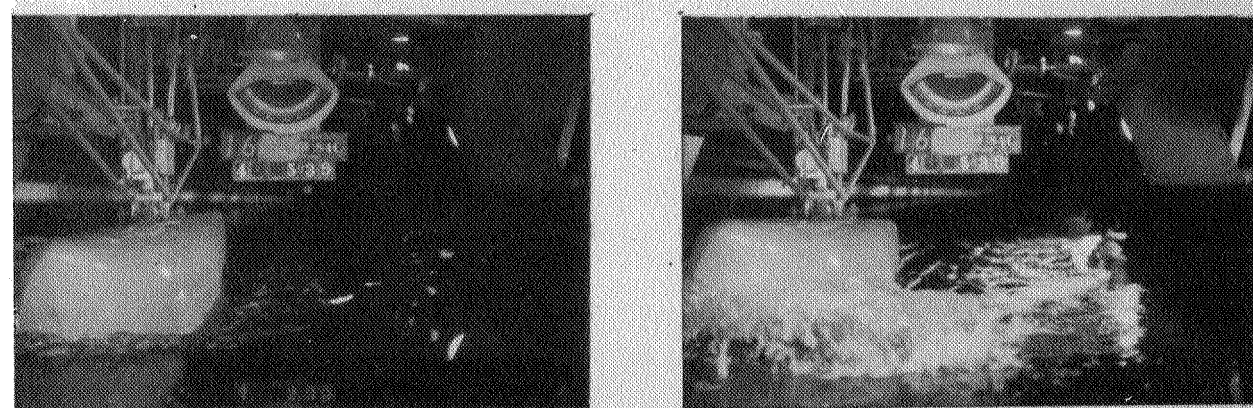

 $C_{\Delta} = .4$ 

 $C_{\Delta} = .6$ 

 $C_{\Delta} = .8$ 
 $C_V = .66$ 
 $C_V = 1.12$ 

Figure 11 (a). Model 84C, Bow 3, Stern 3.  
Without chine flare

L-277

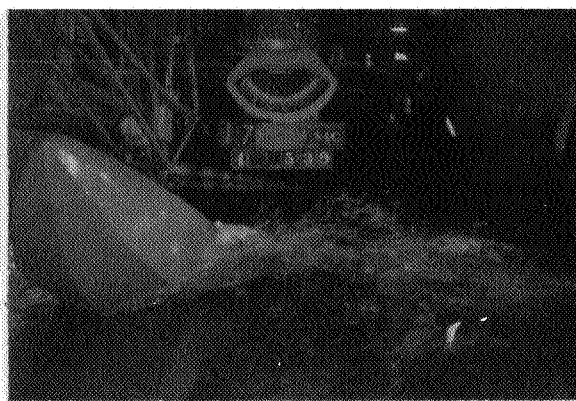
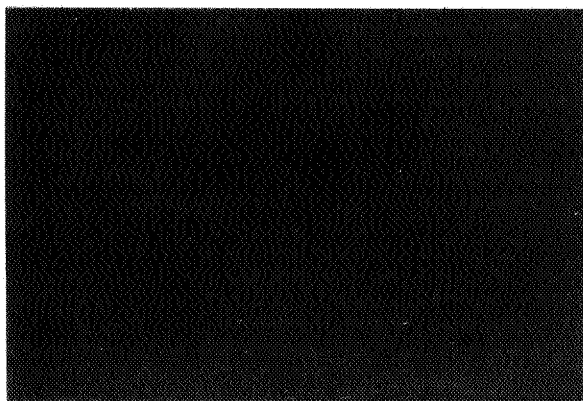
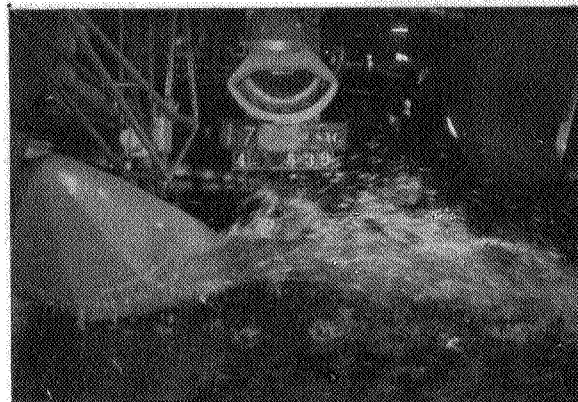
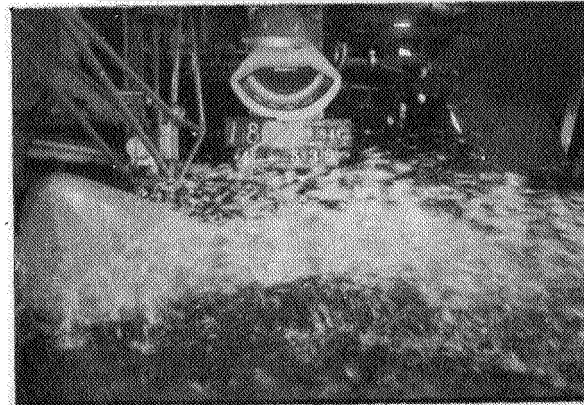
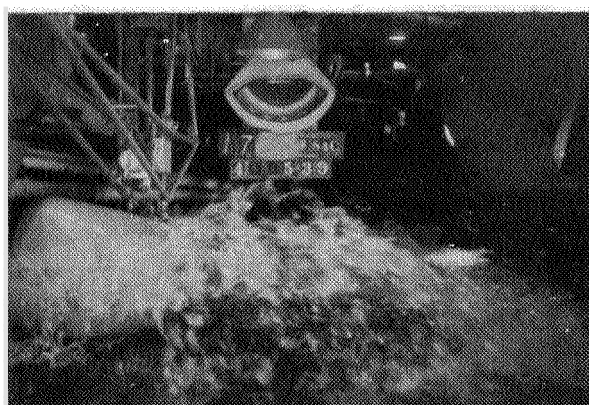
 $C_D = .4$  $C_D = .6$  $C_D = .8$  $C_v = 1.69$  $C_v = 2.09$ 

Figure 11 (b). Model 84C



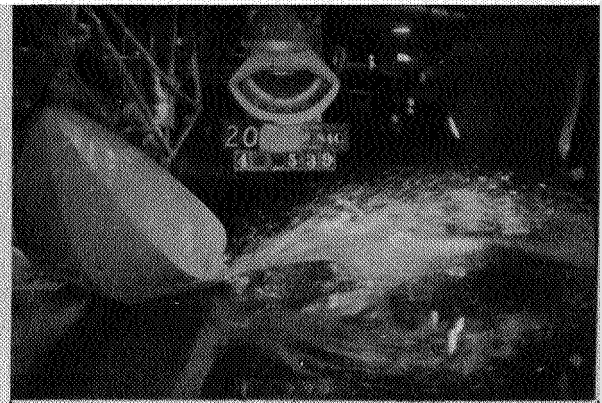
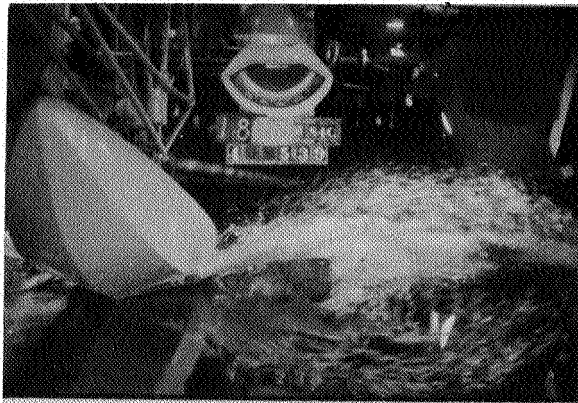
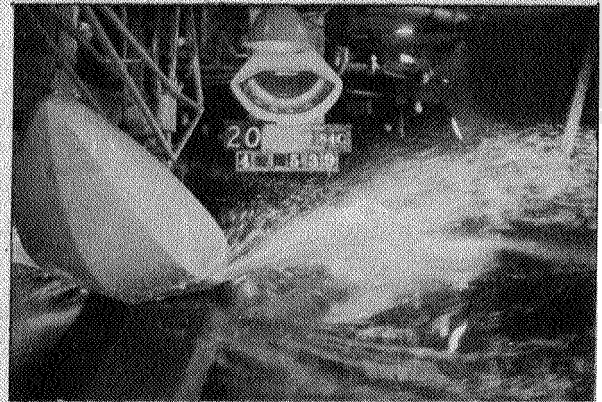
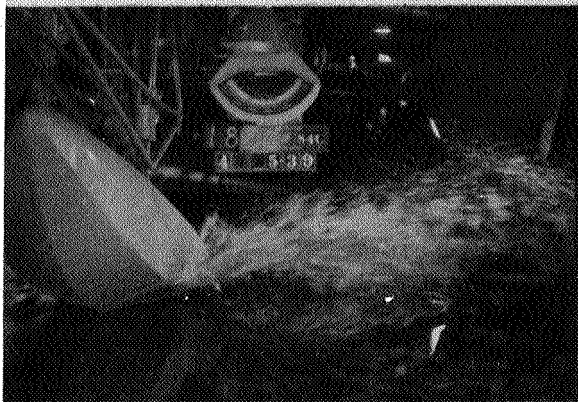
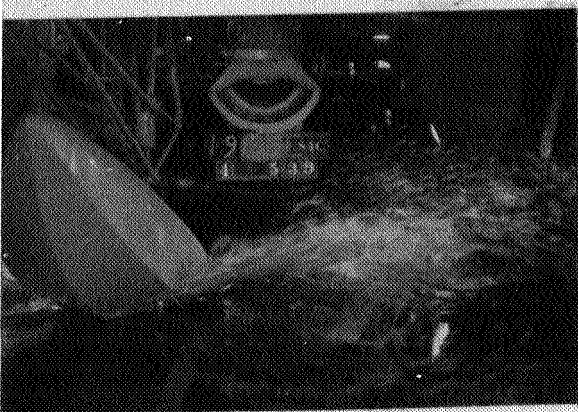
 $C_D = .4$  $C_D = .6$  $C_D = .8$  $C_V = 2.60$  $C_V = 3.20$ 

Figure 11 (c). Model 84C

NACA

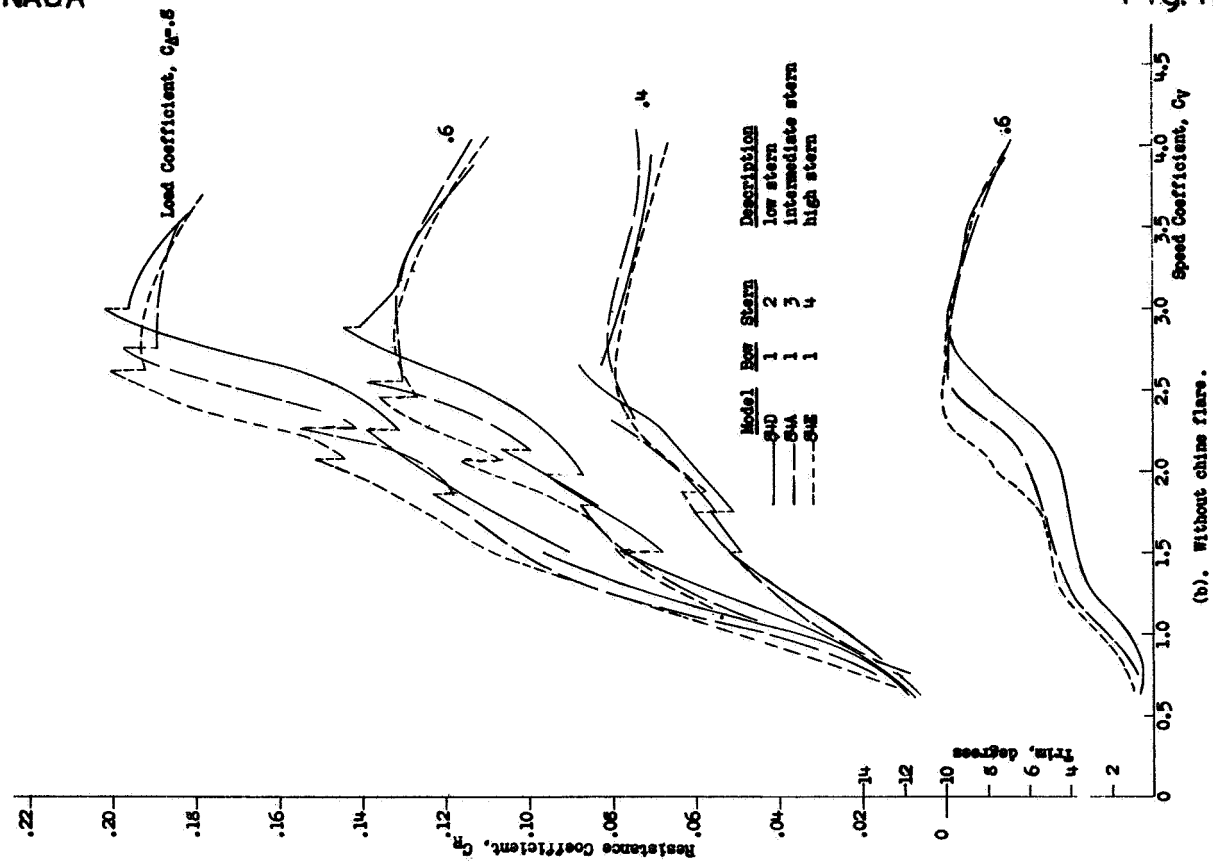
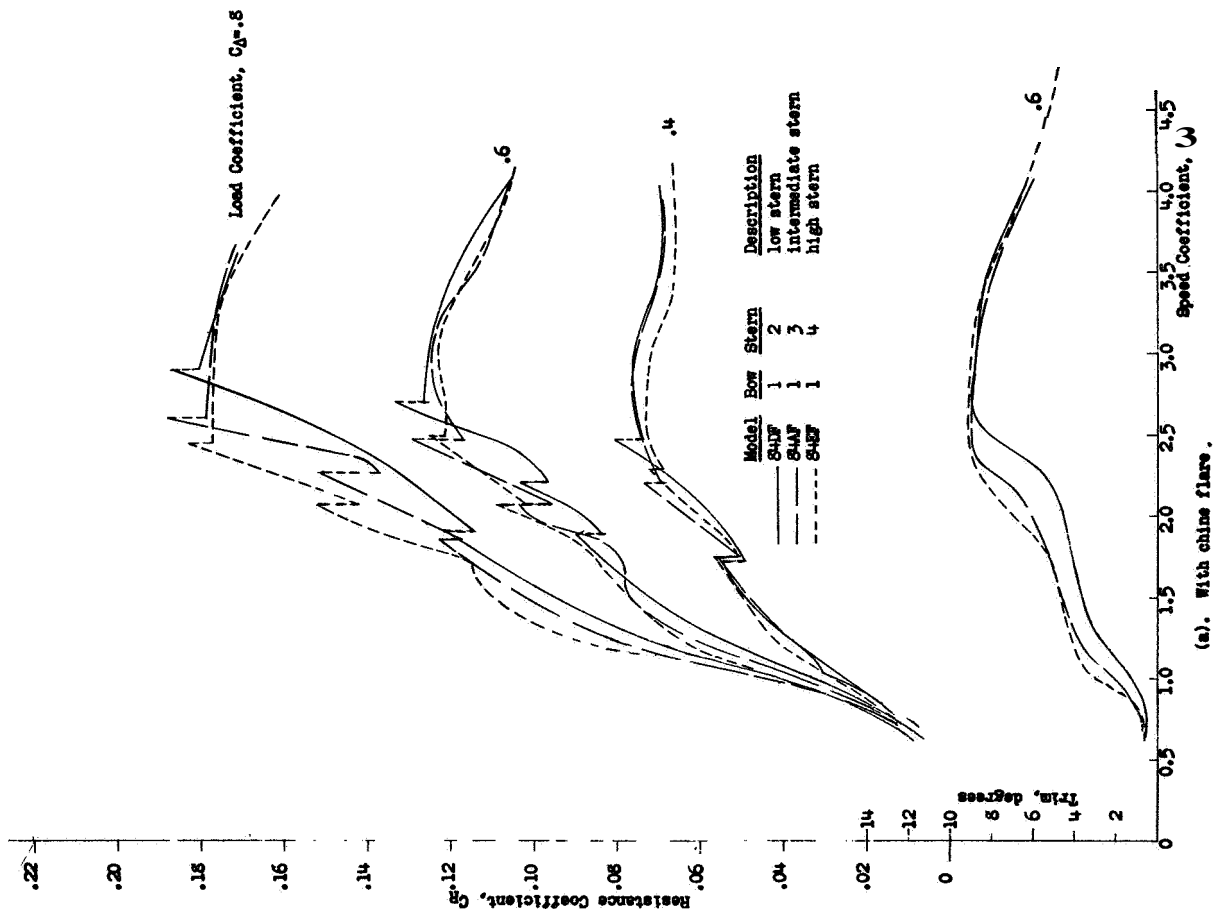


Figure 12. - Effect of height of stern.

Fig. 12

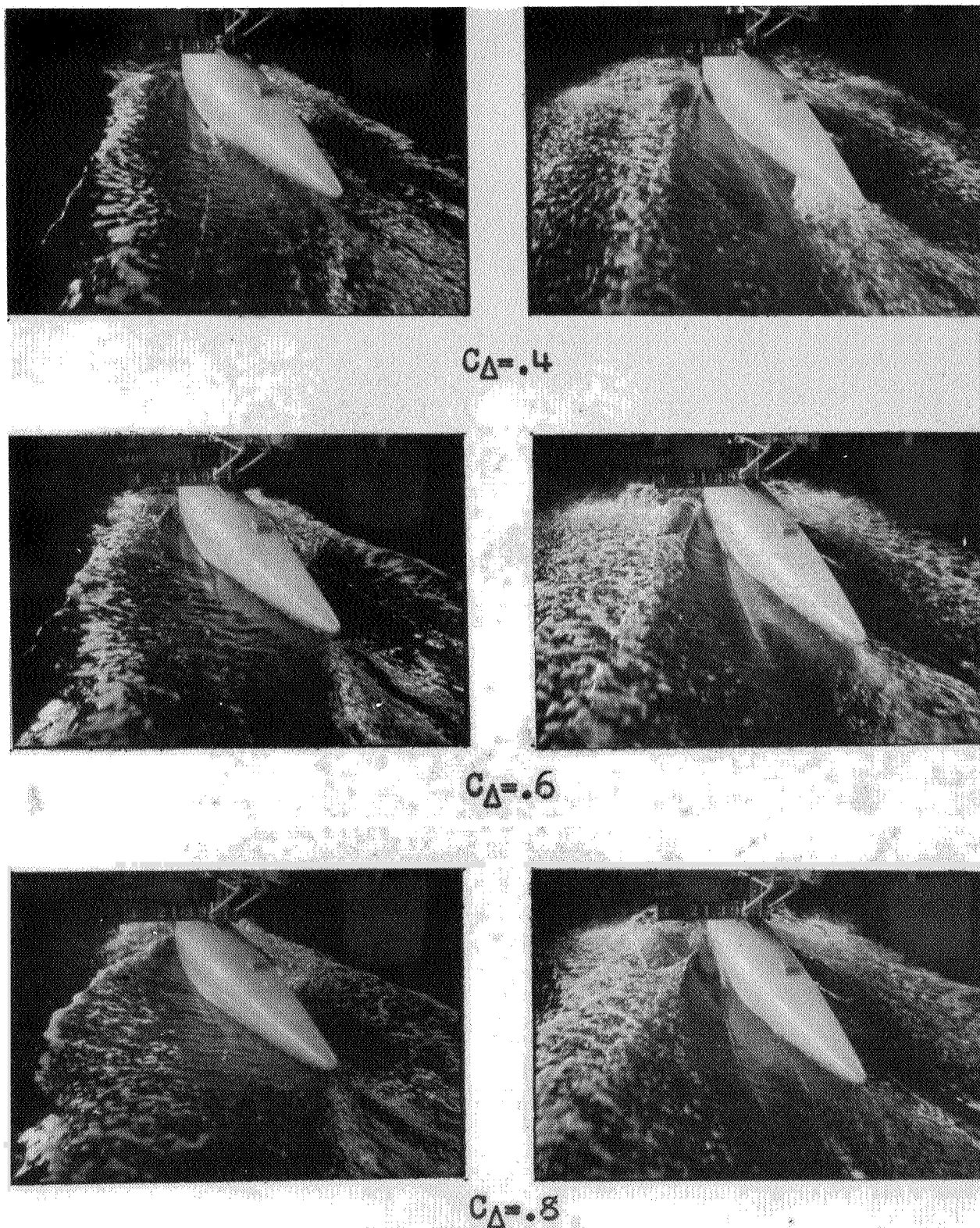
 $C_v = 1.15$  $C_v = 1.67$ 

Figure 13 (a). Model 84DF, Bow 1, Stern 2.

With chine flare

NACA  
20499



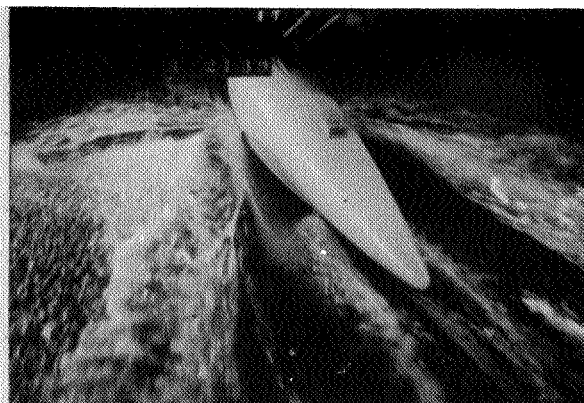
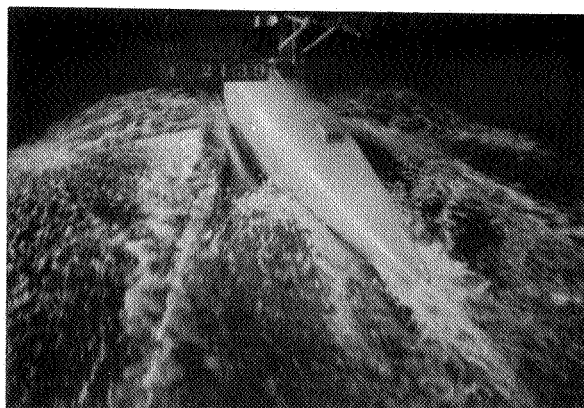
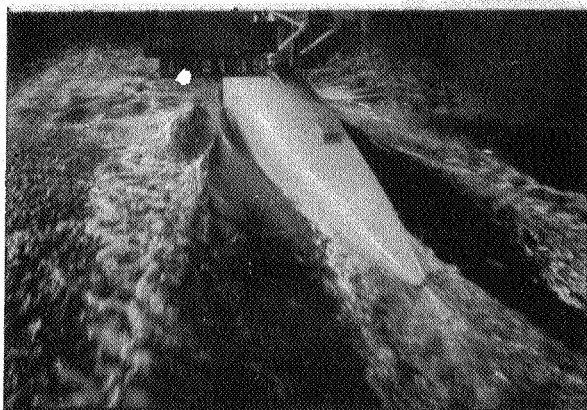
 $C_D = .4$  $C_D = .6$  $C_D = .8$  $C_V = 2.16$  $C_V = 2.58$ 

Figure 13 (b). Model 84DF



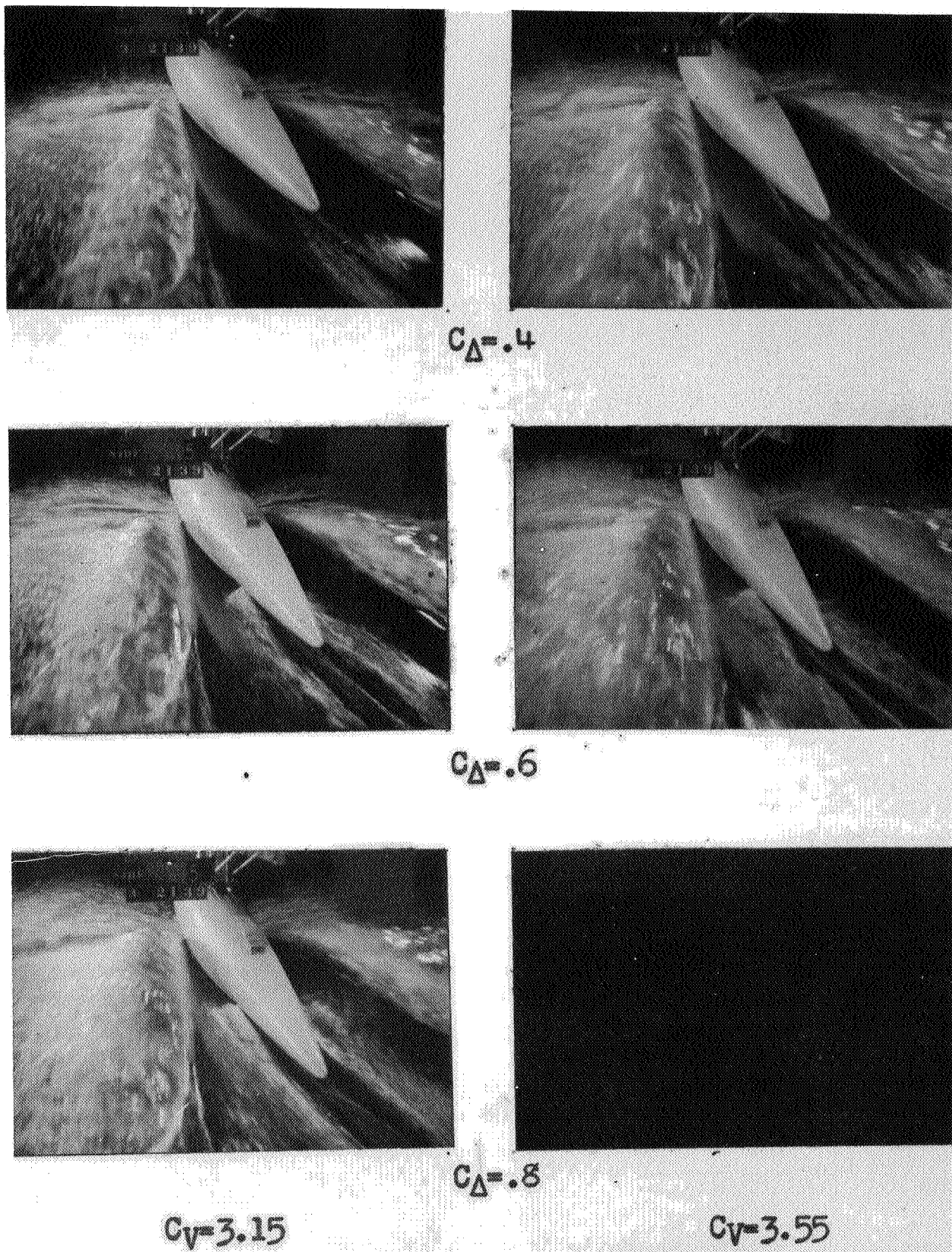


Figure 13 (c). Model 84DF

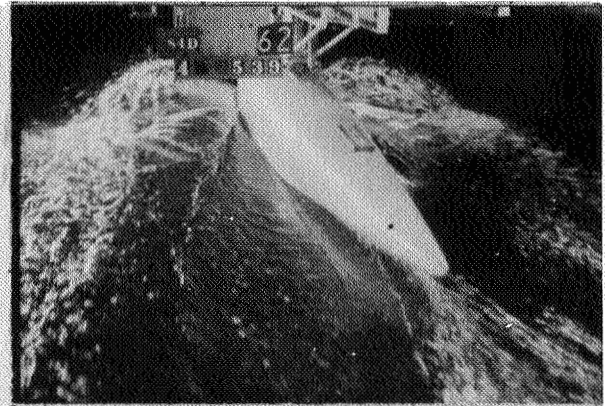
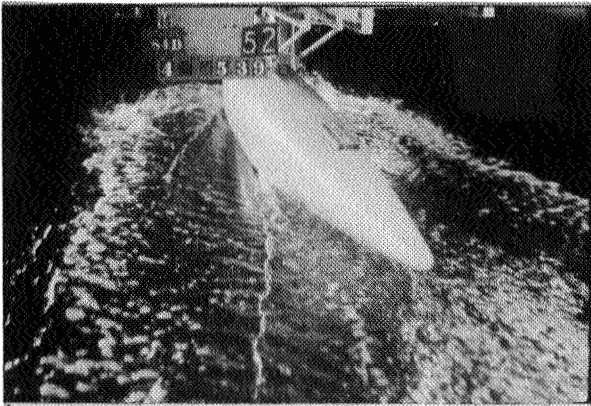
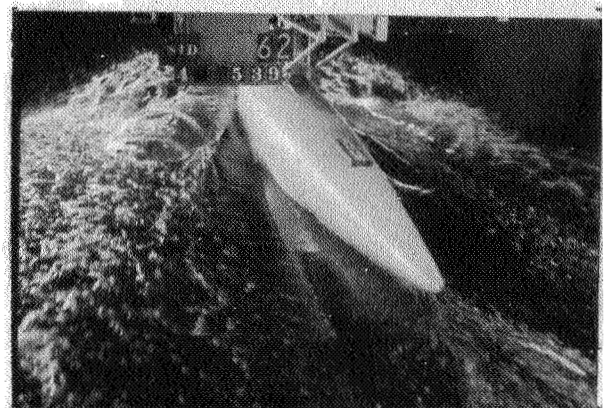
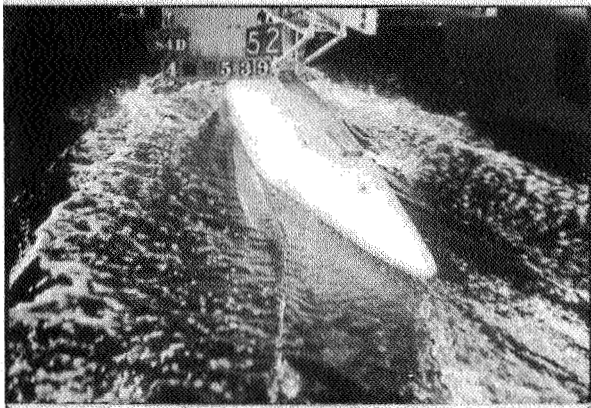
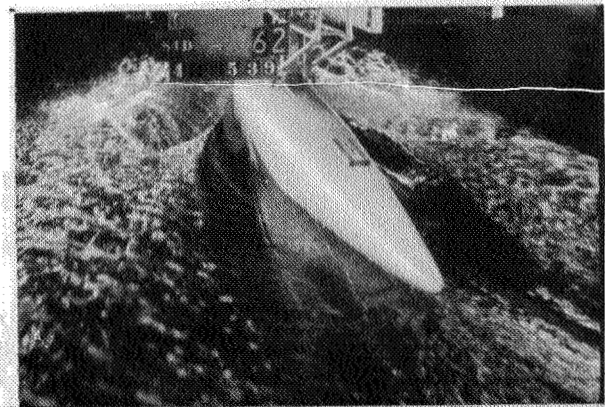
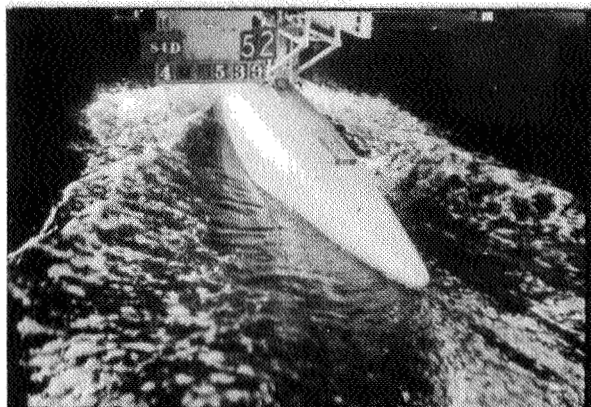

 $C_{\Delta} = .4$ 

 $C_{\Delta} = .6$ 

 $C_{\Delta} = .8$ 
 $C_V = 1.24$ 
 $C_V = 1.62$ 

Figure 14(a). Model 84D, Bow 1, Stern 2.

Without chine flare.

NACA  
20502



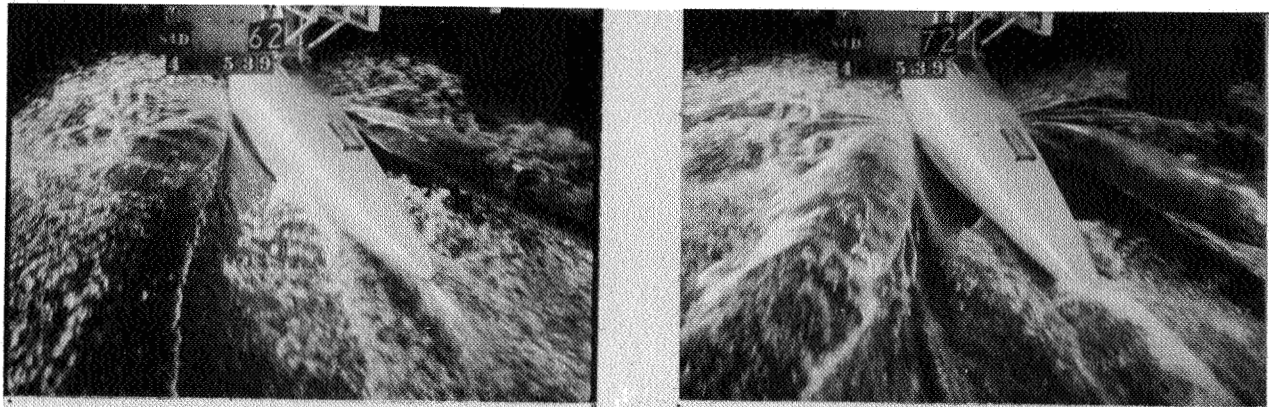
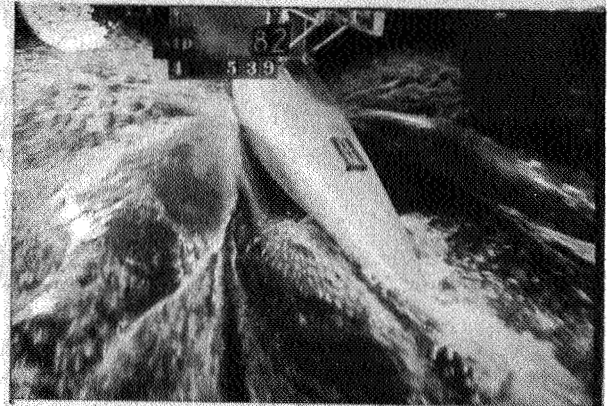
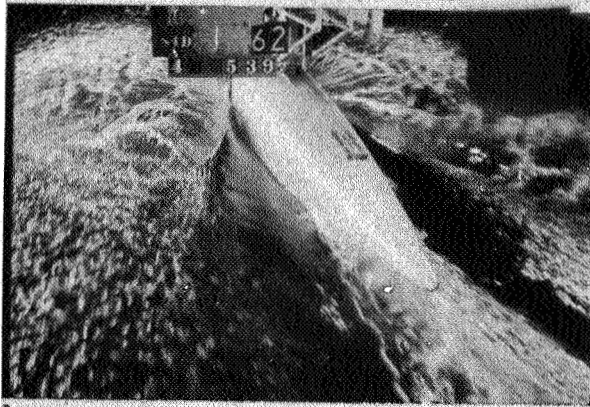
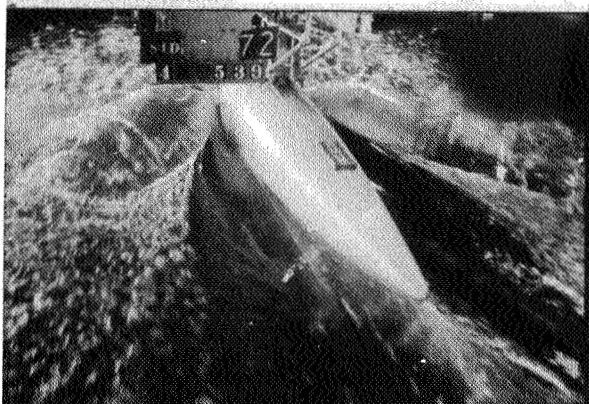

 $C_{\Delta} = .4$ 

 $C_{\Delta} = .6$ 

 $C_{\Delta} = .8$ 
 $C_V = 2.08$ 
 $C_V = 2.60$ 

Figure 14(b). Model 84D.

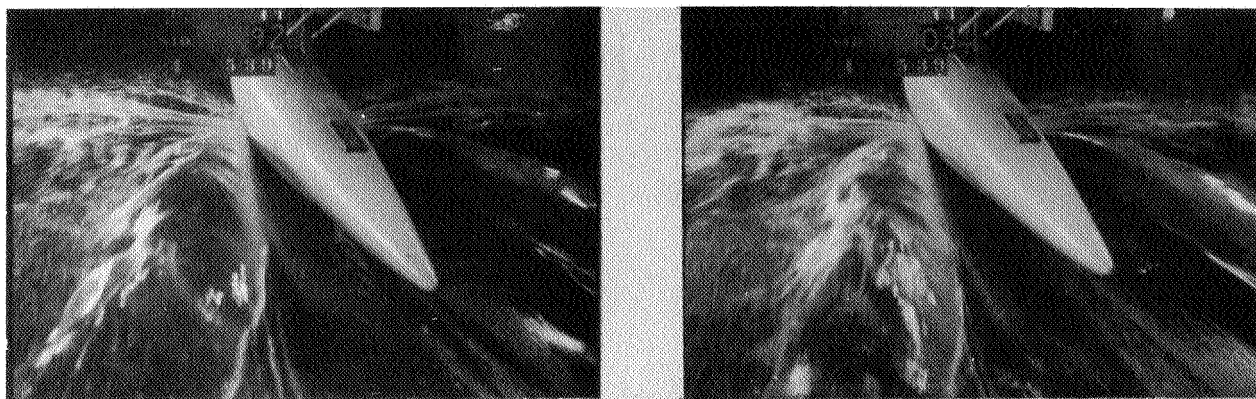
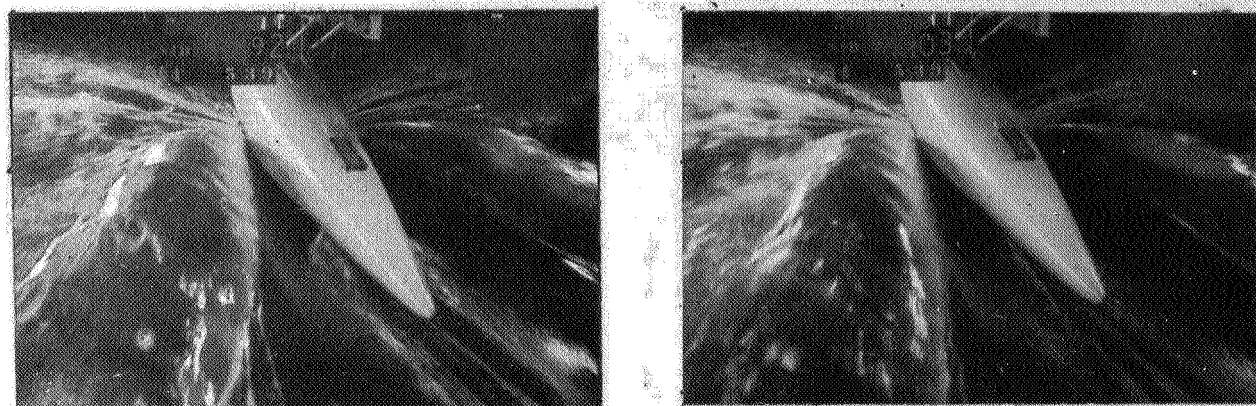
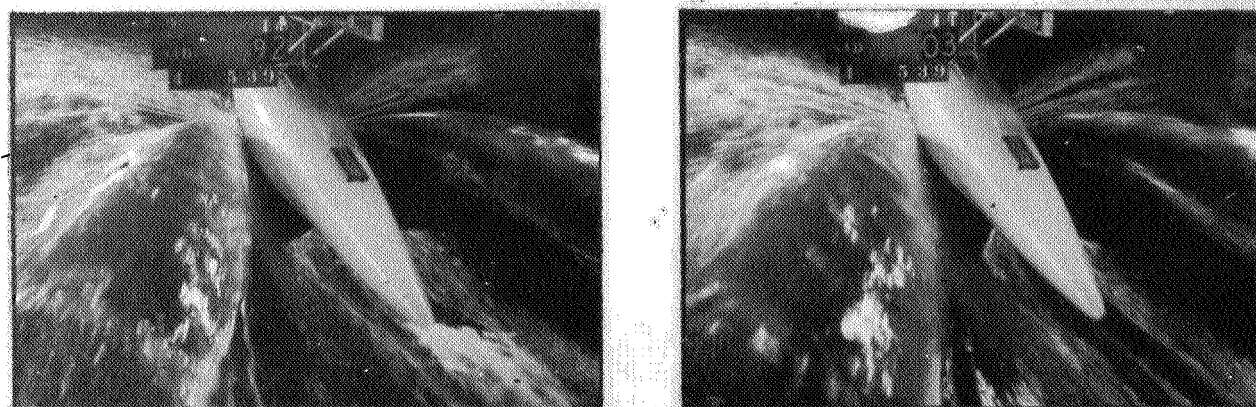
 $C_{\Delta} = .4$  $C_{\Delta} = .6$  $C_{\Delta} = .8$  $C_v = 3.11$  $C_v = 3.52$ 

Figure 14(c). Model 84D



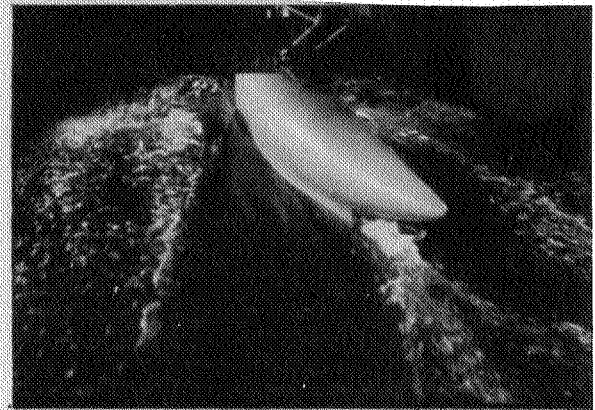
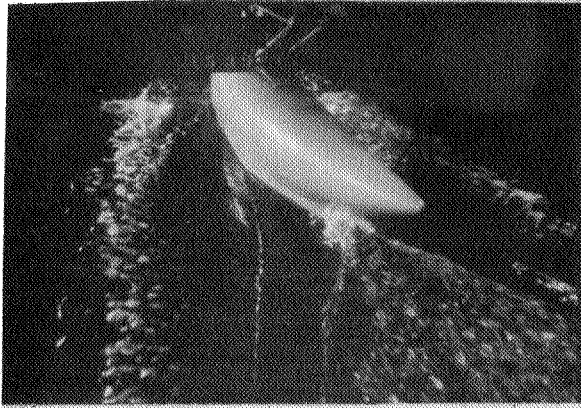
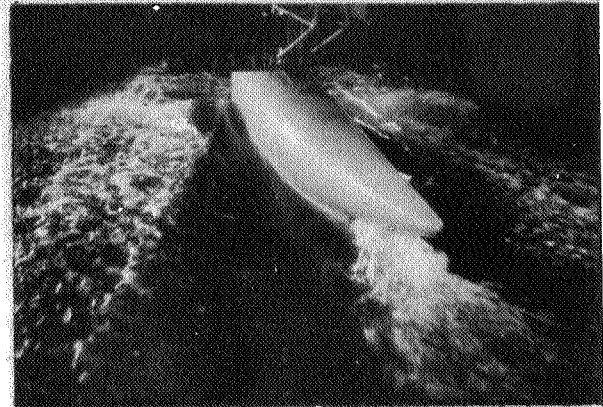
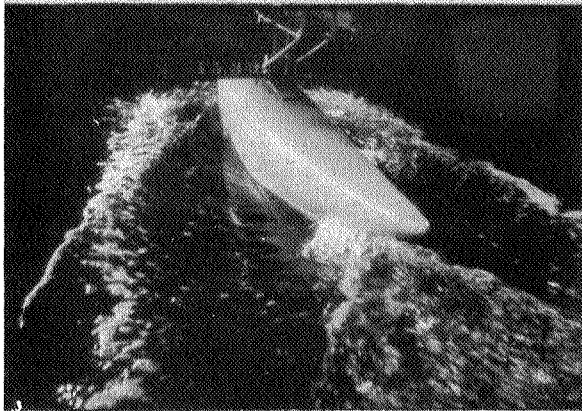
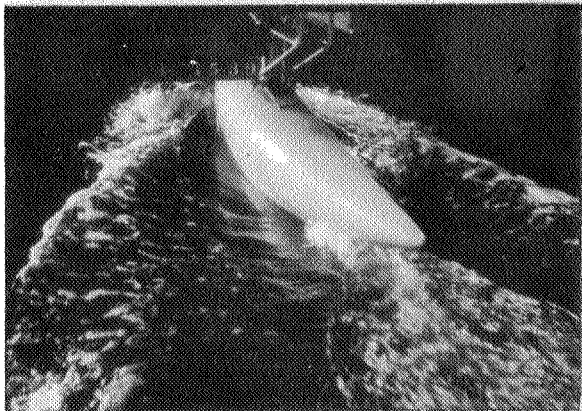

 $C_D = .4$ 

 $C_D = .6$ 

 $C_D = .8$ 
 $C_V = 1.21$ 
 $C_V = 1.68$ 

Figure 15 (a). Model 84EF, Bow 1, Stern 4

With chine flare

C.G. 7.20 in. fwd.

NACA  
20505

L-277

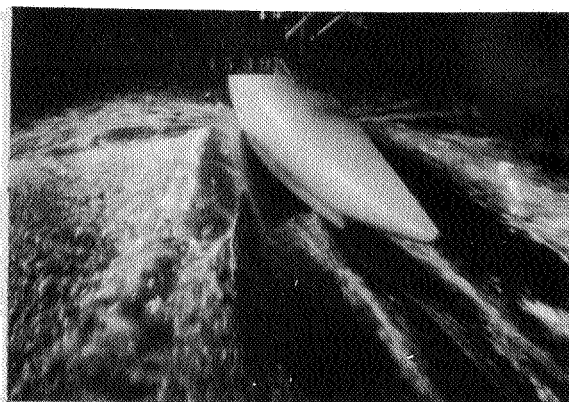
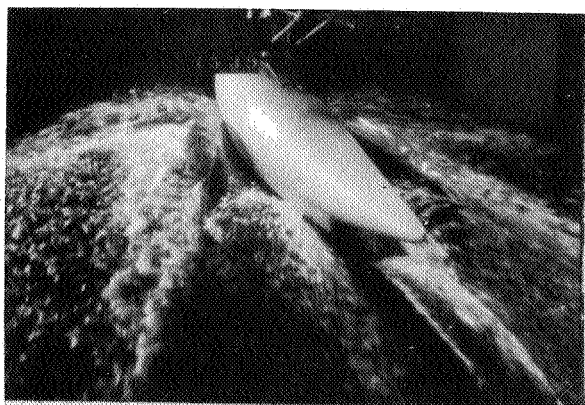
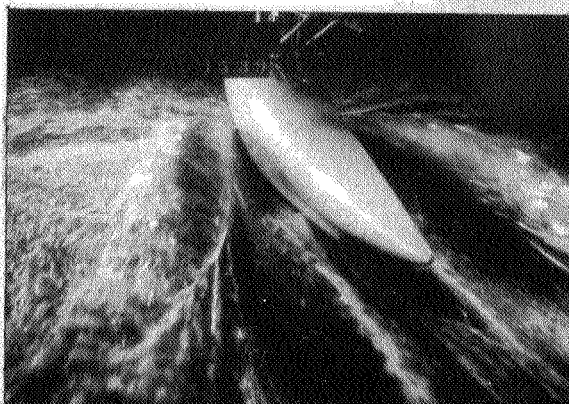
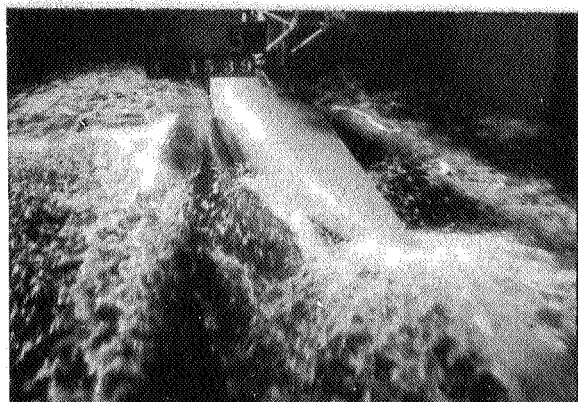
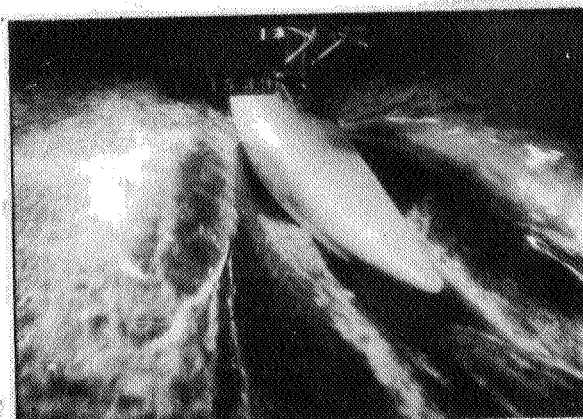
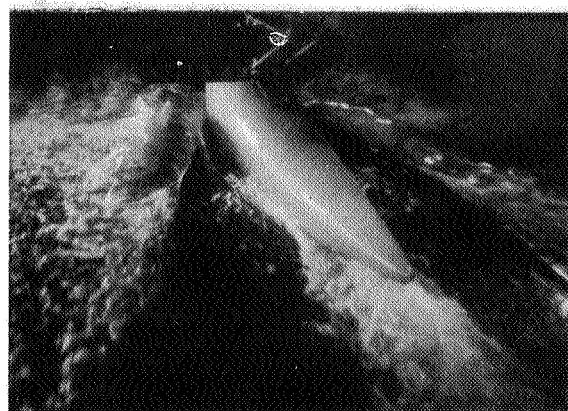
 $C_D = .4$  $C_D = .6$  $C_D = .8$  $C_Y = 2.15$  $C_Y = 2.65$ 

Figure 15 (b). Model 84EF.



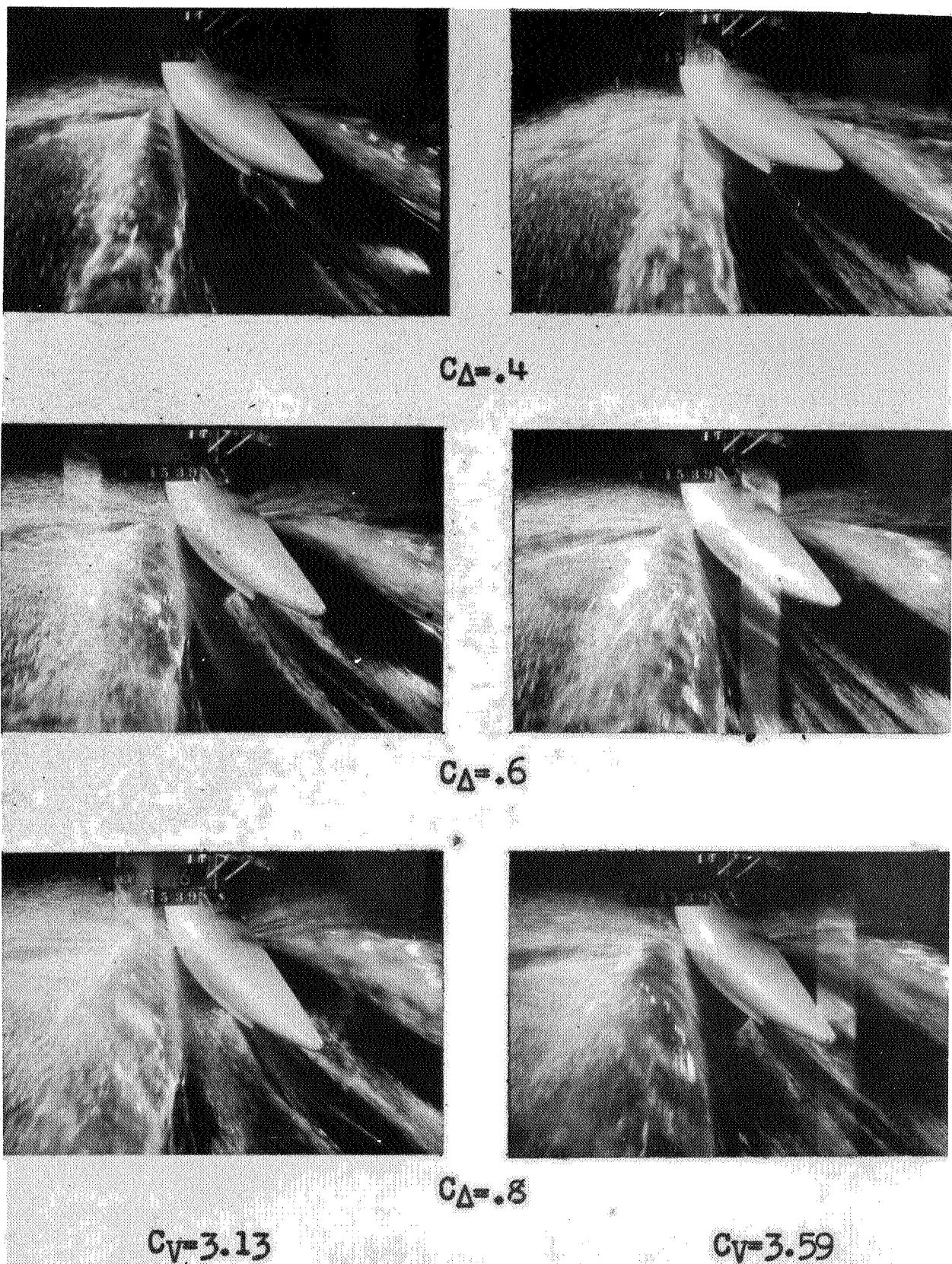


Figure 15 (c). Model 84EF.

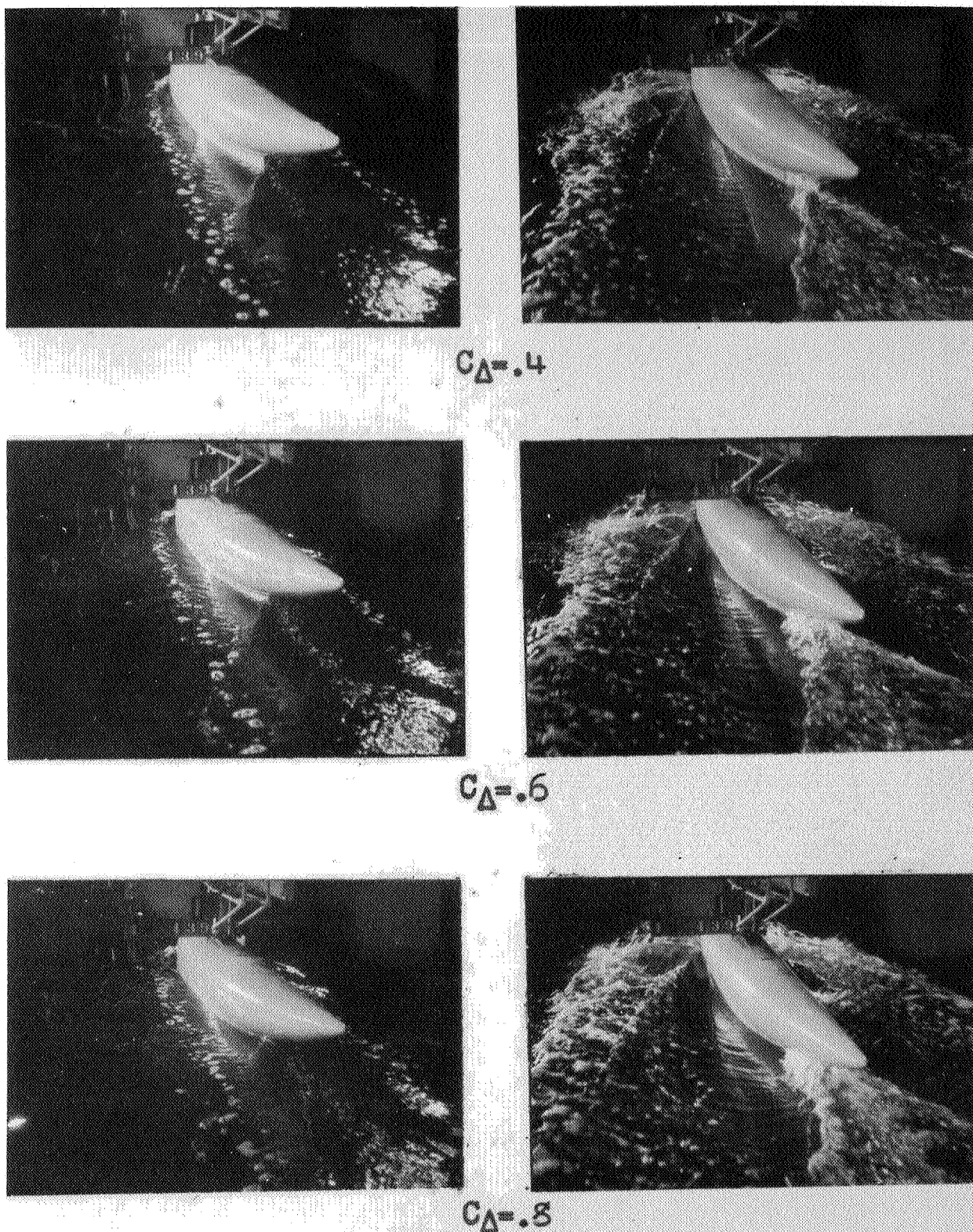

 $C_V = .70$ 
 $C_V = 1.38$ 

Figure 16 (a). Model 84E, Bow 1, Stern 4 .

Without chine flare

NACA  
20508



L-277

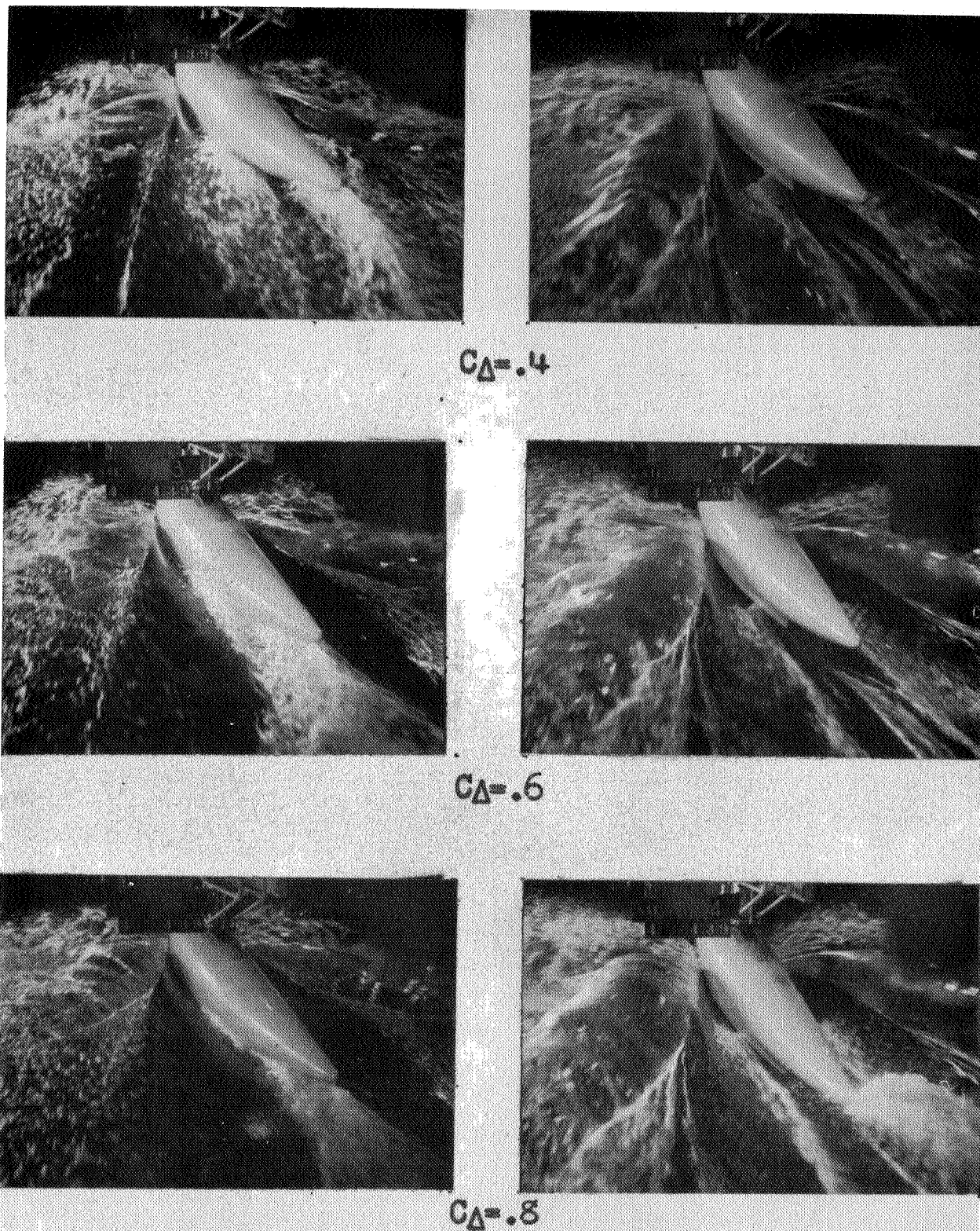
 $C_V = 2.00$  $C_V = 2.55$ 

Figure 16 (b). Model 84E

NACA  
20509

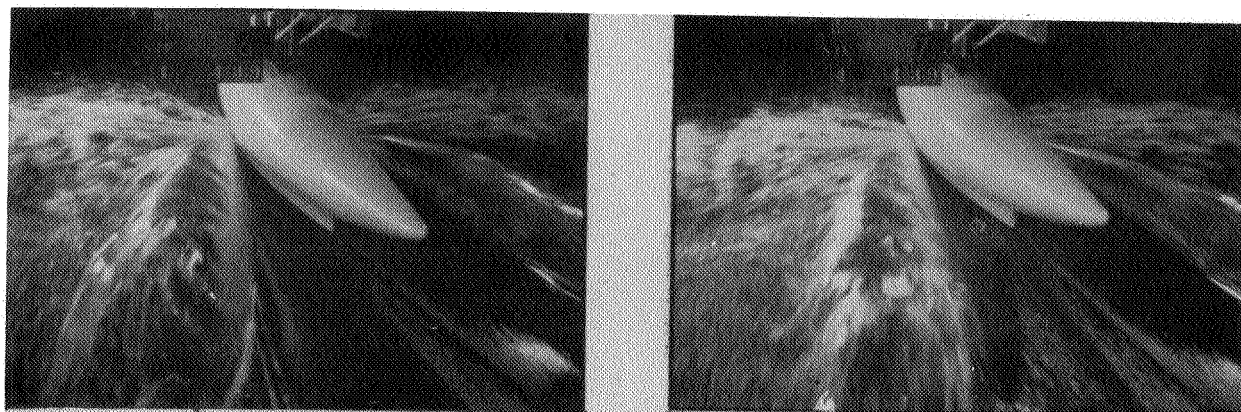
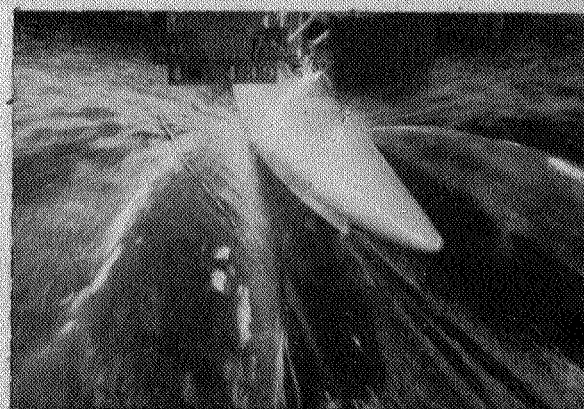
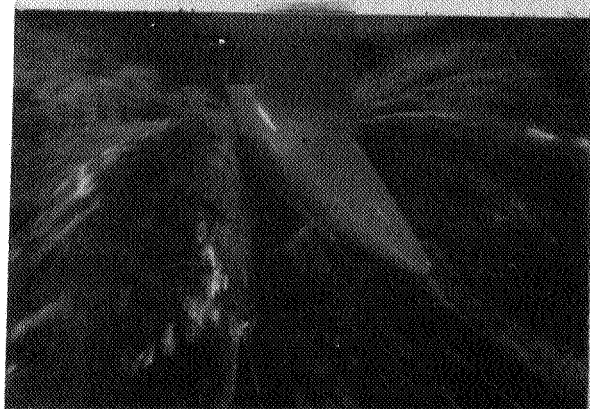
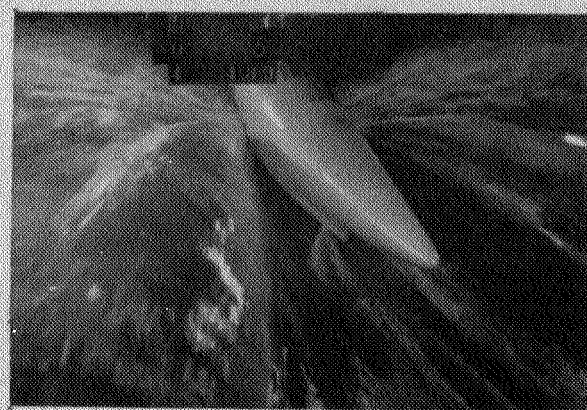
 $C_{\Delta} = .4$  $C_{\Delta} = .6$  $C_{\Delta} = .8$  $C_v = 3.31$  $C_v = 3.64$ 

Figure 16 (c). Model 84E.

NACA

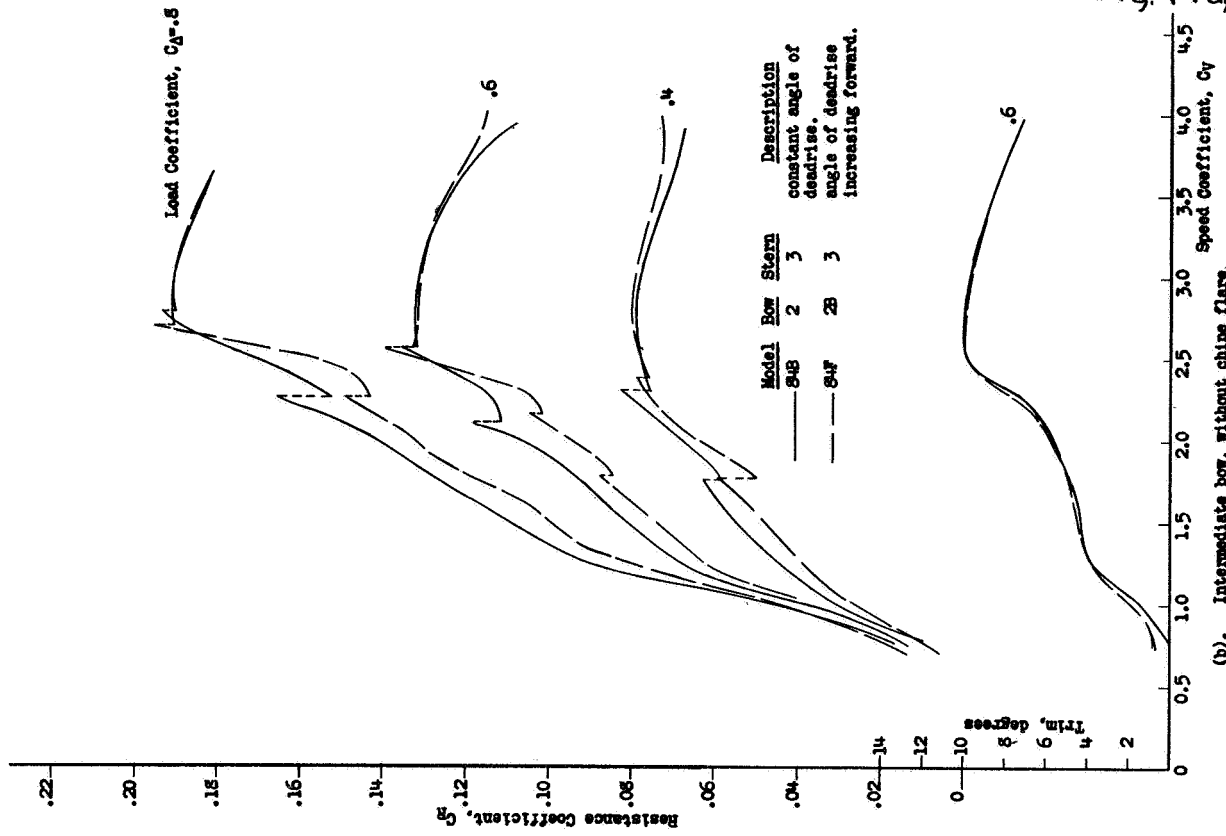
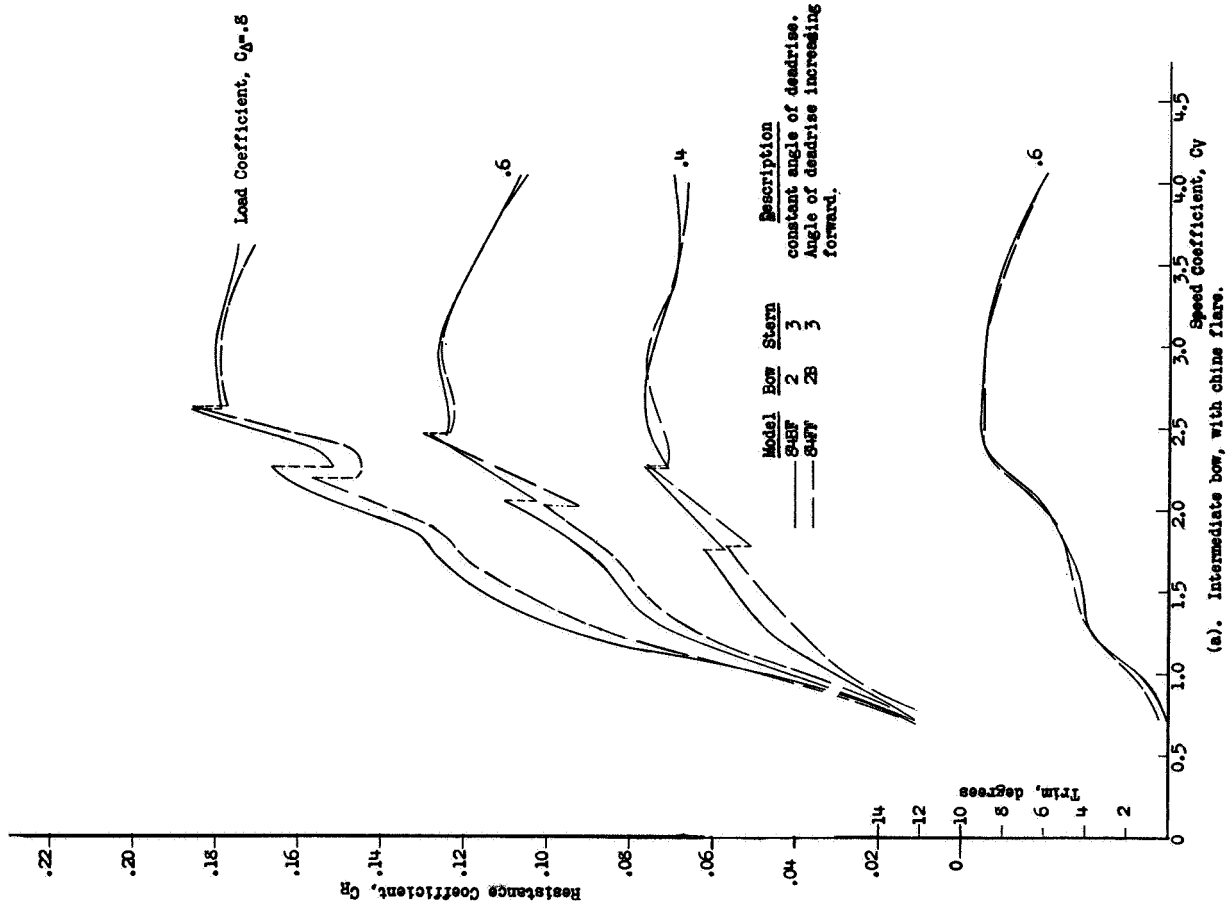


Figure 17 - Effect of angle of deadrise at bow.

Fig. 17a,b

$L=2.1$

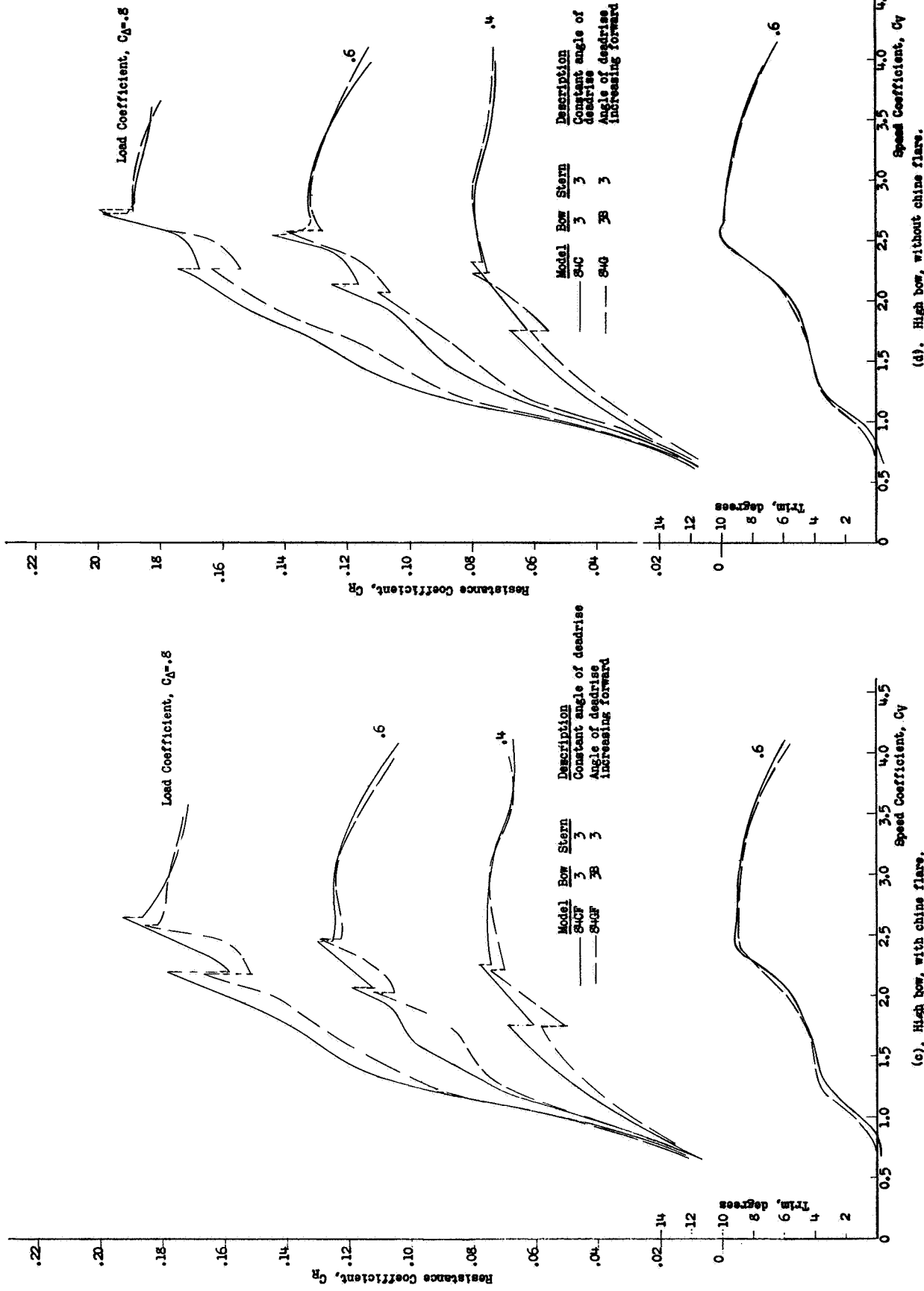


Figure 17. - Effect of angle of deadrise at bow.



L-277

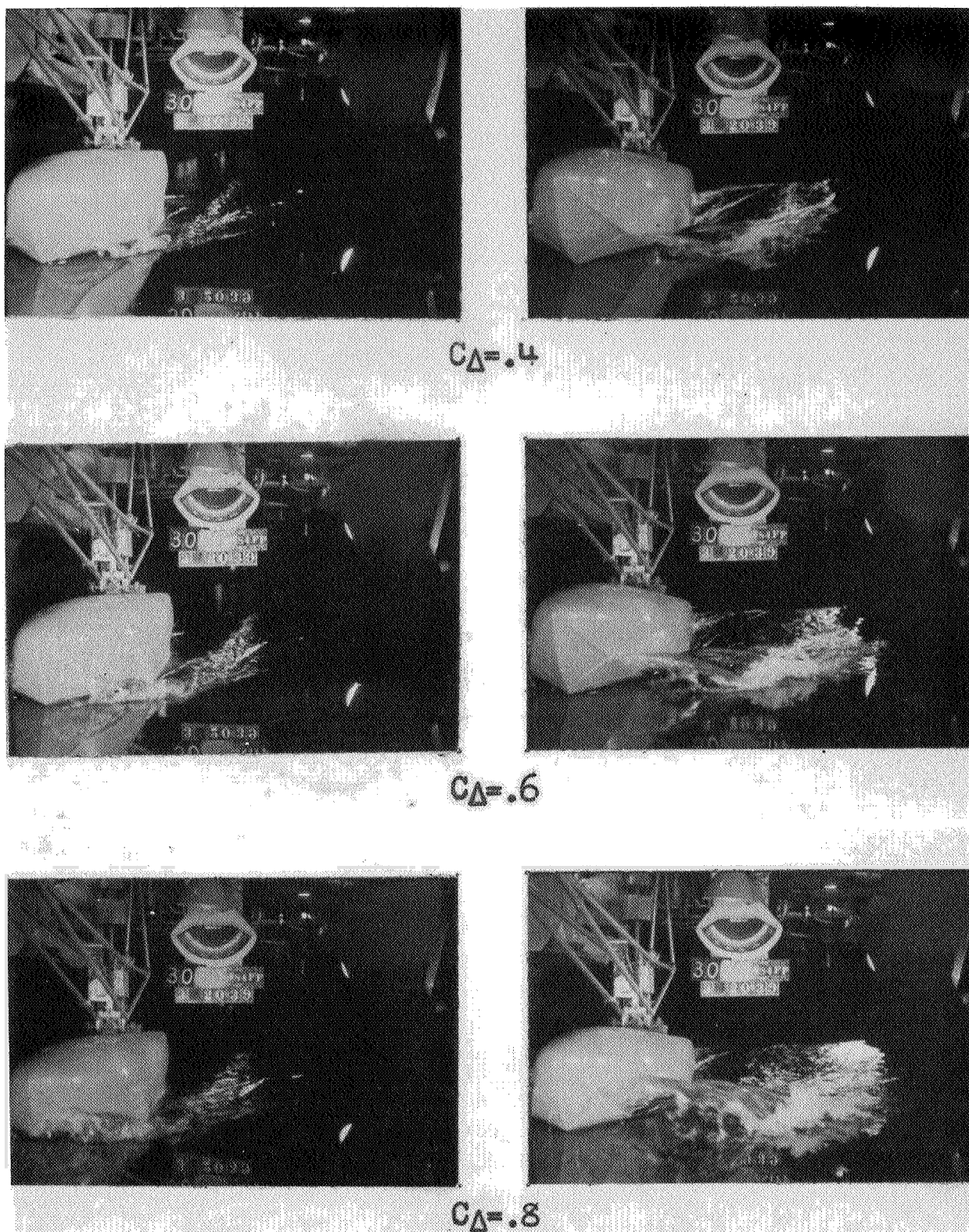
 $C_v = .78$  $C_v = 1.22$ 

Figure 18 (a). Model 84FF, Bow 2B, Stern 3.  
With chine flare

NACA  
20511



L-277

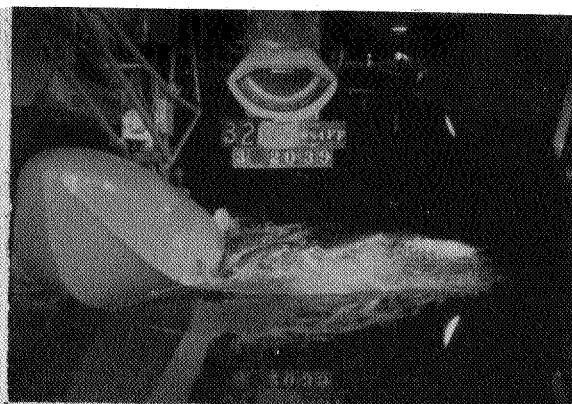
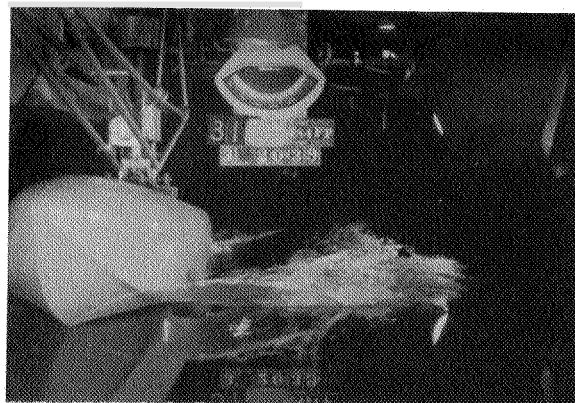
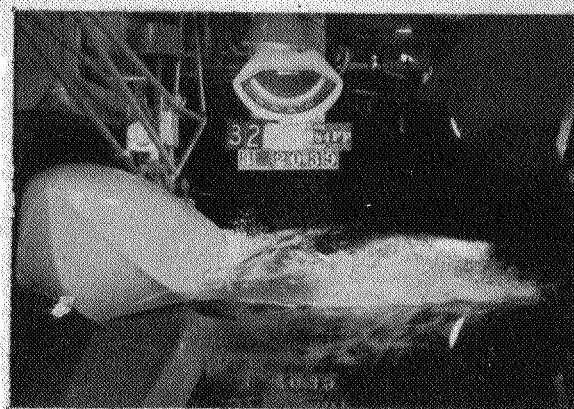
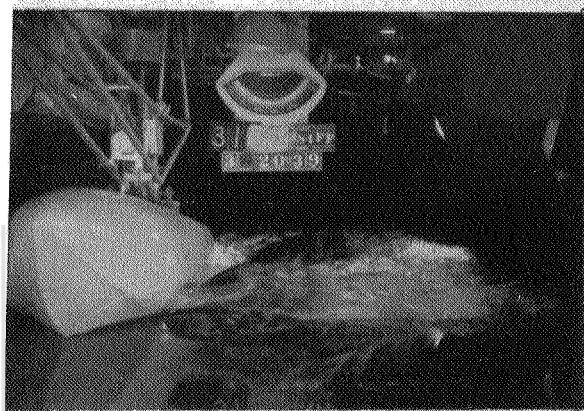
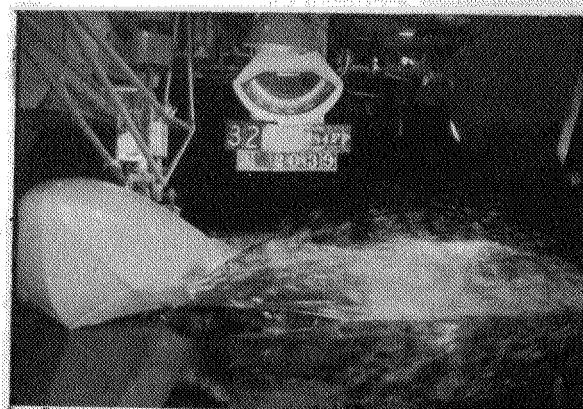
 $C_{\Delta} = .4$  $C_{\Delta} = .6$  $C_{\Delta} = .8$  $C_v = 1.70$  $C_v = 2.15$ 

Figure 18(b). Model 84FF.

L-277

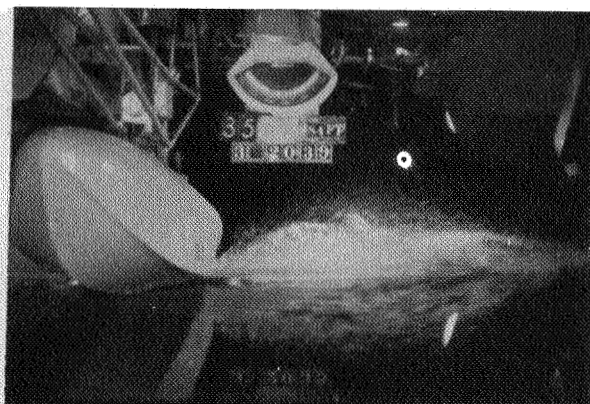
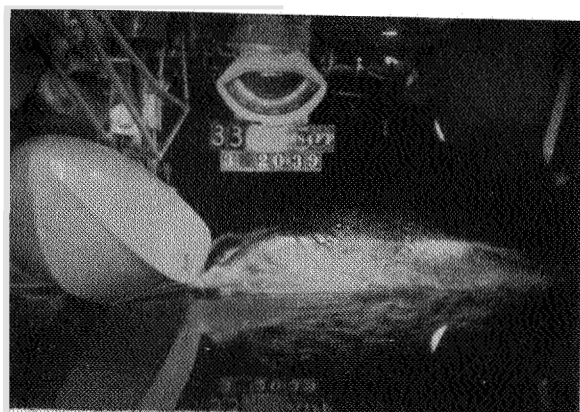
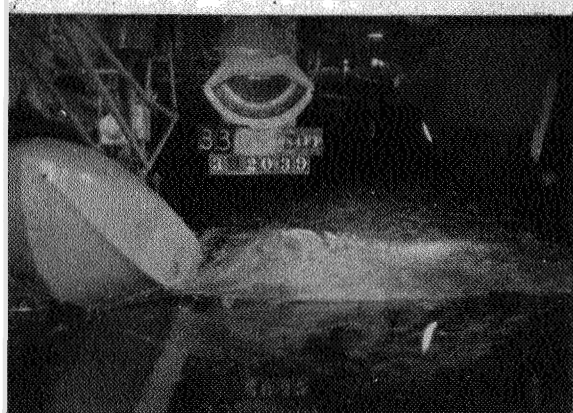
 $C_D = .4$  $C_D = .6$  $C_D = .8$  $C_V = 2.62$  $C_V = 3.12$ 

Figure 18(c). Model 84FF

NACA  
20513



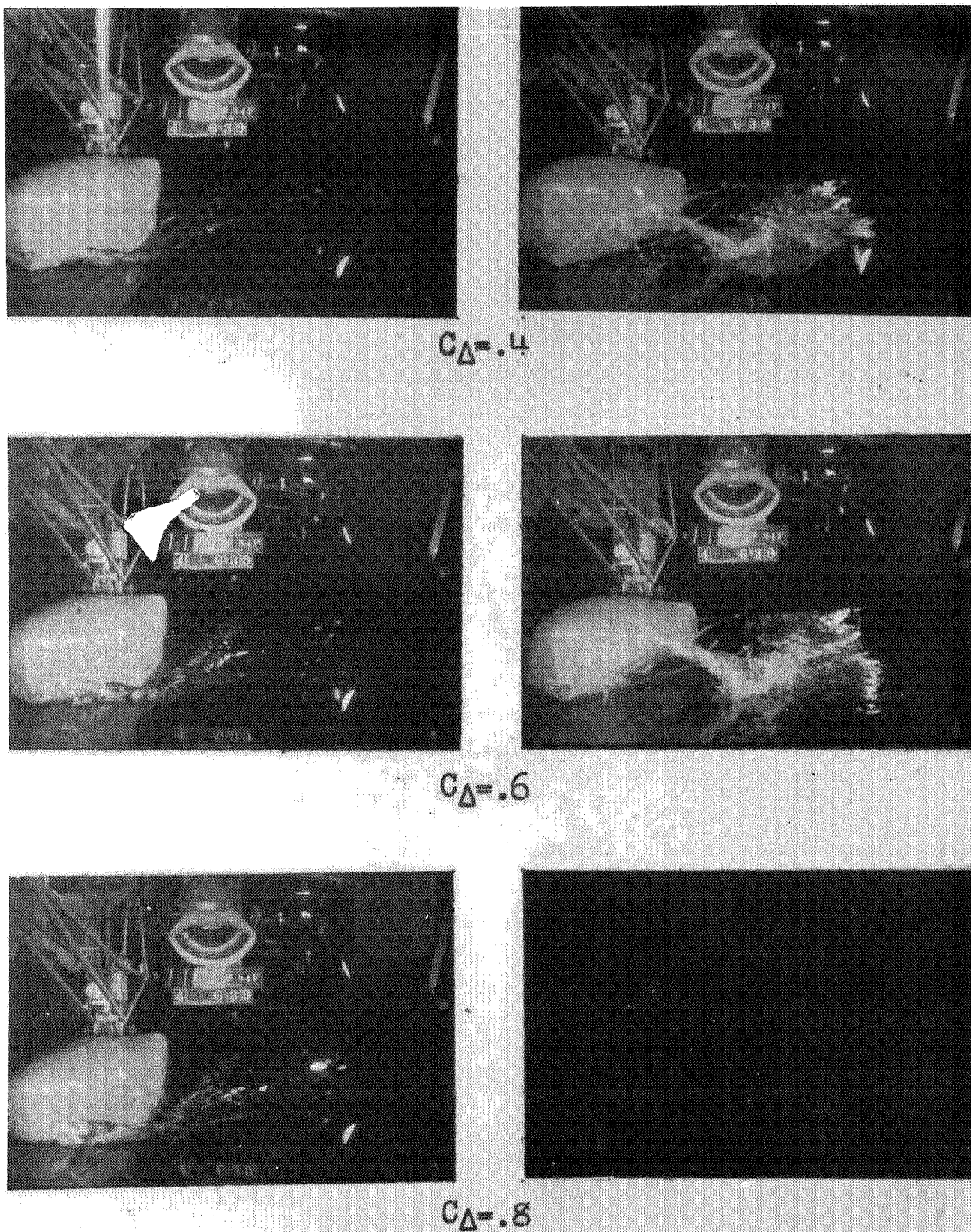
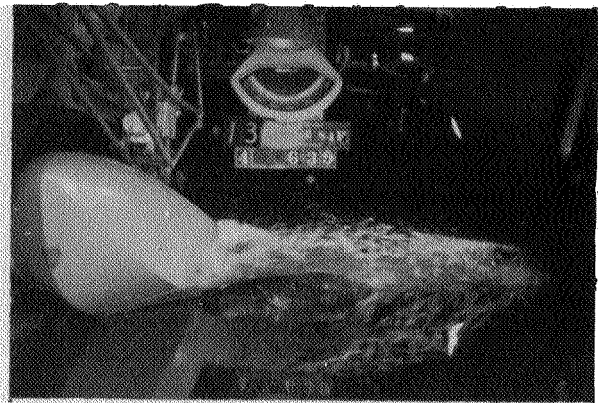
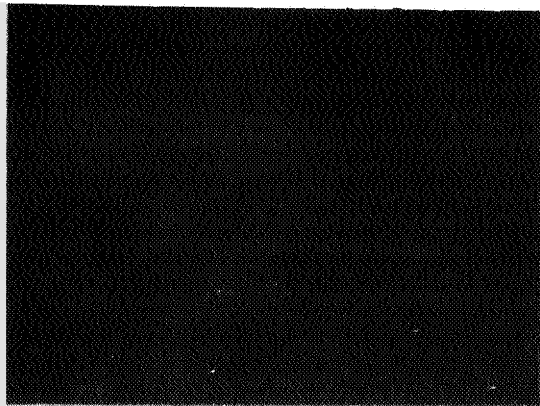
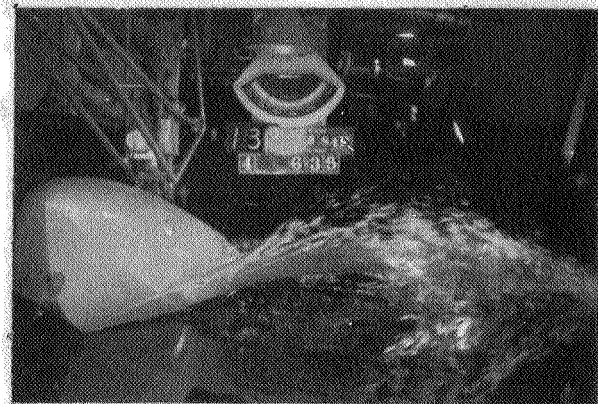
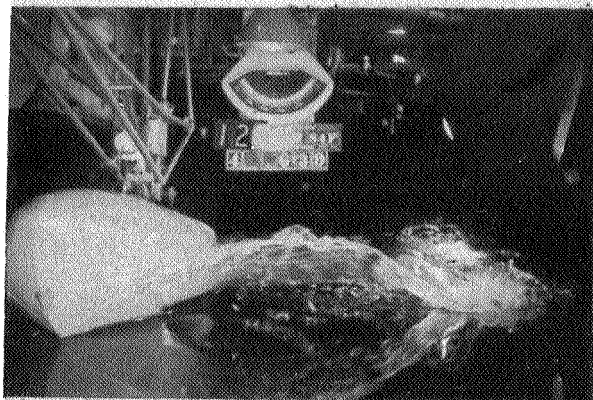


Figure 19(a). Model 84F, Bow 2B, Stern 3.  
Without chine flare

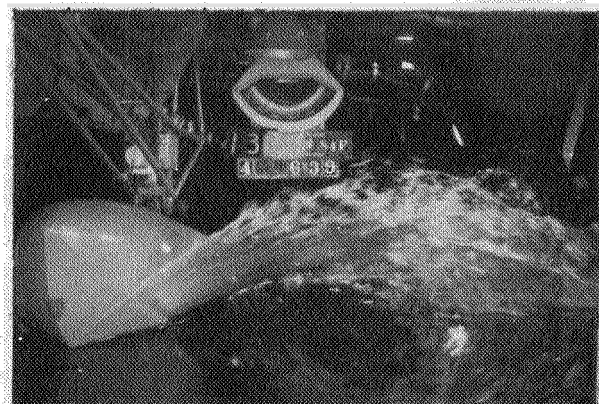
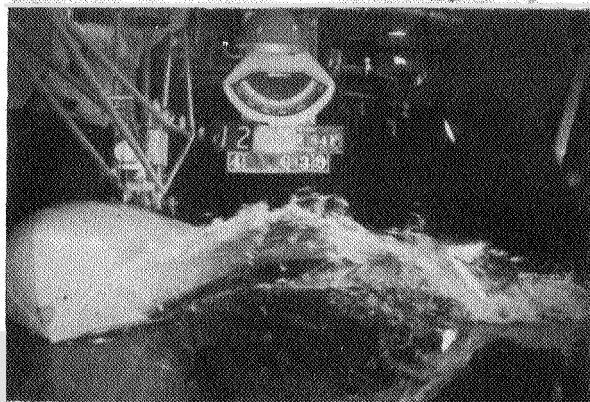
L-277



$C_D = .4$



$C_D = .6$



$C_D = .8$

$C_V = 1.70$

$C_V = 2.10$

Figure 19 (b). Model 84F.



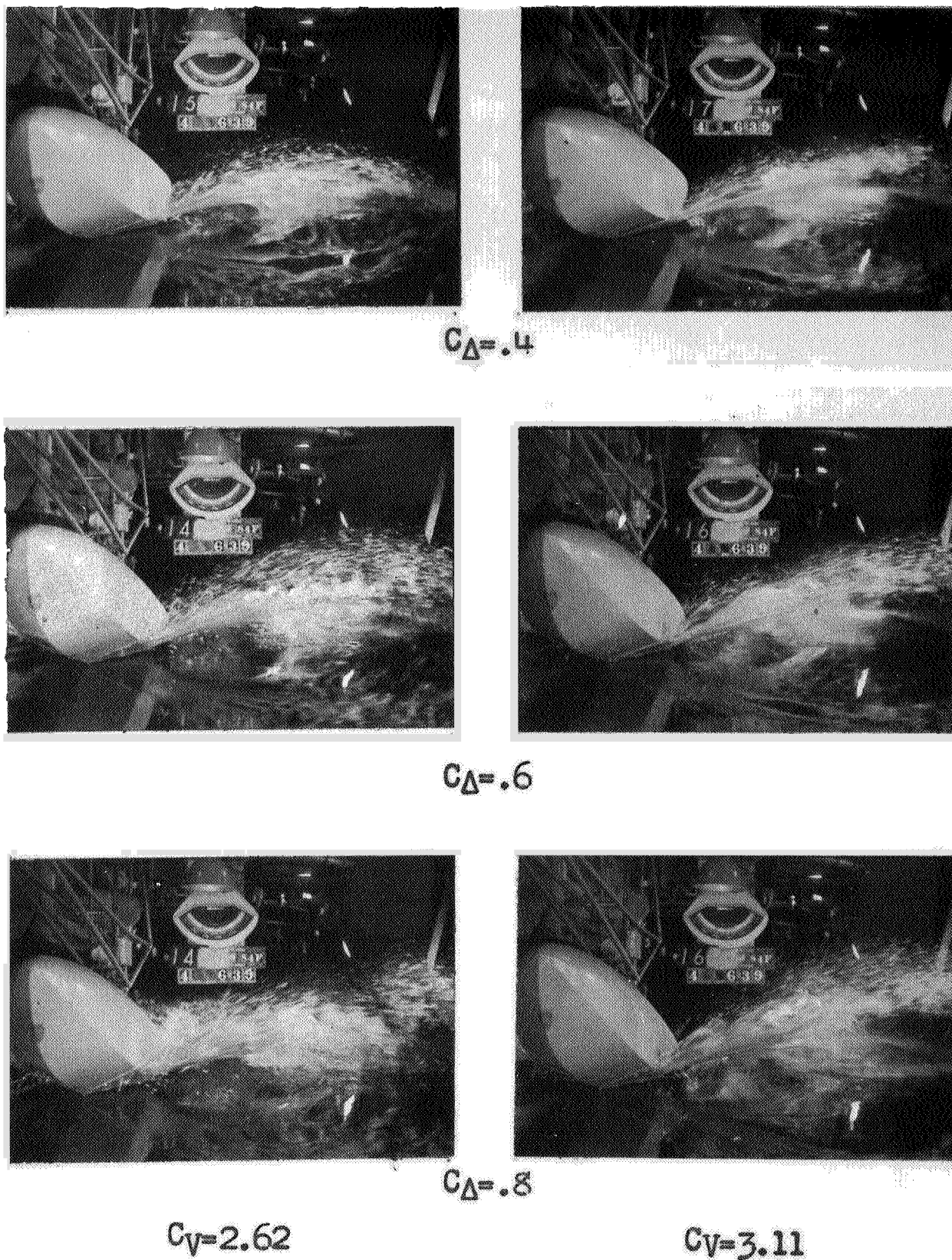


Figure 19 (c). Model 84F



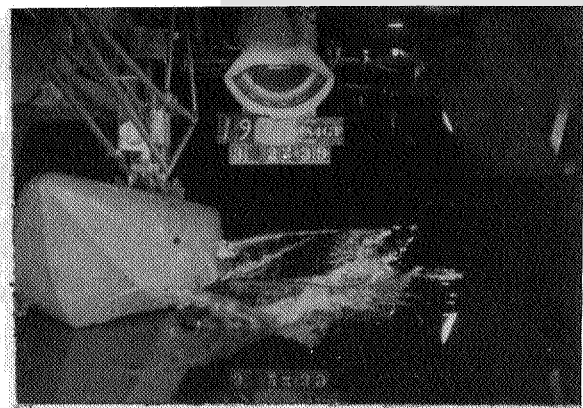
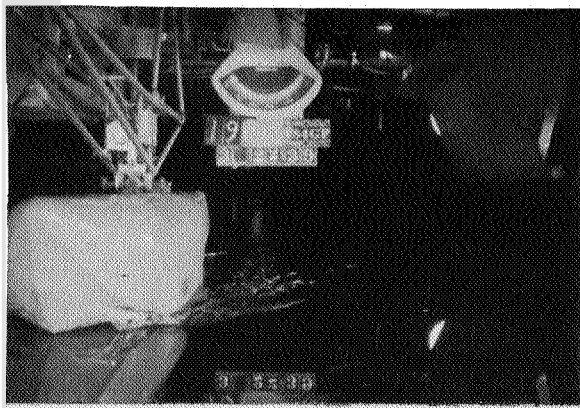
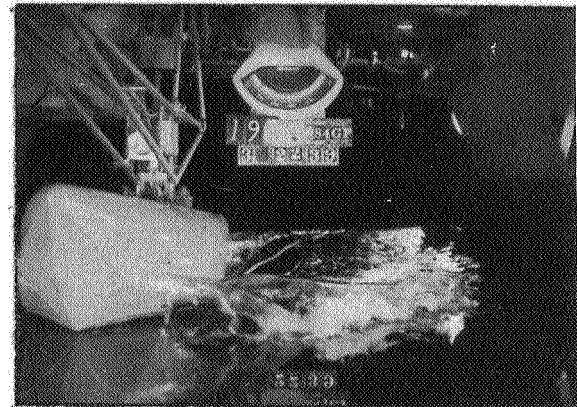
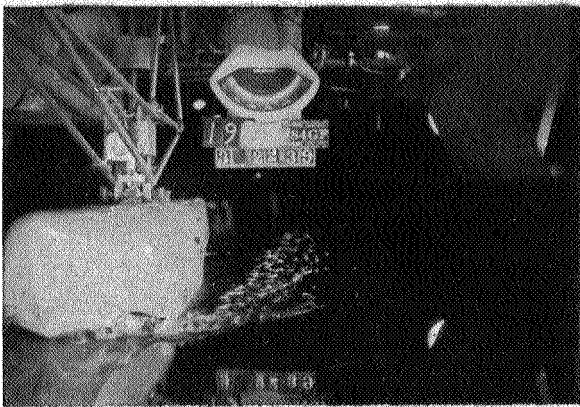
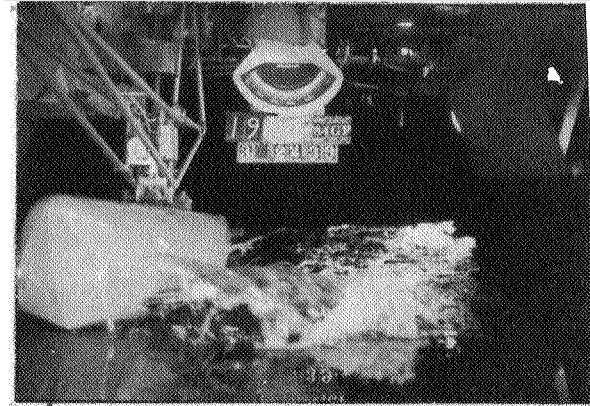

 $C_D = .4$ 

 $C_D = .6$ 

 $C_D = .8$ 
 $C_V = .71$ 
 $C_V = 1.20$ 

Figure 20(a). Model 84GF, Bow 3B, Stern 3.  
With chine flare.

NACA  
20520

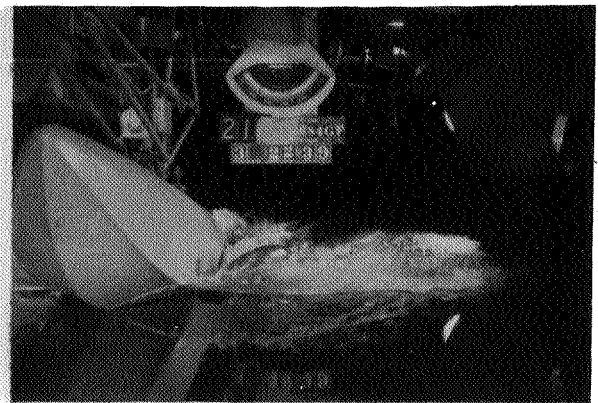
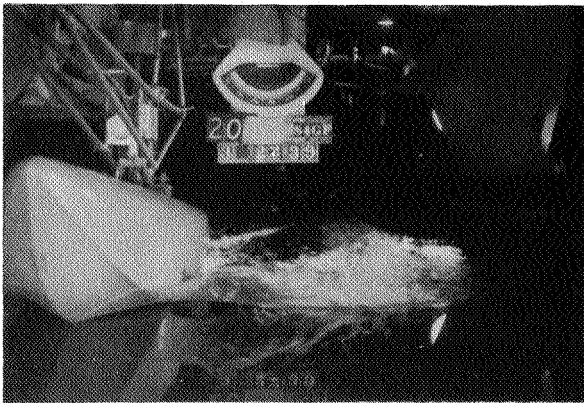
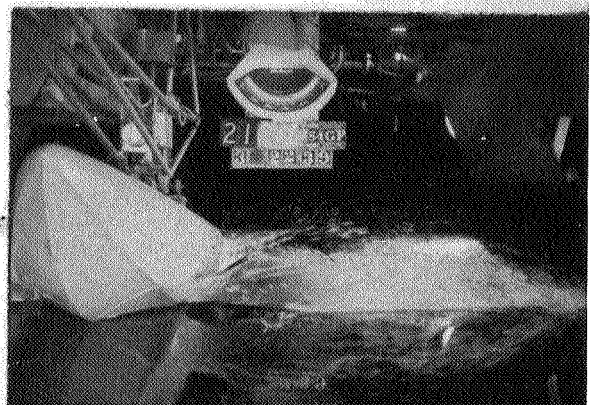
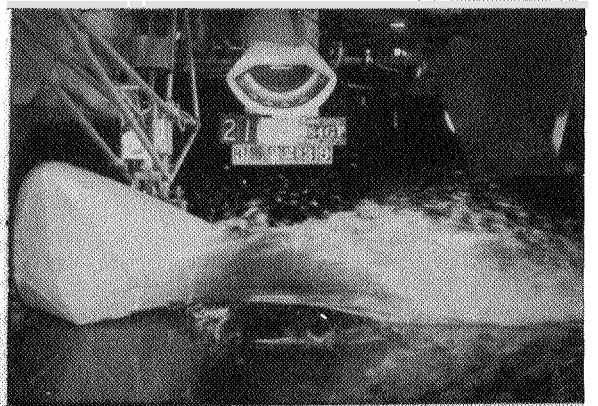

 $C_D = .4$ 

 $C_D = .6$ 

 $C_D = .8$ 
 $C_V = 1.79$ 
 $C_V = 2.08$ 

Figure 20 (b). Model 84GF.

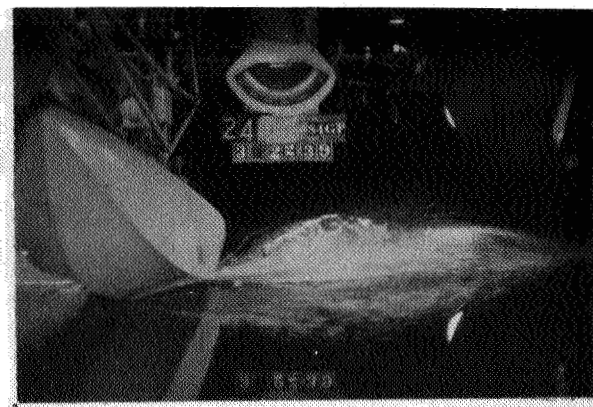
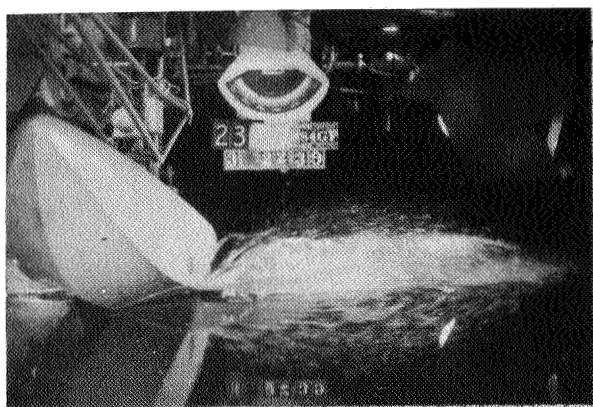
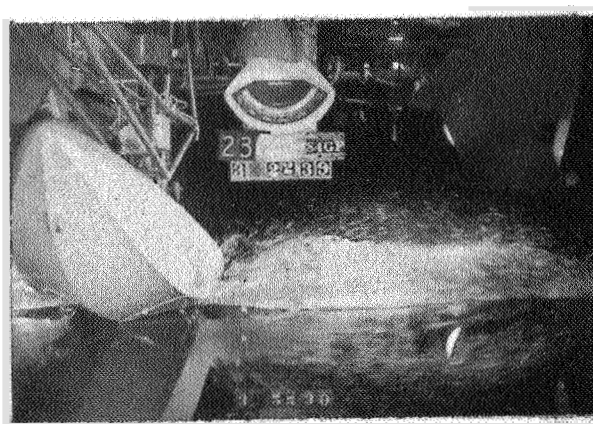
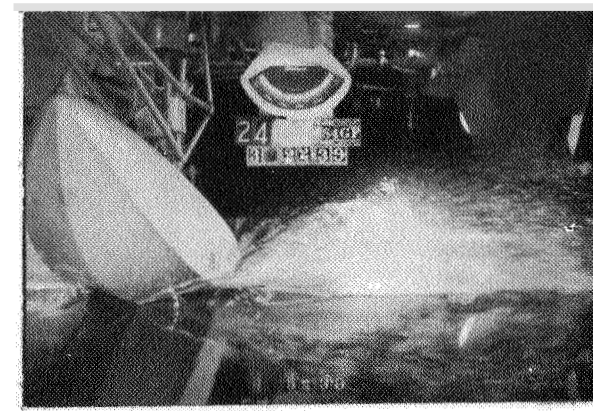

 $C_D = .4$ 

 $C_D = .6$ 

 $C_D = .8$ 
 $C_V = 2.60$ 
 $C_V = 3.05$ 

Figure 20(c). Model 84GF



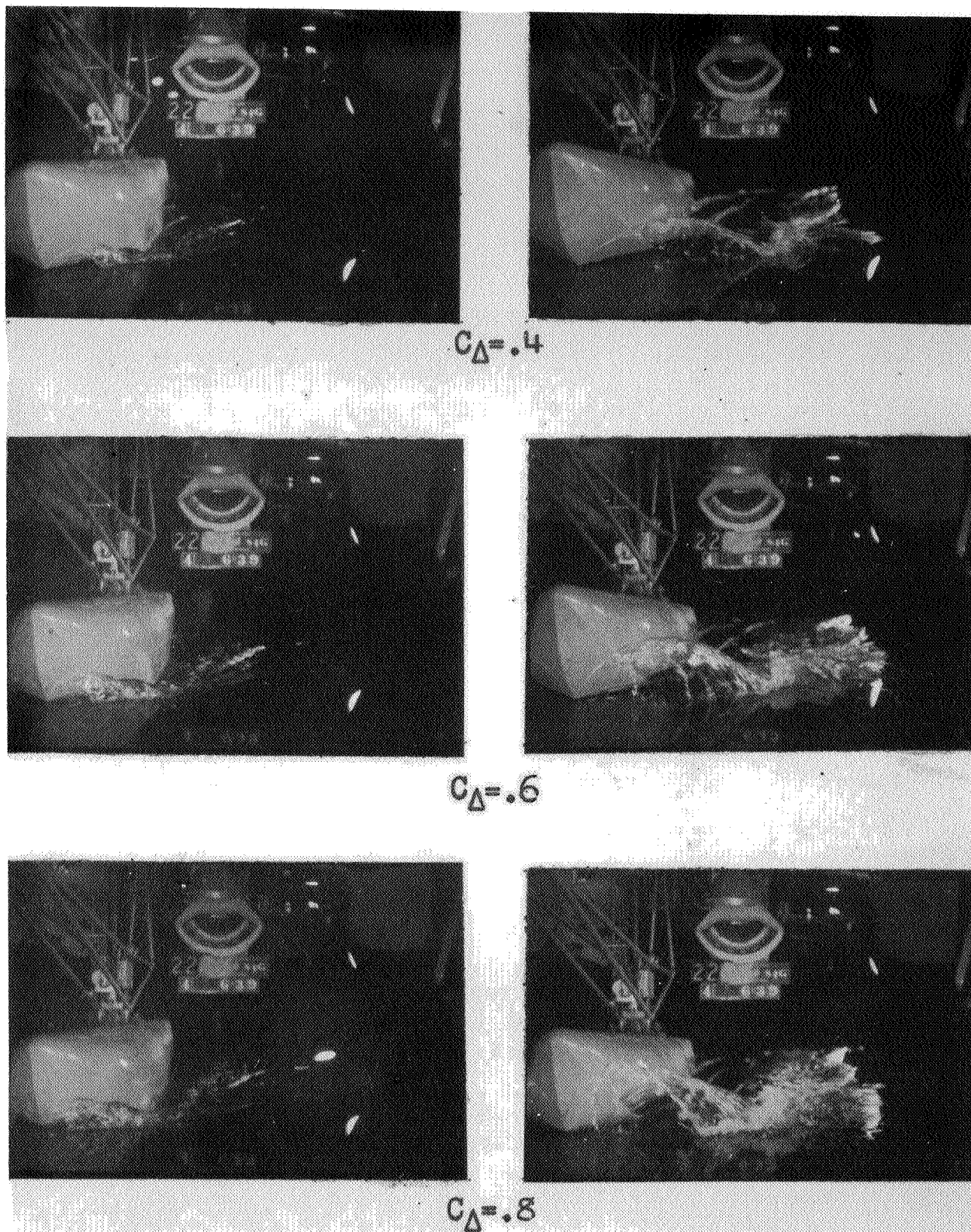
 $C_V = .75$  $C_V = 1.18$ 

Figure 21 (a). Model 84G, Bow 3B, Stern 3  
Without chine flare

L-277

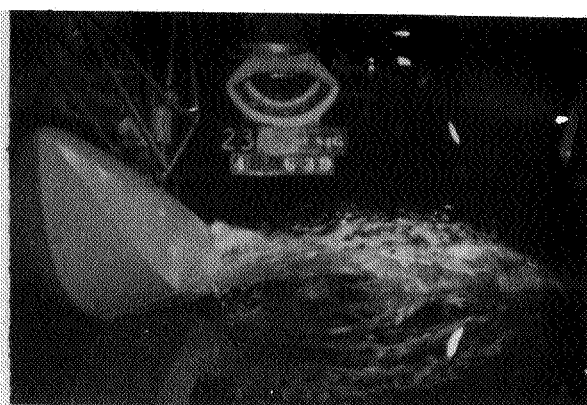
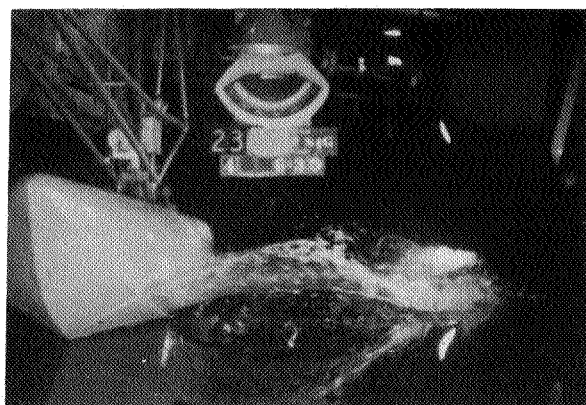
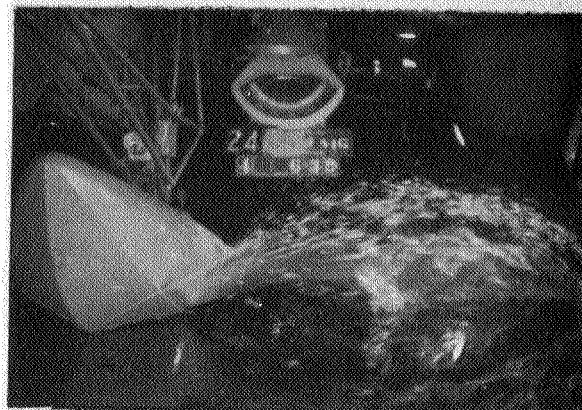
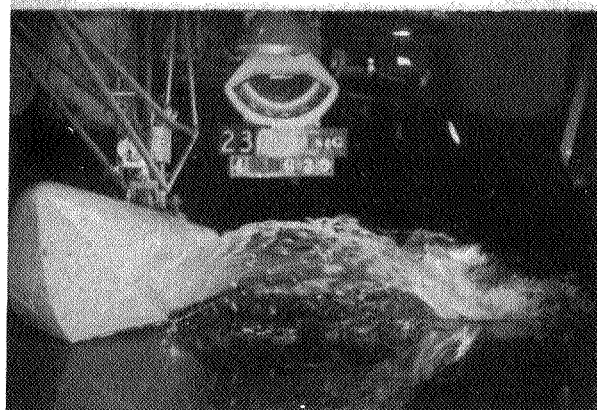
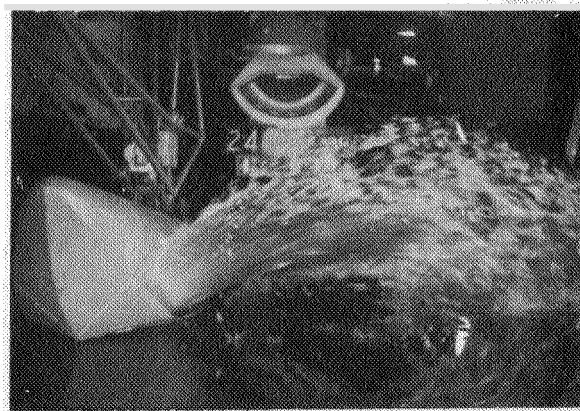
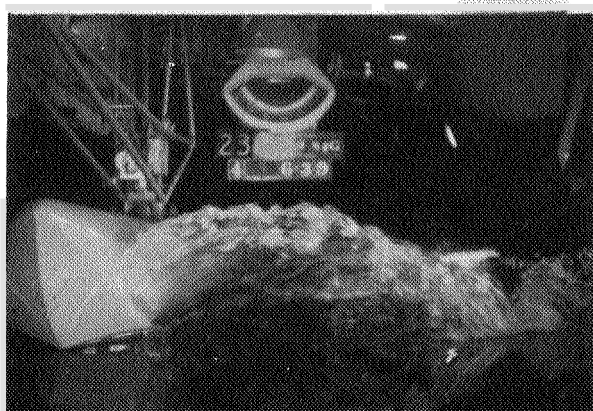
 $C_\Delta = .4$  $C_\Delta = .6$  $C_\Delta = .8$  $C_V = 1.64$  $C_V = 2.14$ 

Figure 21(b). Model 84G

NACA  
20525



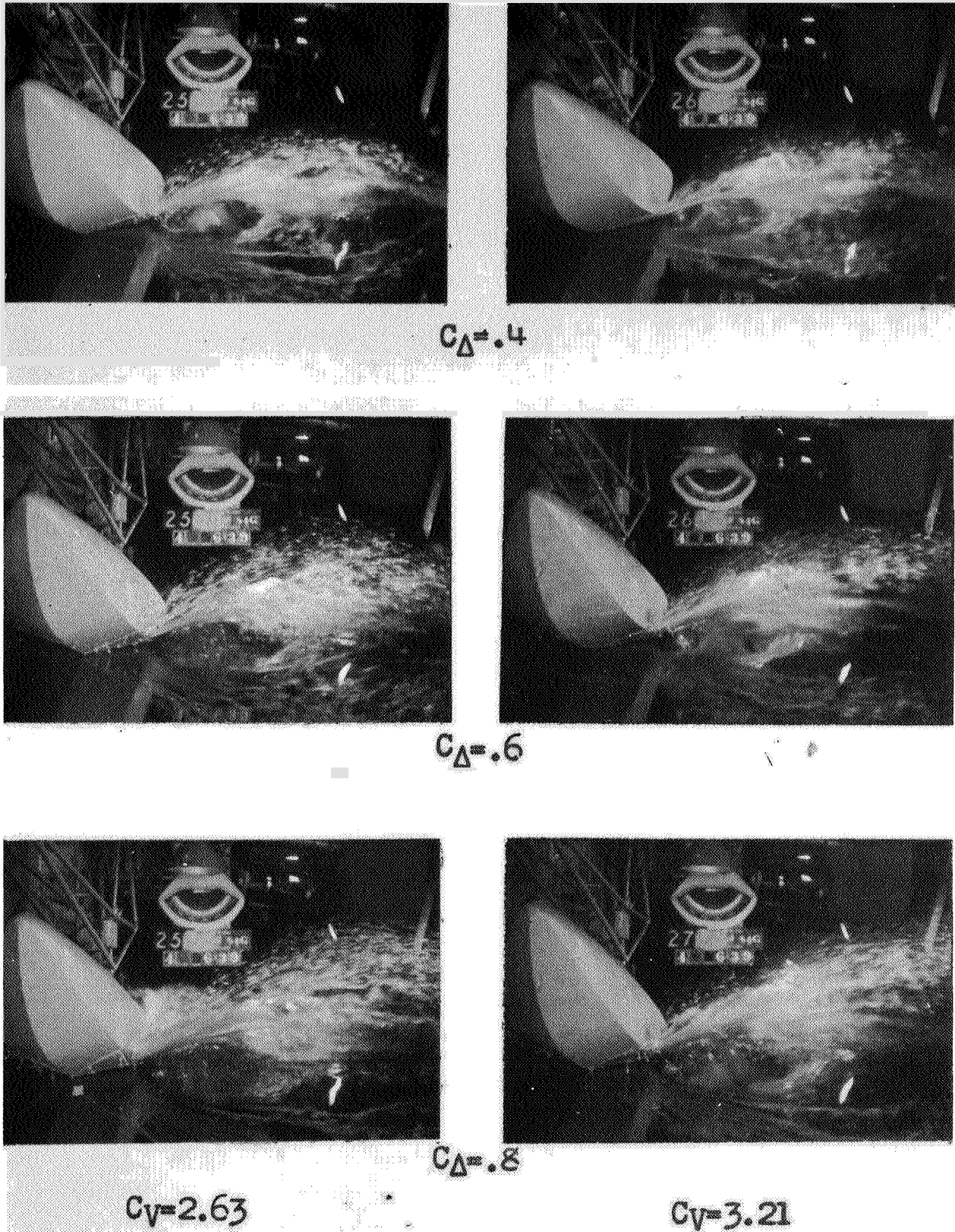


Figure 21 (c). Model 84G

Fig. 22

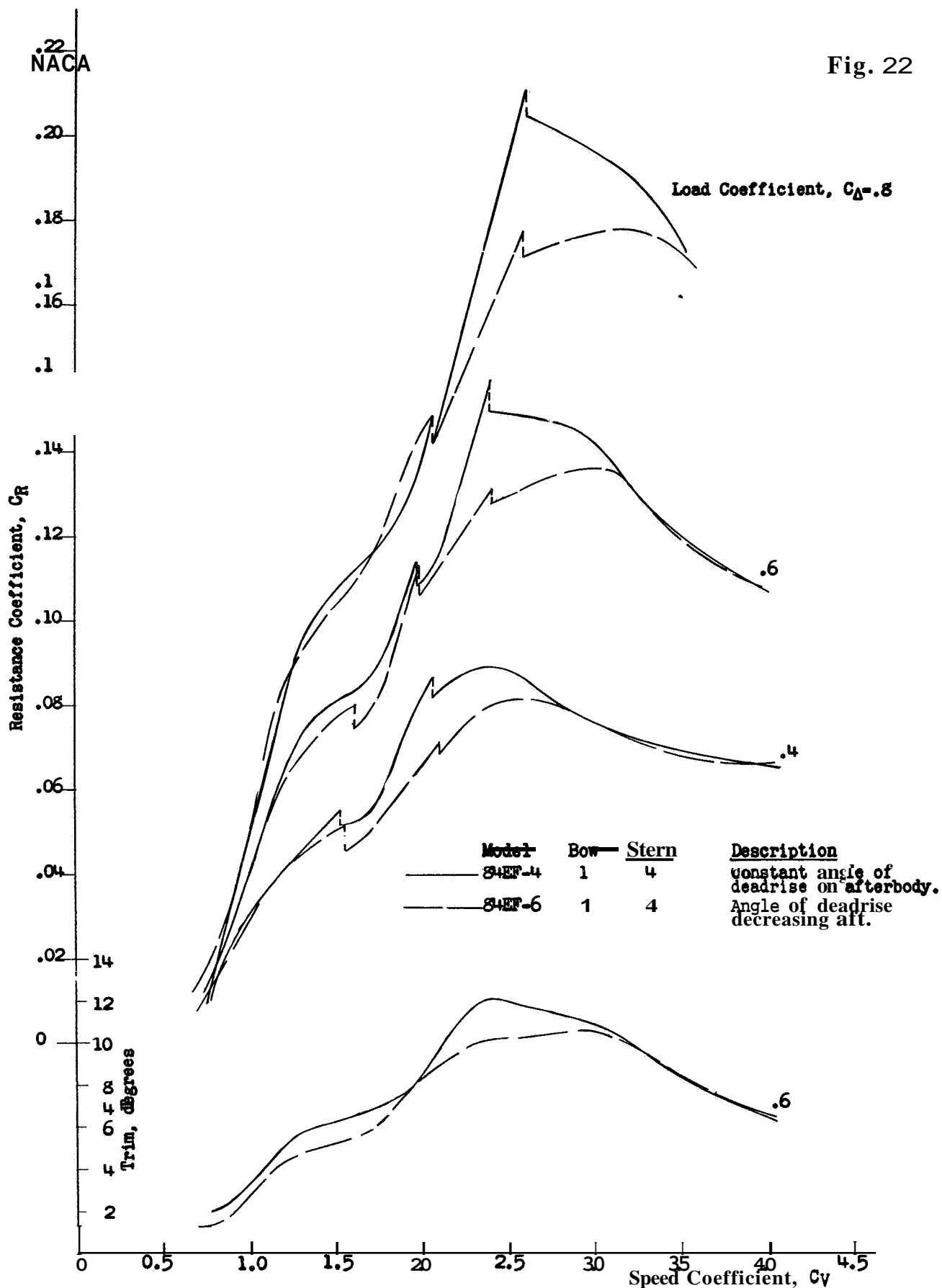


Figure 22 . Effect of decreasing angle of deadrise on afterbody, .40 in. depth of step; 7.25 deg. angle of afterbody keel. Chine flare on forebody only.

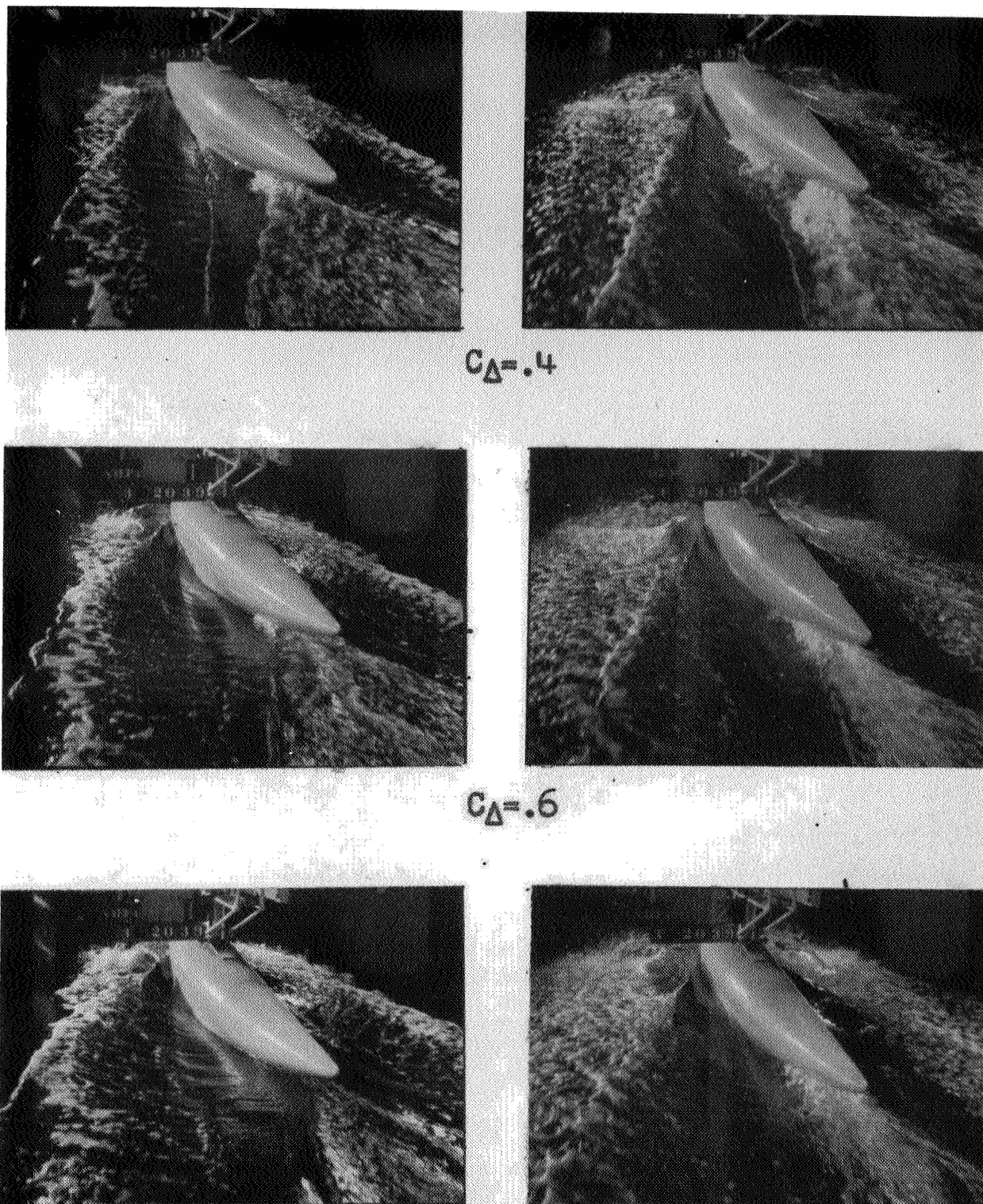
 $C_D = .4$  $C_D = .6$  $C_D = .8$  $C_V = 1.25$  $C_V = 1.71$ 

Figure 23(a). Model 84EF-4, Bow 1, Stern 4.  
 Depth of step .40 in., Angle of afterbody keel  $7.25^\circ$   
 Chine flare on forebody only.

NACA  
 20527



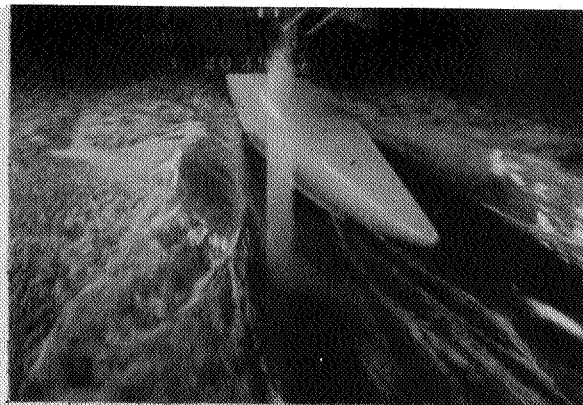
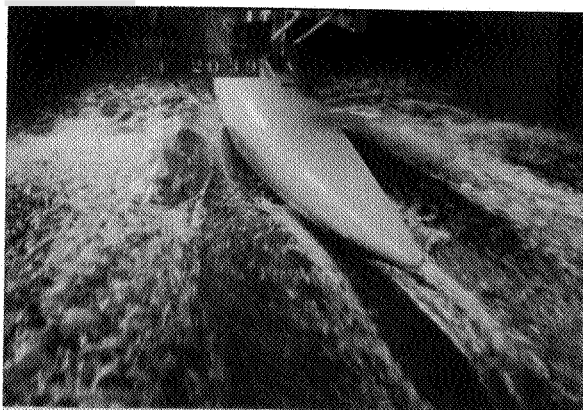
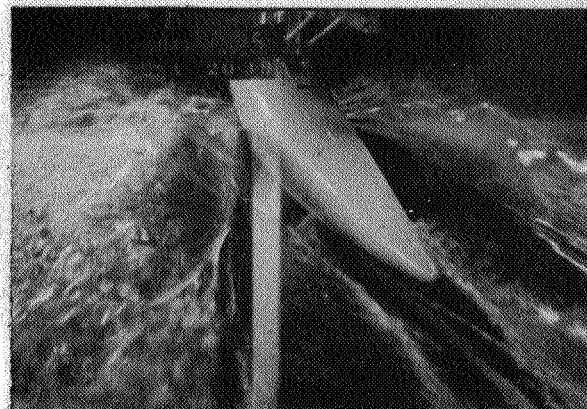
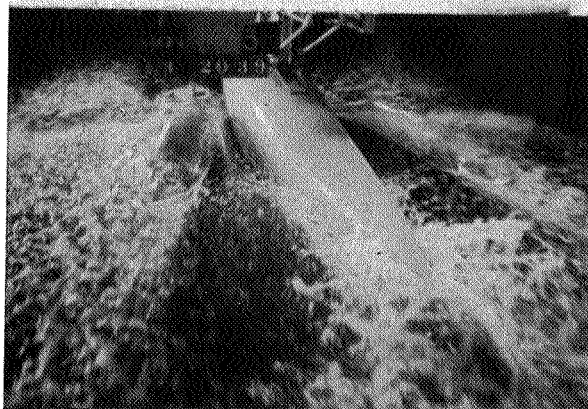
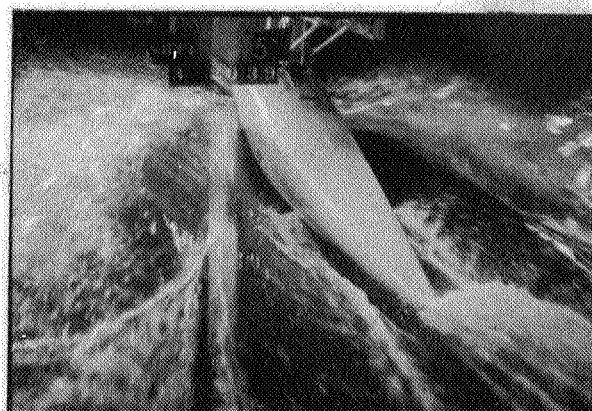
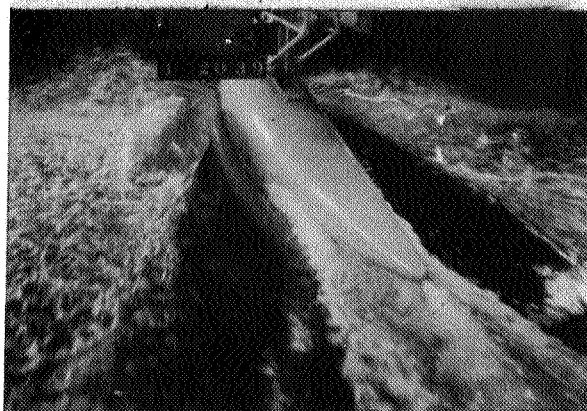
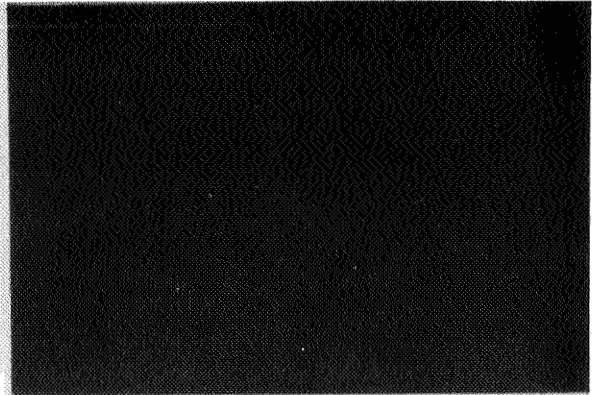
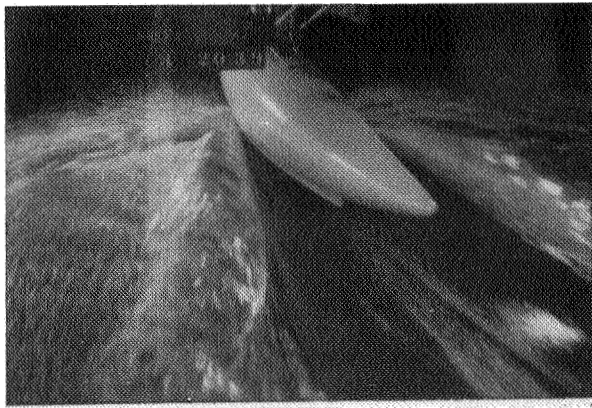
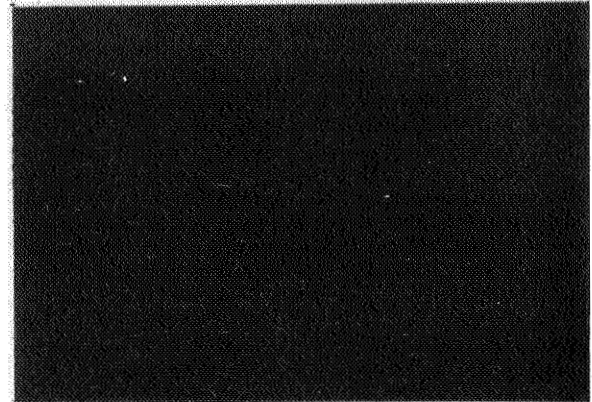
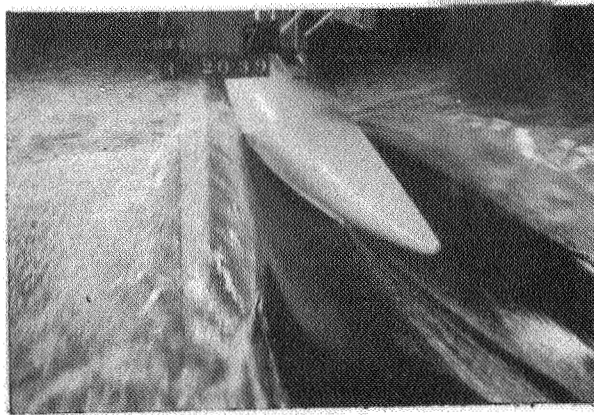
 $C_D = .4$  $C_D = .6$  $C_D = .8$  $C_V = 2.13$  $C_V = 2.59$ 

Figure 23 (b). Model 84EF-4.

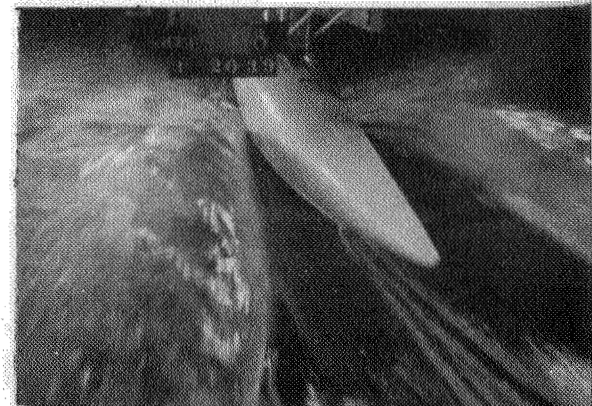
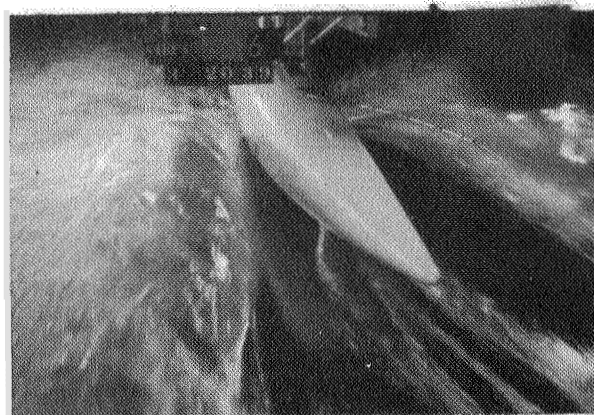




$C_D = .4$



$C_D = .6$



$C_D = .8$

$C_V = 3.21$

$C_V = 3.50$

Figure 23 (c). Model 84EF-4.

NACA  
20529

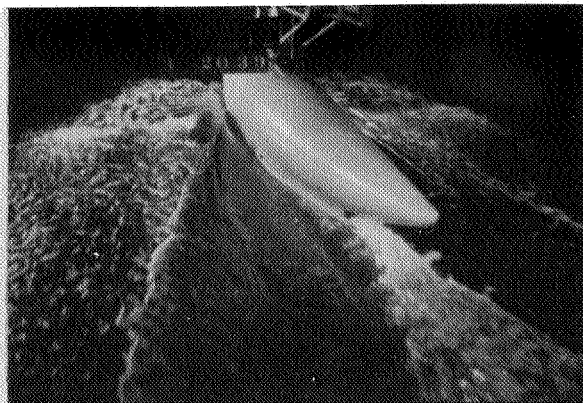
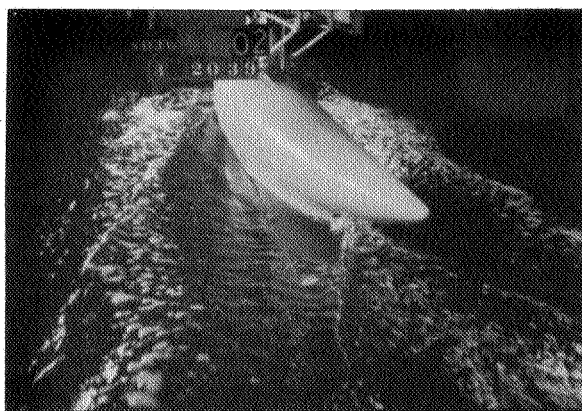
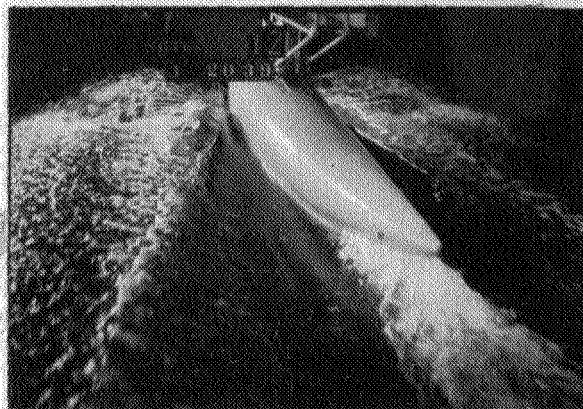
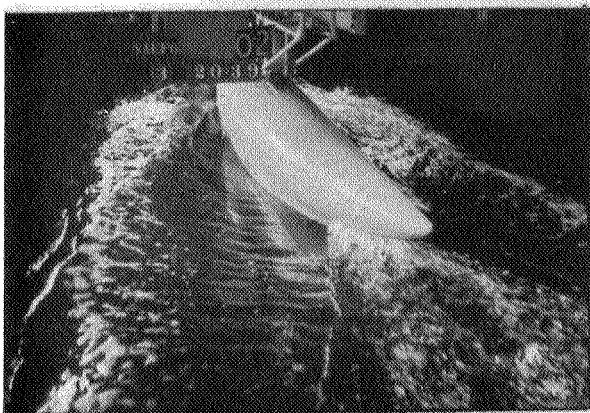
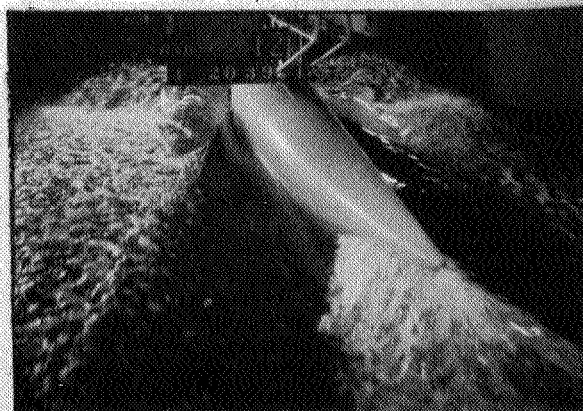
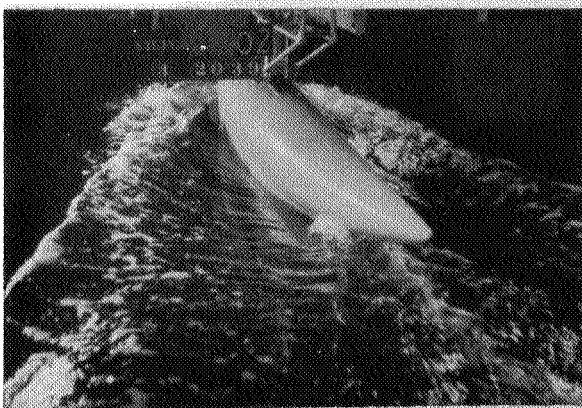

 $C_{\Delta} = .4$ 

 $C_{\Delta} = .6$ 

 $C_{\Delta} = .8$ 
 $C_V = 1.17$ 
 $C_V = 1.76$ 

Figure 24(a). Model 84EF-6, Bow 1, Stern 4.  
 Depth of step .40 in., Angle of afterbody keel  $7.25^\circ$   
 Chine flare on forebody only.

 NACA  
 20530

L-277



L-277

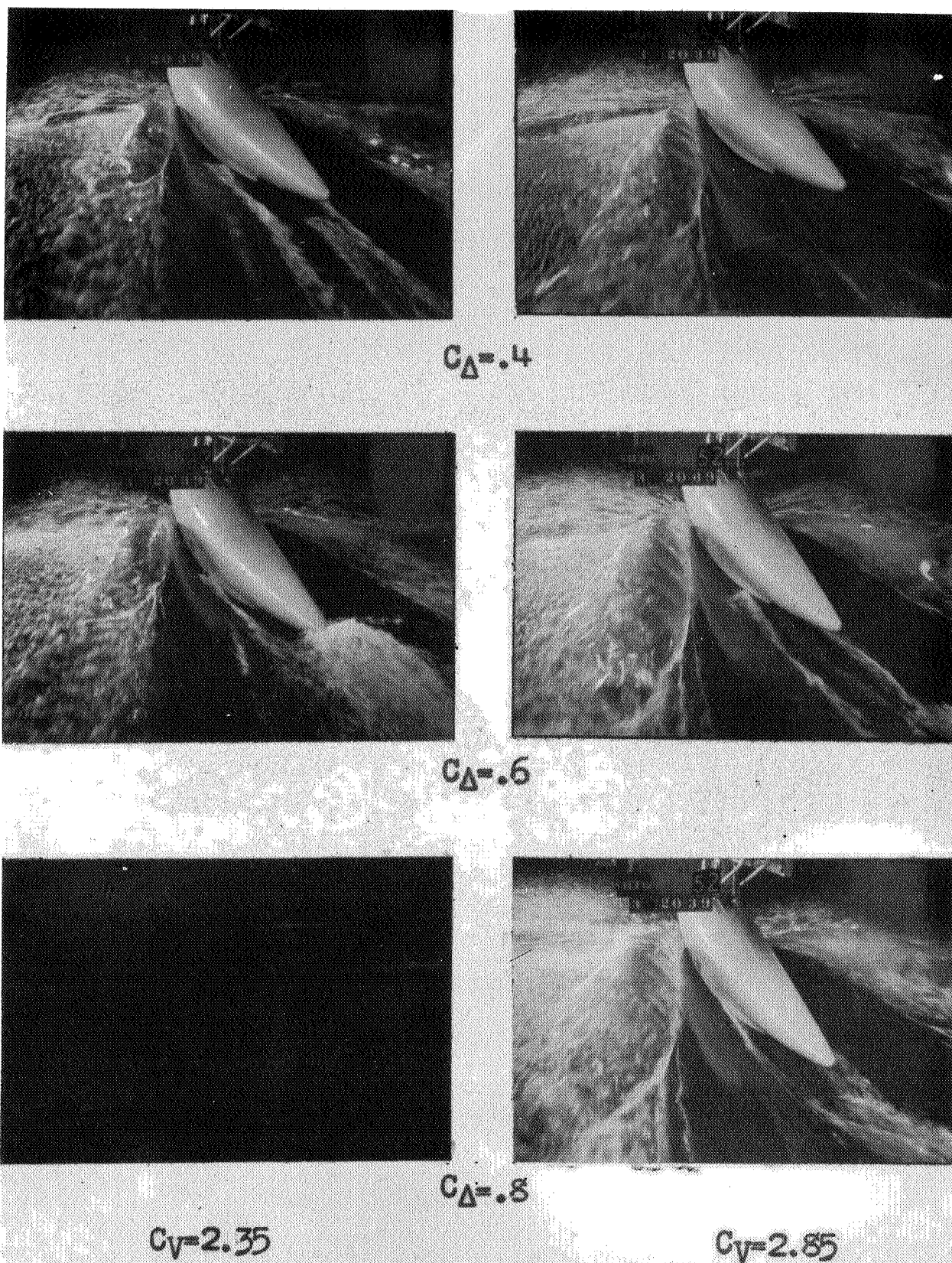


Figure 24(b). Model 84EF-6.

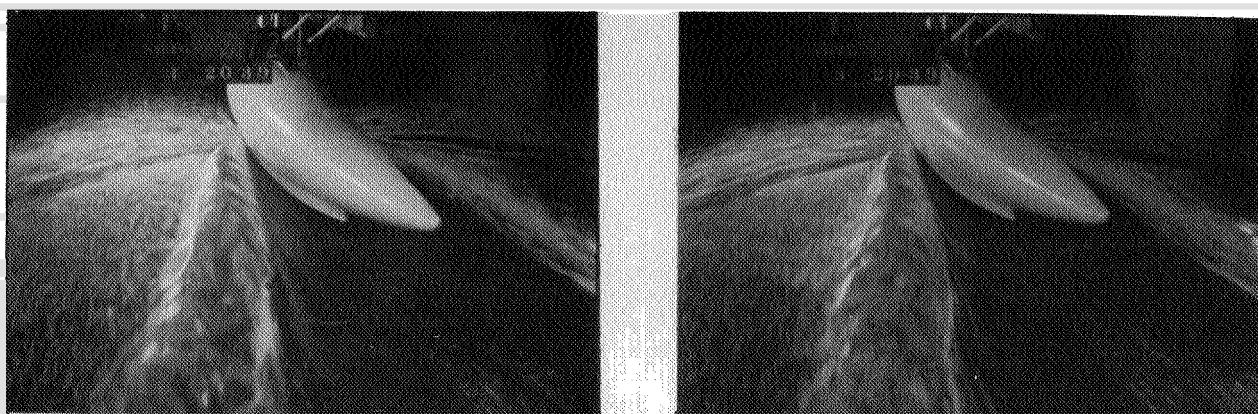
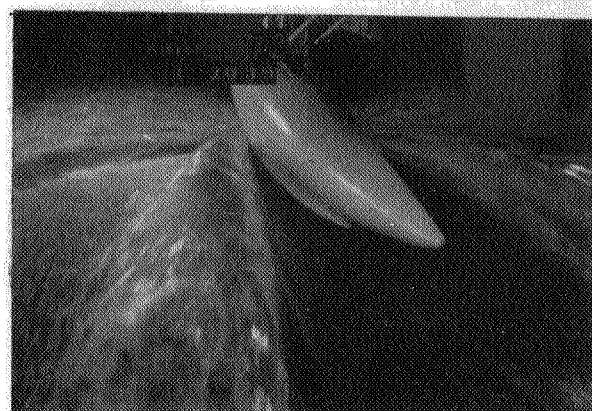
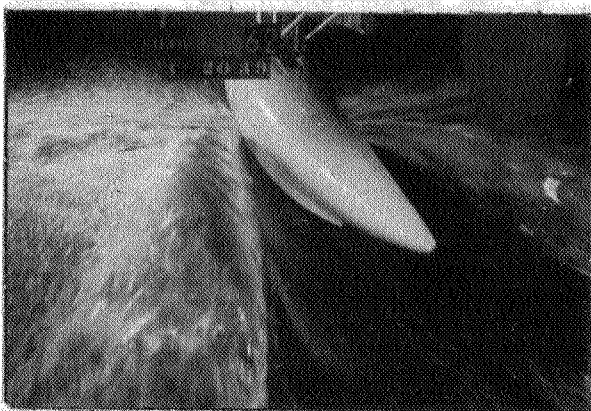
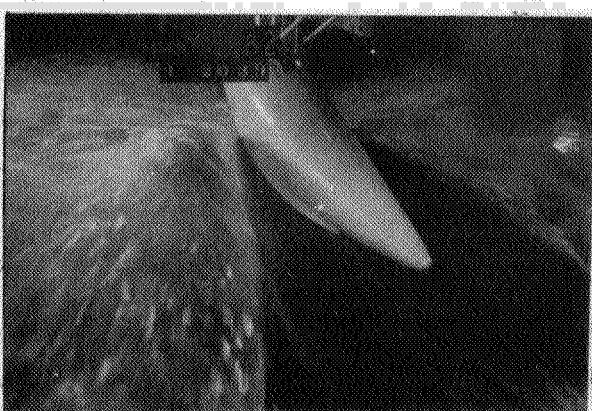
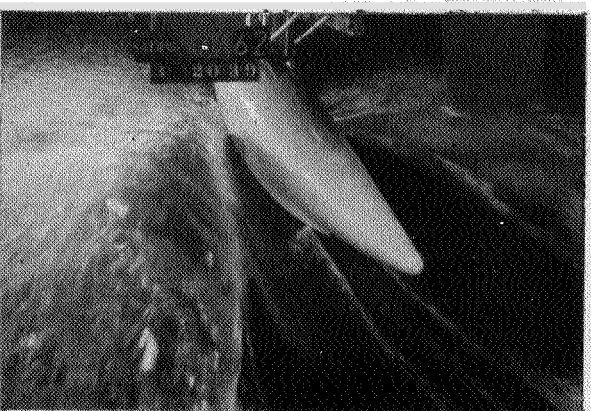
 $C_D = .4$  $C_D = .6$  $C_D = .8$  $C_V = 3.35$  $C_V = 3.55$ 

Figure 24(c). Model 84EF-6.

NACA  
20532



Fig. 25

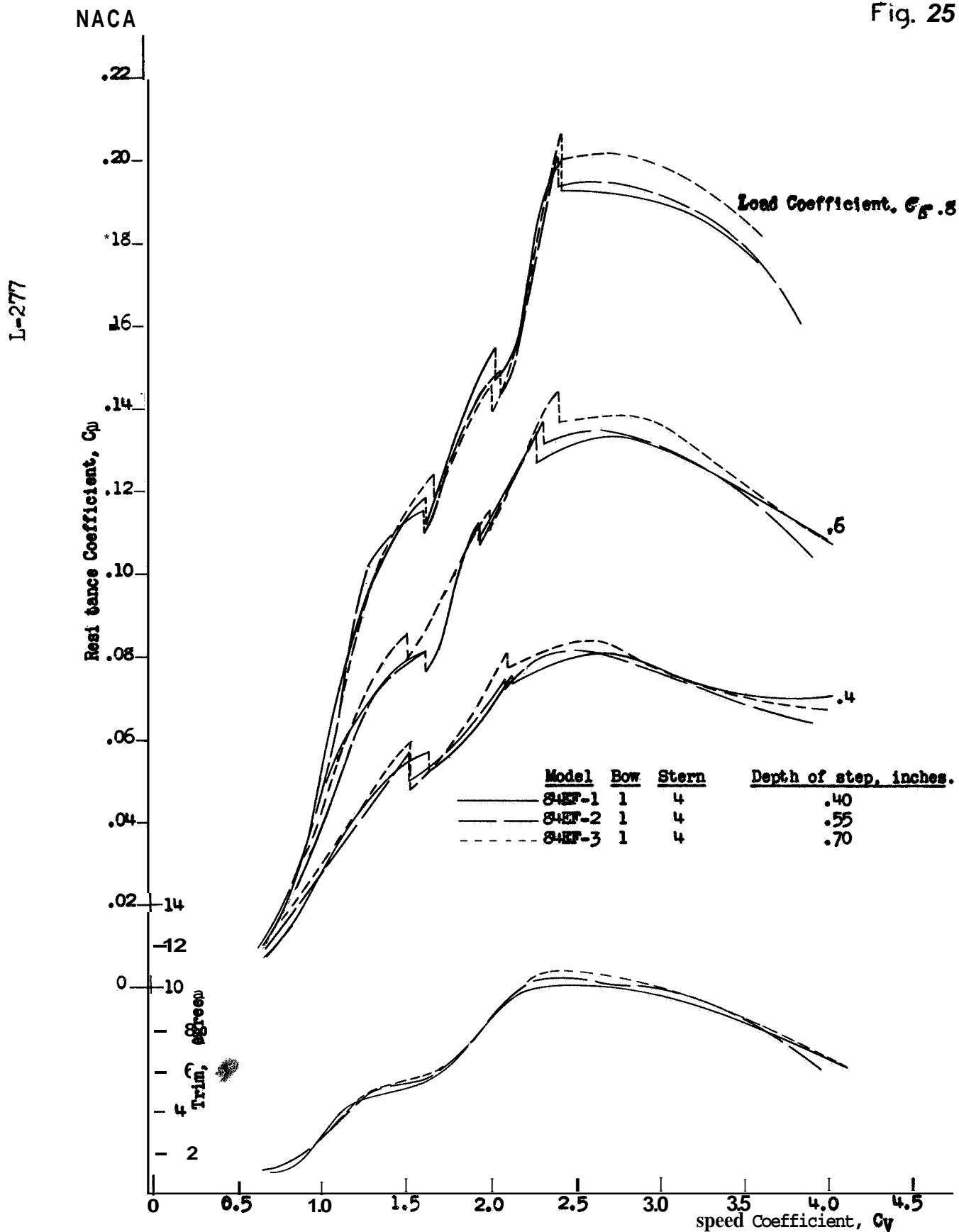


Figure 25 - Effect of depth of step.  
5.5° angle of afterbody keel. Chine flare OR forebody only.

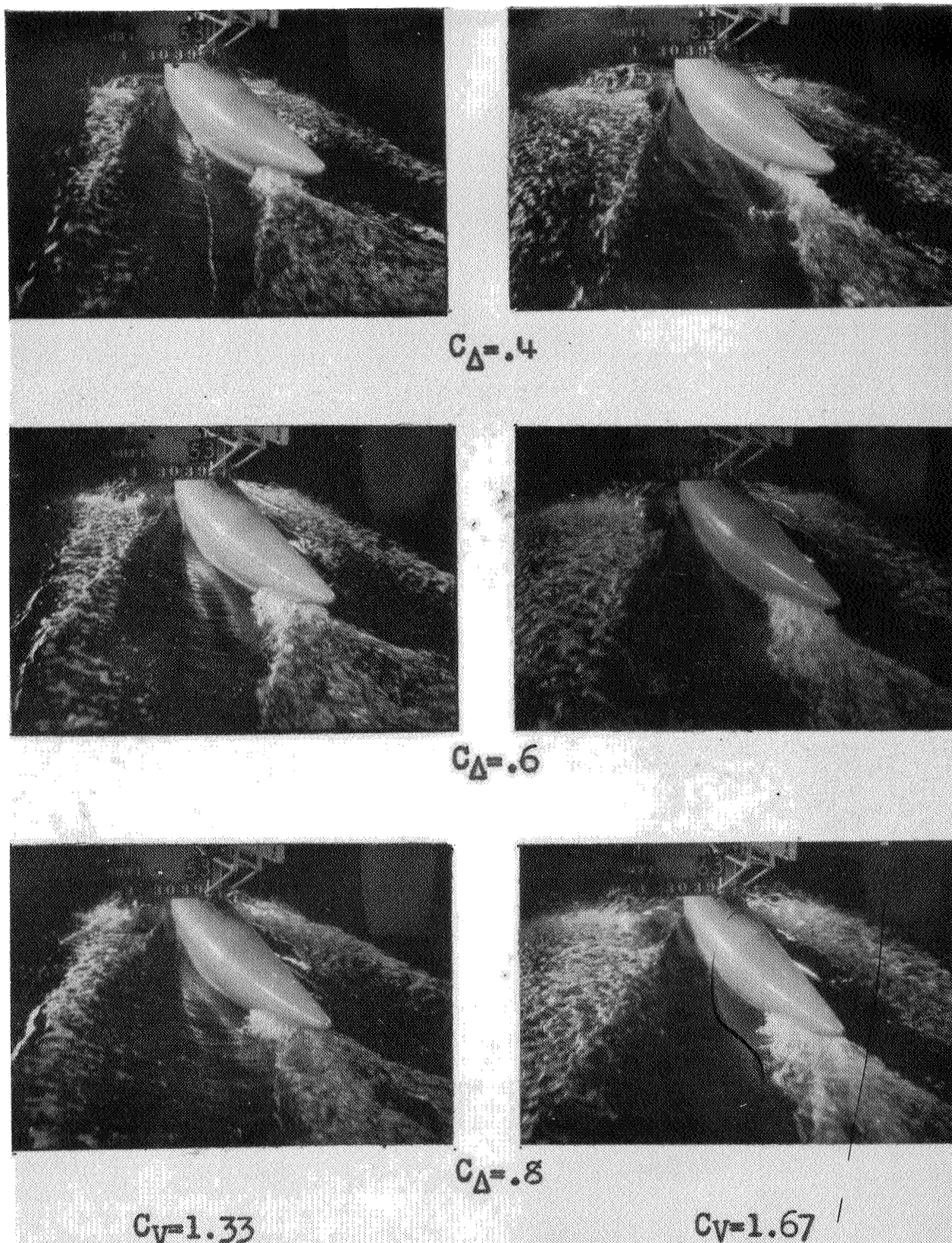
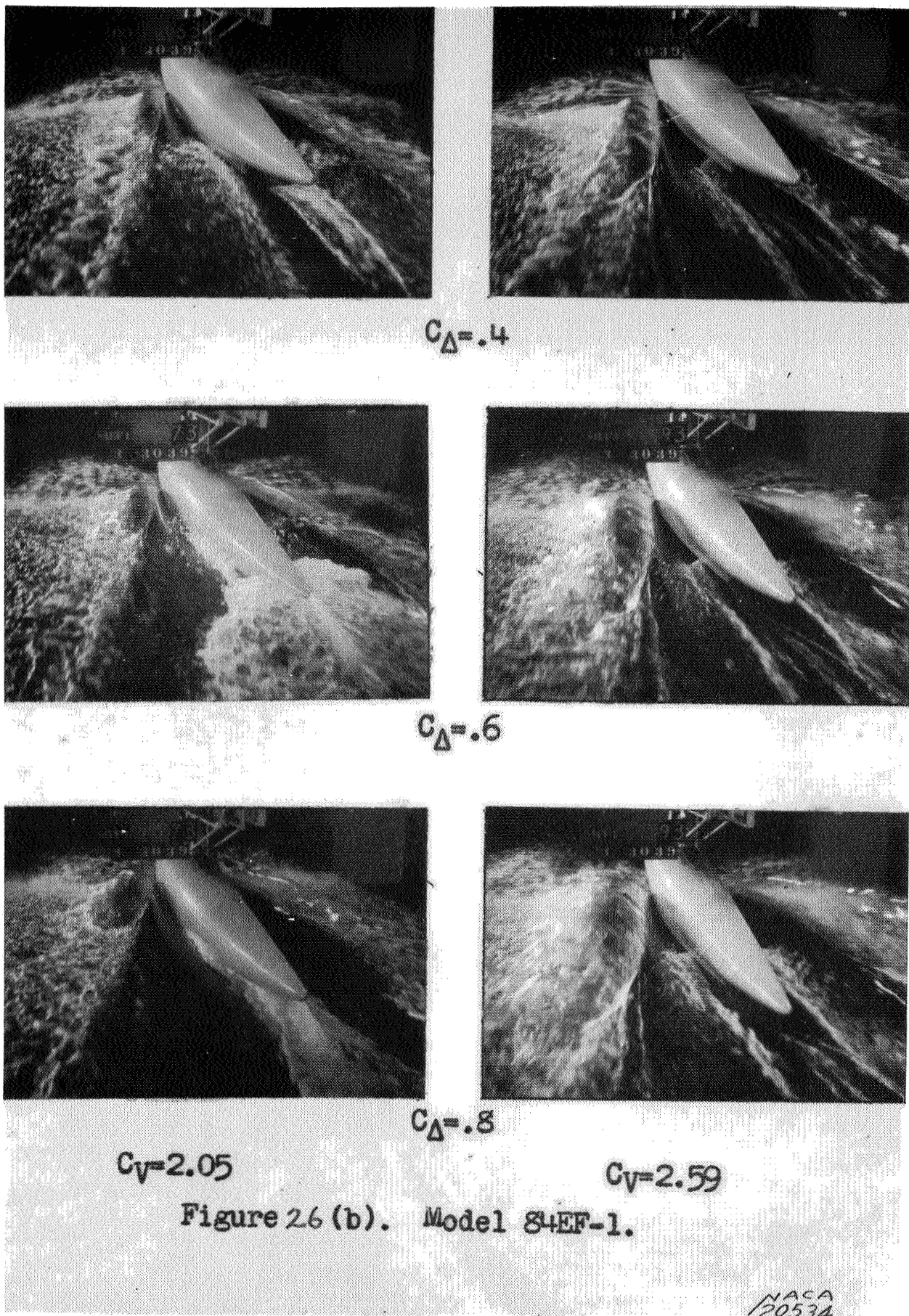


Figure 26(a). Model 84EF-1, Bow 1, Stern 4.  
 Depth of step .40 in., Angle of afterbody keel  $5.5^\circ$   
 Chine flare on forebody only.





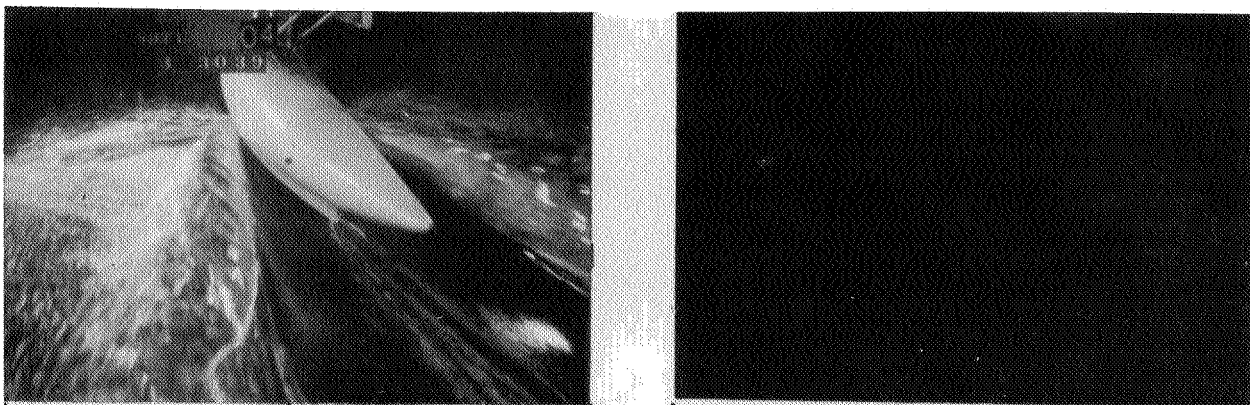
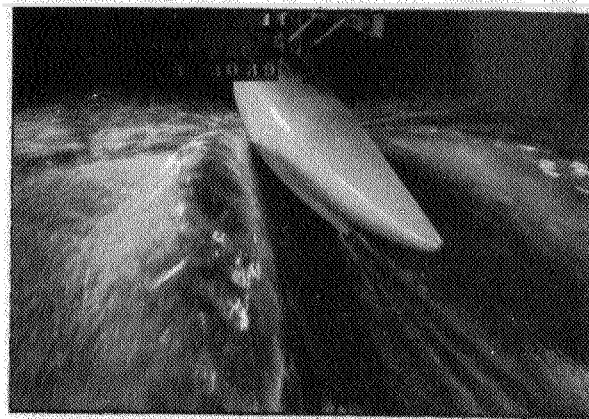
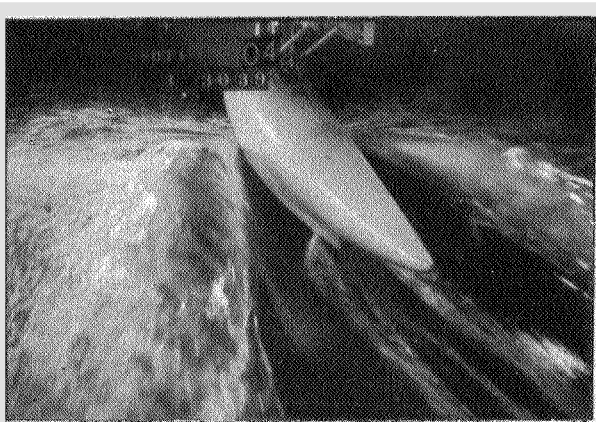
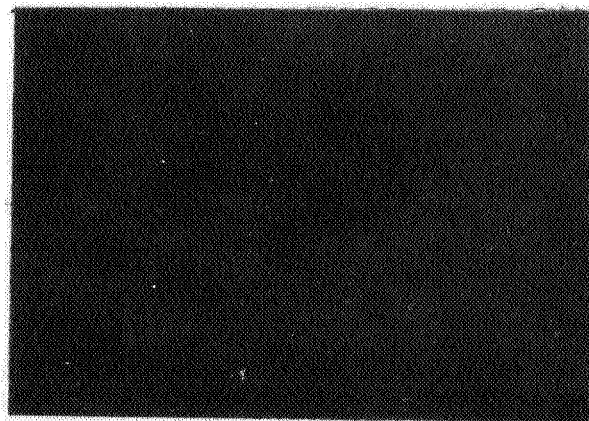
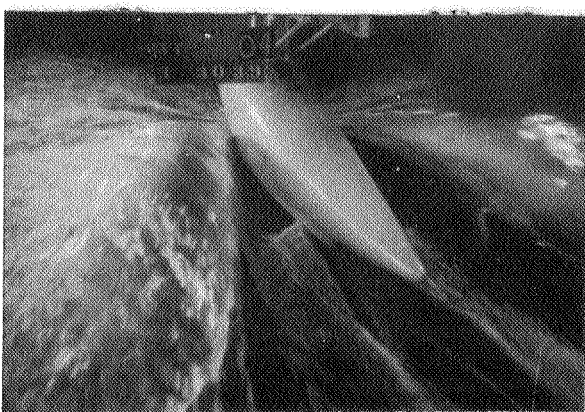
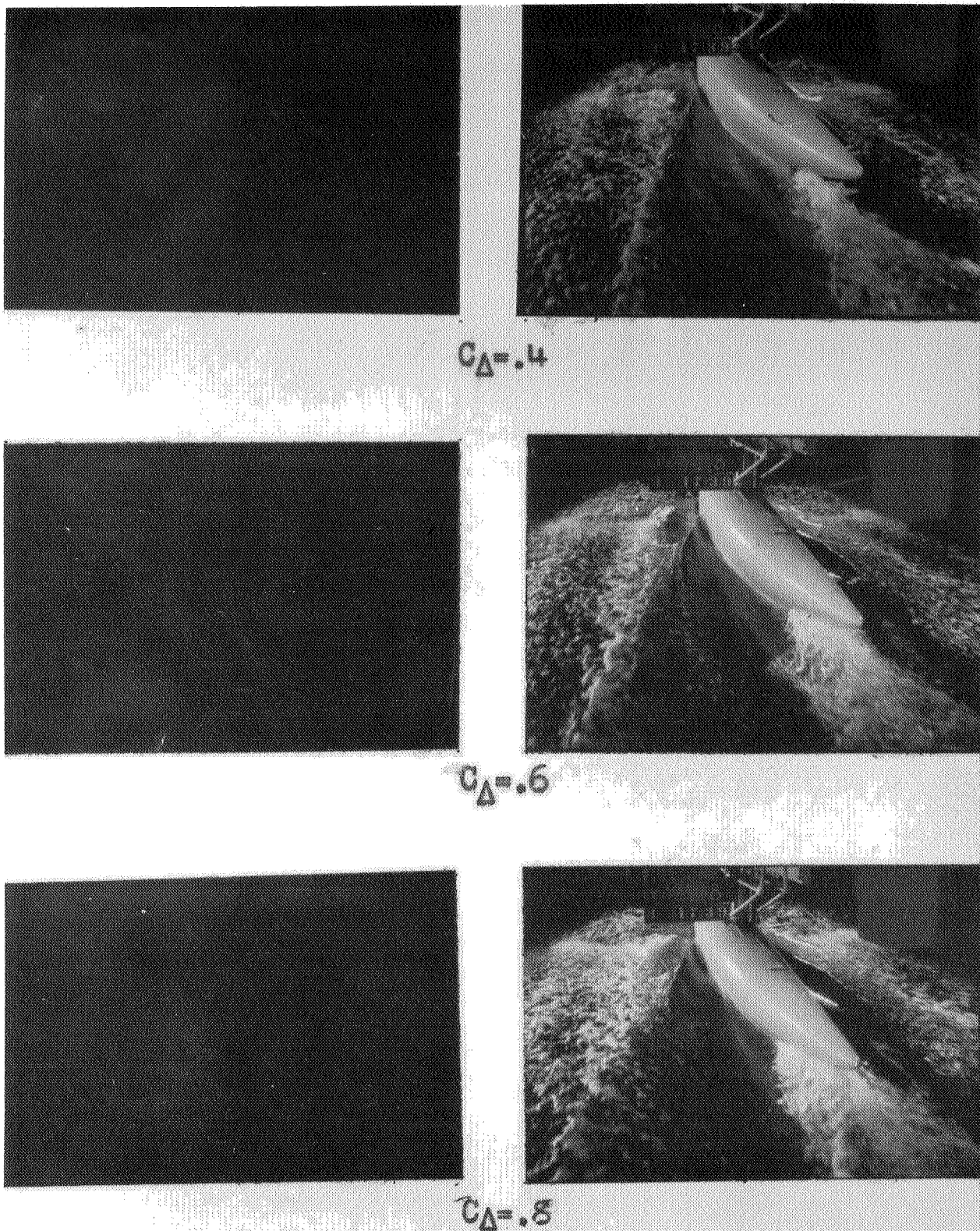

 $C_{\Delta} = .4$ 

 $C_{\Delta} = .6$ 

 $C_{\Delta} = .8$ 
 $C_V = 3.13$ 
 $C_V = 3.46$ 

Figure 26(c). Model 84EF-1.



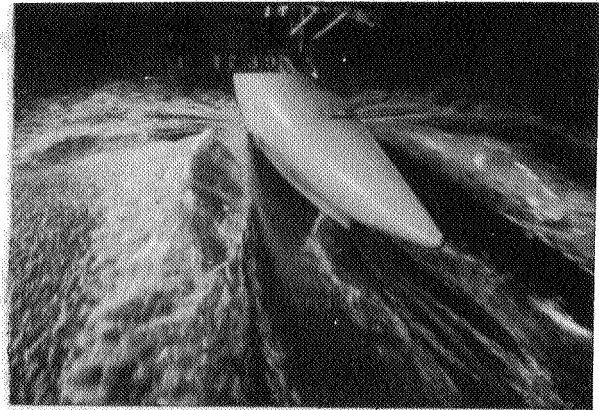
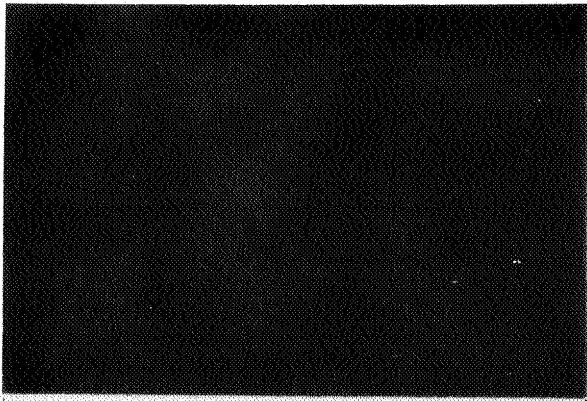


$C_V = 1.25$

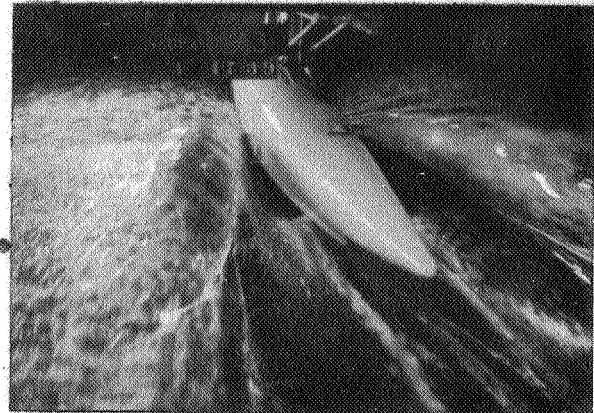
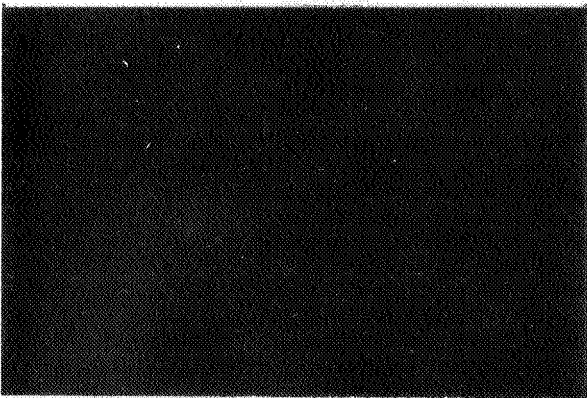
$C_V = 1.70$

Figure 27(a). Model 84EF-2, Bow 1, Stern 4.  
Depth of step .55 in., Angle of afterbody keel  $5.5^\circ$   
Chine flare on forebody only.

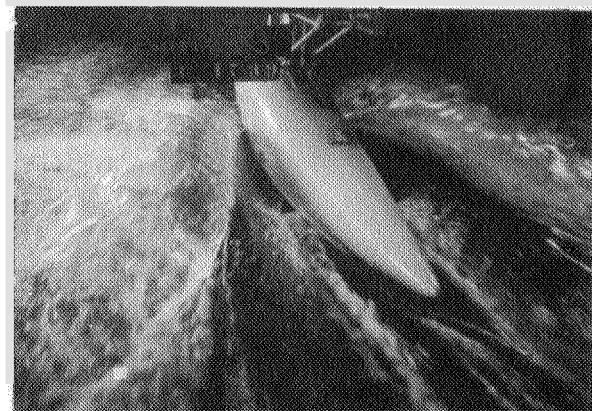
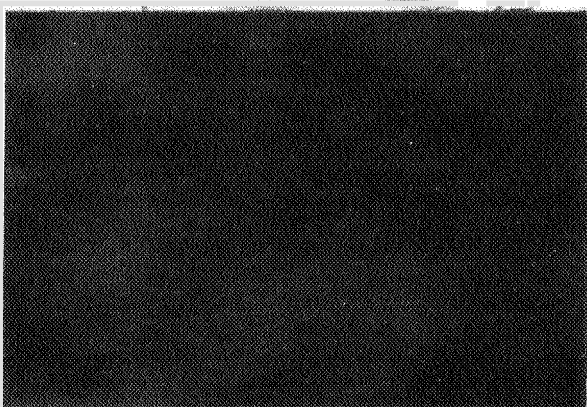
NACA  
20536



$C_D = .4$



$C_D = .6$



$C_D = .8$

$C_V = 2.15$

$C_V = 2.65$

Figure 27(b). Model 84EF-2.



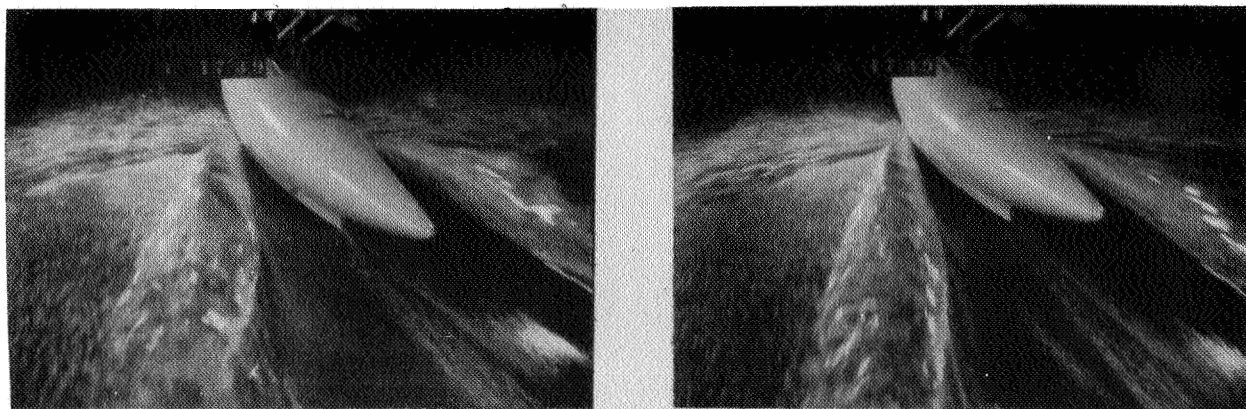
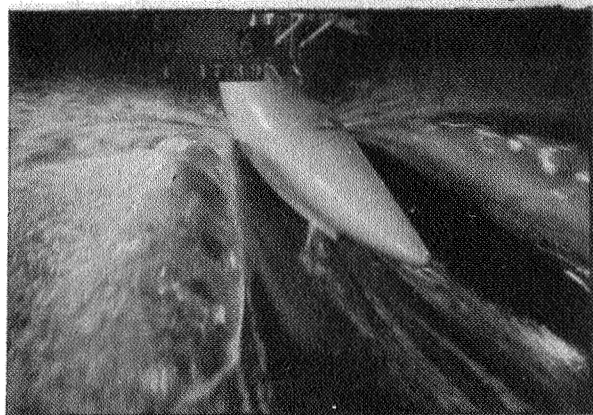
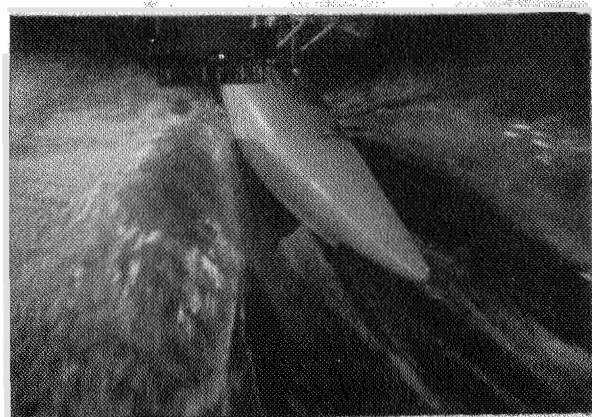
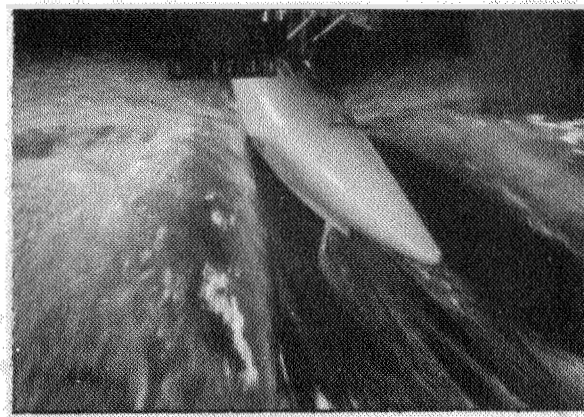
 $C_{\Delta} = .4$  $C_{\Delta} = .6$  $C_{\Delta} = .8$  $C_V = 3.10$  $C_V = 3.50$ 

Figure 27 (c). Model 84EF-2

L-277

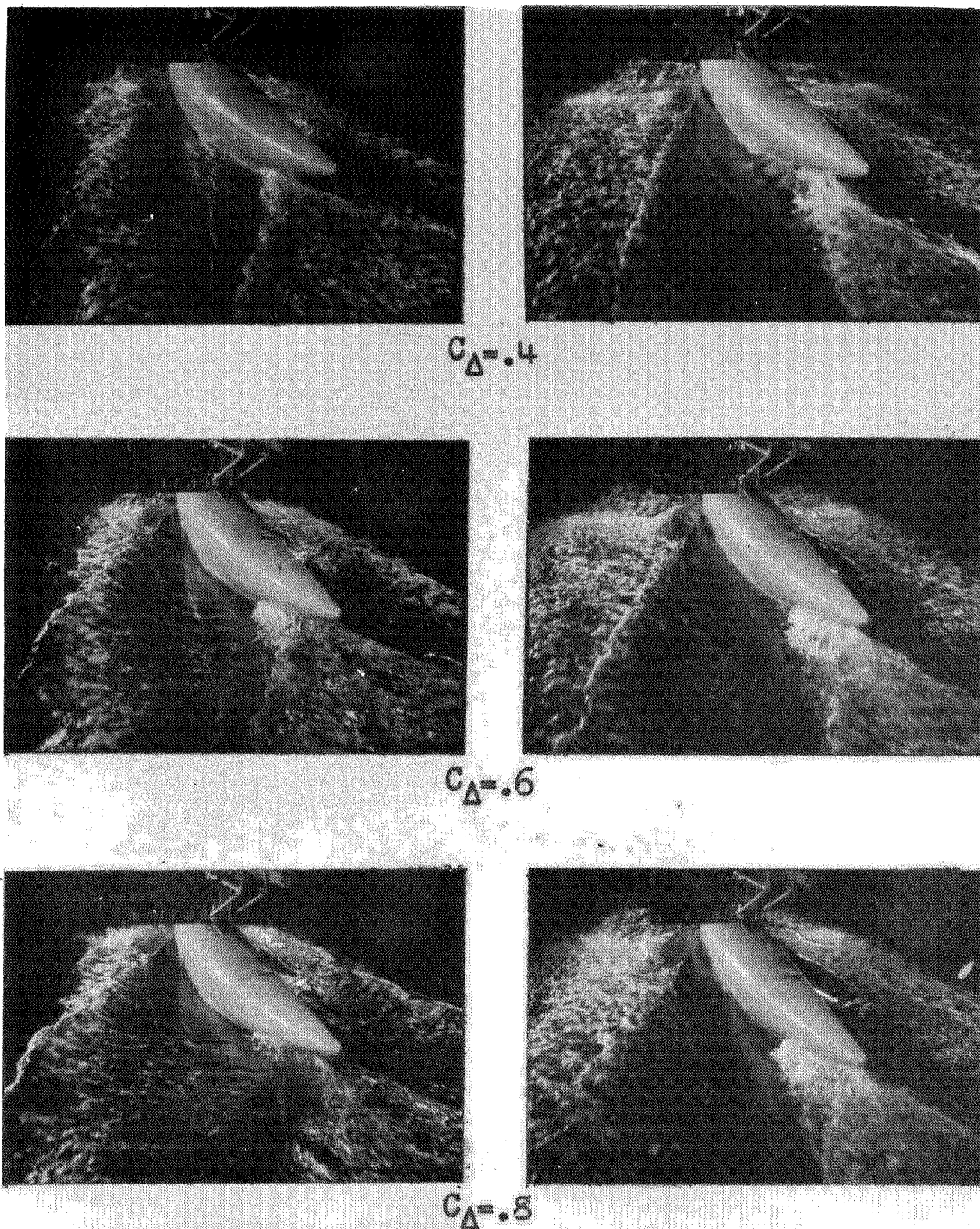
 $C_V = 1.27$  $C_V = 1.66$ 

Figure 28(a). Model 84EF-3, Bow 1, Stern 4.  
 Depth of step .70 in., Angle of afterbody keel 5.50  
 Chine flare on forebody only.

NACA  
20539



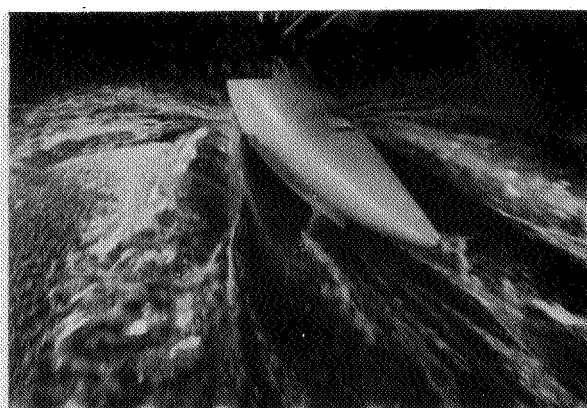
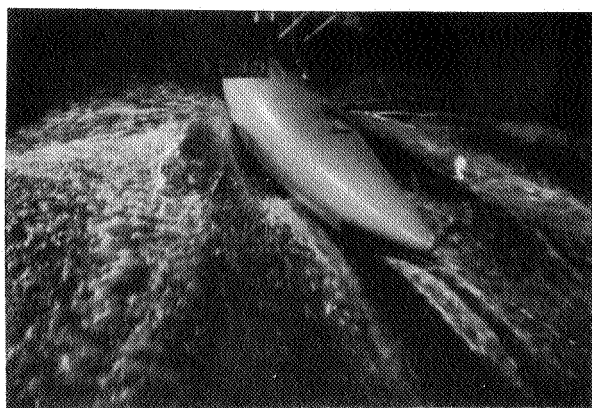
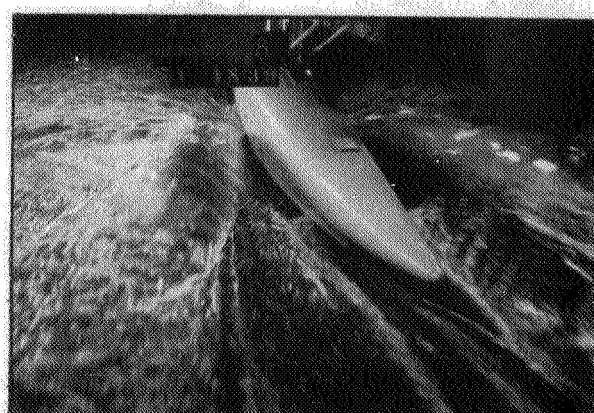
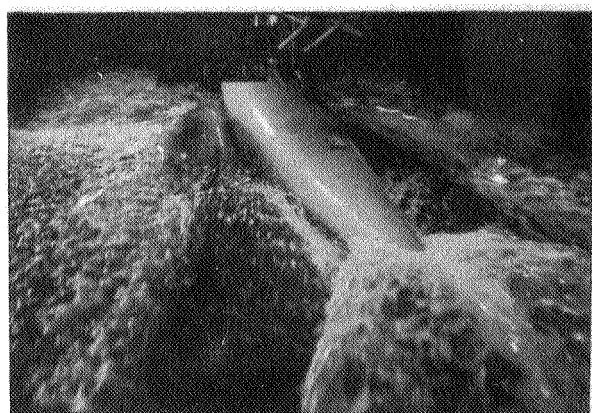
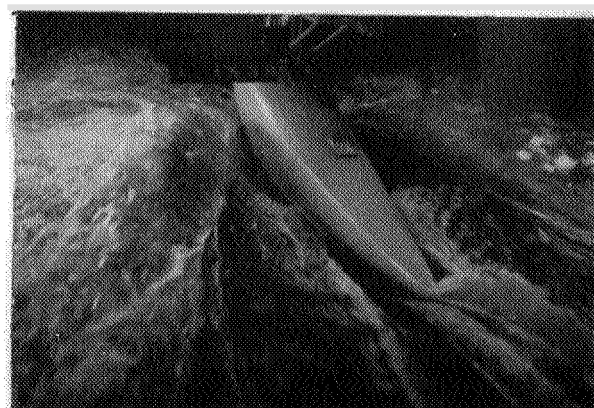
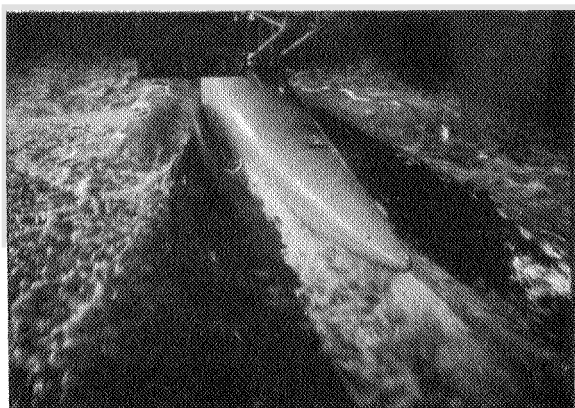
 $C_D = .4$  $C_D = .6$  $C_D = .8$  $C_V = 2.14$  $C_V = 2.55$ 

Figure 28(b). Model 84EF-3.

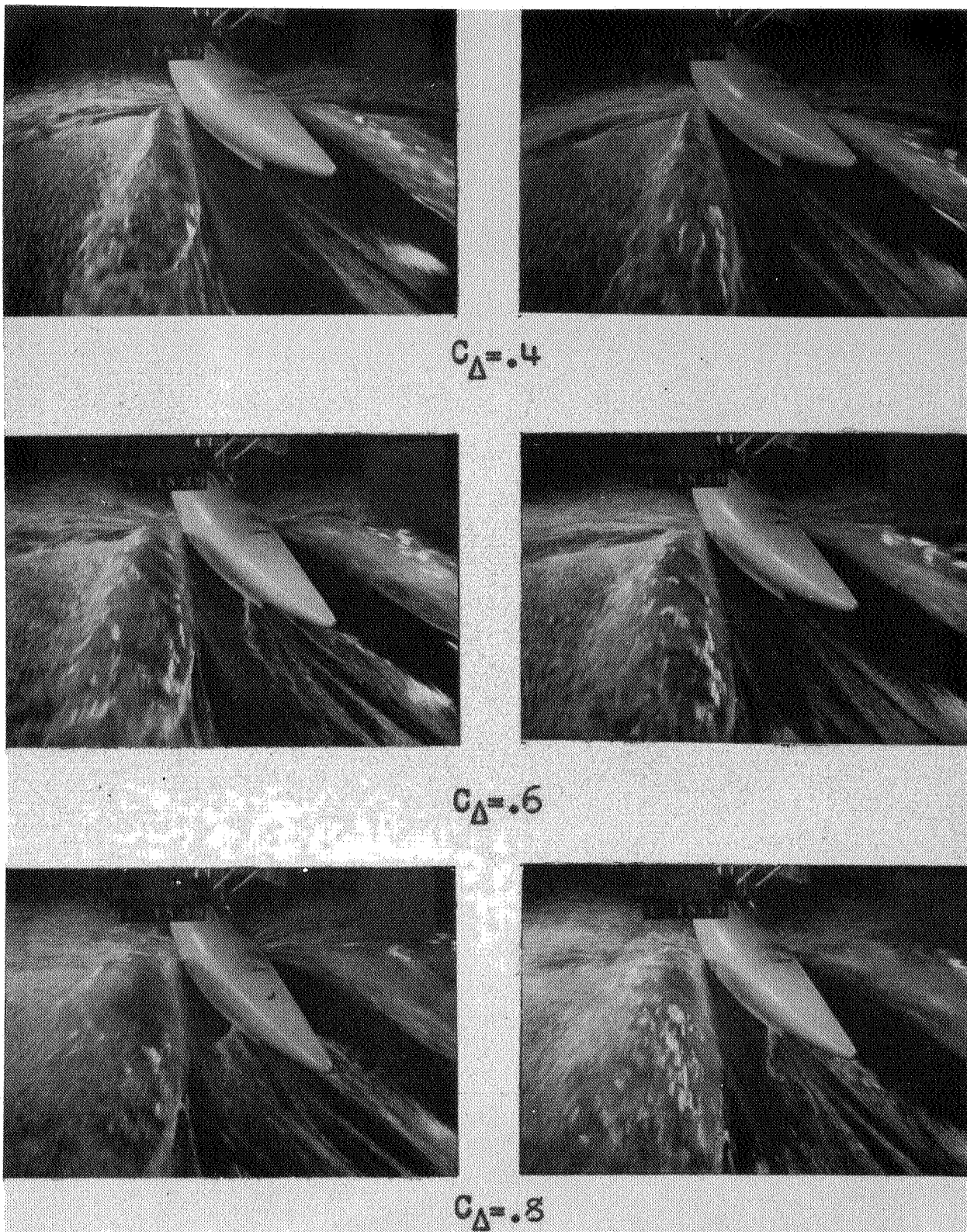


Figure 28(c). Model 84EF-3.

L-277

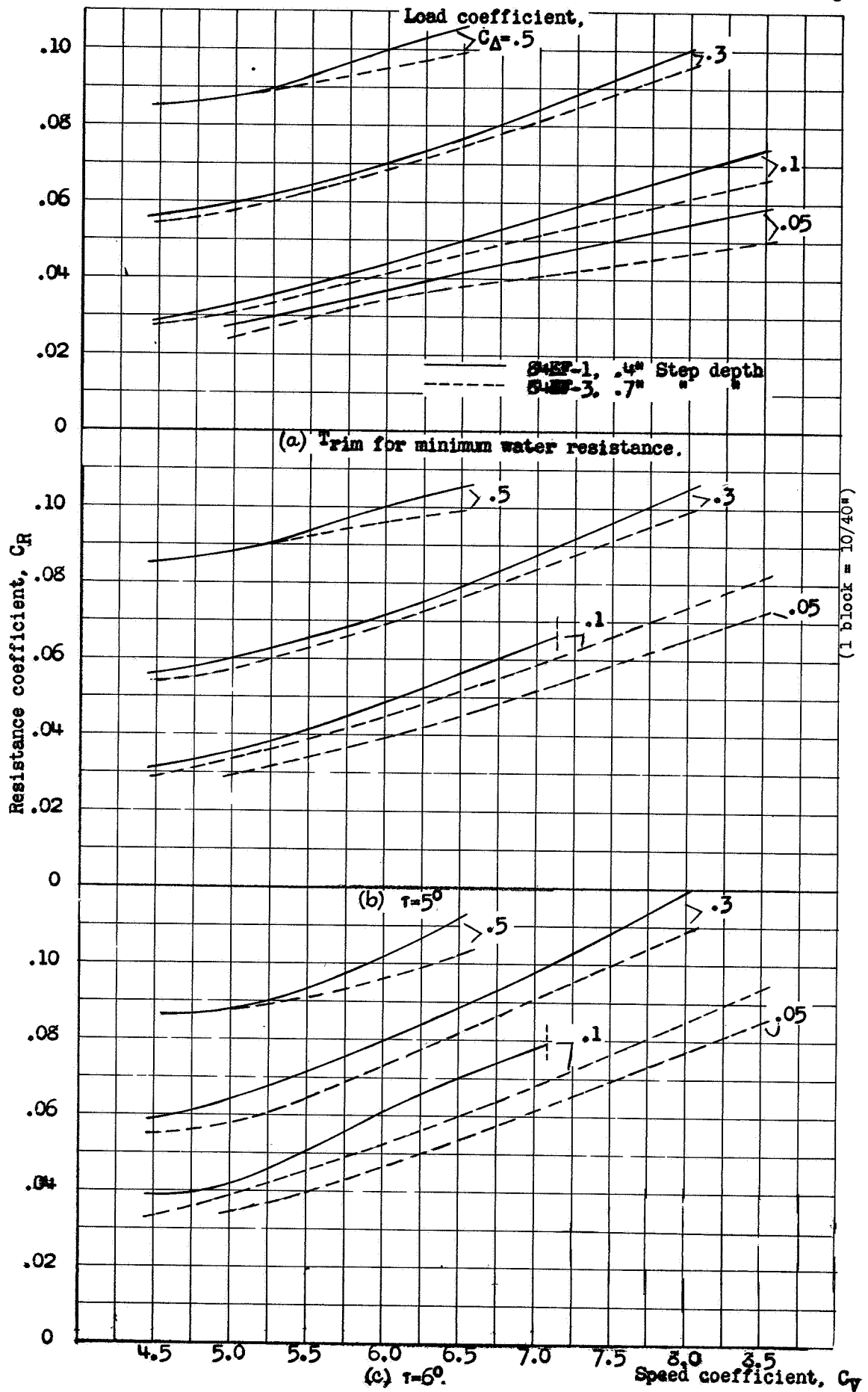


Figure 29.- Effect of variation of step depth at planing speeds.

NACA

Fig. 30

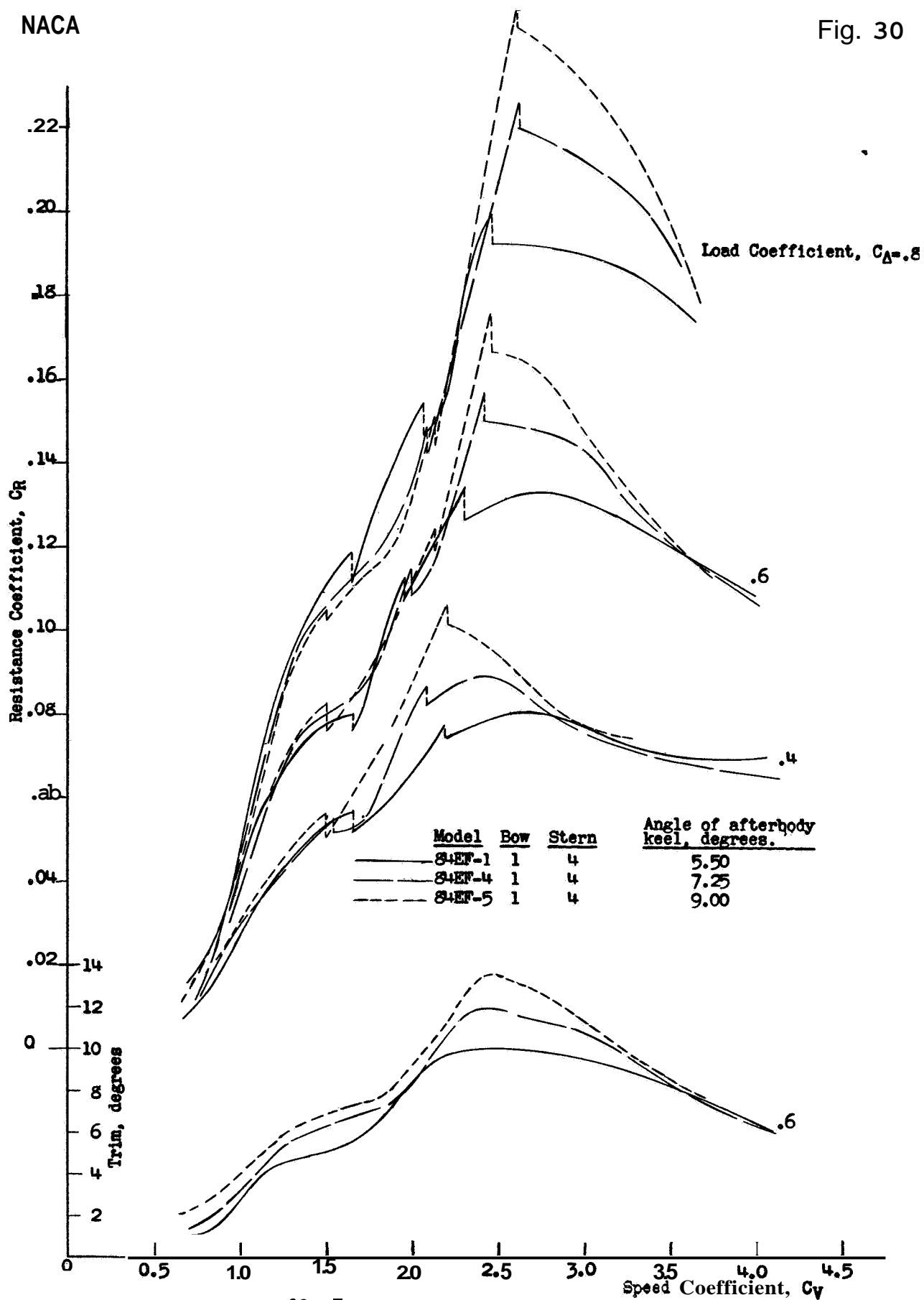


Figure 30 . Effect of angle of afterbody keel.  
 .40 in. depth of step. Chine flare on forebody only.



L-2777

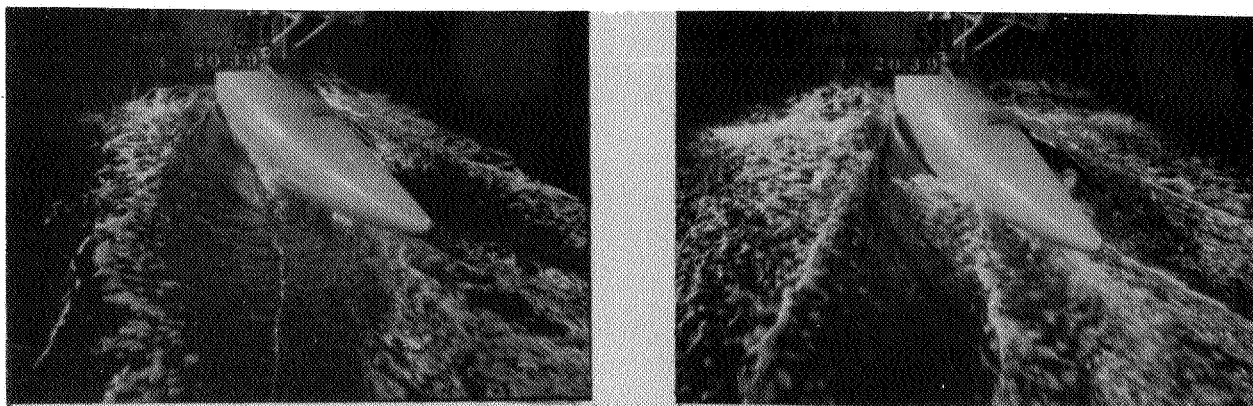
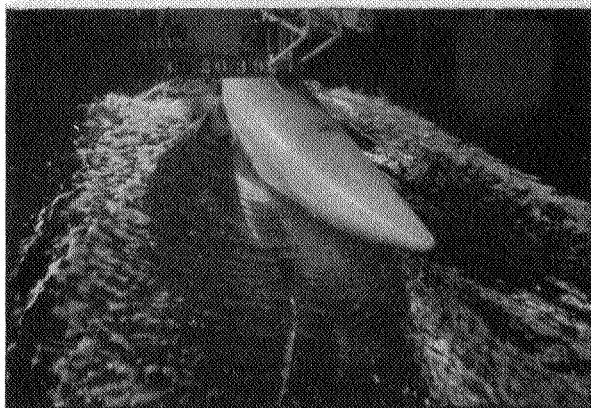
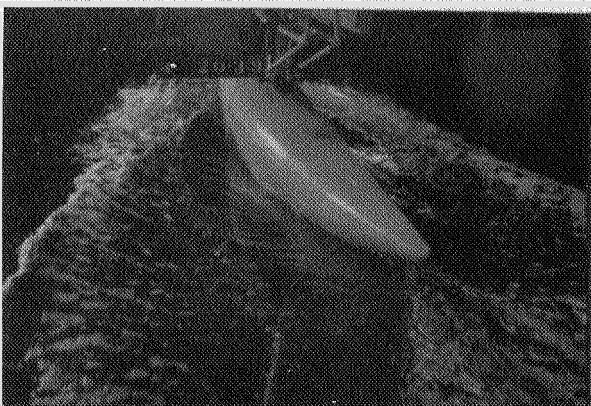
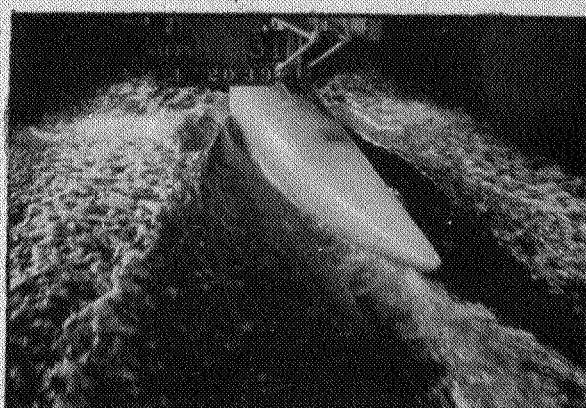
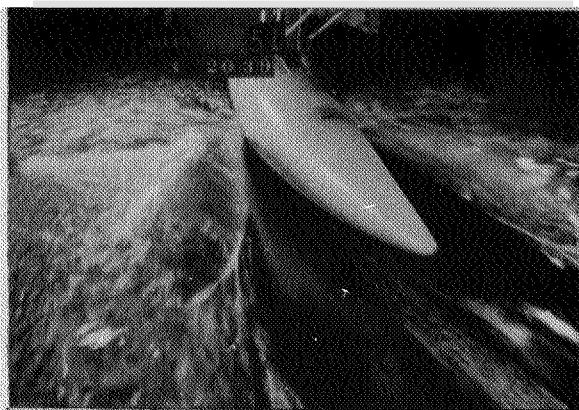
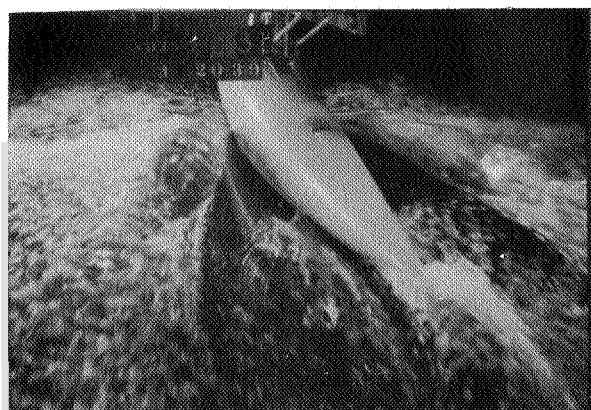
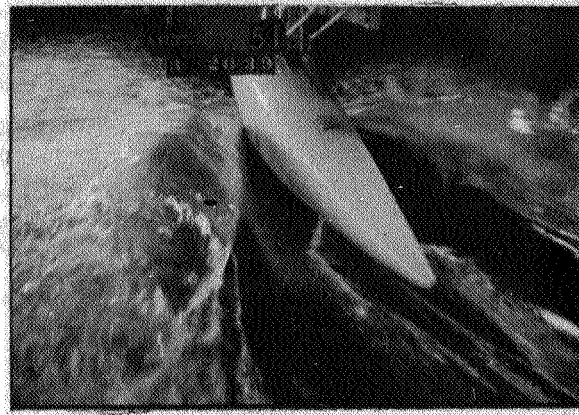
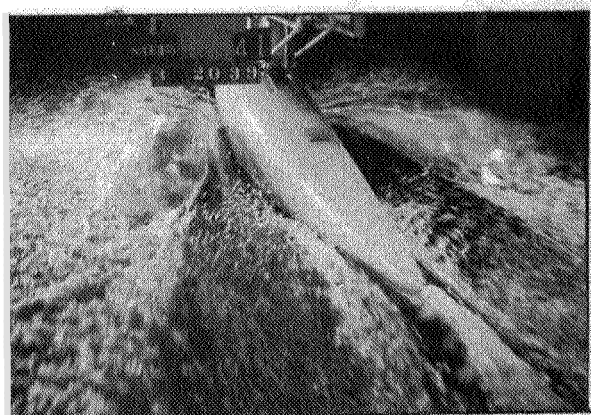
 $C_{\Delta} = .4$  $C_{\Delta} = .6$  $C_{\Delta} = .8$  $C_v = 1.25$  $C_v = 1.67$ 

Figure 31 (a). Model 84EF-5, Bow 1, Stern 4.  
 Depth of step .40 in., Angle of afterbody keel  $9.00^\circ$   
 Chine flare on forebody only.

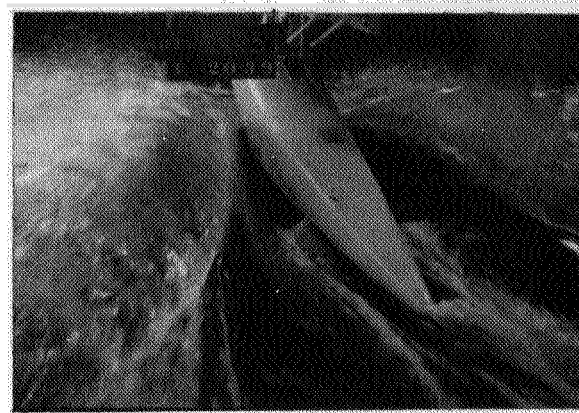
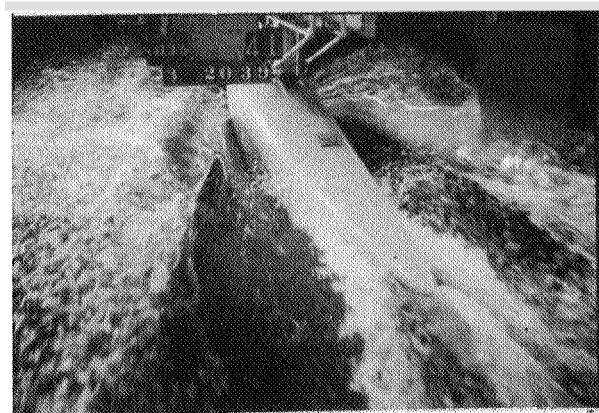
NACA  
 20542



$C_D = .4$



$C_D = .6$



$C_D = .8$

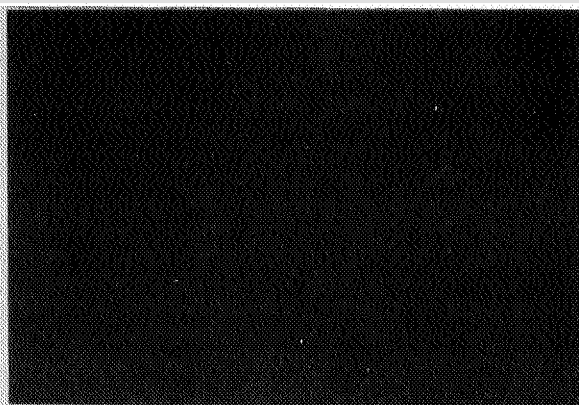
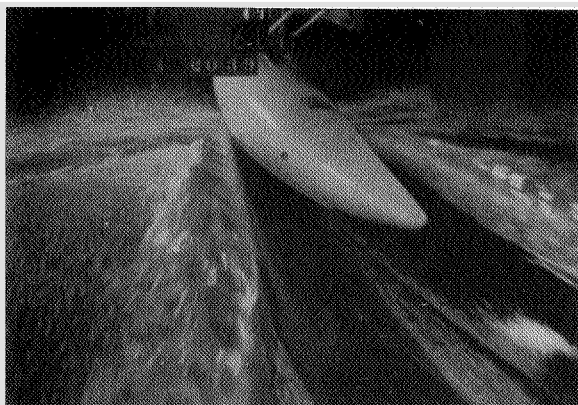
$C_V = 2.20$

$C_V = 2.70$

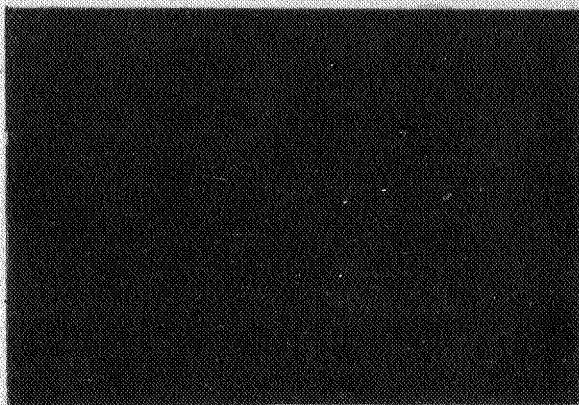
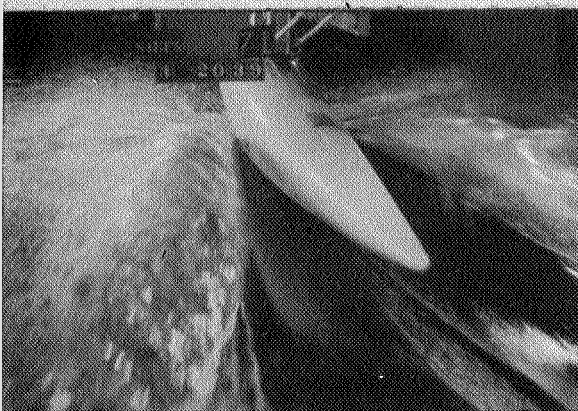
Figure 31 (b). Model 84EF-5.



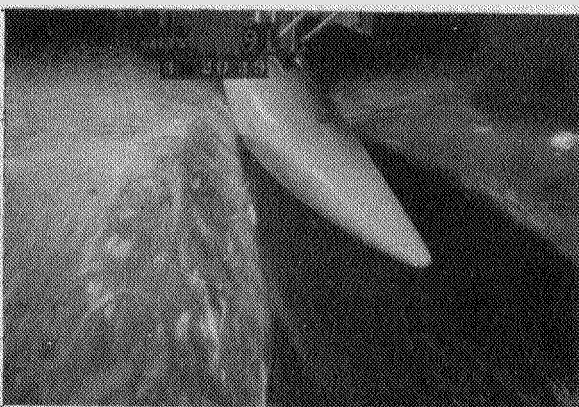
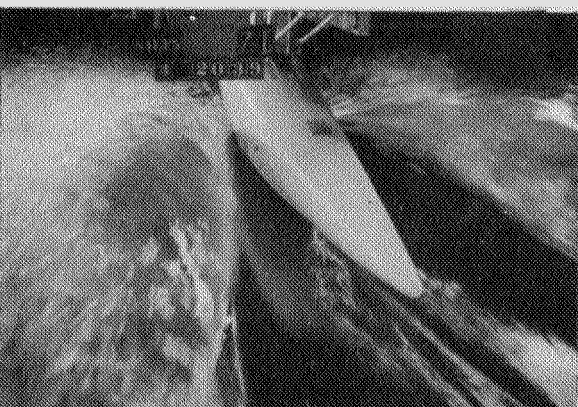
L-277



$C_D = .4$



$C_D = .6$



$C_D = .8$

$C_V = 3.12$

$C_V = 3.63$

Figure 31 (c). Model 84EF-5.

NACA  
20544

L-277

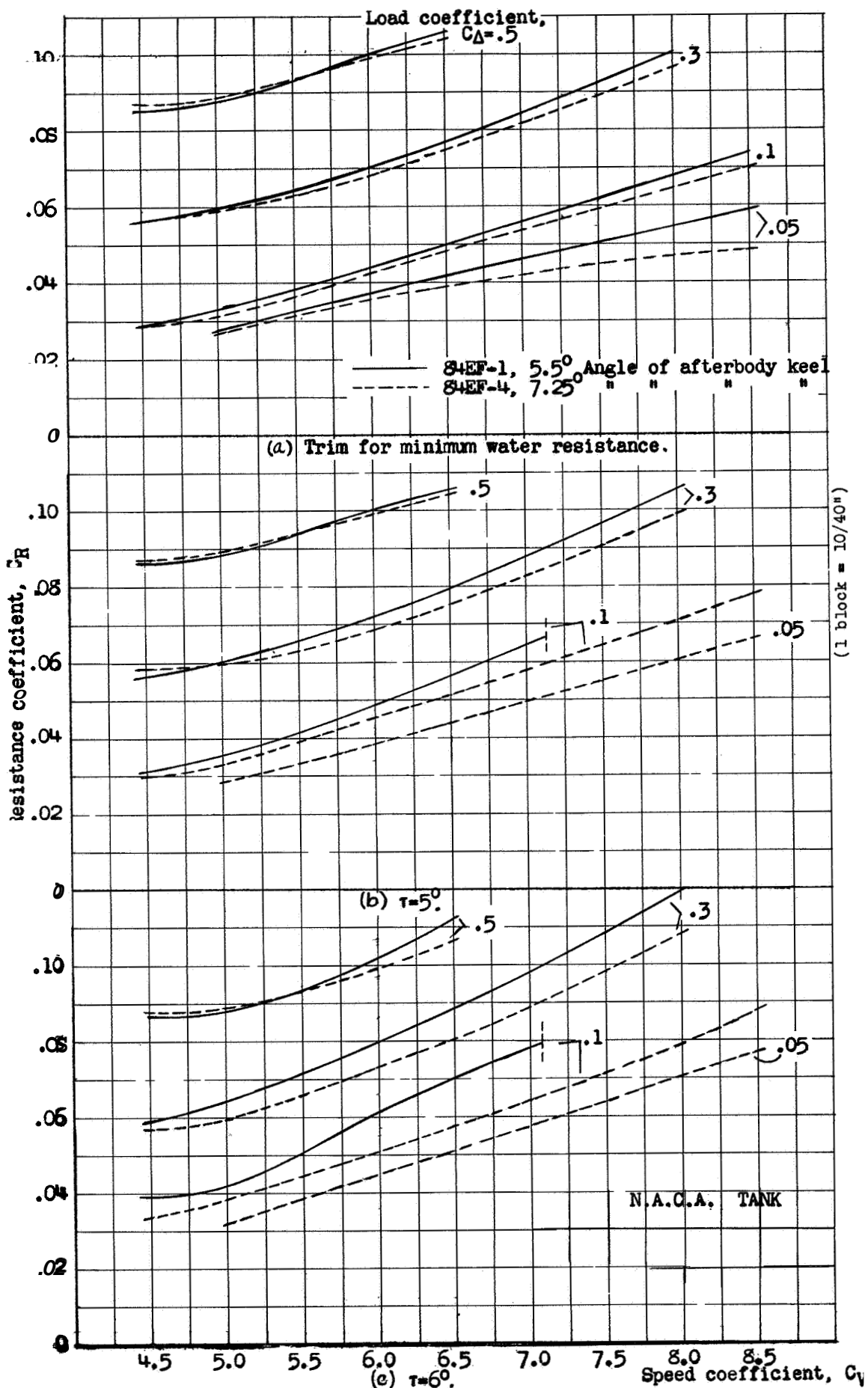


Figure 32.- Effect of angle of afterbody keel at planing speeds.



NACA

Fig. 33

L-277

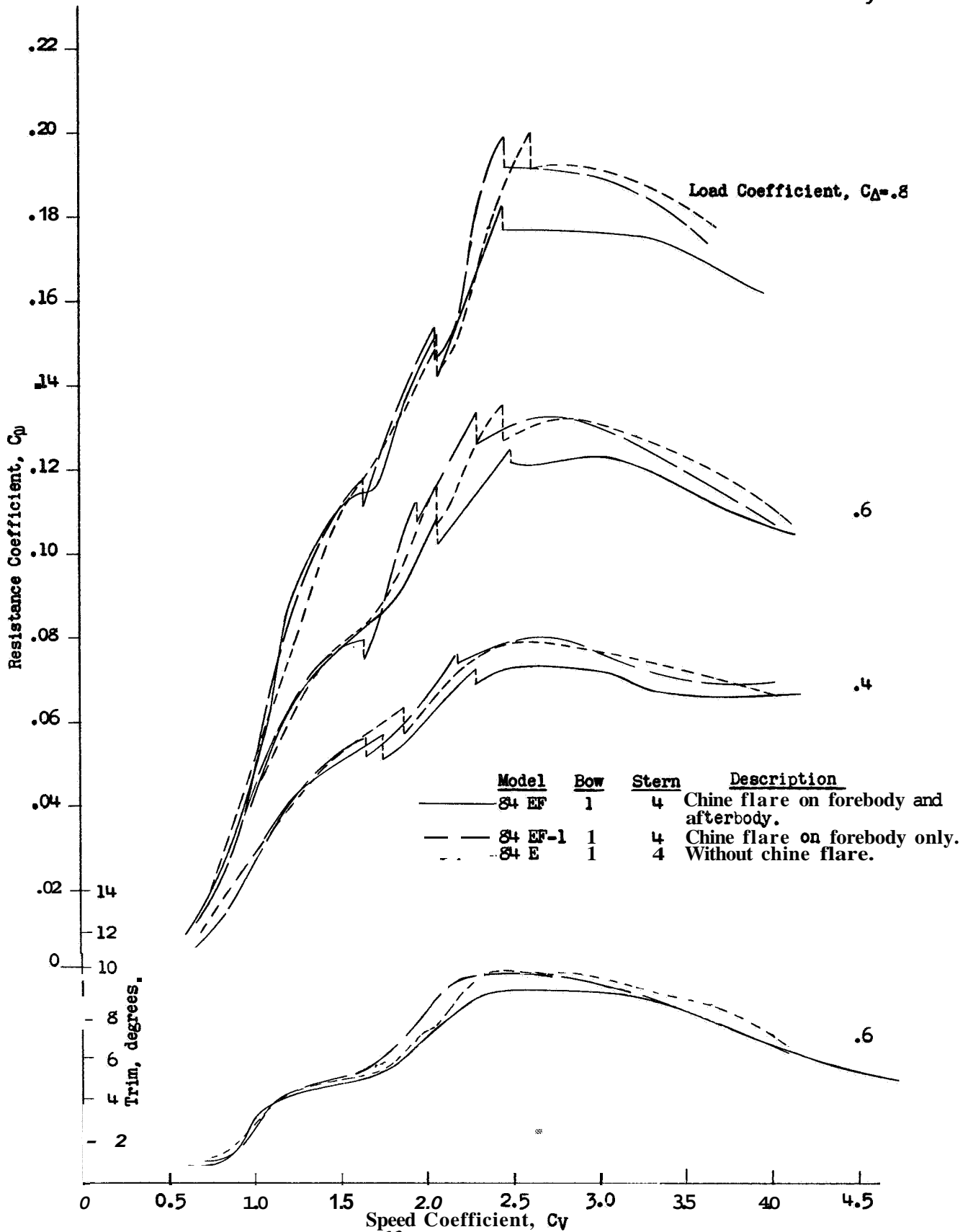


Figure 33 Effect of chine flare

L-277

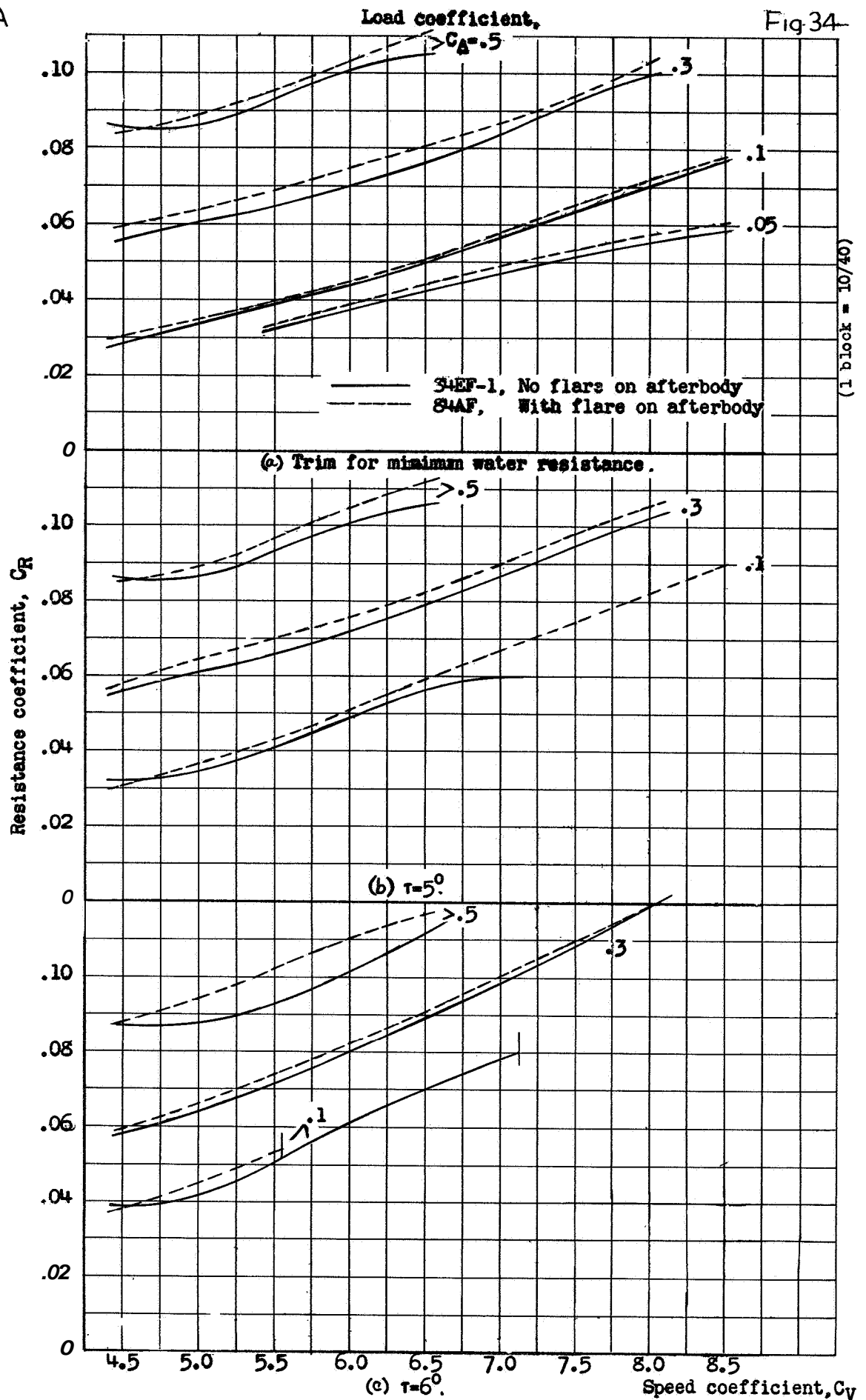


Figure 34. - Effect of flare on afterbody at planing speeds.

L-277

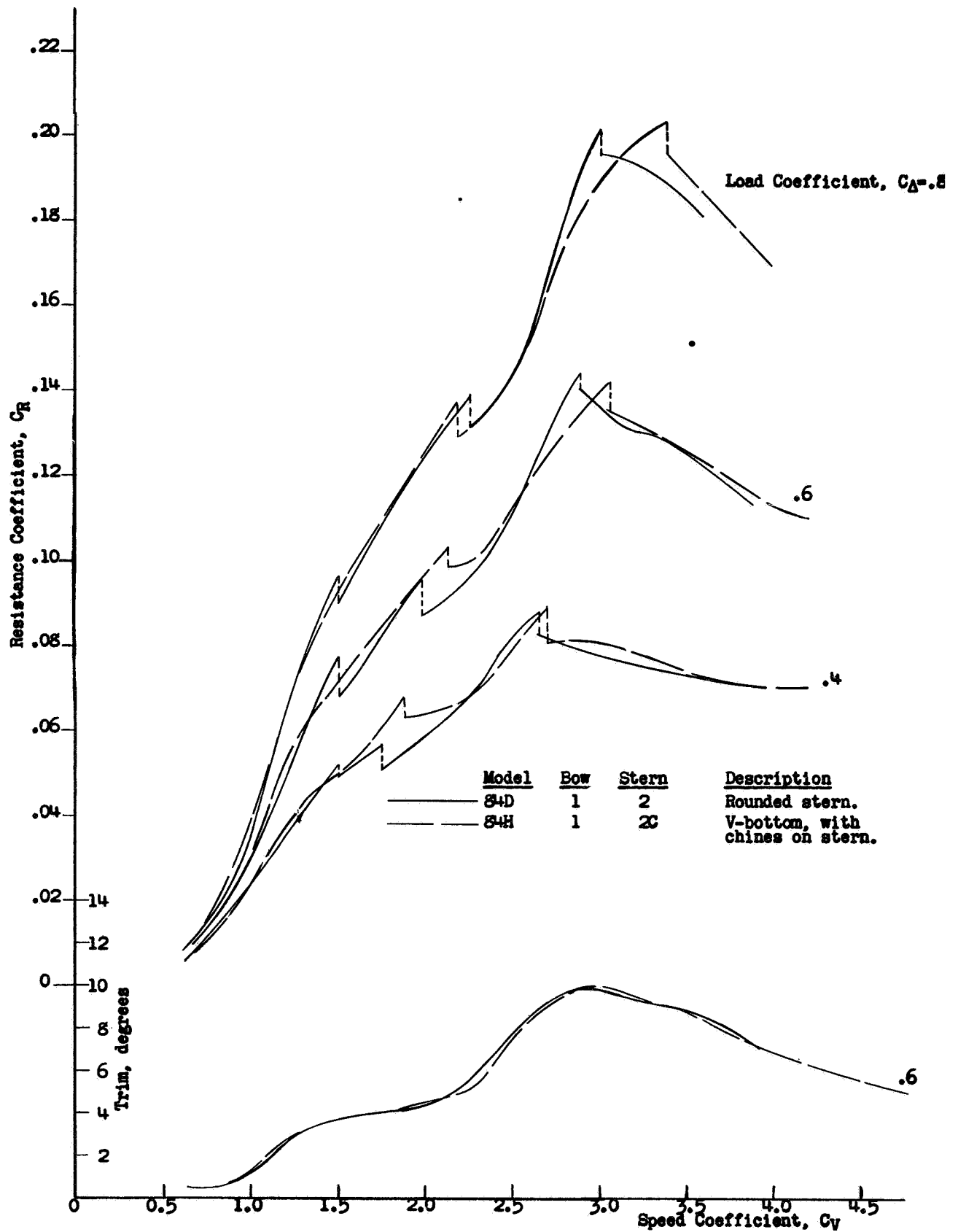
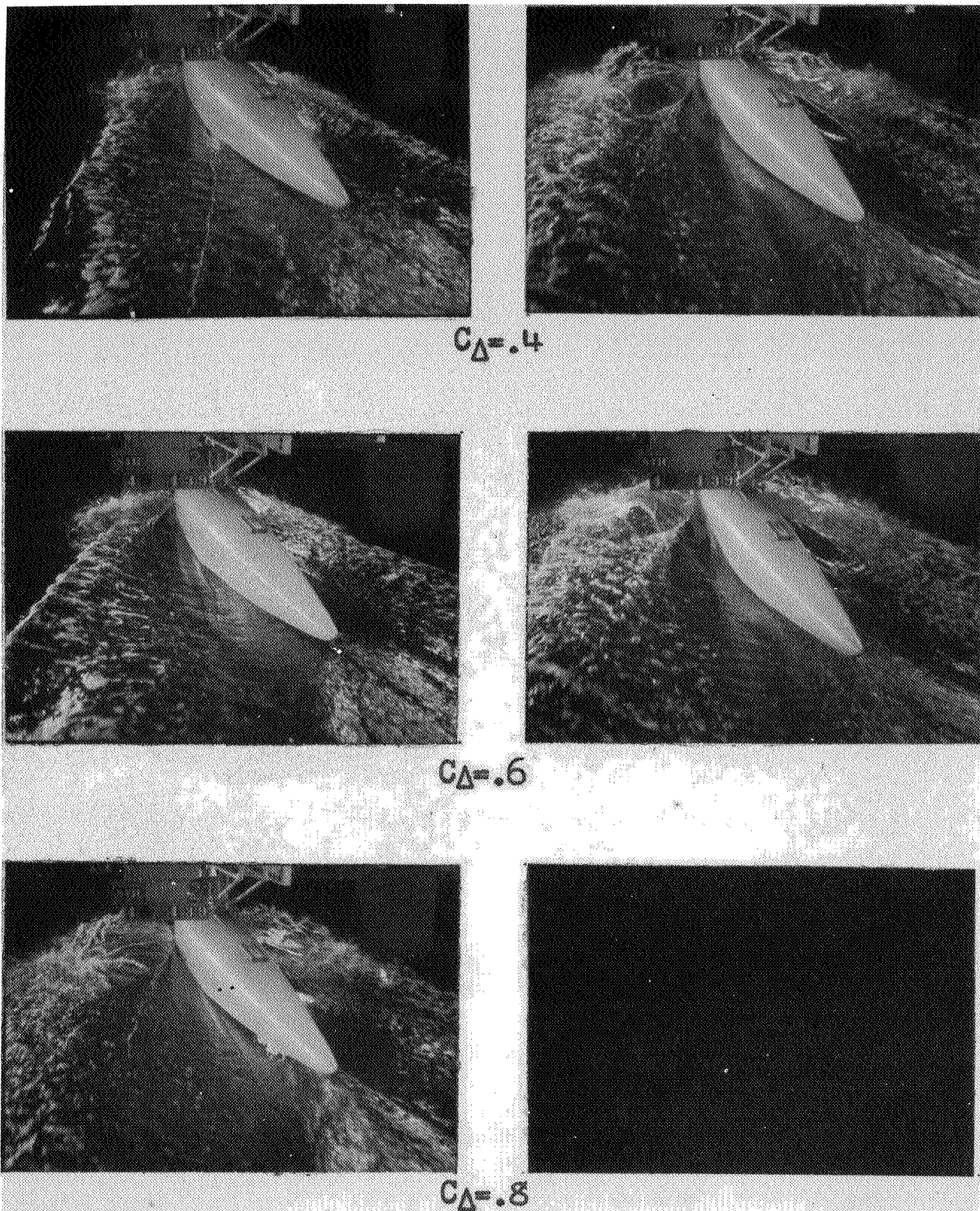


Figure 35.- Effect of chines on low stern,  
Without chine flare.



$C_v = 1.16$   $C_v = 1.58$   
 Figure 36(a). Model 84H, Bow 1, Stern 2C.  
 Without chine flare.



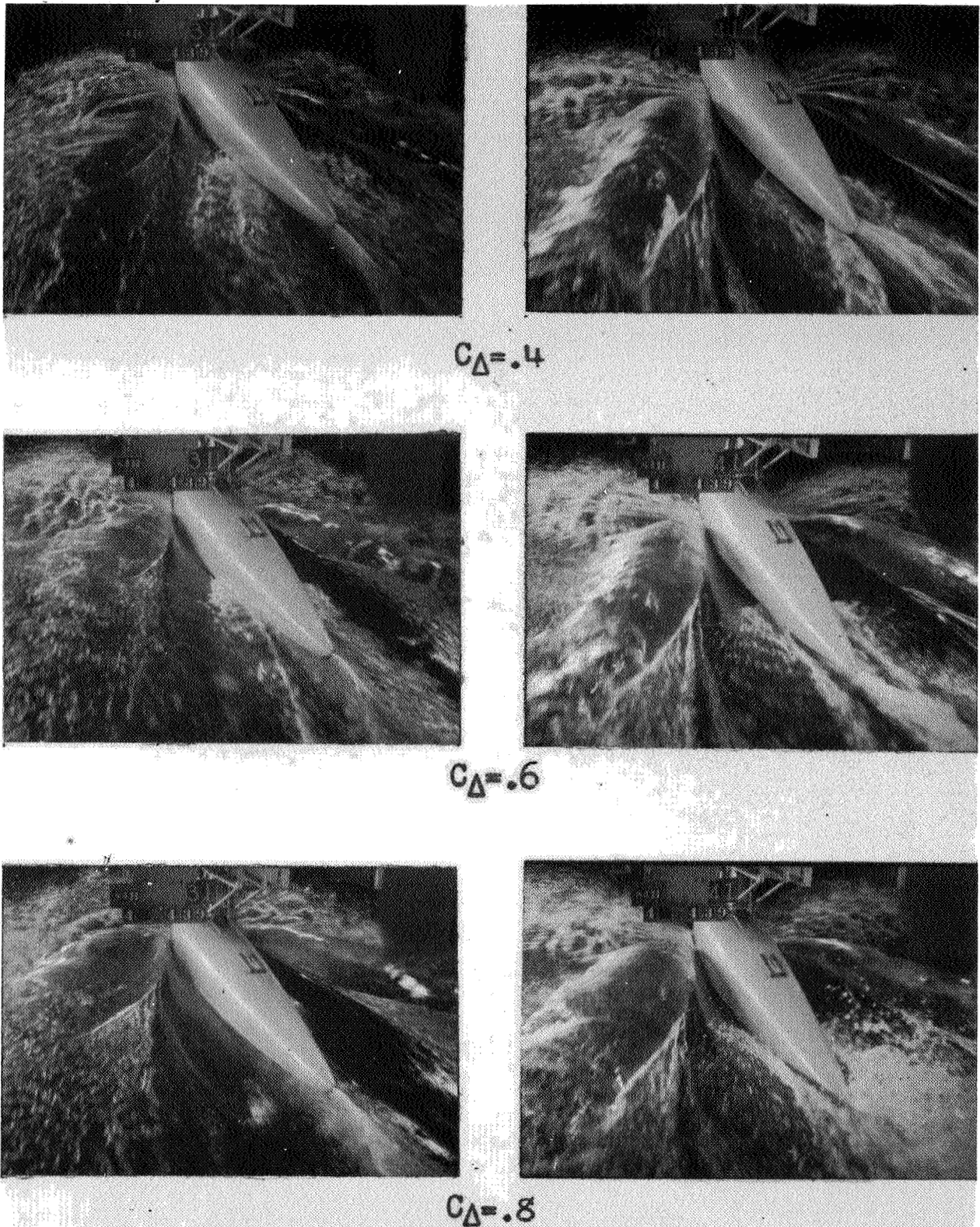


Figure 36(b). Model 84H.

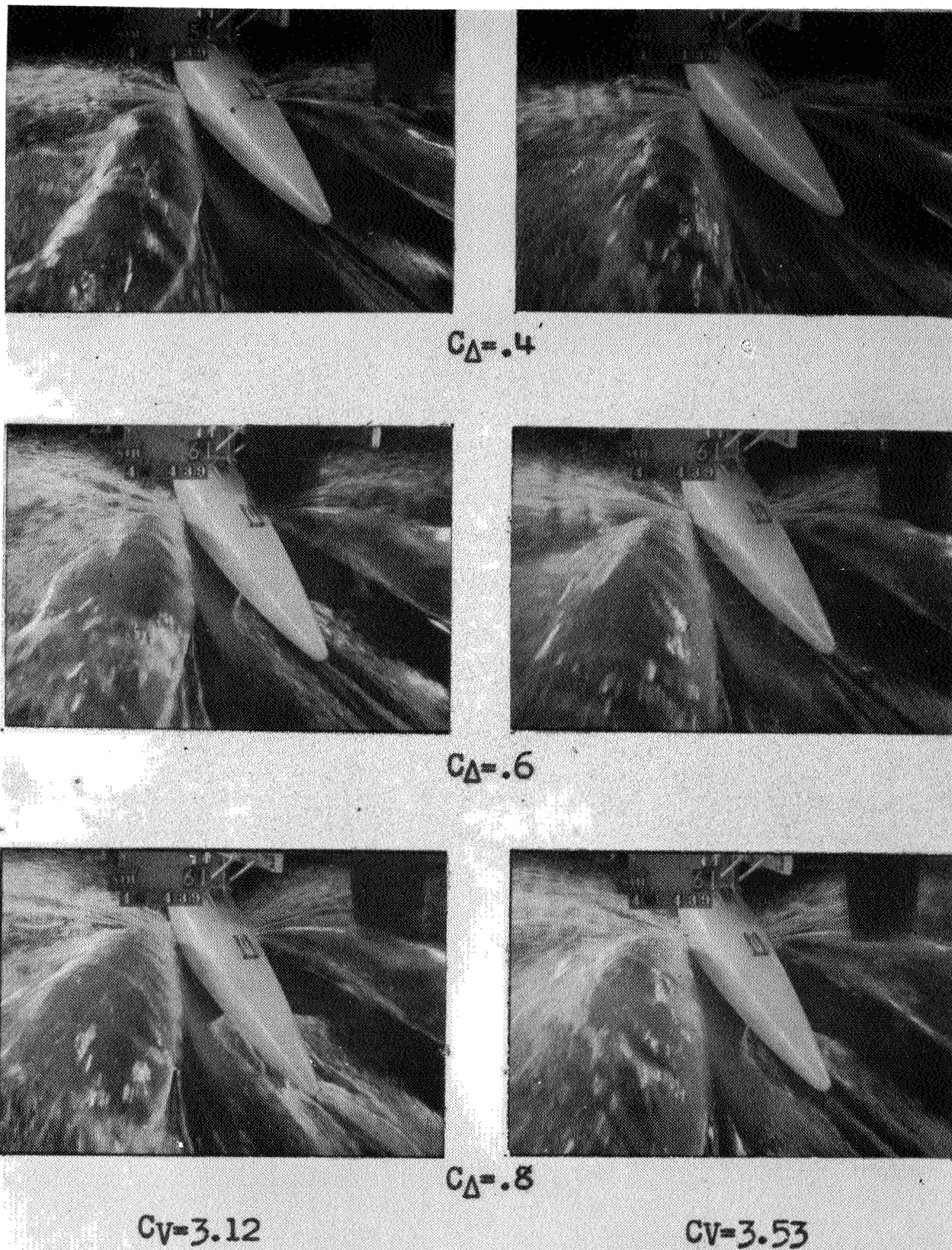


Figure 36 (c). Model 84H.

L-277

Fig. 37

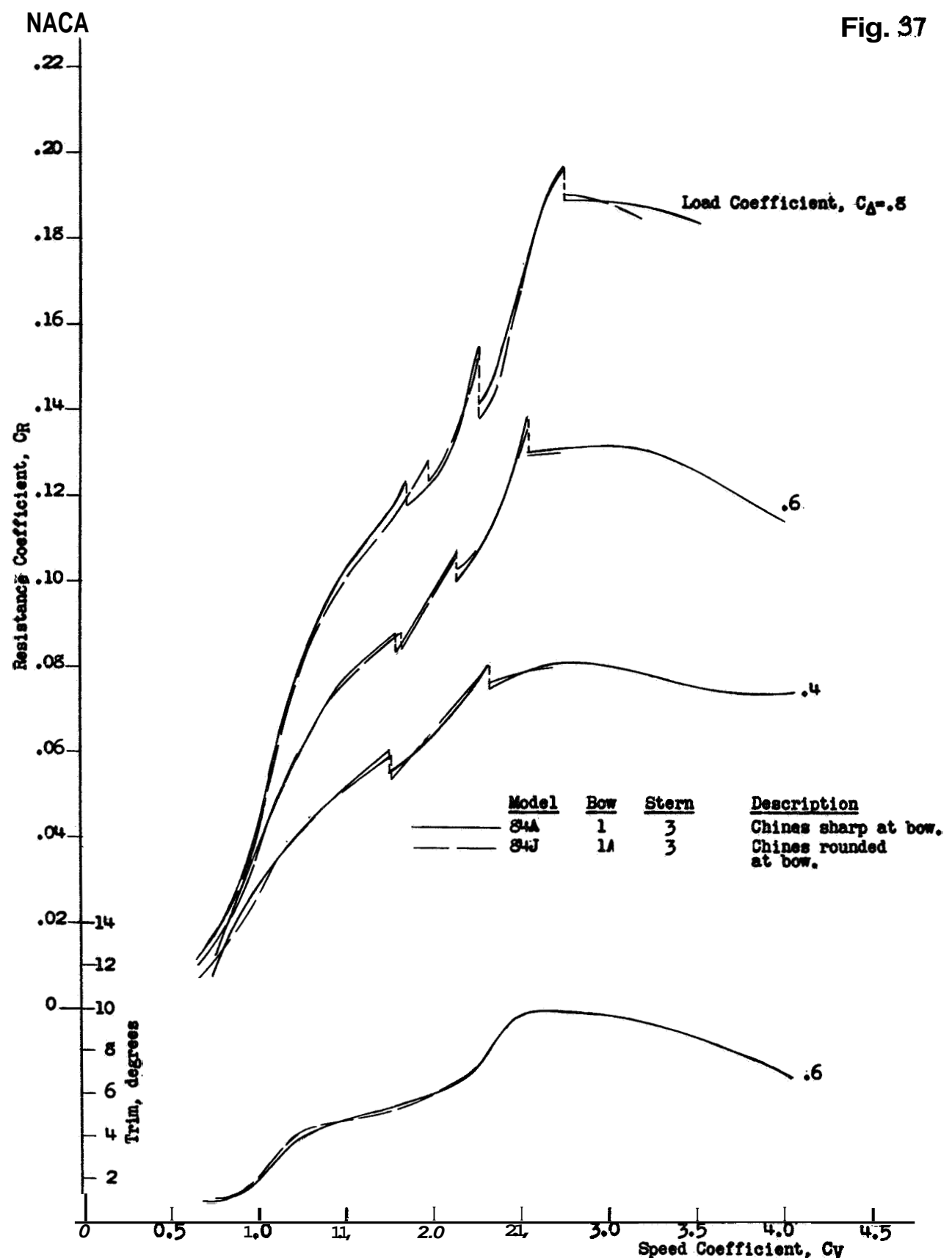


Figure 37 .- Effect of chines on low ban.  
Without chine flare.



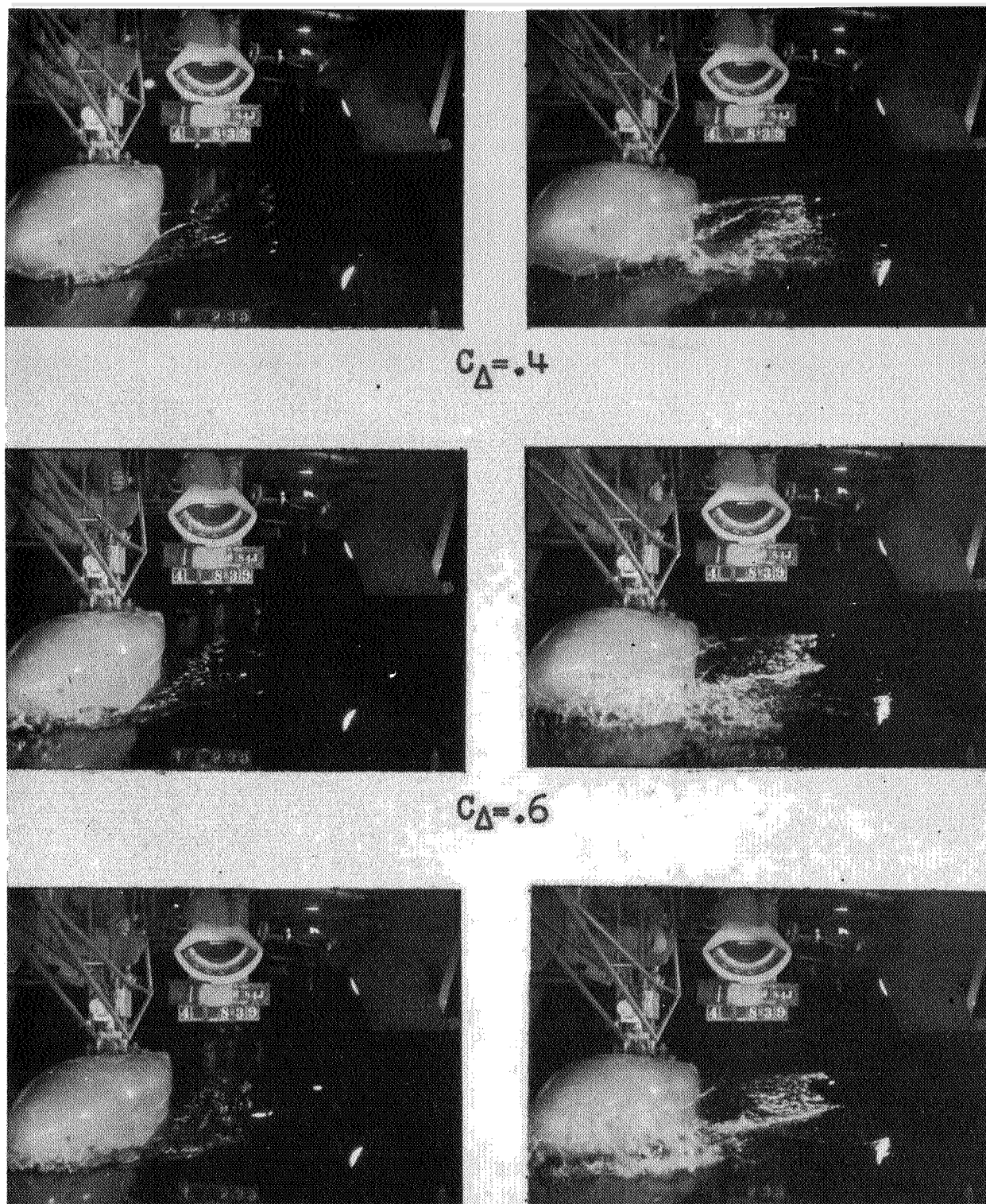
 $C_D = .4$  $C_D = .6$  $C_D = .8$  $C_V = .70$  $C_V = 1.17$ 

Figure 38 (a). Model 84J, Bow 1A, Stern 3.

Without chine flare.

NACA  
20550



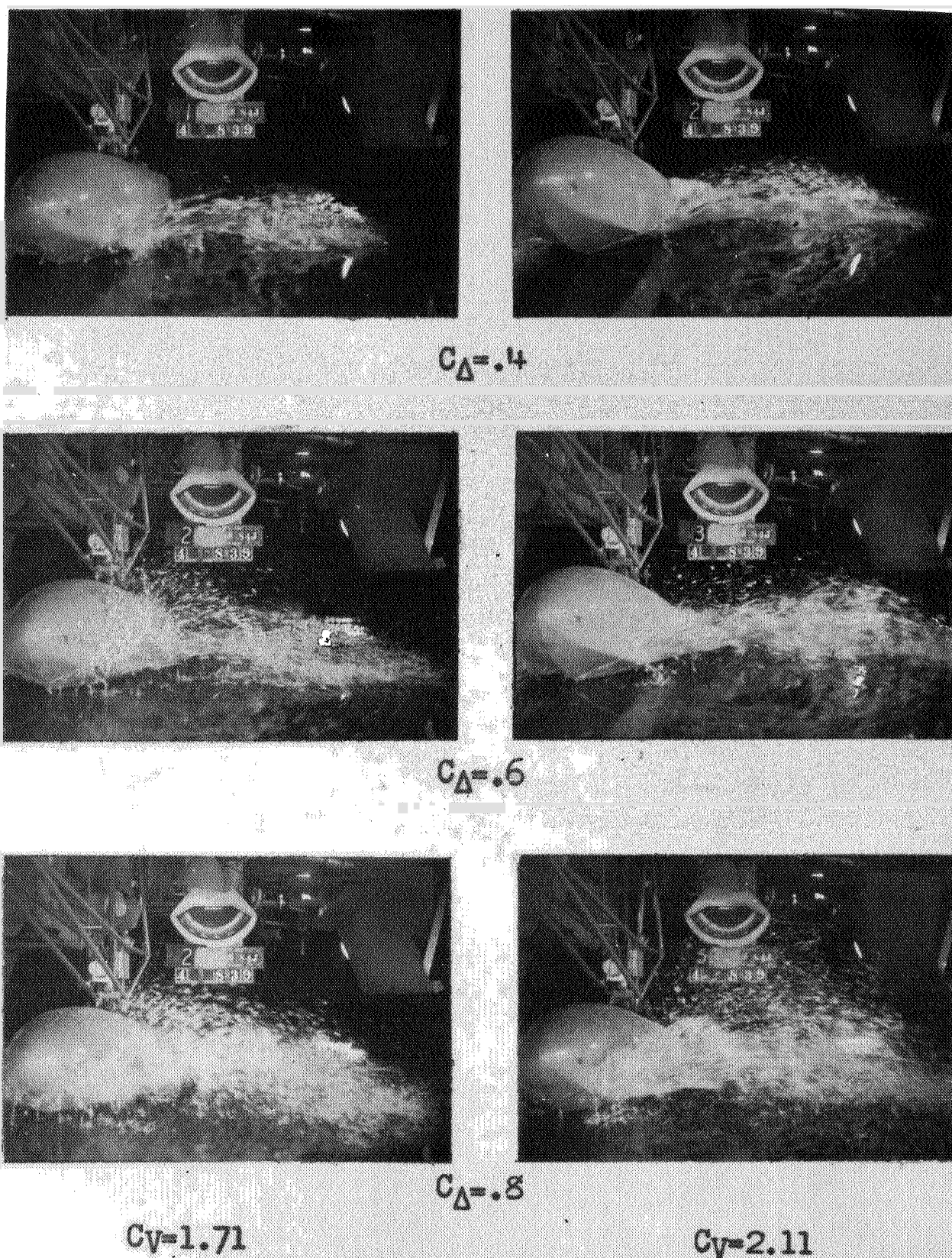
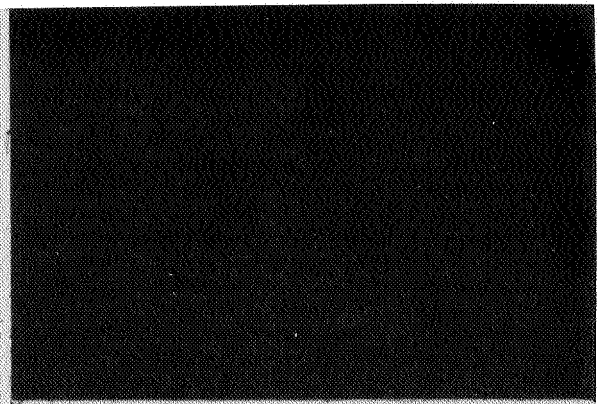
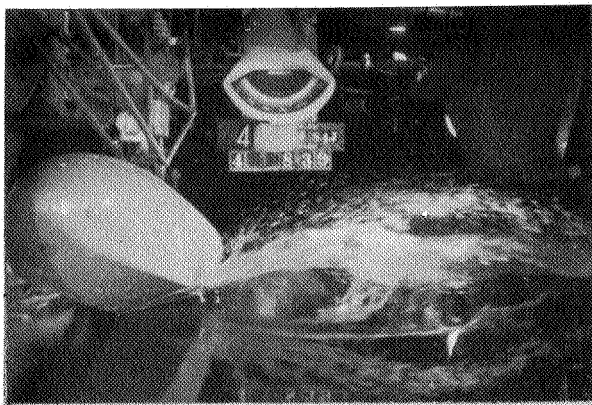
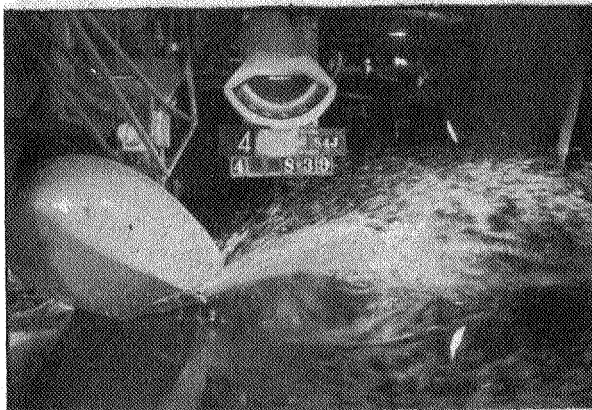


Figure 38 (b). Model 84J.

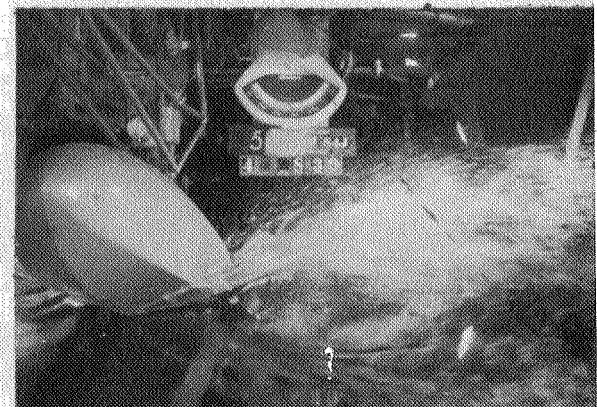
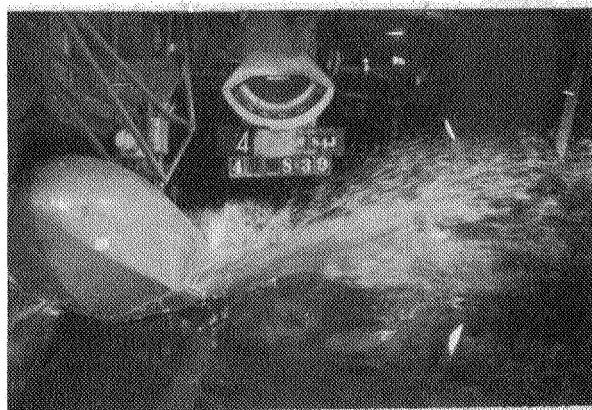
L-277



$C_D = .4$



$C_D = .6$



$C_D = .8$

$C_V = 2.63$

$C_V = 3.12$

Figure 38 (c). Model 84J.

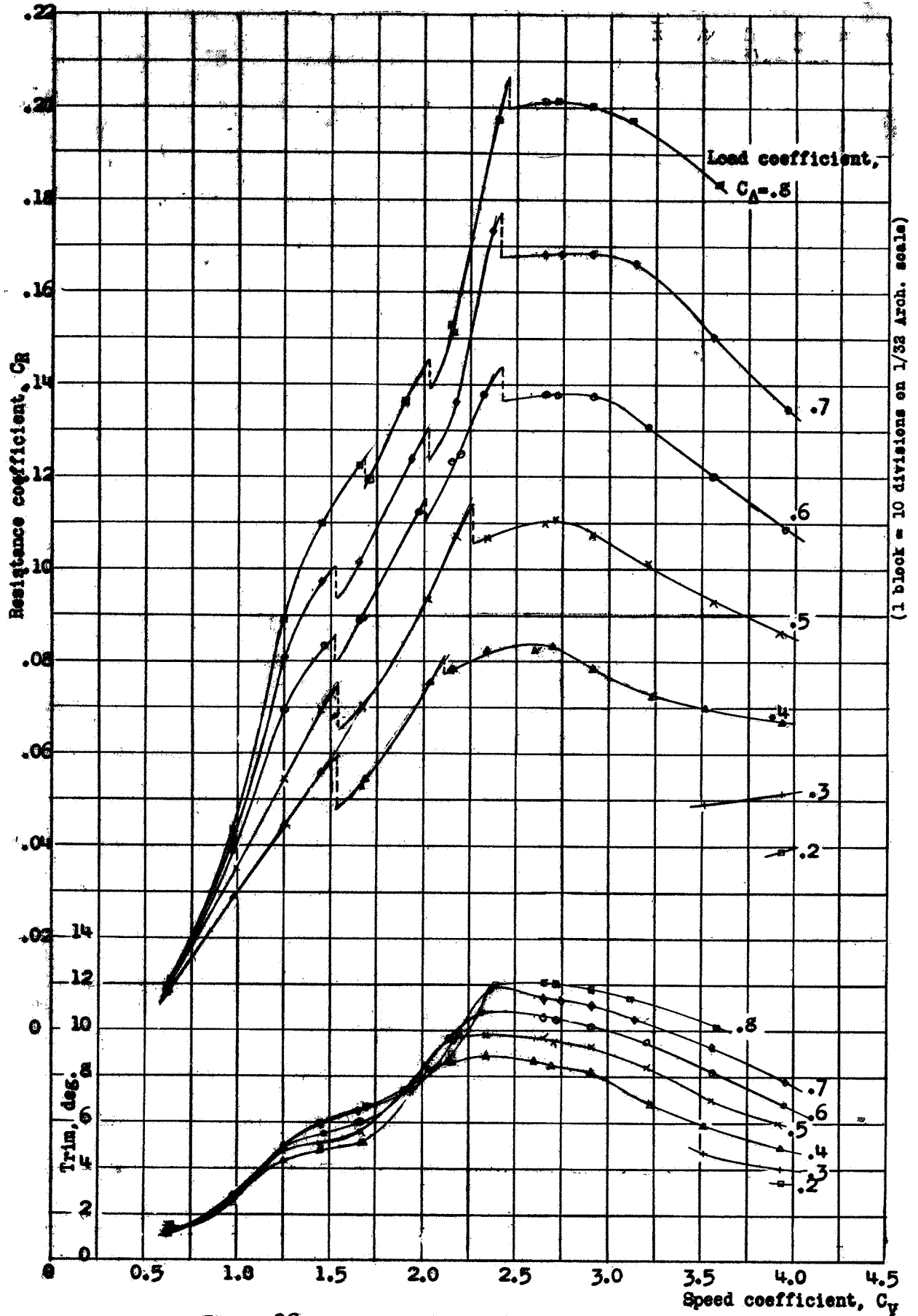


Figure 39. - Model 84-EF-3, Free-to-trim characteristics.

L-277

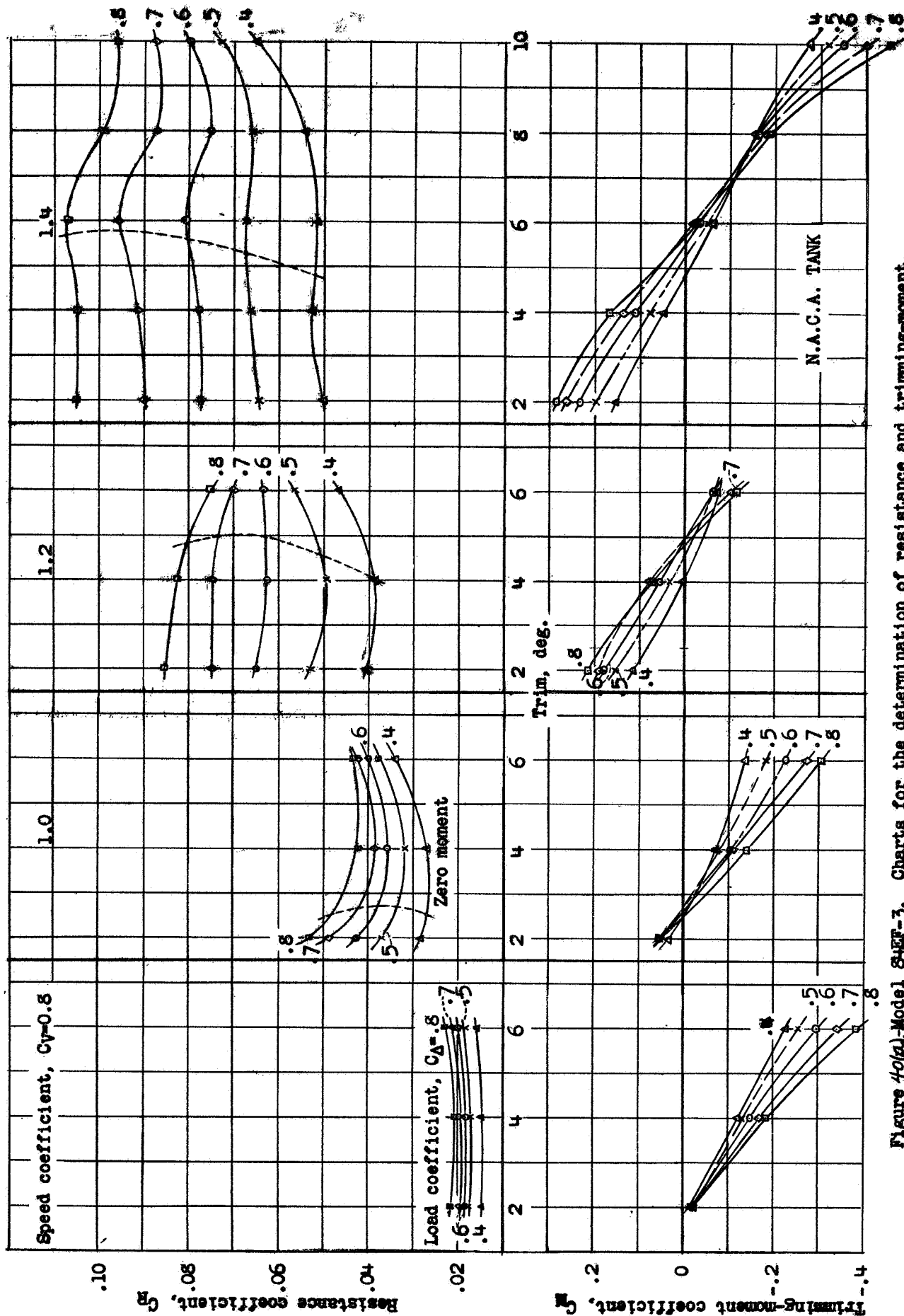


Figure 40(a). Model SAEF-3. Charts for the determination of resistance and trimming-moment.



L-277

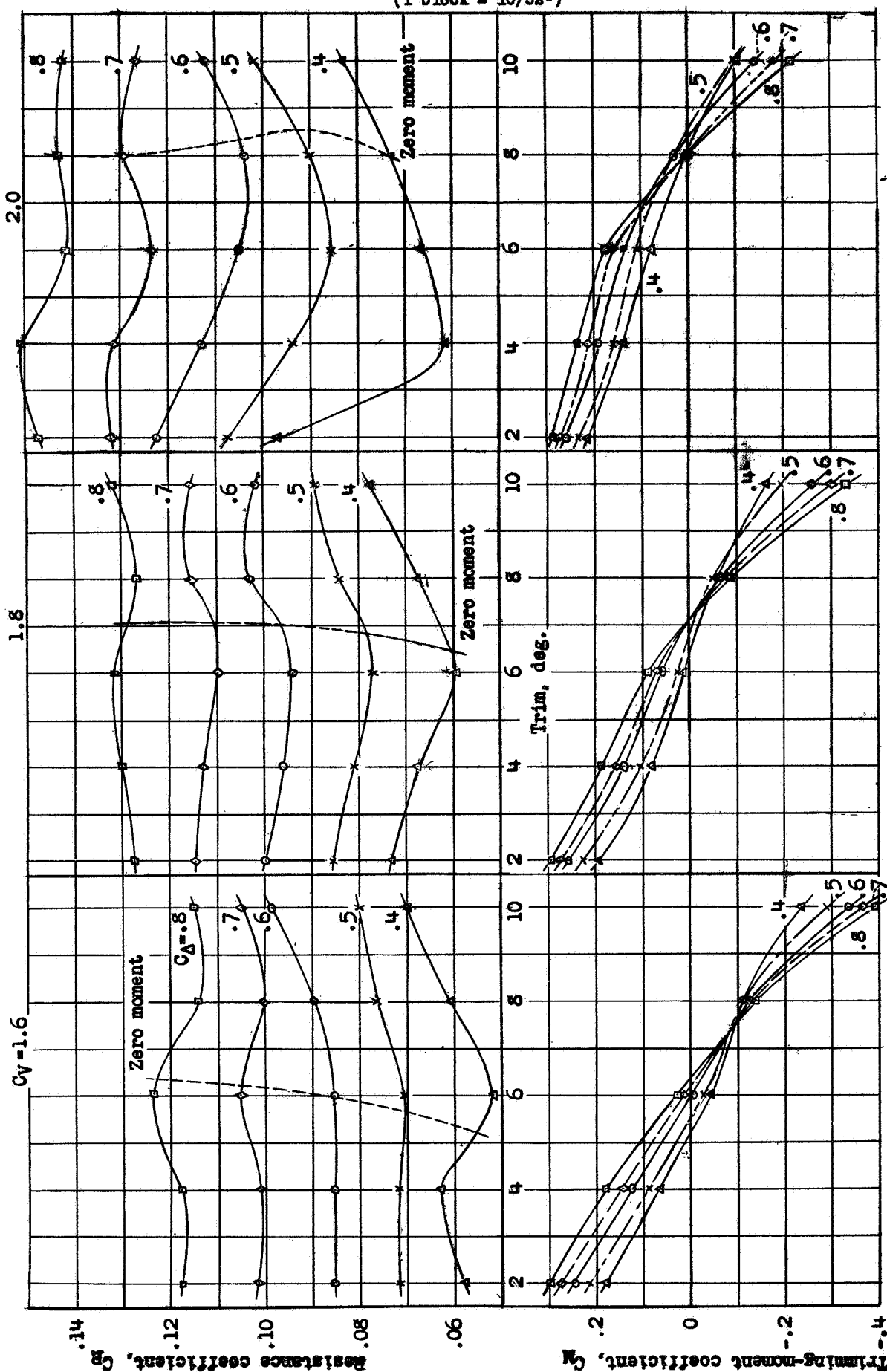


Figure 40(b), - Model S1-EF3.

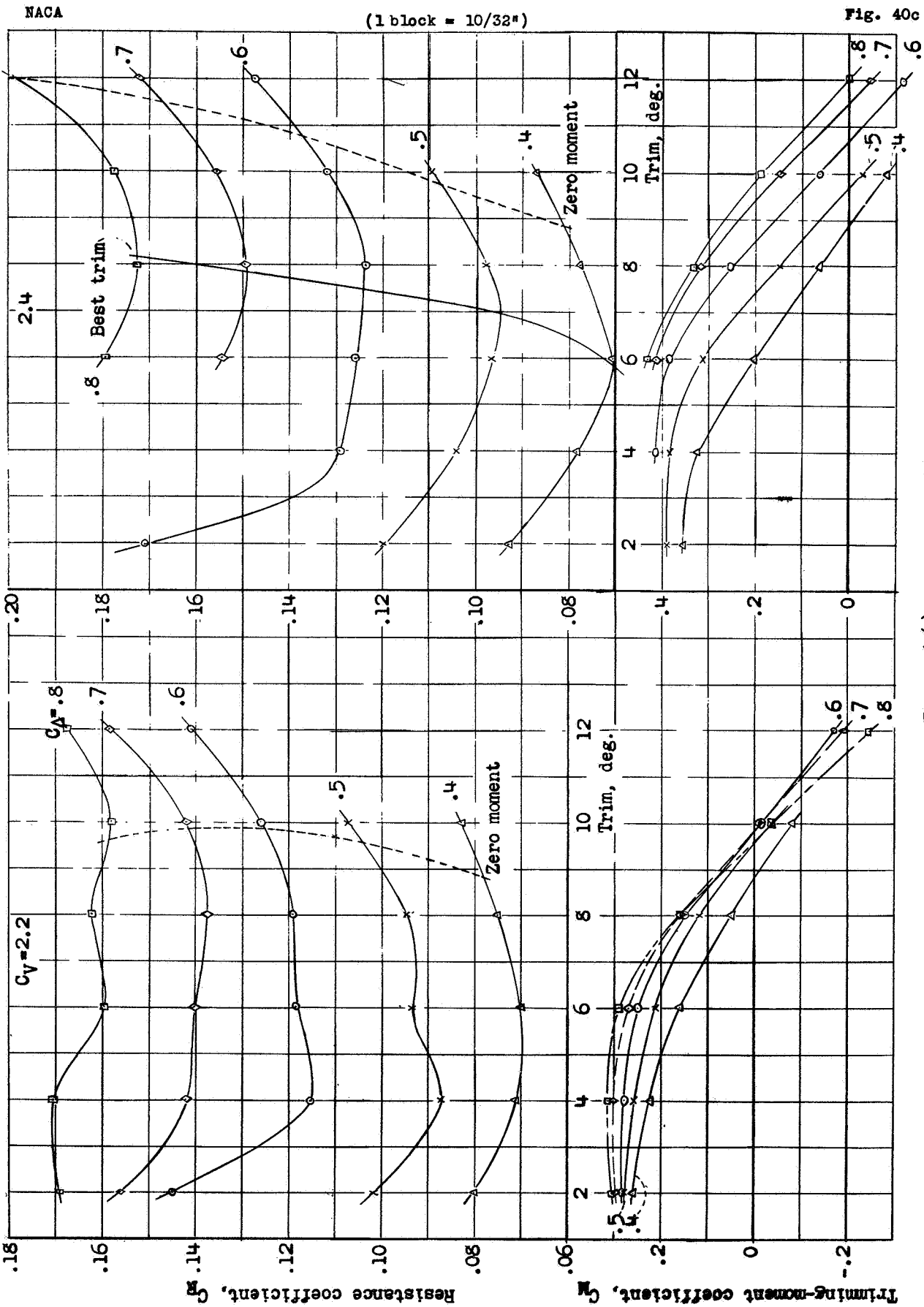


Figure 40(c). - Model 84-EF3.

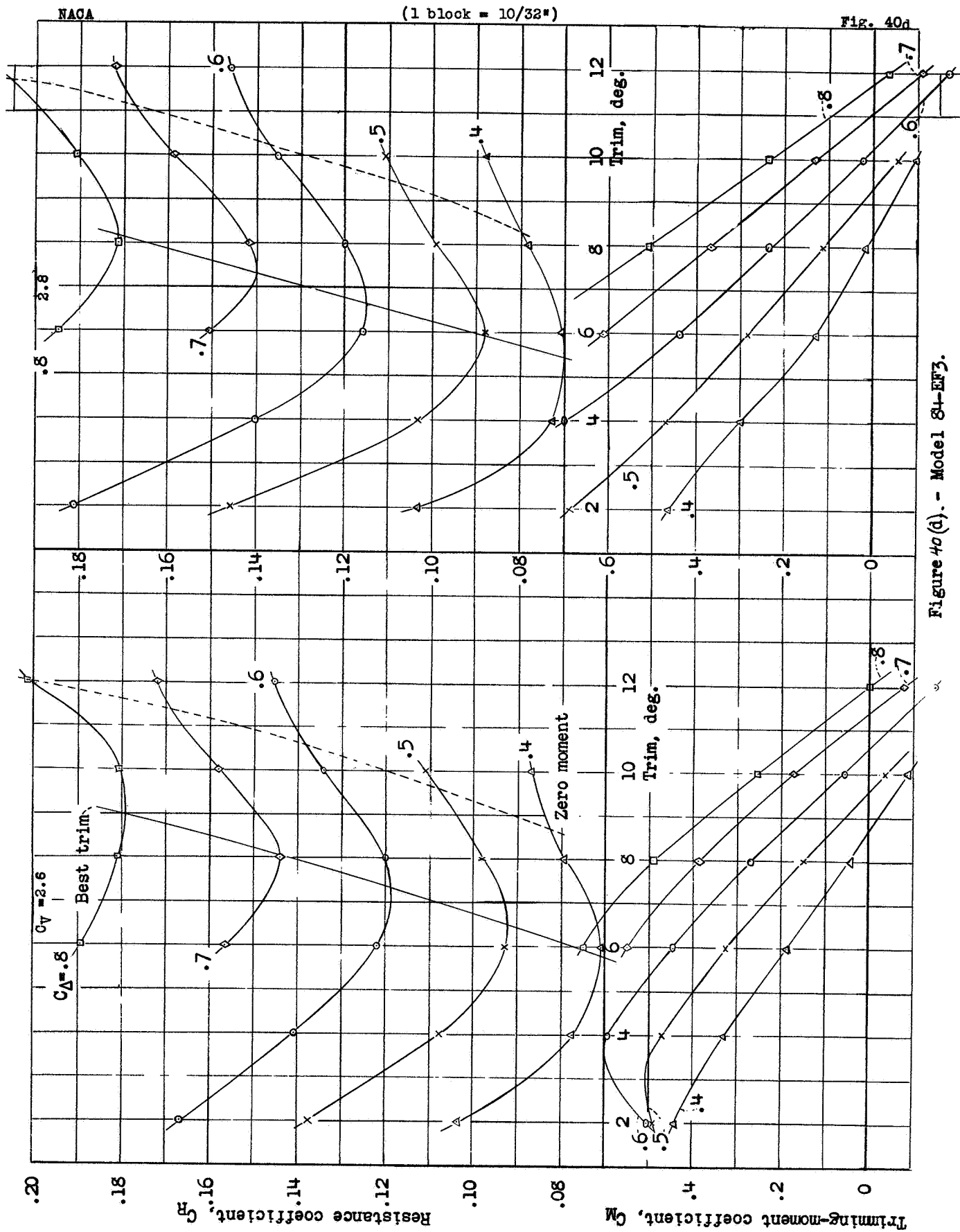


Figure 40(d). - Model 84-EF3.

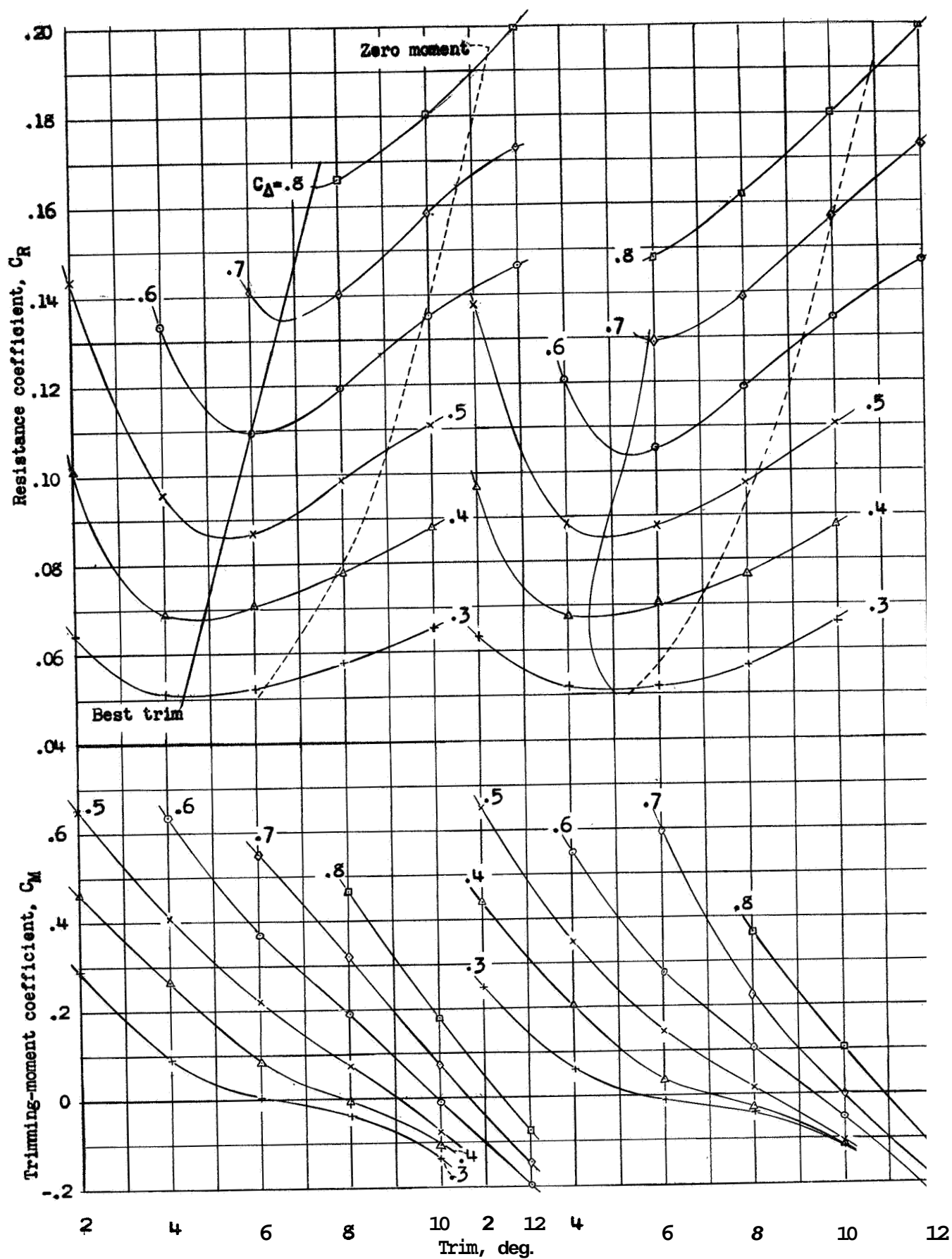


Figure 40 (e). - Model 84-EF3.



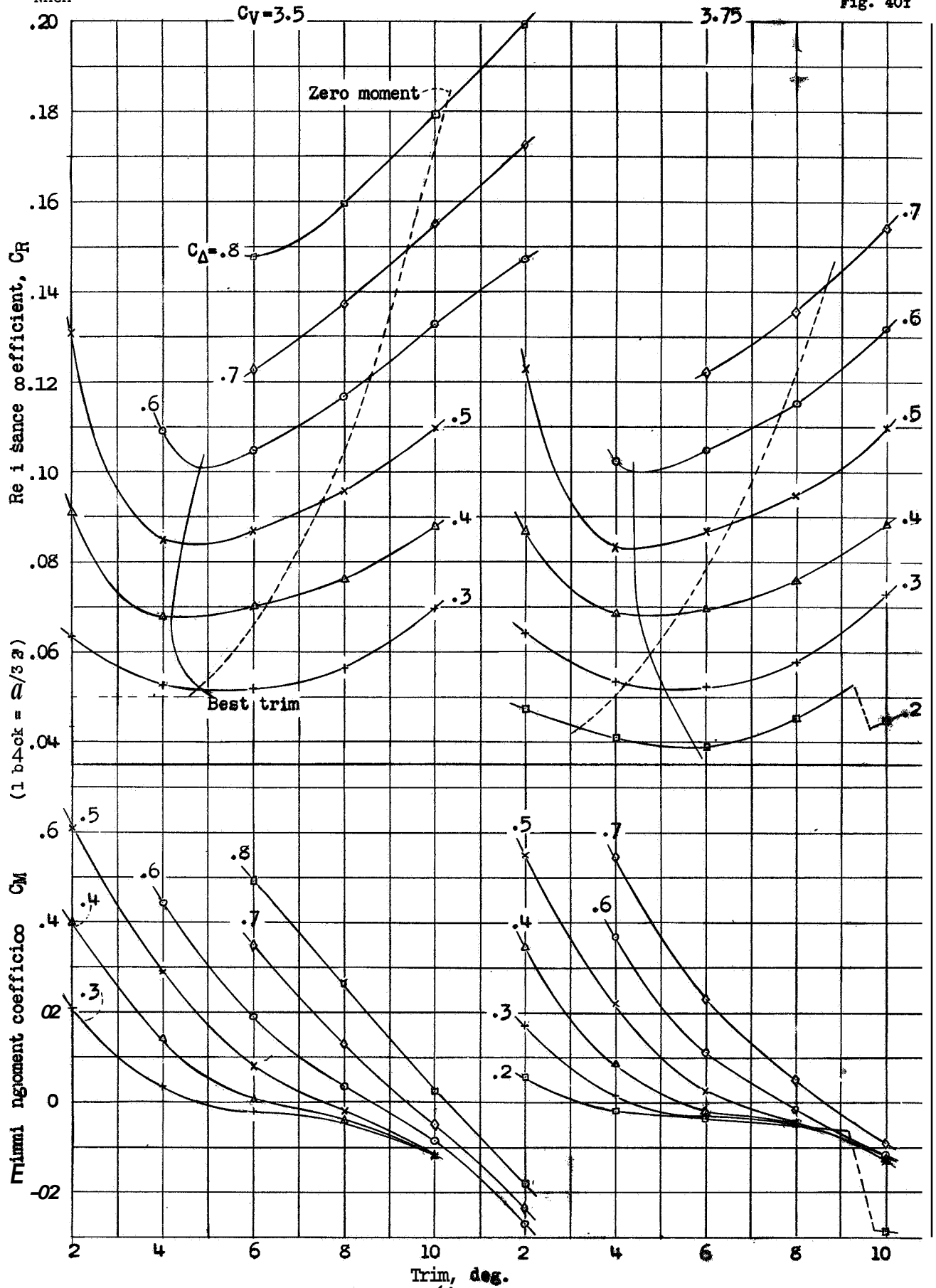
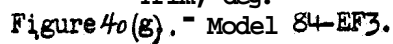


Figure 40(f) - Model 84-EF3.



L-277

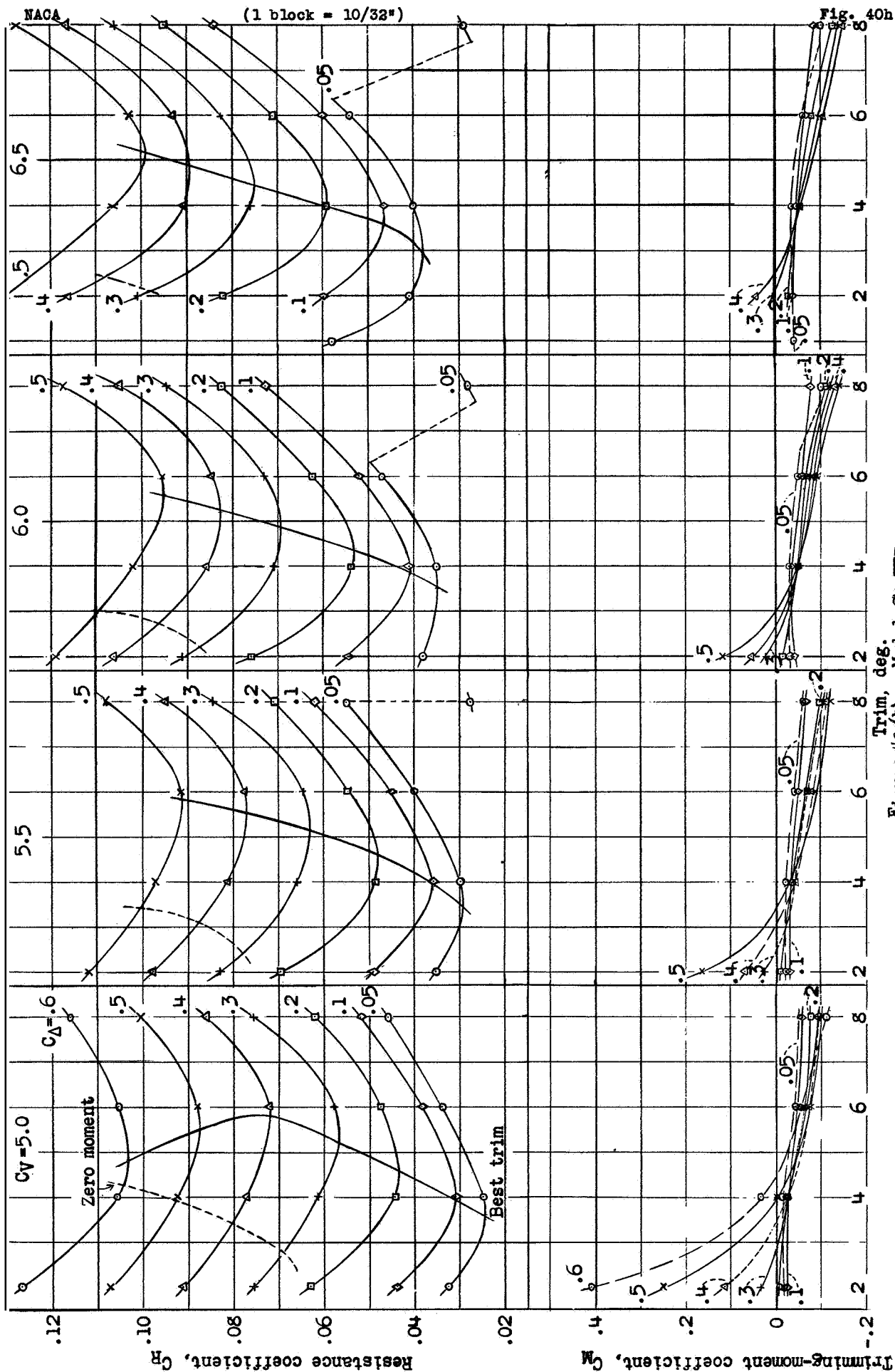


Figure 40 (h). - Model 84-EF3.

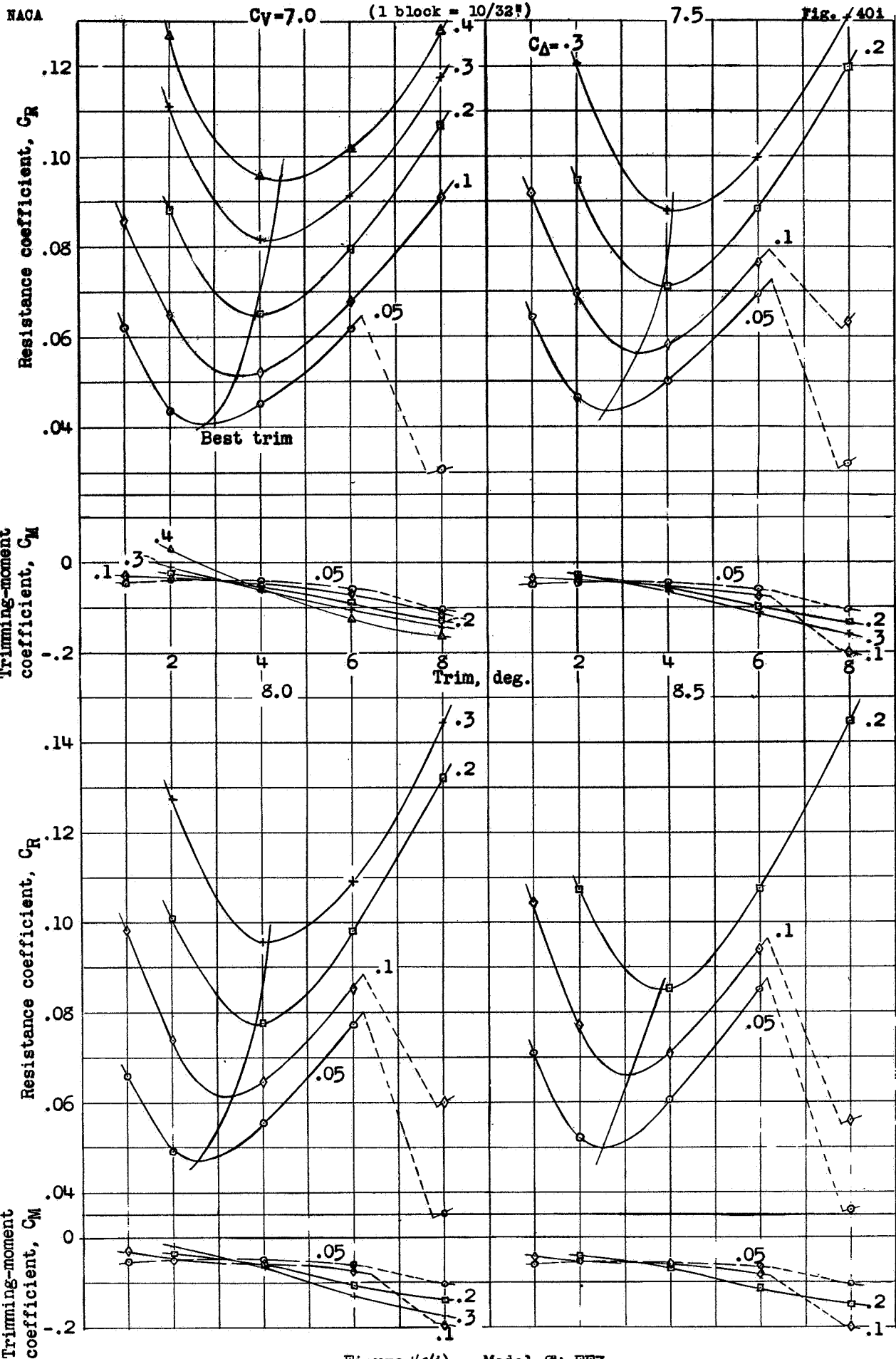


Figure 40(i). - Model 84-EF3.



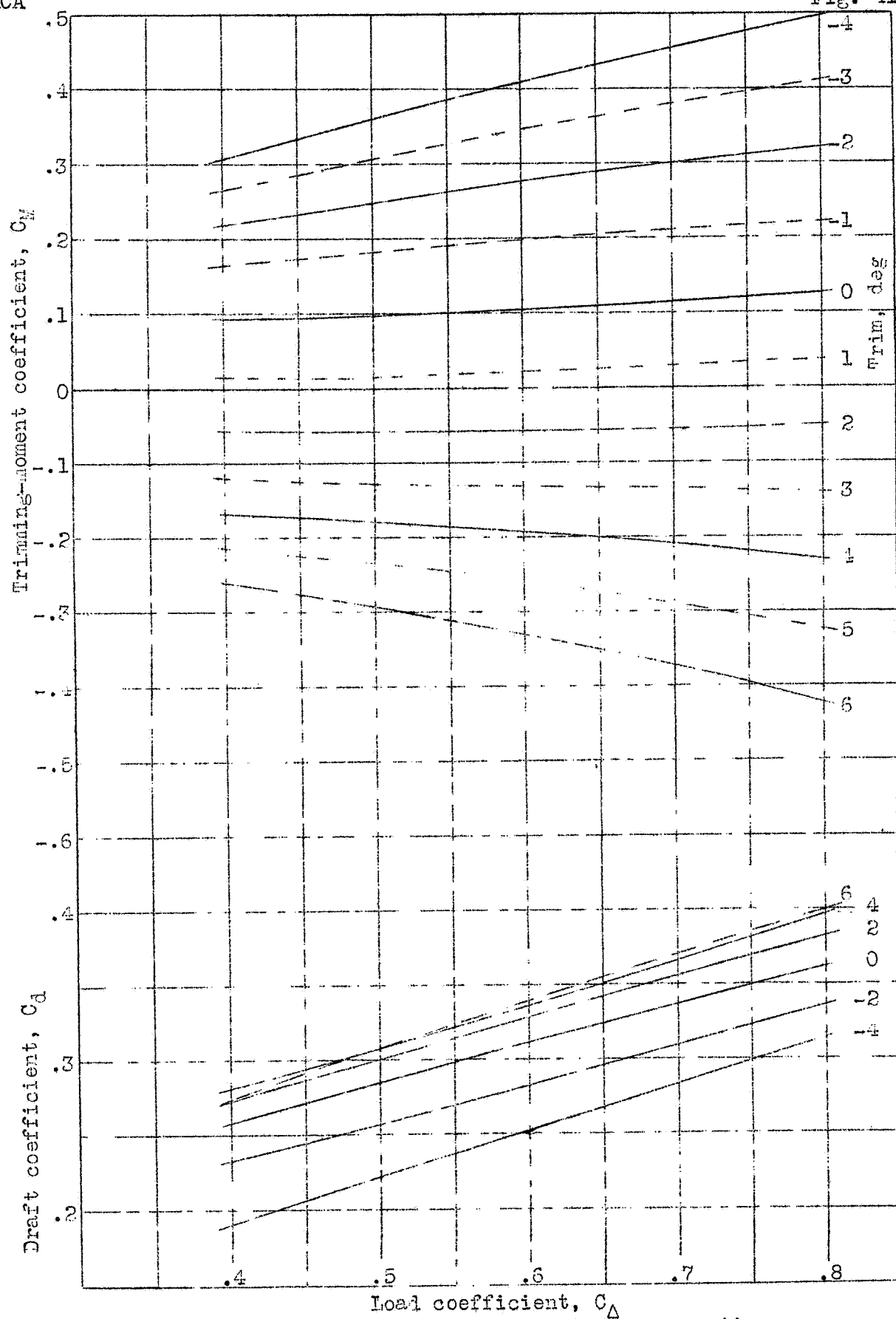


Figure 41.- Model 84EF-3, static properties.

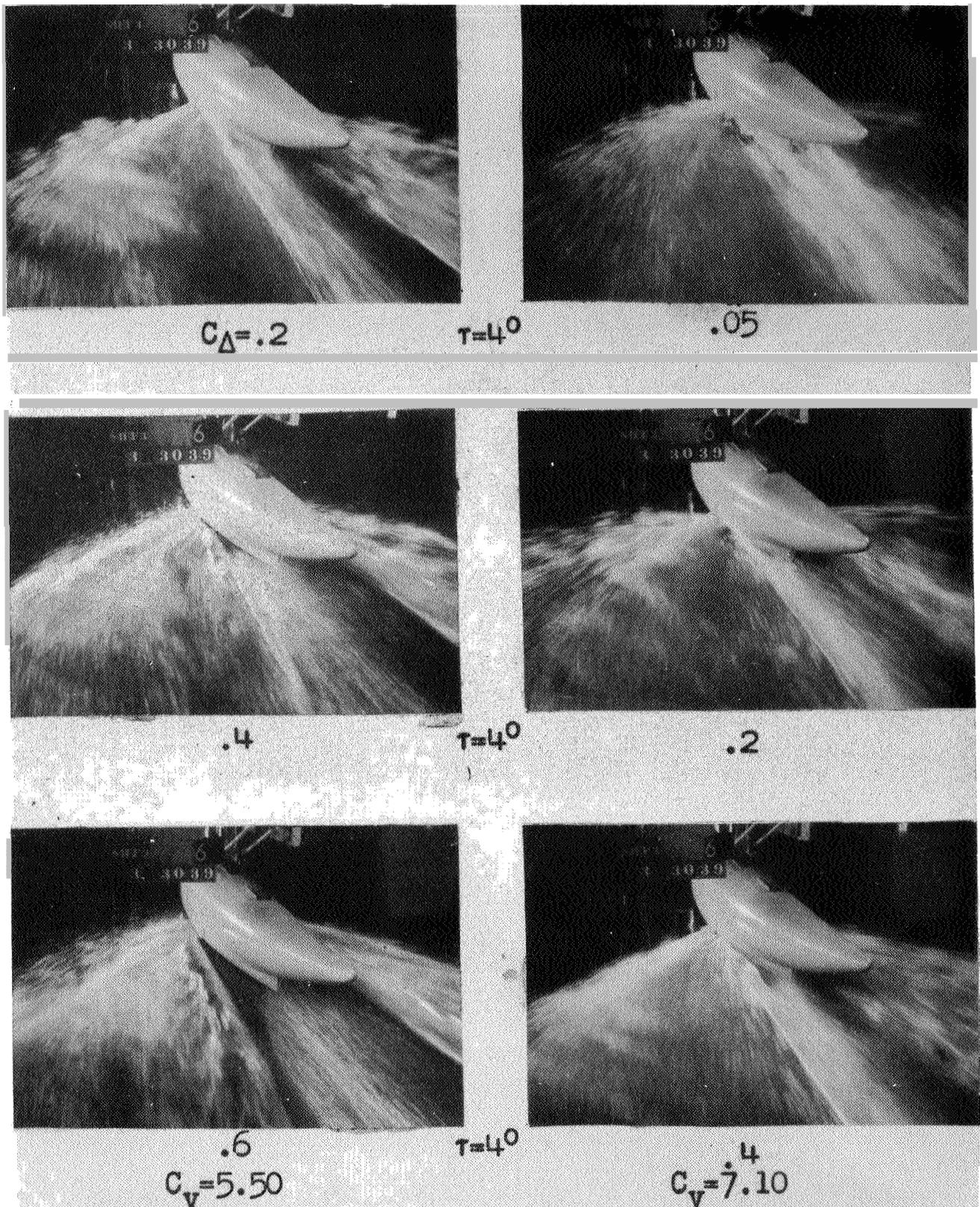


Figure 42.- Model 84 EF-3, Bow 1, Stern 4.  
 Depth of step .70 in., Angle of afterbody keel  $5.5^\circ$   
 Chine flare on forebody only.

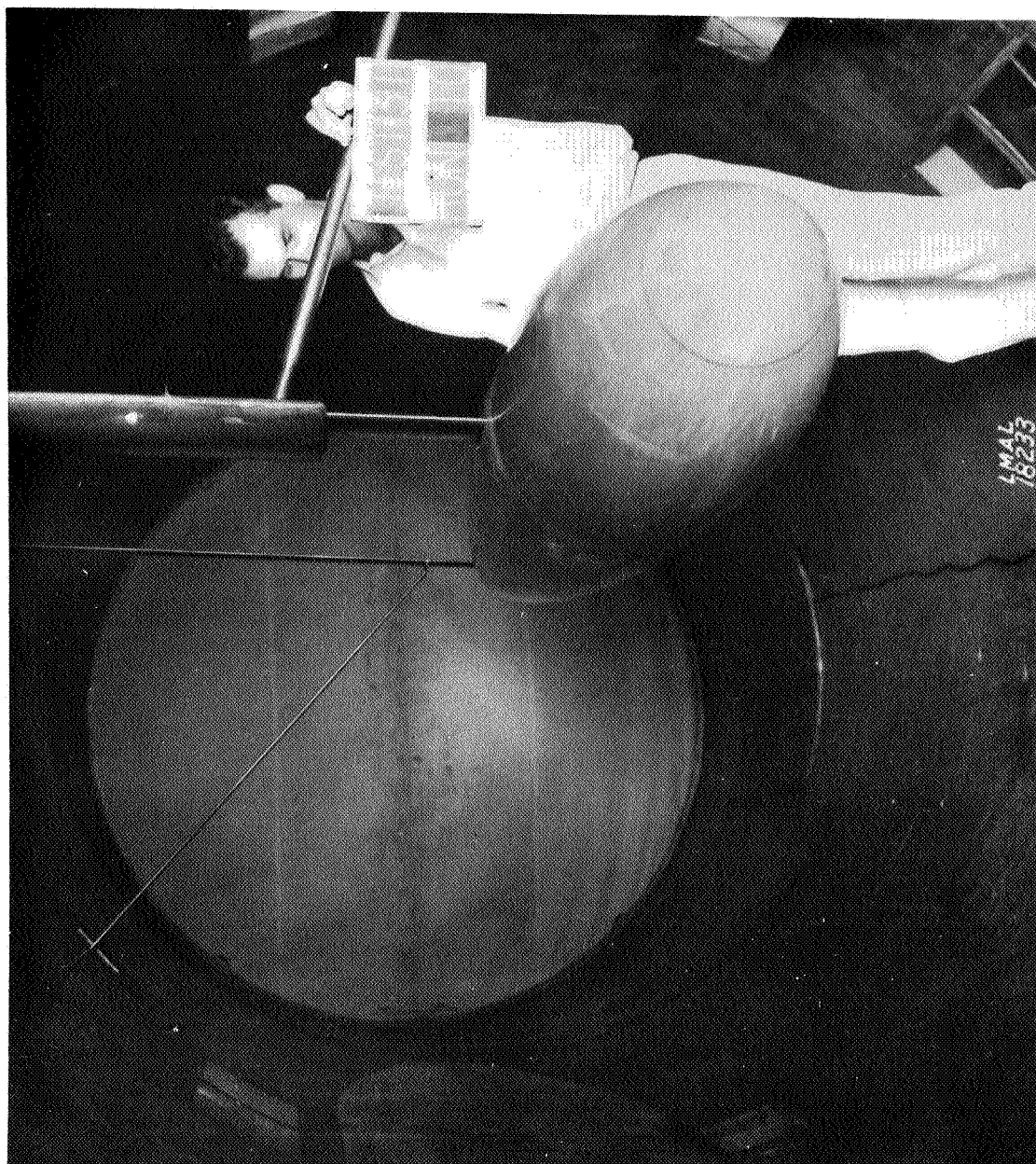


Figure 43.- The installation of streamline body, nose 1 and tail 1, in the 8-foot high-speed wind tunnel.



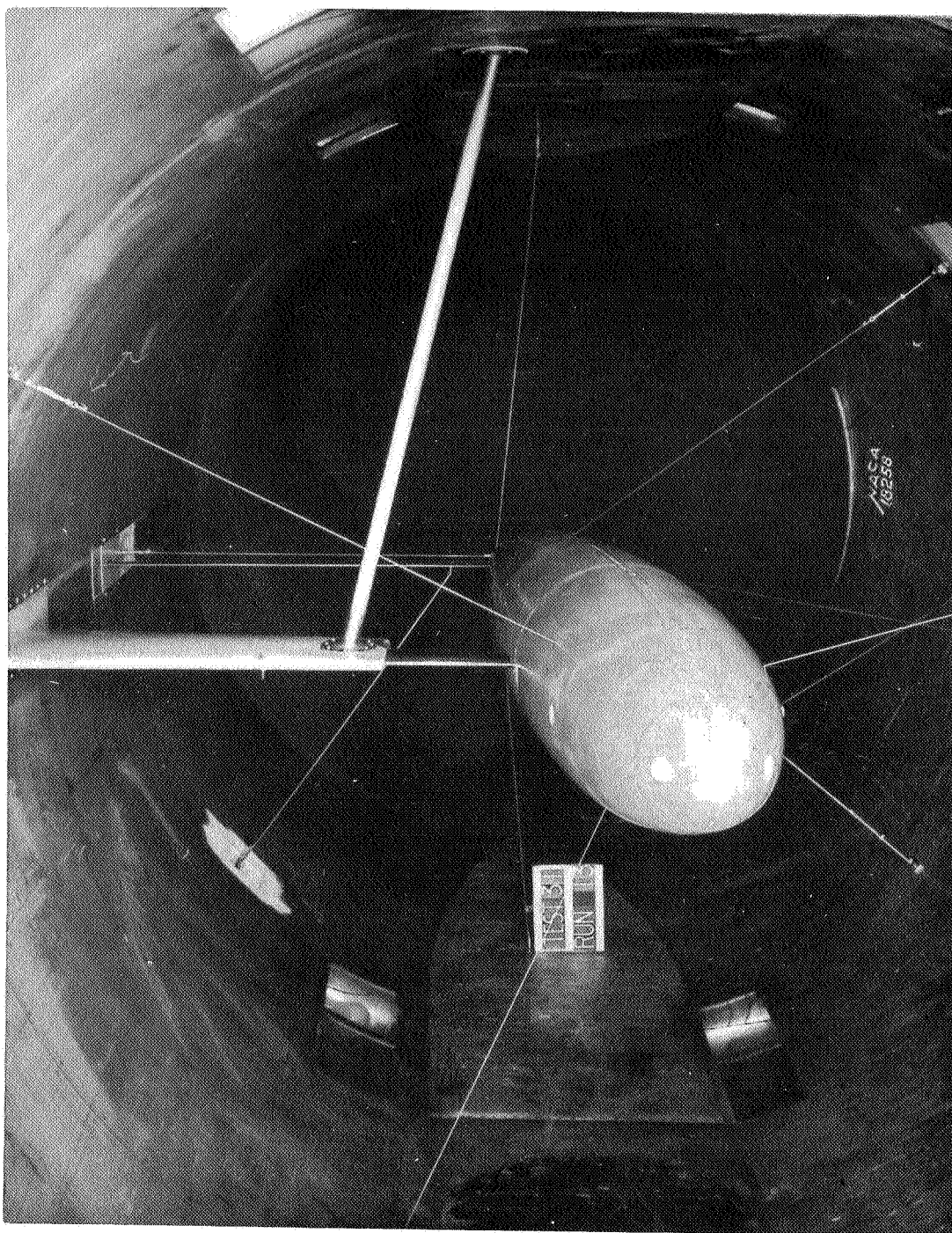


Figure 44.- Tare-drag installation to hold model in place by wires so that the model does not touch struts.



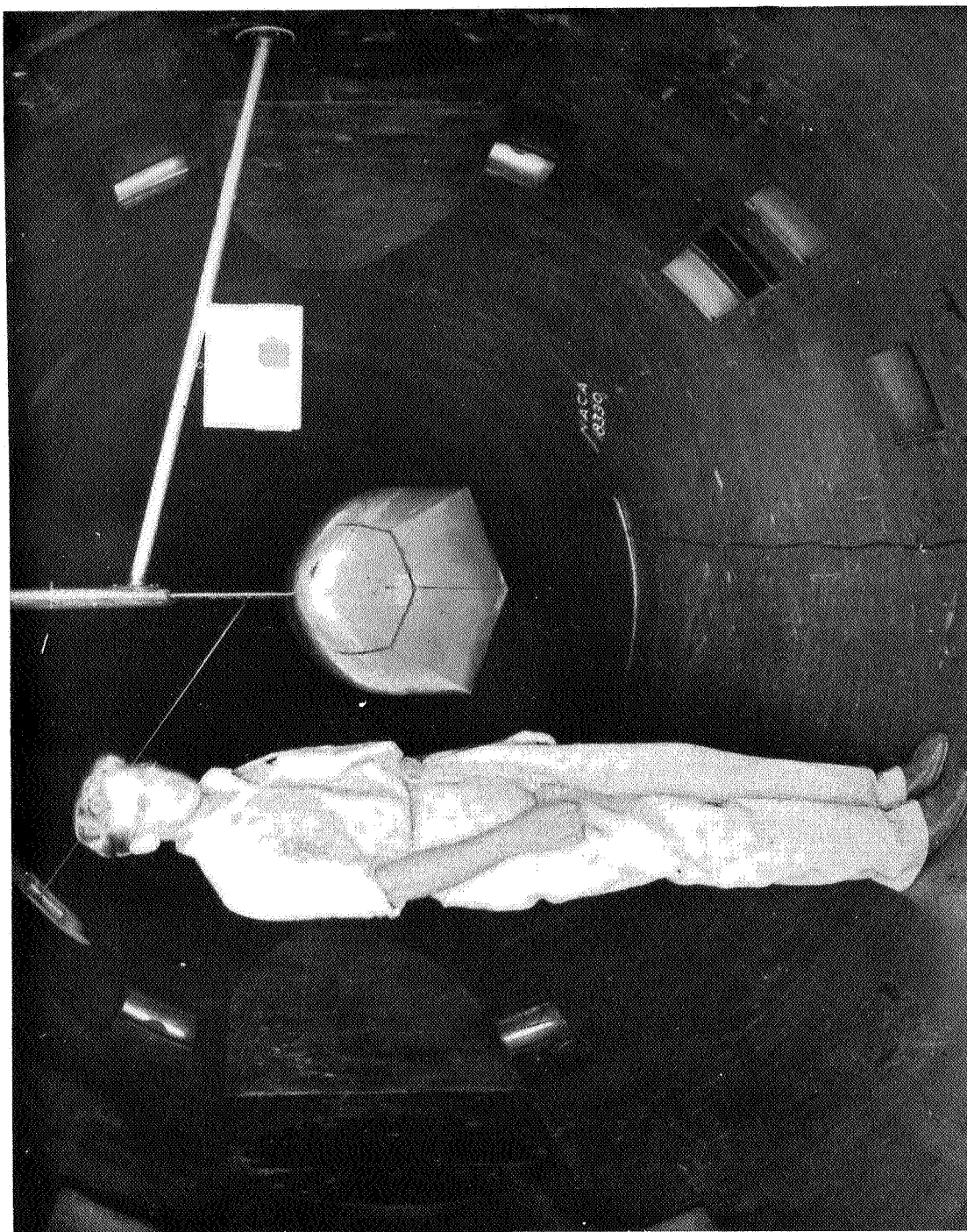


Figure 45.- The installation of the hull combination of bow 3-stern 3 in the 8-foot high-speed wind tunnel.

NACA

Fig 46

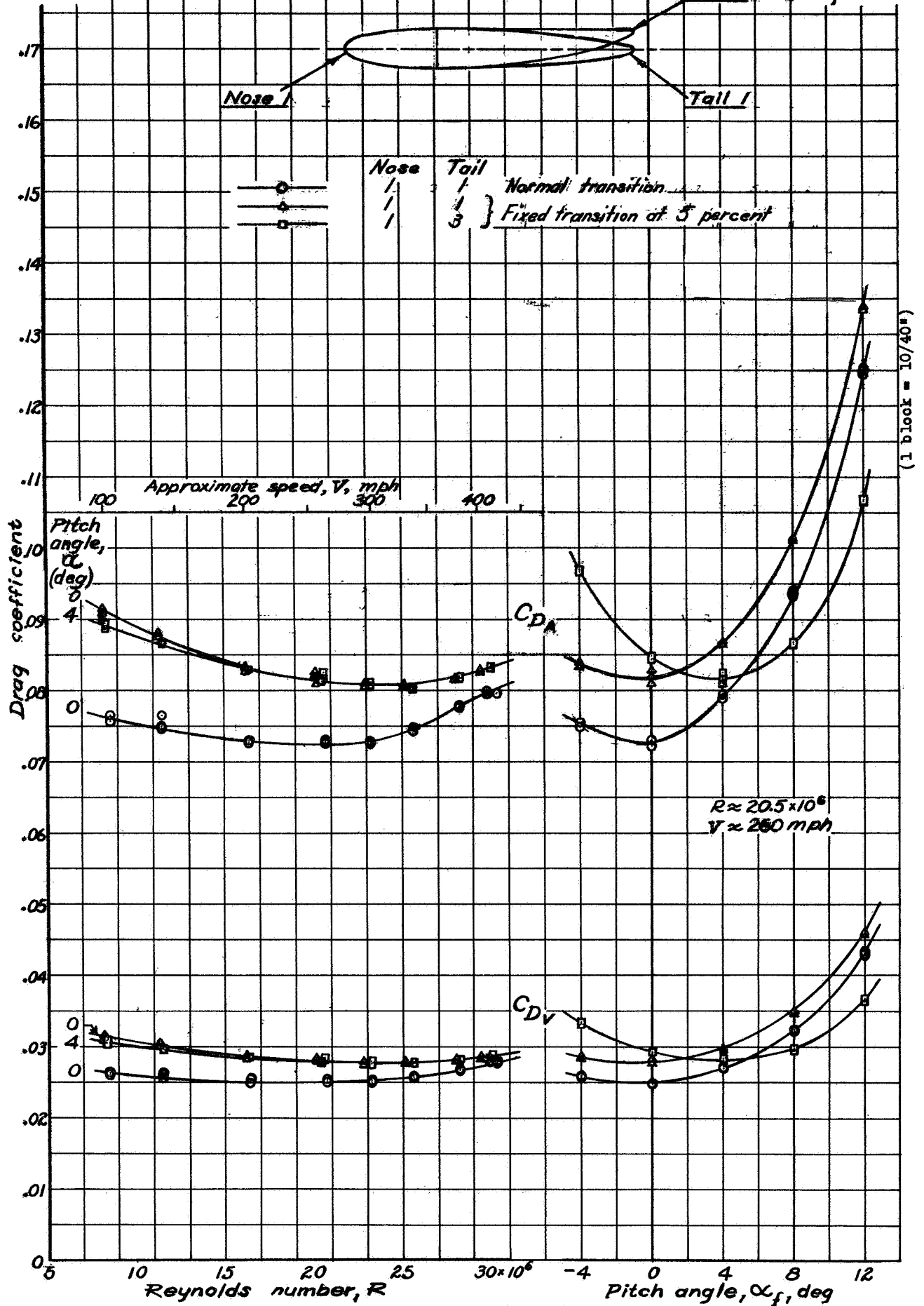


Figure 46.- Drag effects of height of tail of streamline bodies.

NACA

Fig. 47

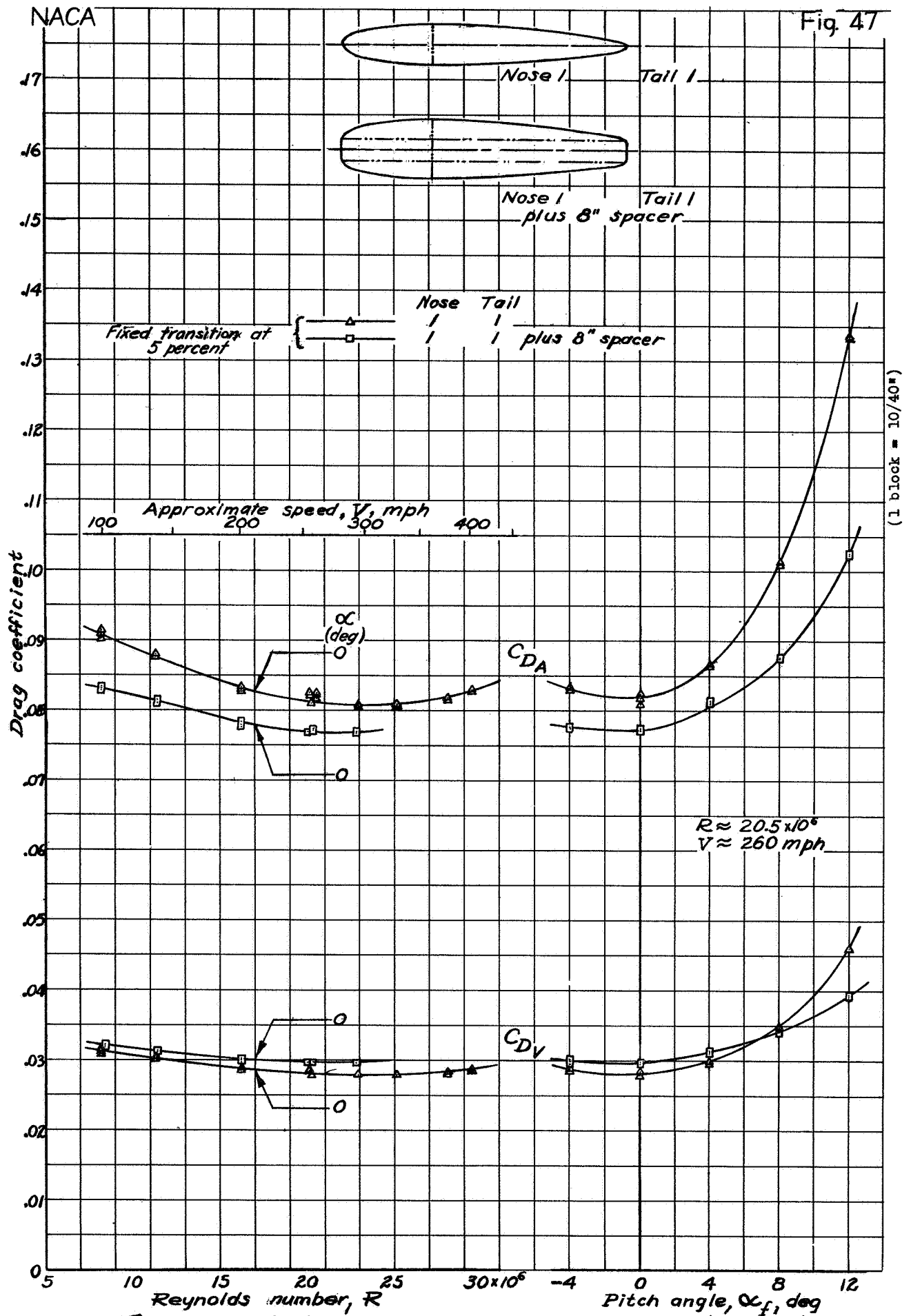


Figure 47.-Drag effects of increased depth on streamline bodies.

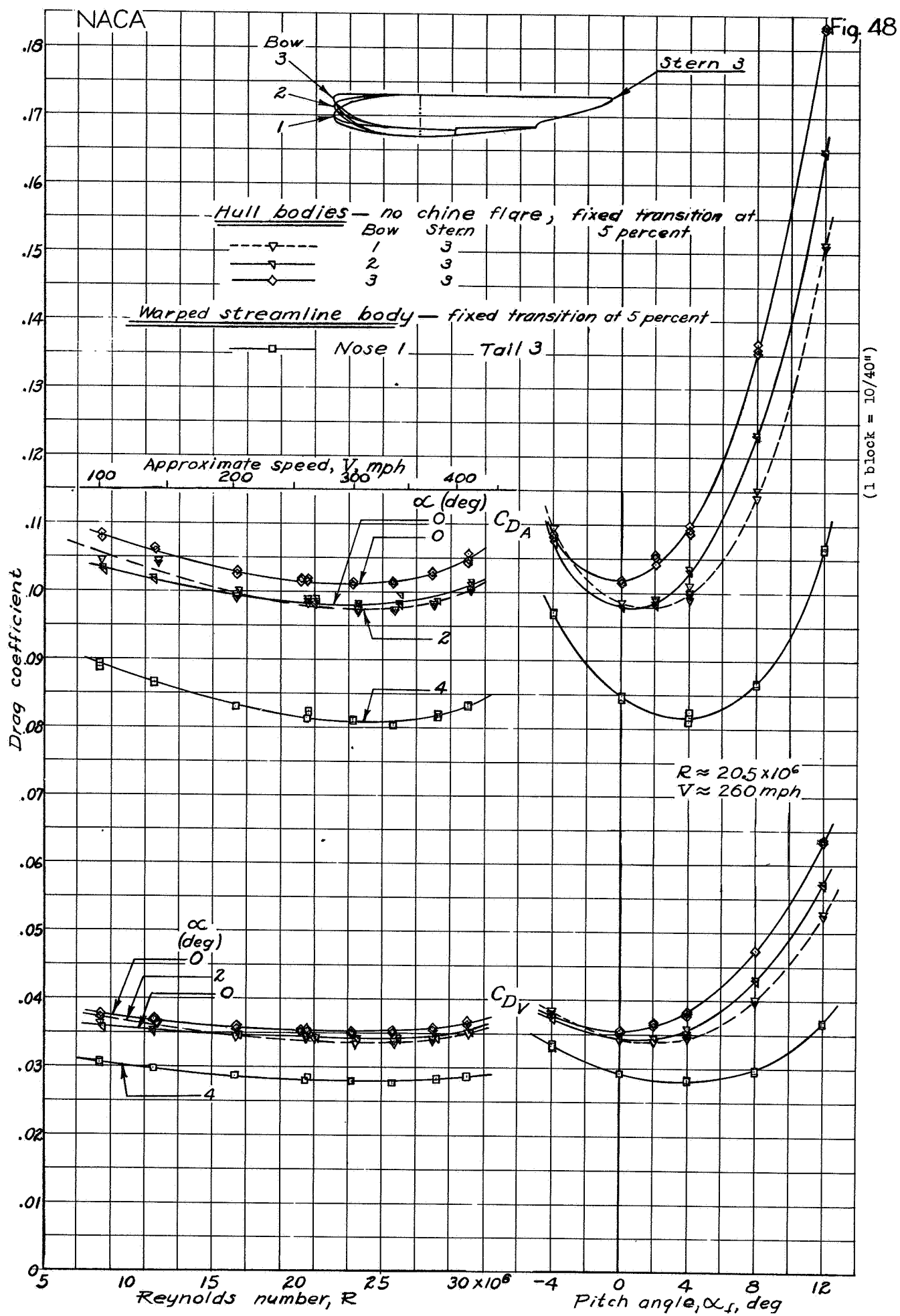


Figure 48 - Effect of bow height of hulls.



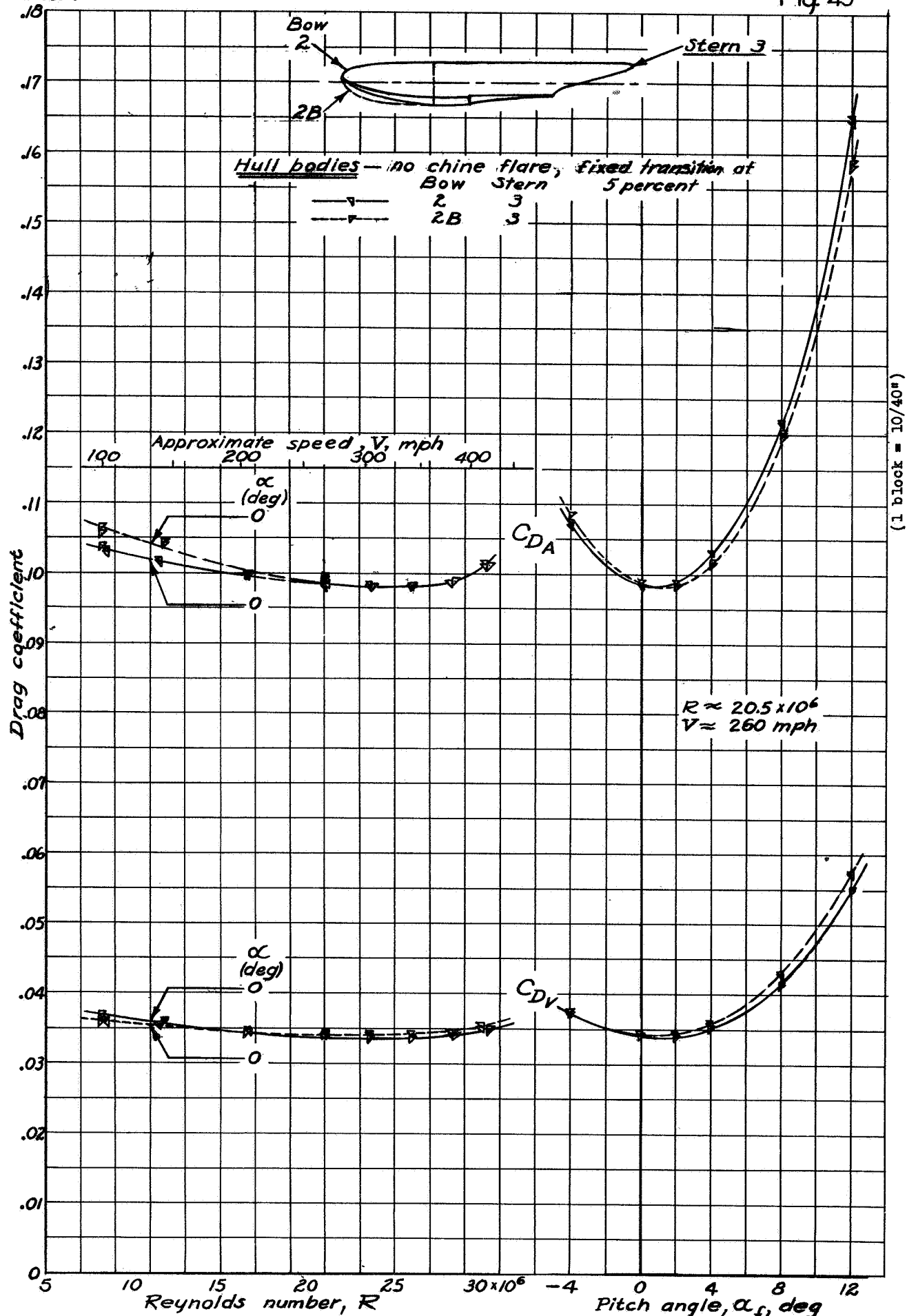


Figure 49.— Effect of angle of dead rise at bow of hull.

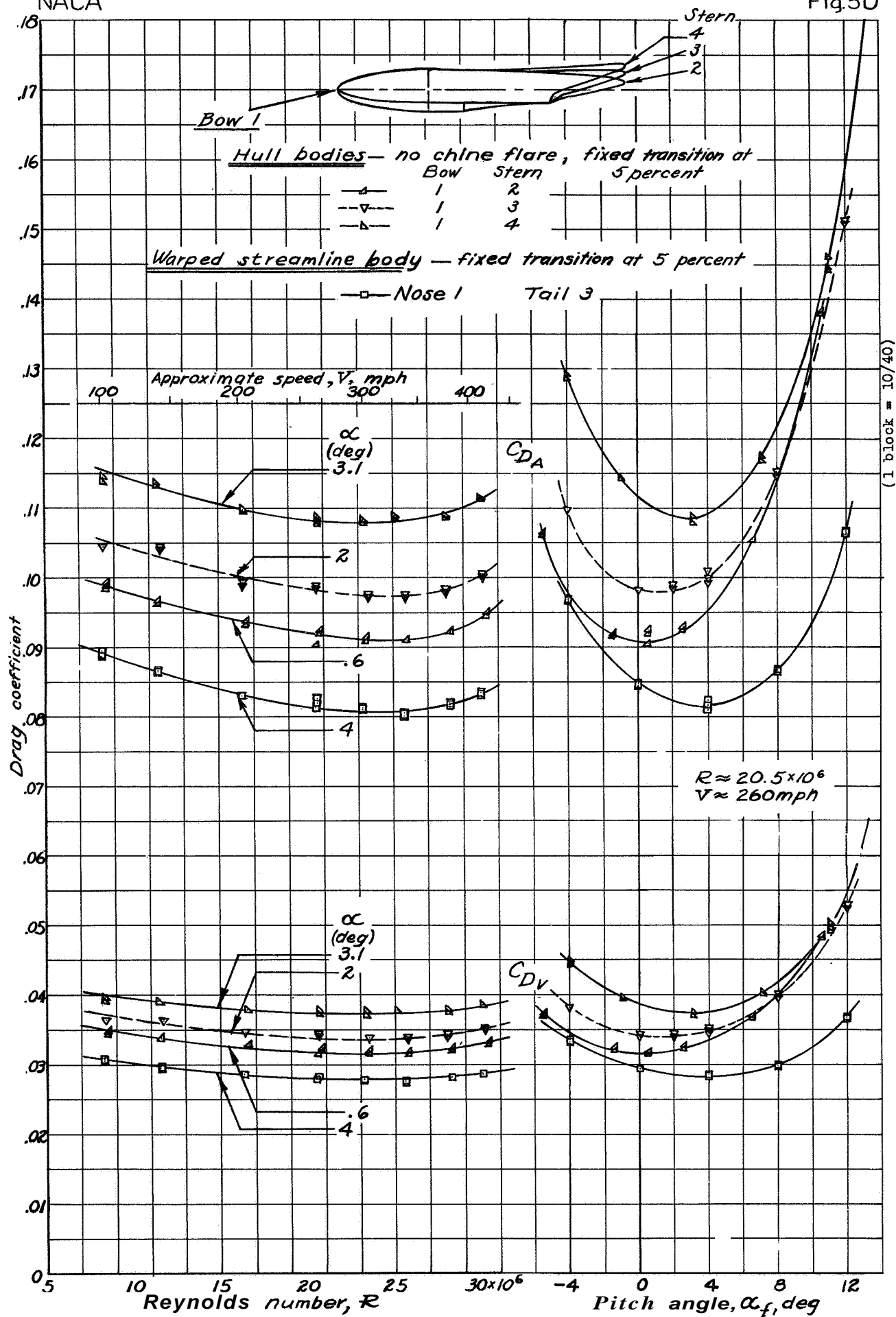


Figure 50.— Effect of height of stern of hulls

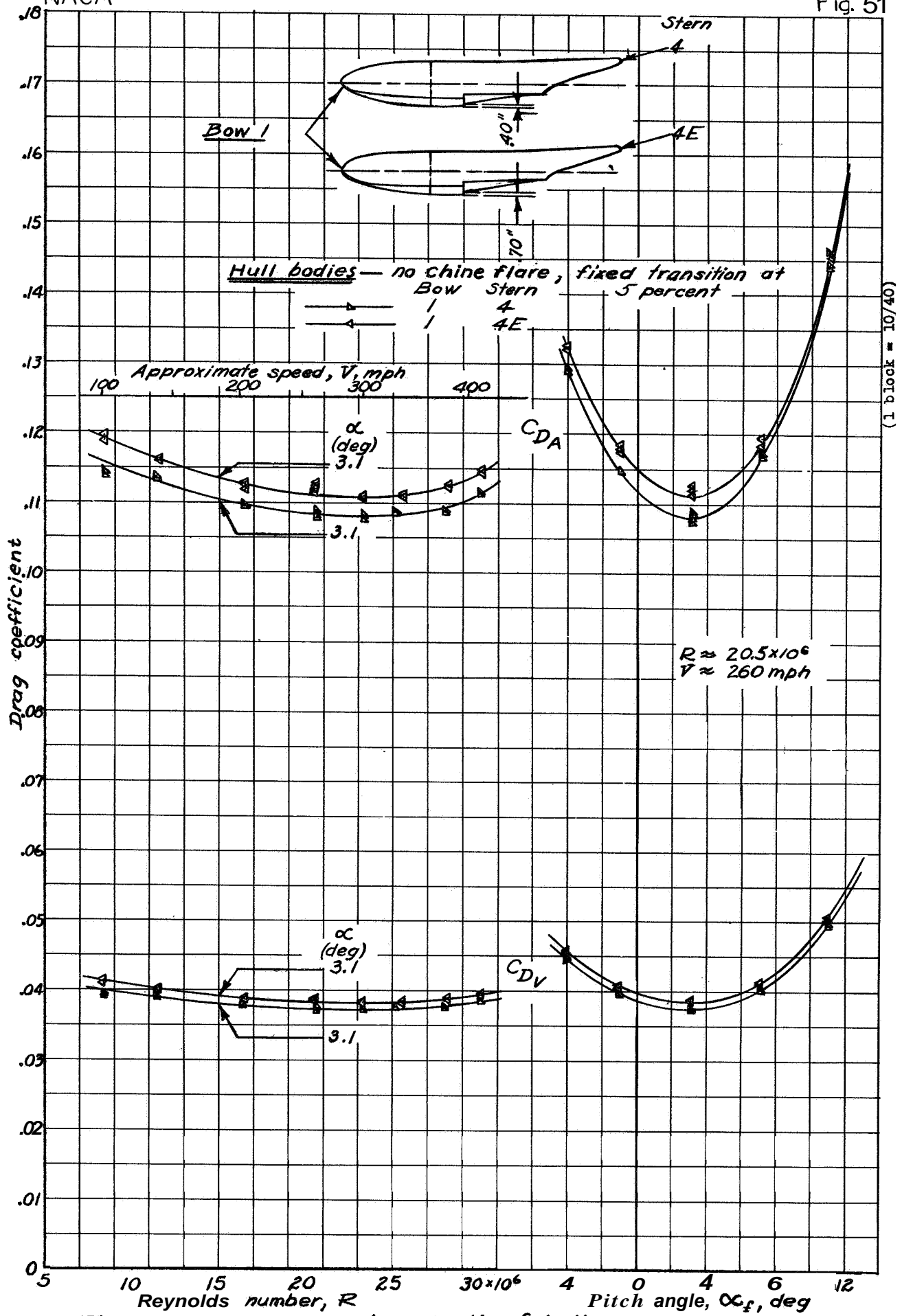


Figure 51.— Effect of step depth of hulls.

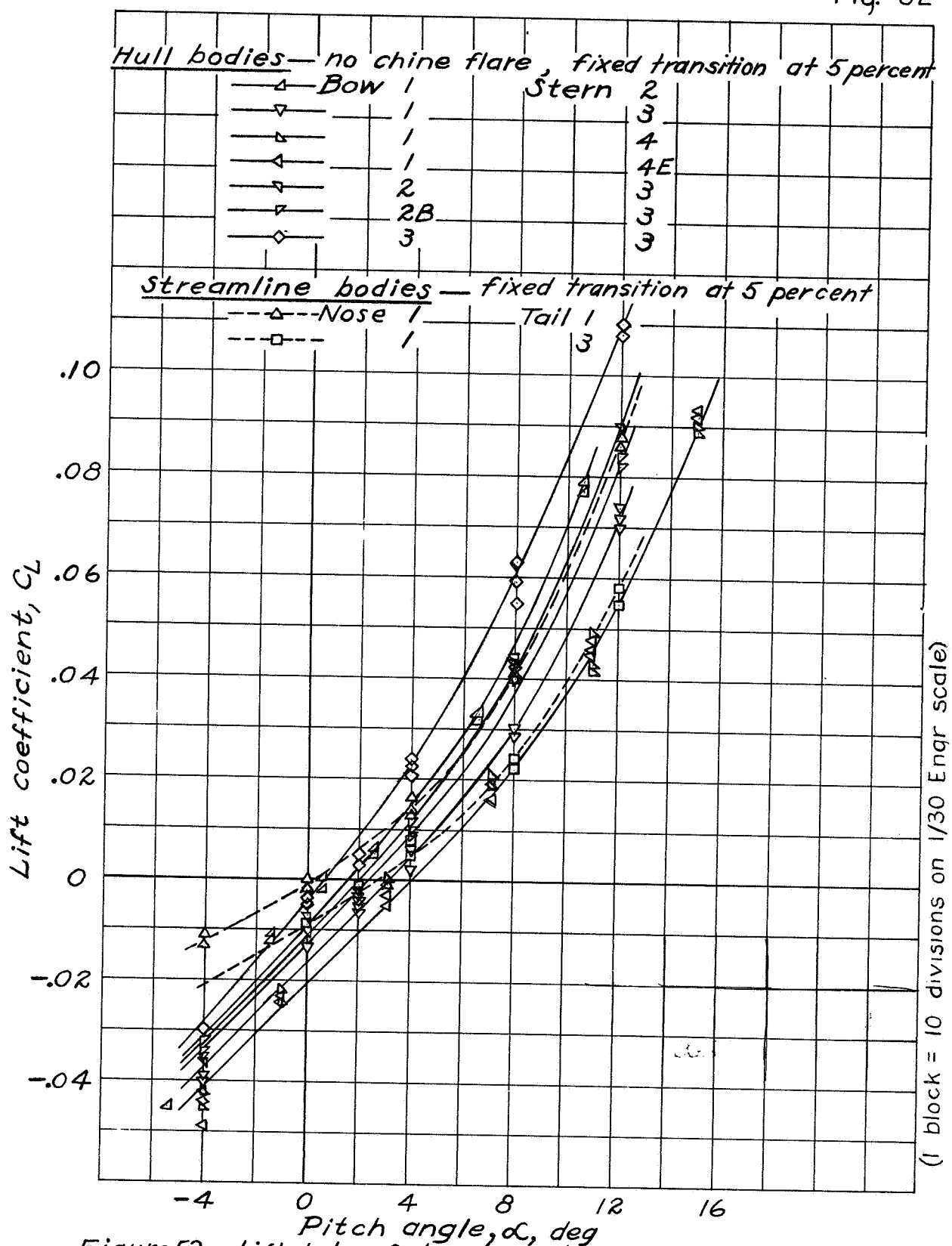
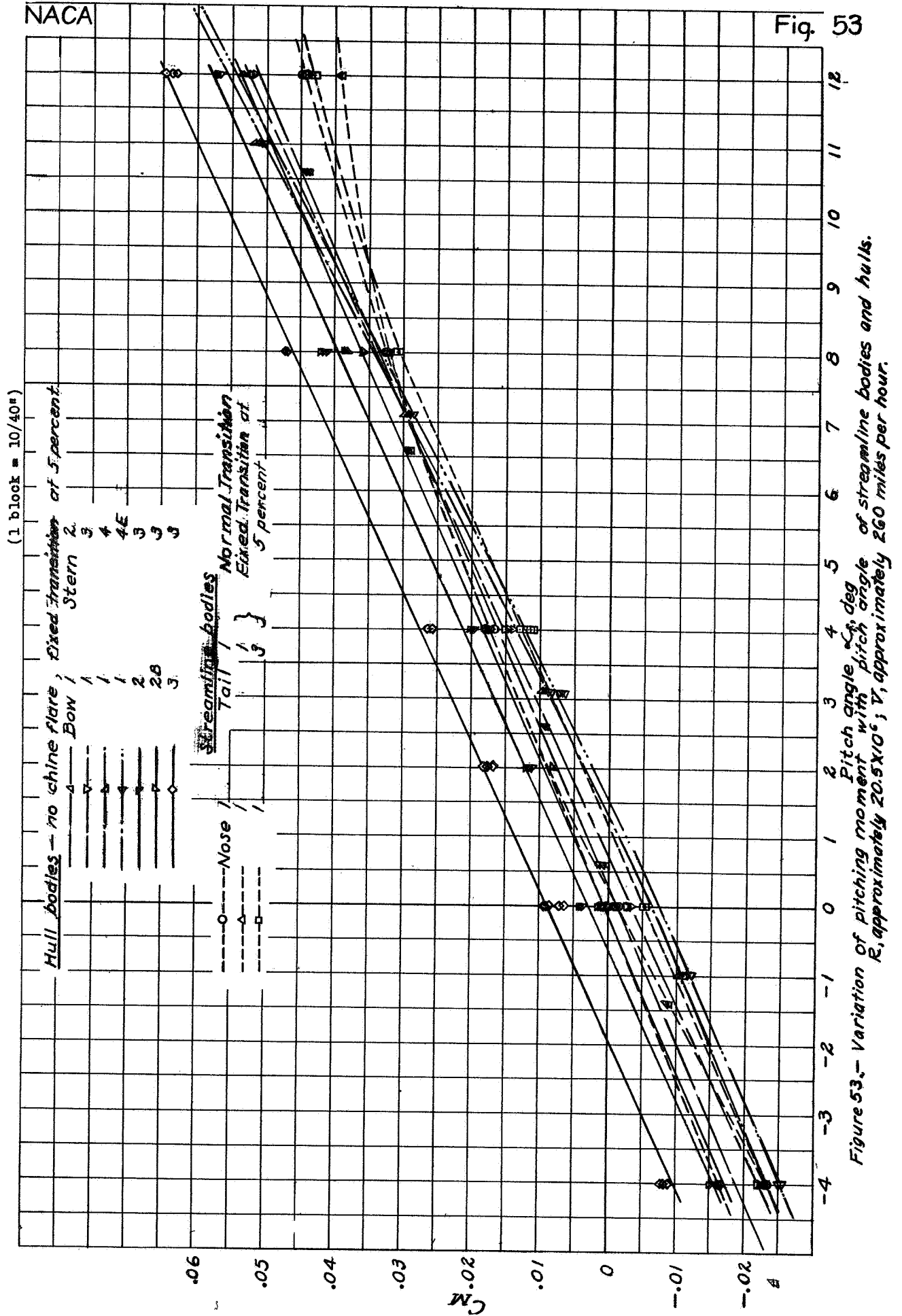


Figure 52.—Lift data of streamline bodies and hulls.  
 $R$ , approximately  $20.5 \times 10^6$ ;  $V$ , approximately 260 miles per hour.





(1 block = 10/40")

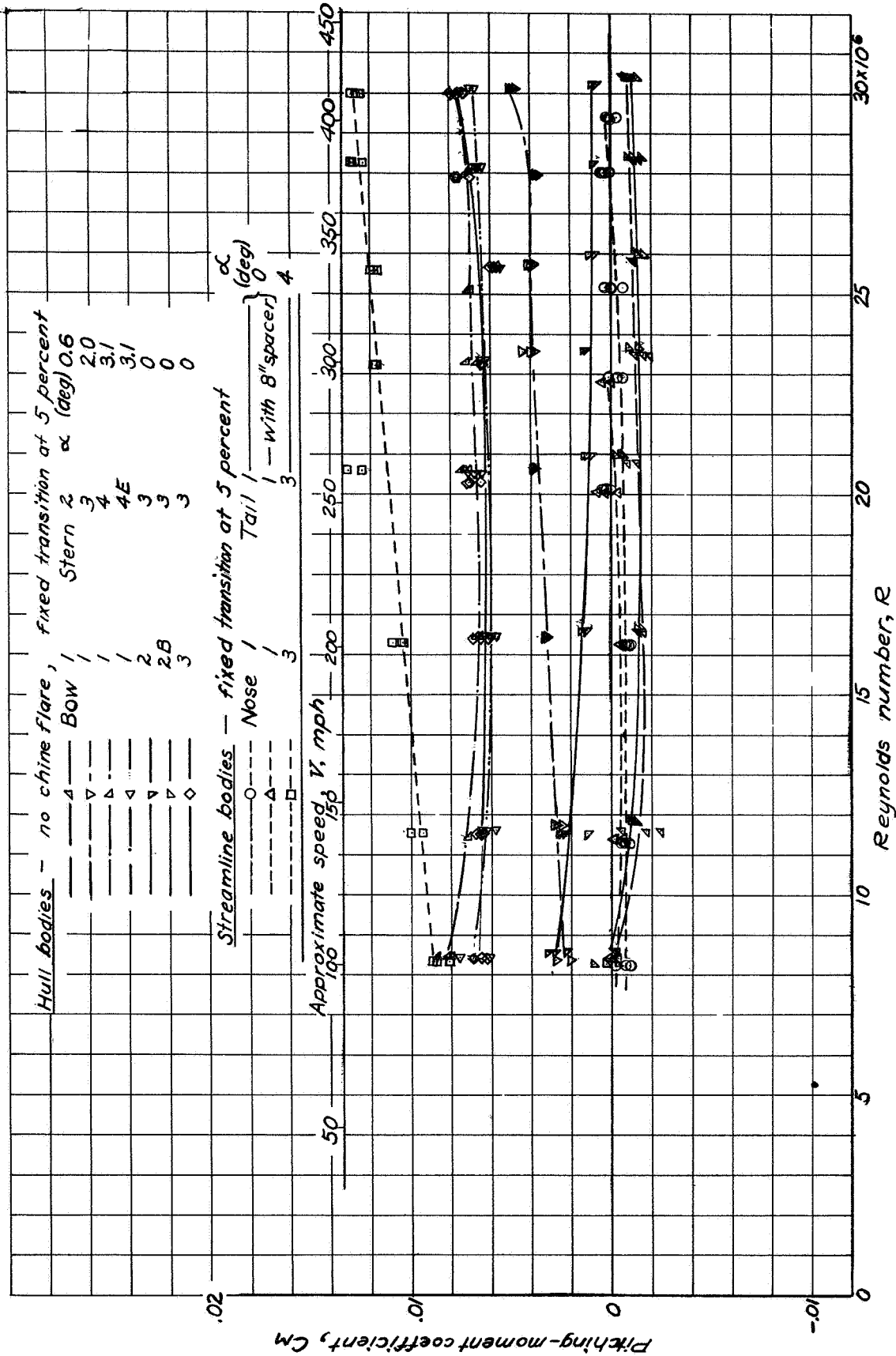


Figure 54.- Variation of pitching moment with Reynolds number of streamline bodies and hulls.